BIOMECHANICAL ALTERATION OF CORNEAL MORPHOLOGY AFTER CORNEAL REFRACTIVE THERAPY

by

Fenghe Lu

A thesis
presented to the University of Waterloo
in fulfillment of the
thesis requirement for the degree of
Doctor of Philosophy
in
Vision Science

Waterloo, Ontario, Canada, 2006

I hereby declare that I am the sole author of this thesis. This is a true copy of the thesis, including any required final revisions, as accepted by my examiners.

I understand that my thesis may be made electronically available to the public.

Abstract

Purpose: Although orthokeratology (non-surgical corneal reshaping, Corneal Refractive Therapy, CRT®) has been used for almost a half century, contemporary CRT's outcomes and mechanisms still require investigation. A series of studies was designed to examine different aspects of non-surgical corneal reshaping for myopic and hyperopic corrections, including the efficacy and stability of this procedure, the effect of the lens material characteristics (Dk/t), and the corneal or superficial structural change (e.g. corneal/epithelial thickness) in corneal reshaping.

Methods: Details are in the following summary Table A-1.

Results: In the CRT1 study, after one night of CRT® for myopia, the central cornea flattened and the mid-periphery steepened, and myopia reduced. In the CRTH study, after one night of CRT® for hyperopia, the central cornea steepened and the para-central region flattened, myopia was induced or hyperopia was reduced, all aberrations except for the astigmatism increased and signed spherical aberration (SA) shifted from positive to negative. In the CRT2 study, after 4 weeks of CRT® lens wear, in general, the treatment zones stabilized by day 10, vision improved, myopia diminished, total aberration and defocus decreased and higher order aberrations (HOAs) including coma and SA increased. The visual, optical and subjective parameters became stable by day 10. In the CRTHDK study, after one night of CRT® [Menicon Z (MZ) vs. Equalens II (EII)] lens wear, the central corneal curvature and aberration were similar with a slight exception: The mid-peripheral corneal steepening was greater in the EII (lower Dk/t) lens-wearing eyes compared to the MZ (higher Dk/t) eyes. In the STOK study, after brief CRT® and CRT®H lens wear, significant changes occurred from

the 15 minutes time point: The corneal shape and optical performance changed in a predictable way; the central cornea swelled less than the mid-periphery after CRT® lens wear, whereas the central cornea swelled more than the para-central region after CRT®H lens wear; the central epithelium was thinner than the mid-periphery after CRT® lens wear and was thicker than the para-central region after CRT®H lens wear.

Conclusion: After one night of lens wear, CRT® and CRTH® lenses were effective for myopia and hyperopia correction, respectively. In the 4 week CRT® study, the treatment zone changed during the first 10 days. Its size was associated with VA, refractive error, aberrations, and subjective vision. In the CRTHDK study, after one night of lens wear, changes in corneal shape were slightly different, with more mid-peripheral steepening in the lower Dk lens-wearing eyes compared to the higher Dk lens-wearing eyes. Changes in central corneal shape and optical performance were similar in both eyes. In the STOK study, CRT® lenses for myopia and hyperopia induced significant structural and optical changes in as little as 15 minutes. The cornea, particularly the epithelium, is remarkably moldable, with very rapid steepening and flattening possible in a small amount of time.

Table A-1. Summary of the Methods and Materials in this Series of Studies

Studies	Corneal Refractive Therapy for myopia (CRT1)	CRT for hyperopia (CRTH)	Relatively long term CRT for myopia (CRT2)	Effects of Dk/t on CRT for myopia (CRTHDK)	Short term effects of CRT for myopia and hyperopia (STOK)
Study Design	Double masked randomized controlled	Single masked randomized controlled	Prospective cohort	Double masked randomized controlled	Cross-over randomized
Study Duration	One night	One night	4 weeks overnight study	One night	15, 30 and 60 minutes
Subjects	20 myopes	20 ametropes	30 myopes (23 completed)	20 myopes	20 ametropes
Lenses (Materials)	CRT (Paragon HDS 100)	CRTH (Paragon HDS 100)	CRT (Paragon HDS 100)	CRT (Menicon Z and Equalens II)	CRT and CRTH (Paragon HDS 100)
The time when measurements were taken	The night before lens insertion and immediately after lens removal, 20 min, and 1, 3, 6, and 12 hours later	The night before lens insertion and immediately after lens removal, 1, 3, 6, 12 and 28 hours	The night before lens insertion and immediately after lens removal, and 14 hours on day1, and on day 4, 10 and 28.	The night before lens insertion and immediately after lens removal, 1, 3, 6, and 12 hours later	Before lens insertion and after lens removal.
Outcome Variables	Corneal Curvature and Auto-refraction	Corneal Curvature, Aberrations and Auto-refraction	Corneal Curvature, Treatment Zone Size, Aberrations, Auto-refraction, Visual Acuity, and Subjective Vision	Corneal Curvature, Aberrations and Auto-refraction	Corneal Curvature, Aberrations, Auto-refraction, and Corneal/Epithelial Thickness

Acknowledgements

First, I would like to thank my supervisor, Dr. Trefford Simpson, from the bottom of my heart for his great guidance and mentoring. During the last four years, Dr. Simpson has guided me with his profound academic knowledge and rich experience in a variety of ways. From the selection of courses to the writing of my dissertation and papers, from study design to discussion and analyses of the experimental results, Dr. Simpson has put significant effort into my graduate study and research. I really admire his enthusiasm for scientific research and his kind patience with students. I also would like to express my deep appreciation to Dr. Desmond Fonn for supporting my enrolment in the Ph.D program, providing valuable input for my thesis and his constant support and encouragement in each aspect through these years. I also thank Dr. Luigina Sorbara, who taught me the critical clinical skill of fitting these specialty lenses in this series of the projects, and Dr. Lyndon Jones who gave me special guidance from different perspectives, which expanded my understanding in my research. I would like to thank Dr. Douglas G Horner and Dr. Mungo Marsden for their willingness to be my external and internal examiners and giving me valuable feedback and advice for my thesis.

I would like to thank Drs. P. Situ and Y. Feng for their sharing, listening and help. Also my gratitude goes to our CCLR team, who provided assistance for me at each stage of my graduate study with a kind smile. Your warm and overwhelming welcome especially at the baby shower was a window for me to see my good fortune being part of this big family.

My appreciation extends to our graduate officers (Drs. E. Irving, C. Hudson, J. Hovis, and T Singer) and graduate coordinators (Ms. S. Dahmer, Ms. K. Snell and Ms. K. Parsons), for keeping me on track during these years. The library staff are very helpful, especially Mr. T. Ireland, in literature searching. I also would like to thank Mr. T. Germen for his help in developing the software for data collection and data analysis, and Mr. J. Davidson for his constant support and maintenance of my computer to keep it functioning properly. Thank our fellow graduate students in school over these years!

My thanks go to all subjects for their participation in these projects. Without their helps, these projects would not be possible.

Finally, I would like to thank my parents, parents-in-law, and my husband, Hongming Dong. Without their strong and continuous support, I would not have been able to overcome the many hardships that occurred.

This research was funded by grants from Paragon Vision Sciences and the Canadian Optometry Education Trust Fund (COETF). I also would like to acknowledge my appreciation of the Ontario Ministry of Training, Colleges and University and University of Waterloo for awarding the following scholarships to support me: Ontario Graduate Scholarship (OGS); Provost's Graduate Women Incentive Fund Scholarship, President's Graduate Scholarship and University of Waterloo Graduate Scholarship.

Without the support of the above mentioned people and funding agencies, my Ph.D would not have been possible.

Table of Contents

List of Tables

List of Figures

List of Abbreviations

ASZ	Annular Steepened Zone
ASZ_{n+t}	The sum of the width of the Nasal and Temporal side of the Annular Steepened Zone
CFZ	Central Flattened Zone
CRT	Corneal Refractive Therapy
CRTH	Corneal Refractive Therapy for Hyperopia
Dk	Oxygen Permeability
Dk/t	Oxygen transmissibility
HCVA	High Contrast Visual Acuity
HOAs	Higher Order Aberrations
LCVA	Low Contrast Visual Acuity
LogMAR	Logarithm of the Minimum Angle of Recognition
OCT	Optical Coherence Tomography
OK	Orthokeratology
Rx	Refractive Error
RM-ANOVA	Repeated Measure of Analysis of Variance
RMS	Root-Mean-squared
SA	Spherical Aberration
SD	Standard Deviation
SE	Standard Error
SV	Subjective Vision

TA	Total Aberration
Tukey HSD post hoc tests: Tukey Honestly Significantly Different post hoc tests	
TZ	Treatment Zone
VA	Visual Acuity
CRT1 study	Efficacy of Corneal Refractive Therapy for Myopia
CRTH study	Efficacy of Corneal Refractive Therapy for Hyperopia
CRT2 study	Relatively long-term corneal refractive therapy for myopia
CRTHDK study	Effects of Dk/t on corneal reshaping after CRT for myopia
STOK study	Short-term effects of corneal refractive therapy for myopia and hyperopia
95% CI	95% Confidence Interval

Chapter 1 Introduction and the Purpose of the Study

1.1 Introduction

Orthokeratology can be defined as the temporary reduction, modification or elimination of a refractive error by the programmed application of rigid contact lenses (Kerns, 1977d). Overnight orthokeratology, also known as corneal reshaping or Corneal Refractive Therapy (CRT®), is one of the promising myopia correction modalities, because it can enable reasonable daytime vision without correction. Recently, rapid improvement in technology and understanding of the modality has renewed interest in Orthokeratology (Mountford, 1997; Swarbrick et al., 1998; Nichols et al., 2000; Rah et al., 2002; Sridharan and Swarbrick, 2003; Alharbi and Swarbrick, 2003; Tahhan et al., 2003; Wang et al., 2003; Soni et al., 2003; Jayakumar and Swarbrick, 2005; Sorbara et al., 2005). The advent of high Dk (oxygen permeability) materials, reverse geometry multicurve lens designs, and novel corneal topographers partially account for this renewed interest (Lui et al. 2000).

1.2 Purpose of the Study

Although the practice of, and research in, orthokeratology have developed relatively rapidly recently, there are still various unknowns. In this series of corneal reshaping studies, the questions we attempt to answer are:

First, due to the lack of the well-controlled corneal reshaping study, a double masked randomized study was designed to examine the temporal efficacy of the corneal reshaping for myopia using corneal refractive therapy (CRT) lens (2002)---CRT 1 study;

Second, since understanding hyperopic corneal reshaping is poorer than that for myopia, a single masked randomized study was conducted to examine the temporal efficacy of corneal reshaping for hyperopia (2004)---CRTH study;

Third, a prospective cohort study was designed and conducted to investigate the relatively long-term (4 weeks or one month) effects of corneal reshaping for myopia, and to determine the time when the treatment effect became stable, something of concern for both the practitioner and the patient (2003-2004) ---CRT 2 study;

Fourth, since the lens material (i.e. Dk/t) not only influences the ocular health, but also the clinical effects, practitioners need to choose the appropriate material for corneal reshaping lenses in clinical practice. Therefore, a double masked randomized study was designed to compare the effects of two materials (Menicon Z and Equalens II) with different Dk/t values on the corneal shape and optical performance (2005)---CRTHDK study;

Fifth, the efficacy of corneal reshaping partially depends on how moldable the cornea is. Therefore, a randomized cross-over study was designed to determine the moldability of ocular surface by local mechanical stress through examining the acute effects of corneal reshaping for myopia and hyperopia after a brief use of lenses wear (2005-2006)---STOK study.

The remainder of this thesis is organized in 10 chapters. Chapter 2 presents the literature review with respect to corneal biomechanics and orthokeratology. Chapter 3 introduces the instruments, subjects, and lenses used. The next five chapters (Chapters 4-8) are devoted to the corneal reshaping experiments including introduction, protocol, results and discussion. Chapter 9 reports the corneal posterior surface change after corneal reshaping.

Chapter 10 summarizes the present work. Finally, Chapter 11 gives some recommendations the future work in this field.

Chapter 2 Literature Review

The cornea is a unique portion of the outer, fibrous ocular tunic that is transparent and serves a refractive function while maintaining mechanical strength. These dual responsibilities of the cornea are the basis of many refractive procedures. This review covers the biomechanics of the cornea and the non-surgical corneal reshaping with respect to the refractive function.

2.1 Biomechanics of the Cornea

In microscopic view, the cornea can be divided into five layers: epithelium, Bowman's layer, stroma, Descemet's membrane and endothelium (Klyce and Beuerman, 1997). Before I review the biomechanics of the cornea, a brief review of the corneal structure is given.

2.1.1 Corneal Structure

2.1.1.1 Epithelium

The nonkeratinized, stratified squamous epithelium of the cornea consists of four to six layers of cells and represents 10 percent of the corneal thickness. Morphologically, the epithelium is divided into three layers: the superficial cell, the wing (middle) cell and basal (deep) cell layers. It turns over approximately every 7 days. The epithelium has several mechanical cell junctions. For example, tight junctions have large areas of membrane fusion. In addition to the tight junctions, the desmosomes and hemidesmosomes also maintain some intercellular attachments and adhesion (Klyce and Beuerman, 1997).

2.1.1.2 Bowman's Layer

The Bowman's layer is below the epithelium and in the anterior of the stroma. It is composed of collagen fibrils with diameters of 20-25 nm. These fibrils run in various directions and form an 8 to 12 μm-thick sheet. Bowman's layer is attached to the stroma by collagen fibrils that insert in Bowman's layer and become part of the anterior stromal lamellae (Komai and Ushiki, 1991). Bowman's layer functions as a domelike structure that is anchored to the limbus. It is difficult, if not impossible, to change the shape of Bowman's layer, and hence the anterior corneal curvature, without first cutting through it and the underlying anterior stromal lamellae (Klyce and Beuerman, 1997).

2.1.1.3 Stroma

Stroma constitutes about 90 percent of the corneal thickness, featuring stacked lamellae of collagen fibrils. The collagen fibrils, which are packed in parallel arrays, make up the 300 to 500 lamellae of the stroma centrally and peripherally. The lamellae extend from limbus to limbus and are oriented at various angles to one another, less than 90 degrees in the anterior stroma but nearly orthogonal in the posterior stroma (Klyce and Beuerman, 1997). In the anterior one third of the stroma, collagen lamellae are narrow (0.5-30μm width) and thin (about 0.2-1.2 μm thick), run in random direction and often branch and interweave in an irregular manner. However, the collagen lamellae in the posterior two thirds of the stroma are wider (0.5-250 μm) and thicker (0.2-2.5 μm), and tend to be parallel to the corneal surface. The fibrils appear to have uniform diameters of 23-35nm (Pouliquen, 1984; Komai and Ushiki, 1991). These collagen lamellae are embedded in the amorphous, compressible and elastic ground substance. The ground substance plays a role in the absorbance of the mechanical force and can be remodeled through the enzymes (Alberts et

al., 1994). The stroma, particularly the collagen fibrils, is the component responsible for the mechanical strength of the cornea. The biomechanical features of the cornea are heavily influenced by this layer (reviewed in a later section).

2.1.1.4 Descemet's Membrane

Descemet's membrane is the thick basal lamina secreted by the endothelium. It increases from 5 to 13 μm thick with age. It is loosely attached to the stroma (Klyce and Beuerman, 1997) and is more plastic and flexible than Bowman's layer (Jue and Maurice, 1986). As a consequence, corneal swelling is mainly towards the posterior surface.

2.1.1.5 Endothelium

The corneal endothelium forms a single layer of cells approximately 4 to 6 μm thick, and 20um wide, on the posterior corneal surface.

2.1.2 Biomechanical Features of Corneal Tissue

2.1.2.1 Elasticity

Different microstructures of the cornea have different mechanical properties. The elastic modulus, or Young's modulus, is the ratio of change in stress to the associated change in strain. It is a measure of "strength" of a material. When the elastic modulus is high, little deformation occurs with a increase in strain (Battaglioli and Kamm, 1984). Modulus of the Bowman's membrane is greater than that of a typical layer of the stroma. Due to being approximately 2-6% of the corneal thickness, Bowman's membrane may not influence the effective modulus of the whole cornea dramatically (Hoeltzel et al., 1992). However, in non-surgical corneal reshaping, the higher modulus of the Bowman's membrane may play an important role in the corneal epithelial alteration. Compared to the high moduli of the rigid contact lenses and Bowman's membrane, the modulus of the corneal epithelium is much

lower. Accordingly, the epithelial alteration may occur from eyelid tension, the hydraulic force underneath the corneal reshaping lens and intraocular pressure (IOP). Hoeltzel et al. (1992) stated that the Descemet's membrane had a lower modulus than a typical layer of stromal lamellae.

Besides the different elasticity of layers, the regional variation of elasticity has been reported. A higher modulus of elasticity in a certain direction and region corresponds to an increased resistance to deformation. Hjortdal et al. (1996) explored the regional elastic performance of the human cornea *in vitro* by changing the IOP (2-100 mmHg). The pressure-induced meridional strains were smallest at the corneal para-centre and periphery, and largest at the limbus. The circumferential strains varied less between regions with the para-centre straining the most. In the meridional direction, Young's modulus was highest at the central and para-central corneal regions, whereas the highest circumferential elastic modulus was found at the limbus (Hjortdal, 1996). In brief, the cornea is anisotropic.

The detailed estimates of the in-plane elastic modulus of the central human cornea are different depending on the method of measurement (for example, mercury droplets or laser-scanning confocal microscope), different corneal tissue (for instance, the intact cornea or strip extensiometry) and the hydration state. Detailed information has been provided in a thesis paper (Hjortdal, 1998) and by others (Hennighausen et al., 1998).

2.1.2.2 Extensibility

Human stroma is poorly extensible, a pressure change of 5–20 mmHg causing only 0.25% stretching (Maurice, 1988). As discussed in the microscopic view of the corneal structure, the anterior corneal contour is more stable than the posterior (Carney, 1975; Rom

et al., 1995; Muller et al., 2001). The stroma is less extensible than Descemet's membrane in rabbit and human corneas (Jue and Maurice, 1986; Maurice, 1988).

Corneal hydration affects the deformation pattern (strain) of the human cornea *in vitro* (Hjortdal, 1995; Hjortdal and Jensen, 1995). In humans, the increase in the epithelial corneal strain was approximately 1% and was 3% on the endothelial side in swollen corneas. However, in normally hydrated corneas, strain changes were approximately 10% higher on the endothelial side compared with the epithelial side. After raised IOP for 2 hours to thin the cornea, the epithelial corneal strain gradually decreased, whereas the endothelial corneal strain increased. In rabbits, the posterior stromal strain was greater than the anterior stroma, and the swollen cornea strain was greater than the normally hydrated cornea (Hennighausen et al., 1998). Therefore, the elastic and visco-elastic behaviour of the cornea is related to changes in corneal hydration. A possible consequence of this is that when corneal edema occurs, corneal swelling is greater in posterior cornea than in the anterior (Kikkawa and Hirayama, 1970; Van Horn et al., 1975; Lee and Wilson, 1981; Cristol et al., 1992; Edelhauser et al., 1994; Erickson et al., 1999; Muller et al., 2001; Moezzi et al., 2004).

2.1.2.3 Stromal Cohesive Strength

Maurice (1999) observed that the stroma immersed in water swelled up to 10 times, but did not fall apart. This was quantified as adhesive strength, measuring the force required to tear apart two layers of a strip of tissue. In humans, stromal cohesive strength varied with different regions and depth, i.e., it increased approximately twice from the centre to the periphery horizontally (Smolek and McCarey, 1990), and from the posterior to the anterior stroma (McTigue, 1967). A study also revealed that inferior peripheral cornea had the lowest cohesive strength compared to the superior, nasal and temporal regions (Smolek, 1993).

These findings supported the anisotropic property of the human cornea. However, in the rabbit stroma, it is relatively uniform and not sensitive to tissue hydration (Maurice, 1988).

2.1.2.4 Shear Force of the Cornea

The ground substance in the corneal stroma may not play a role in the elastic modulus, but it has importance for shear strength. Low resistance to shear deformation was found in the rabbit and the relationship between the shear stress and shear strain was dependent on the stromal hydration (Maurice, 1988). Although the shear force resistance possibly plays no role in the intact cornea, it may become important when the cornea is bent, for instance, during tonometry. Due to the tight and increasing lamellar interweaving in the anterior stroma (Komai and Ushiki, 1991; Muller et al., 2001), the resistance to shear force would be expected to be greater in the anterior than the posterior stroma.

2.1.3 Mechanical Stress

In addition to the biomechanical characteristics of the cornea itself, the mechanical stress or pressures on the cornea from the neighboring structures (for example, the eyelid tension/pressure), intraocular pressure and hydraulic forces underneath the contact lens should also be taken into consideration when discussing influences on the corneal reshaping.

2.1.3.1 Eyelid Tension/Pressure

Eyelid tension is applied to the corneal anterior surface. Burton (1942) has demonstrated that the upper lid exerted a squeeze force of 50 to 70 gm when pulled against the closed lid with a hook device connected to a spring scale. Mϕller (1954; 1955) used a modified Tybjærg Hansen manometer to directly measure the change in pressure that accompanies blinking, and found that the average lid pressure was 10 mm of water during a gentle blink and 50 mm of water with a forced blink. Lydon and Tait (1988) also measured

the lid pressure and found similar findings to Mϕller. However, Miller (1967) reported that the average lid pressure during a blink was within 10.3mmHg and 51mmHg during a hard lid squeeze, and 3.2 mmHg during a gentle closure, which is much greater than others. Miller (1967) also reported that the interposition of a small thick mass could easily exert some 5gm of force over a small area and thus indent the globe, indicating that a rigid corneal reshaping lens could induce a pressure on the corneal surface. Hung et al. (1977) reported that the amplitudes of blinks for upward loading forces ranging from 2 to 80 gm, giving estimates of the driving forces of the eyelid during normal blinks. Ehrmann et al. (2001) reported that the averaged lid tensions for Asian and Caucasian groups were 15.7 and 14.9 mN/mm, respectively, using a novel lid tensiometer.

The evidence of the effects of eyelid tension on the cornea is inconclusive. Several groups found the normal cornea exhibited a high degree of stability, and the ocular topography remained essentially constant even during forced blinking (Kiely and Carney, 1978; Lydon and Tait, 1988). However, Lieberman and Grierson (2000) used a surface modeling technique to demonstrate the corneal shape difference with and without the lid forces, illustrating the effect of eyelid pressure on corneal surface.

The eyelid tension is an important variable to be taken into consideration in contact lens fitting. Dickinson (1971) discussed the relationship of the eyelids to the contact lens performance. Swarbrick and Holden (1996) used linear discriminant analysis and revealed that the greater eyelid tension could increase the frequency of lens adherence. Holden et al. (2001) hypothesized that the inward pressure of upper eyelid might be a cause of the superior epithelial arcuate lesions (SEALs) through mechanical chaffing at the peripheral cornea. Herman (1983) suggested that the upper lid was a major factor in causing flexure of rigid gas

permeable lenses, indicating the lid pressure might contribute to the corneal shape. However, other authors did not draw the same conclusion (Harris and Appelquist, 1974; Lydon and Tait, 1988).

Lid tension decreases with age (Vihlen and Wilson, 1983). Lid tension and associated contact lens forces could be at or near a maximum during the second decade, which is a common age for the corneal reshaping. Therefore, lid tension appears to be an important influence on corneal reshaping.

2.1.3.2 Eyelid Shear Force

The shear force of the eyelid is tangent to the corneal surface. Shear forces assist epithelial desquamation (Ren and Wilson, 1997), regulate some epithelial activities (Srinivas et al., 2002) and spread tears uniformly during blinking, to maintain the tear film as an optically smooth refractive layer (Trinkaus-Randall et al., 1998). Due to its tangential direction, it is not a critical force when a corneal reshaping lens is in place. However, the eyelid shear force may play an important role in the corneal shape regression after the lens removal.

2.1.3.3 Hydraulic Forces underneath the Contact Lens

In addition to the eyelid tension, the hydraulic forces underneath the contact lens are important in cornea reshaping. Allaire and Flack (1980) modeled the hydrodynamic forces of tear films during squeeze motions and found that the forces were related to the tear film thickness profile. A tear film with a peripheral film thickness of one-half of the central film thickness produces over three times the squeeze force produced by a constant tear film thickness with the same central clearance. The pressure was associated with the lens bearing relationship (Martin and Holden, 1986). When the lens bearing relationship decreased

(steeper fit), the pressure at the central cornea decreased (more negative pressure). Flat fitting contact lenses had a greater positive pressure at the corneal centre (apex). Mountford (2004b) also modeled the hydraulic forces under the orthokeratology lens and profiled the tear film and corresponding forces. Tear film hydraulic force may be influenced by the amount of tear film and Fan et al. (1999) reported that in a group of orthokeratology subjects, eyes with insufficient tears had a slower response and consequently, the treatment effect was less.

2.1.3.4 Intraocular Pressure (IOP)

Like other living tissues, the cornea is constantly under stress (Fung, 1995), with the primary load from IOP (Berkley, 1971). IOP (approximately 20mmHg above atmospheric pressure) is outward at the posterior surface, opposite to the eyelid tension/pressure and the forces derived from atmospheric pressure (760 mmHg or 101 kPa) at the anterior surface, into the eye. When homeostatic conditions of stable stress in tissues are disturbed, remodeling may take place (Fung, 1995). For example, in congenital glaucoma without timely treatment, progressive enlargement of the eye may occur throughout the first two years (Walton, 1983). Besides the pathological condition, the disturbed homeostatic conditions also occur with surgical intervention. For example, after corneal refractive surgery, corneal ectasia has been reported (Wang et al., 1999; Randleman et al., 2003).

One study showed that the lower intraocular pressure appeared to be a predictor of orthokeratologic changes (Joe et al., 1996). Subjects with relatively low IOP, whose ocular rigidity was hypothesized to be low, would be more easily reshaped. Others have not found this relationship (Lui and Edwards, 2000).

2.1.4 Mechanisms of the Corneal Reshaping

To understand the non-surgical corneal reshaping, the mechanisms during this procedure have been explored and hypothesized, and include epithelial compaction, epithelial redistribution/ migration, the combination of both and corneal bending. The corneal stroma has also been hypothesized to be involved.

In 1964, Dixon stated, "The cornea epithelium is soft and pliable. It is easily molded mechanically and the cells are more loosely attached to Bowman's membrane than they are to each other. The absence of keratinization makes the surface easily indented. Foreign bodies readily become imbedded in this soft tissue, but defects are rapidly repaired" (Dixon, 1964). This comment indicates the compressible, movable and moldable features of the corneal epithelium, which are particularly important in the field of non-surgical corneal reshaping.

2.1.4.1 Epithelial Compression

Greenberg and Hill (1973) fit rabbits' eyes with steep rigid contact lenses and found that the epithelial thickness at bearing sites became thinner (only approximately 64%) than areas of the corneas without lens wear. The average basal cell width increased to 10 microns compared to only 7 microns in the non-bearing area. The corneal epithelium has been shown to be compressed after corneal reshaping lens wear in cat and rabbit eyes histologically (Choo et al., 2004c; Matsubara et al., 2004).

2.1.4.2 Epithelial Migration/Redistribution

Although it has not been directly shown that there is epithelium migration or redistribution *in vivo* during the mechanical stress of corneal reshaping, the following

indirect evidence from different groups suggested and supported the theory of epithelium migration and redistribution.

1) Matsubara et al. (2004) showed that the number of layers of epithelium decreased in rabbits after corneal reshaping, compared to the control corneas. Greenberg and Hill (1973) fitted steep rigid contact lenses on rabbit corneas and demonstrated that the number of the epithelium layers in the bearing areas was less than the non-bearing sites.
2) Ladage et al. (2002) used a confocal microscope to scan the areas of mucin balls and found that these produced indentations extending into the corneal epithelium, reaching as far as the basal lamina. This rabbit model also showed no epithelial nuclei within the indentation, suggesting that epithelial migration occurred.
3) Dixon (1964) reported that the dimple veiling occurred in corneas of the living rabbits, but did not occur in the corneas of dead animals, indirectly suggesting that epithelial redistribution would be involved in the formation of dimple veiling rather than only epithelial compression. In addition, the observation that "blinking of the lids later erased the dimples within two or three minutes" also supported the idea that epithelium migration was involved in this recovery.
4) The epithelial compression findings (see section 2.1.4.1) by Greenberg and Hill (1973) also suggested the epithelium in the bearing areas would spread (green central cells in Figure 2-1). Correspondingly, the epithelium around the lens bearing area would migrate outward and redistribute (blue cells in Figure 2-1).
5) Greenberg and Hill (1973) also demonstrated higher mitotic frequency (average one cell in ten) at imprint sites compared to that of the non-fitted corneas (approximately one per

one hundred cells), indicating that the epithelium in the bearing area might migrate and redistribute to the neighboring area.

6) Dierick and Missotten (1992) observed small variations in epithelial thickness, which partly compensated for induced irregularities in the stroma, when ocular hypotony was induced. This experiment suggested that the epithelium was able to move rapidly to fill in the small spatial irregularities induced.

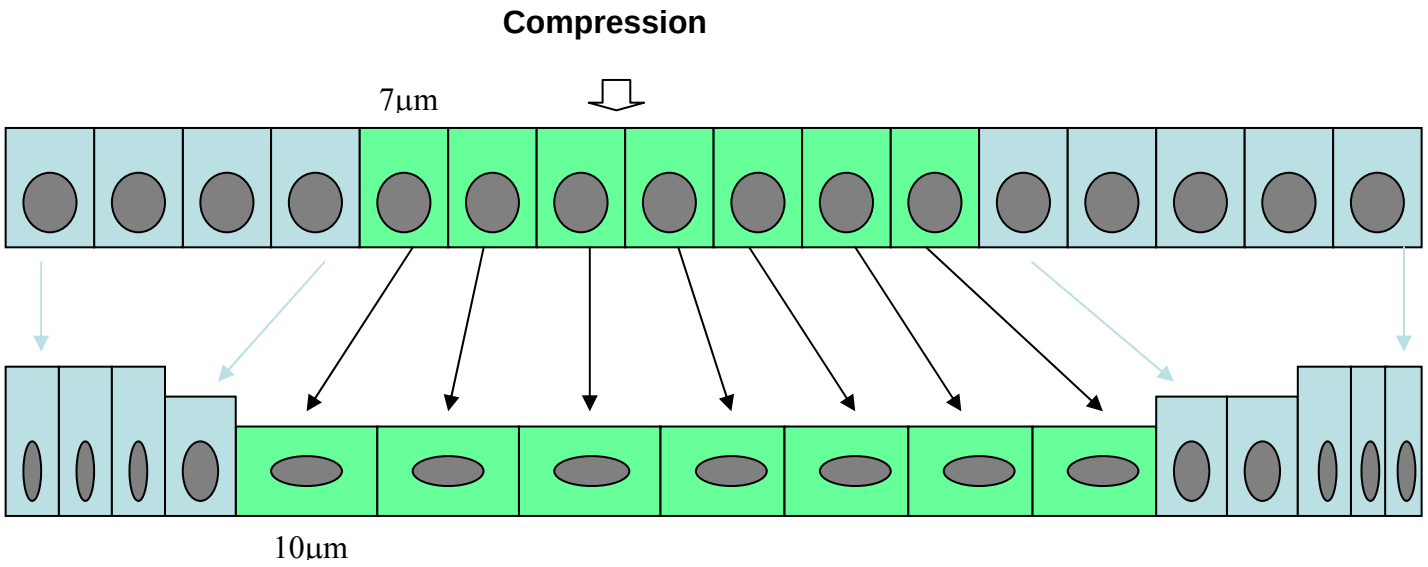

Figure 2-1. Illustration of the epithelial shape change and spatial alteration during compression in a single epithelial layer. Central seven cells are in the lens bearing area in green and the surrounding 4 to 5 cells on each side are in the non-bearing area in blue.

2.1.4.3 Stromal Involvement

Corneal stromal shape change during contact lens wear has been demonstrated and reviewed (Holden, 1988; Holden et al., 1989; Bruce and Brennan, 1990; Efron and Ang, 1990; Liesegang, 2002; Jalbert and Stapleton, 2005). In addition to the epithelial change, the stroma has also been proposed to be involved in corneal reshaping. Choo et al. (2004b) have demonstrated histologically that the stroma was involved in the corneal reshaping in cats. Others (including us) have shown stromal thickness changes after corneal reshaping, indicating that stroma may also contribute to the orthokeratologic effect (Alharbi and Swarbrick, 2003; Wang et al., 2003; Haque et al., 2004b; Alharbi et al., 2005). Recently, the Swarbrick group (2005; 2006) examined the clinical response of overnight orthokeratology using low Dk/t materials (Boston ES vs. XO and EO and XO) and found that the lower Dk/t lens was associated with greater stromal edema and had less clinical OK effects. These suggest that the corneal stroma is involved in corneal reshaping after overnight lens wear.

2.1.4.4 Corneal Bending

When compression was applied to corneal anterior surface, corneal bending would be a reasonable assumption, resulting in the posterior surface flattening, if the cornea were a piece of plastic. Due to the difficulty in measuring the corneal posterior surface, exploring corneal bending has not been extensively examined experimentally. Recently, Owens et al. (2004) reported a significant flattening of the posterior surface during the early adaptive stages of orthokeratology lens wear. In this series of experiments, we could not draw the same conclusion using Orbscan II (see chapter 9).

In summary, the most likely hypothetical mechanism of corneal reshaping is epithelial compaction, but epithelial migration/redistribution cannot be completely excluded.

The corneal stroma is also likely involved in corneal reshaping, but its exact role requires further investigation. It is unclear whether actual corneal bending occurs.

2.2 Orthokeratology (Corneal Reshaping or Corneal Refractive Therapy)

2.2.1 Orthokeratology: Past and Present

Orthokeratology has been refined over years, leading to an effective, faster and more predictable outcome. Corneal reshaping originated in China; the ancient Chinese placed sandbags on their eyes while sleeping in attempt to change the refractive error (Kerns, 1976a; Lebow, 1991). Contact lens to alter ametropia was first proposed by Jessen (1962) who fitted patients with plano power contact lenses so that the tear layer compensated for the myopia. With this technique, the greater the myopia, the flatter the lens fit. As a consequence, discomfort increased, lens decentred and corneal astigmatism/distortion was induced. Due to the concerns of the ophthalmic community at the early stage of orthokeratology, four controlled orthokeratology studies were conducted. They included one by Kerns (1976a; 1976b; 1976c; 1977a; 1977b; 1977c; 1977d; 1978), one by Binder (1980), one by Polse et al. (Brand et al., 1983; Polse et al., 1983b; 1983a; 1983c), and one by Coon (1984). From these studies, it was concluded that orthokeratology was an unpredictable and time-consuming procedure, generally unacceptable in ophthalmology and optometry.

Stoyan and others developed and patented reverse curve designs (base curve flatter than the central cornea with a secondary curve of steeper radius) specifically for orthokeratology in 1986 (Phillips, 1995). The introduction of the reverse geometry lenses generated more rapid and stable alterations in corneal curvature/refraction than the traditional technique (Wlodyga, 1989) and improved lens centration (Phillips, 1995).

Riley et al. (1992) demonstrated that after two hours of lens wear, the refractive error changed by 0.69D for the reverse geometry lens group and 0.25D for the conventional lens group, although the two lens wearing eyes were fitted with same projected correction (1.50D to 1.75D). The reverse geometry lens design has been used for two decades, now, and detailed information with respect to basic concepts, principles and the effectiveness of the orthokeratology can be found in a number of review papers (Coon, 1982; Dave and Ruston, 1998; Lui et al., 2000; Caroline, 2001; Caroline and Choo, 2003; Barr et al., 2003; Walline et al., 2005).

The advance in oxygen transmissibility (Dk/t) of rigid permeable materials made the overnight lens wear modality physiologically plausible. Mountford (1997) first conducted an orthokeratology study with patients wearing reverse geometry contact lenses on a nightly basis and reported that the effect of this type of orthokeratology lens was more predictable and consistent, and myopia was reduced by 2.19D on average.

In addition to the advances of the reverse geometry lens design and high Dk material, the third improvement, which partially accounts for the renewed interest of the orthokeratology, is the improvement in quantifying corneal topography (Mandell, 1996). Furthermore, the advance of computer-controlled lathes has made the manufacture of precise reverse geometry lenses possible. Therefore, Orthokeratology has received renewed interest in recent years (Mountford, 1997; Swarbrick et al., 1998; Nichols et al., 2000; Rah et al., 2002; Sridharan and Swarbrick, 2003; Alharbi and Swarbrick, 2003; Tahhan et al., 2003; Wang et al., 2003; Soni et al., 2003; Jayakumar and Swarbrick, 2005; Sorbara et al., 2005).

2.2.2 Predictors for Success

Although the average success rate and predictability of the modern orthokeratology has been greatly improved, the individual variation in response to the lenses is still evident. Therefore, defining a predictor before the therapy would assist in indicating who would be an appropriate candidate for this procedure. Clinically, this information would be helpful for both the practitioners and the patients.

Kerns (1978) and Binder (1980) found low myopes were more easy to treat. Carkeet et al. (1995) reported that the success of orthokeratology was related to pre-fitting refractive error. Joe et al. (1996) found that the eccentricity was correlated with the auto-refraction and Mountford (1997; 1998) demonstrated the change of eccentricity was well associated with the refractive change. However, we (unpublished data) could not find this relationship. More prolate corneal shapes might achieve more rapid early effects than those with more spherical corneas (Sridharan and Swarbrick, 2003). Lui and Edwards (2000) have found that the corneal thickness, p-value of the nasal semi-meridian and the difference between central and peripheral corneal powers were correlated with refractive change. Age is a significant factor in the short-term (1h) corneal response to orthokeratology lens wear. The older the patient, the less the treatment effect (Jayakumar and Swarbrick, 2005). Joe et al. (1996) found that lower IOP was also a predictor of orthokeratology changes. However, Carkeet et al. (1995) found that the success of orthokeratology lens wear was not related to ocular biomechanical or biometric attributes (intraocular distances, corneal thickness, ocular rigidity, epithelial fragility). In addition, instead of looking at the baseline data before the treatment, Sridharan and Swarbrick (2003) tried to relate the apical corneal power change of short term lens wear (minutes) to the change after overnight lens wear in the same group of subjects, but did not find any relationship, suggesting that the potential of using a short term trial to predict the

eventual success with orthokeratology lens wear still needed to be clarified. Thus, the predictability is more complicated than what we anticipate. Although great efforts were made in this regards, thus far, the results are still inconclusive. Therefore, more work on this topic is needed to help further our understanding.

2.2.3 Recovery after Orthokeratology

A number of reports have appeared about the recovery after discontinuation of lens wear. Wang et al. (2003) found that after one night of CRT® lens wear, the corneal and epithelial thickness returned to baseline after 3 hours of no lens wear, but the refractive error recovered by 37% (about 0.44D) after 12 hours without lens wear. Researchers from Centre for Contact Lens Research reported 72 hour recovery data after 1 month (28 days) of overnight CRT® lens wear (Haque et al., 2004b; Sorbara et al., 2005). Visual acuity, refractive error, keratometry and subjective vision did not recover to baseline after 72 hours without lens wear (Sorbara et al., 2005). Corneal and epithelial thickness recovered to baseline by 72 hours (Haque et al., 2004b). Barr et al. (2004) reported that after 6 to 9 months of CRT® lens wear in 96 subjects, the refractive error returned to baseline by 72 hours after lens wear cessation. Soni et al. (2004) conducted a recovery study with 2 weeks of lens discontinuation after 1 month of CRT lens wear and found that the corneal thickness regressed rapidly (1 day), and the corneal curvature more slowly (1week). Refractive error recovered fully after 2 weeks, but visual acuity did not fully return to baseline after 2 weeks without lens wear. Cho et al. (2003b) described two subjects who developed pigment rings in their corneas and discontinued lens wear for about 2 to 3 months. Their refractive error and corneal topography completely returned to baseline after 3 months without lens wear.

Horner et al. (1992) have demonstrated that the refractive change varied with the period of time reverse geometry lenses were worn and the recovery to baseline also varied with the exposure time in 7 subjects. The cornea could be flattened rapidly with a recovery that generally took twice as long. After 1, 2 and 4 hours of lens wear, the refractive change ranged from 0.10 to 2.37D for 1hour, 1.01 to 1.81D for 2 hours, and 1.34 to 2.56D for 4 hours. The rate of recovery was 50.9% per hour for the 1 hour group, 36.6% per hour for the 2 hours group, and 30.5% per hour for the 4 hours group. After lens removal, the corneas recovered 99% of the induced change in 10 hours, in all groups.

Is the non-surgical corneal reshaping a plastic or elastic deformation (permanent or temporary)? Horner et al. (1992) showed that after 1, 2 and 4 hours of lens wear, the cornea recovered to baseline level in 10 hours. However, thus far, the longest discontinuation has been 2 weeks after 1 month of lens wear and all examined parameters (except visual acuity) recovered completely (Soni et al., 2004). The recovery after long-term (at least a year of) lens wear will provide invaluable information in determining plastic or elastic deformation.

2.2.4 Safety Issue of Orthokeratology

Microbial keratitis (MK) is the most severe complication and the only sight-threatening adverse event that occurs with contact lens wear (Holden et al., 2003). Studies have showed that overnight lens wear, extended-wear and poor lens hygiene practice, among many others, are risk factors (Schein et al., 1989; Dart et al., 1991; Stapleton, 2003). Compared to soft contact lens wear, the risk of microbial keratitis during rigid contact lens wear is low (Schein et al., 1989; Dart et al., 1991; Stapleton, 2003). In this review, I will focus on the orthokeratology related microbial keratitis.

Early orthokeratology reports suggested that microbial keratitis was rare and orthokeratology was therefore safe (Binder et al., 1980; Grant, 1980; Polse et al., 1983a). There was one report of permanent damage of cornea in a patient during orthokeratology (Levy, 1982). More recently the incidence of microbial keratitis appears to have increased but the incidence of it is unknown. Watt and Swarbrick (2005) reviewed the first 50 cases of the microbial keratitis in contemporary orthokeratology, which occurred from 2001 to 2005. They found that 80% of the MK cases were from East Asia and Asia (88%) and mostly occurred in young patients (9 to 15 years old, 61%). *Pseudomonas aeruginosa* (52%) and *Acanthamoeba* infection (30%) were the prominent two organisms in this series of MK cases. They also proposed risk factors for MK in orthokeratology including inappropriate lens care procedures, patient noncompliance with practitioner instructions and persistence with lens wear despite discomfort.

There were 5 case reports from around the world of MK with orthokeratology in 2005 (Tseng et al., 2005; Hsiao et al., 2005; Araki-Sasaki et al., 2005; Wilhelmus, 2005; Yepes et al., 2005) and 2 case reports in 2006 (Sun et al., 2006; Ying-Cheng et al., 2006). 63 cases were reported. 30 cases were from Taiwan, 28 cases from China, 3 cases from Canada, 1 each from the U.S.A and Japan. Pathogens from 50 (79%) cases were cultured and included 21 (33%) cases with *Pseudomonas aeruginosa* infection, 19 (30%) cases of *Acanthamoeba*, 2 cases of *Fugus*, 2 cases of *coagulase negative staphyloccus*, 1 case each of *Nocadia asteroids*, *Proridencia Stuartii, Serratia Marcesens, Gram-negative bacilli,* and *Non-fermentative Gram-negative bacilli*. In 13 (21%) cases the organism was not identified. This series of case reports confirmed that *Pseudomonas aeruginosa* (33%) and *Acanthamoeba*

infection (30%) were the leading pathogens in orthokeratology related MK. The average age in these 63 cases was 15.1±4.8 years (8 to 41).

Patient education and compliance are two key factors to avoid or minimize this MK. The increase of orthokeratology related MK case reminds the practitioner to pay more attention to their orthokeratology patient, for example, repeating the instruction at each follow-up visit, monitoring the lens care procedure, and emphasizing when to stop lens wear and contact the practitioner. The practitioner and the patient closely working together would make this therapy safer.

Chapter 3 Methods

In this chapter, I will introduce the instruments, summarize the criteria for the subjects' inclusion and exclusion, and introduce the lens characteristics and fitting philosophy.

3.1 Instruments

The following instruments were used in this series of the studies: The Humphery Atlas™ corneal topographer to measure the anterior corneal curvature, the LADARWave™ CustomCornea Wavefront System to measure the ocular aberrations, the Humphery Optical Coherence Tomographer (OCT) to quantify the corneal and epithelial thickness, the Nikon auto-refractor to monitor the refraction change and the Orbscan II™ to detect the posterior corneal surface change in terms of the radius of the posterior best-fit sphere.

The repeatability of these devices was examined and will be reported in this chapter. Repeatability or precision of an instrument is the ability to give similar values on different occasions. Repeatability can be assessed by the limits of agreement (Bland and Altman, 1986), the standard deviation of the mean difference and the coefficient of repeatability. These parameters were used to assess the test versus retest measurements. The less the variability, the better the repeatability. Intraclass correlation coefficient (ICC) is a reliability coefficient calculated from variance estimates obtained through an analysis of variance. The maximum ICC value is 1.00 and the closer to the maximum 1.00, the stronger the reliability (Portney and Watkins, 2000).

3.1.1 Humphrey Atlas™ Corneal Topography

The Atlas corneal topographer (Atlas Mastervue, Humphrey Zeiss Instruments, San Leandro, California, U.S.A.) utilizes the reflected image (concentric illuminated rings) formed by the anterior corneal surface to measure the corneal radii or curvature. Topographical data along the horizontal meridian were collected over an 8 mm chord in 1 mm steps using the tangential power map from the computer display in this series of studies.

In order to evaluate the repeatability of corneal curvature using the Atlas ™ corneal topographer, twenty myopic subjects were enrolled. Their ages ranged from 19 to 35 years (mean± SD: 24.2± 3.6) and they were mostly female (13F:7M). Spherical ametropia ranged from –0.25 to – 5.25D, and corneal cylinder was less than 1.50D.

Two consecutive measurements were taken with the topographer on one eye only (randomly selected). The anterior corneal curvature of the centre and the mid-periphery (3mm from the centre horizontally) was measured using the tangential power map. The repeatability was assessed by 95% limits of agreement (LoA) (LoA= mean difference±1.96SD), the standard deviation of the mean difference, coefficient of repeatability (COR), and intraclass correlation coefficient (ICC).

The differences of corneal curvature against their means and the 95% limits of agreement (LoA) (mean difference ± 1.96SD of the difference) were plotted (Bland and Altman, 1986). Intraclass correlation coefficient (ICC) was calculated using the statistical software on the website of The Chinese University of Hong Kong (http://department.obg.cuhk.edu.hk/Researchsupport/IntraClass_correlation.asp).

The anterior corneal curvature from the test/re-test in the centre and mid-periphery was similar (as shown in Table 3-1). The standard deviations of the mean difference, coefficients of repeatability and intraclass coefficients of the corneal curvature for the centre

and mid-periphery are reported in Table 3-2. The limits of agreement of the corneal curvature for the centre and mid-periphery are in Figure 3-1.

Table 3-1. Test/re-test of corneal curvature (D) in the centre and mid-periphery

	Centre	**T3mm**	**N3mm**
Test (mean±SD)	44.14±1.41	42.48±1.40	41.07±1.18
Re-test (mean±SD)	44.12±1.41	42.51±1.33	40.88±1.23
P Values	0.713	0.164	0.670

Table 3-2. Repeatability of the corneal curvature in the centre and mid-periphery

	Centre	**T3mm**	**N3mm**
SD (D)	0.24	0.41	0.38
COR (D)	0.48	0.81	0.76
ICC	0.99	0.96	0.94

SD, Standard deviation of the difference (D). COR, Coefficient of Repeatability (D). ICC, Intraclass Coefficient.

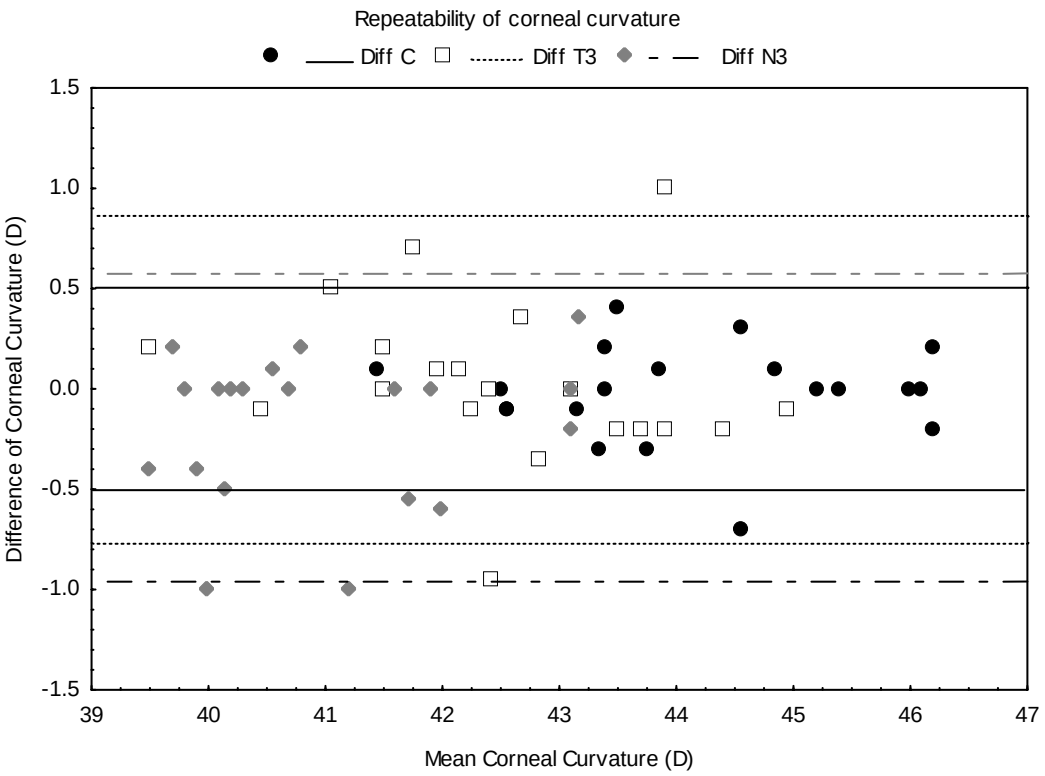

Figure 3-1 The limits of agreement of the central and mid-peripheral corneal curvature

The repeatability of the corneal curvature for the centre was very good in human *in vivo* and accorded with that reported in the previous studies (Jeandervin and Barr, 1998; Cho et al., 2002). The variability was approximately ±1% centrally, and ±2% mid-peripherally (95% confidence interval). In addition, the repeatability was slightly worse toward the mid-periphery, which is similar to the findings of Zadnik et al. (1995).

3.1.2 LADARWave™ CustomCornea Wavefront System

A Shack-Hartmann wavefront sensor (LADARWave™ CustomCornea Wavefront System, Alcon Laboratories, Inc. Orlando, Florida, U.S.A) was used to quantify aberrations using OSA standards. Calibration was performed each day using a specifically aberrated surface provided by the manufacturer. The centre of the pupil served as the alignment target, that is, the instrument's optical axis passed through the center of the subject's pupil, and the line of sight was coaxial with the Shack-Hartmann optical axis and fixation target (Applegate et al., 2000). Five measurements were acquired and the three most similar wavefront shapes were used to generate a composite result. The root-mean-squared (RMS) wavefront error (microns) was used to quantify optical quality. The measurements were taken through undilated pupils, and calculations were made using 4.5mm pupils. The measurements were taken in low room illumination.

Lower order aberrations including defocus (Z_2^0) and astigmatism ($Z_2^{\pm 2}$), are part of the Shack-Hartmann output that make up the clinical spherocylindrical refractive error. The total amount of the higher order aberrations (HOAs, including the sum of the 3rd to 6th order Zernike coefficients), third order coma ($Z_3^{\pm 1}$) and fourth order spherical aberration (Z_4^0, SA)

were analyzed (Thibos et al., 2002). Total aberration was the sum of higher and lower order aberrations.

In order to evaluate the repeatability of aberrations using LadarWave ^{TM}, ten healthy subjects were enrolled. Their ages ranged from 28 to 48 years (mean± SD: 36.1± 6.8) and they were mostly female (8F:2M). Spherical ametropia ranged from +1.75 to – 7.25D, and corneal cylinder was less than 1.25D.

Two independent measurements were taken with LadarWave ^{TM} for the right eye only. The aberrations, including total aberrations, defocus, astigmatism, overall HOA, coma and spherical aberrations, were measured. The repeatability was assessed by 95% limits of agreement (LoA) (LoA= mean difference±1.96SD), the standard deviations of the mean difference, coefficient of repeatability (COR), and intraclass coefficient (ICC), as described in section 3.1.1.

The test/re-test of the aberrations, including the total aberrations, defocus, astigmatism, higher order aberrations, coma, spherical aberration, and signed spherical aberrations, were similar (as showed in Table 3-3). The standard deviations of the mean difference, coefficients of repeatability and intraclass coefficients of the aberrations are presented in Table 3-4. The limits of agreement of the aberrations are plotted in Figures 3-2, 3-3, 3-4.

Table 3-3. Test/re-test of aberrations (mean±SD, um)

	TA	Defocus	Astigmatism	HOA	coma	SA	Signed SA
Test	1.936± 1.983	1.803± 2.057	0.39± 0.258	0.16± 0.035	0.063± 0.031	0.068± 0.034	0.04± 0.067
Re-test	1.91± 1.98	1.773± 2.053	0.384± 0.267	0.162± 0.047	0.061± 0.022	0.072± 0.031	0.04± 0.070
P value	0.191	0.248	0.509	0.785	0.751	0.343	1.000

Table 3-4. Repeatability of the aberrations

	TA	Defocus	Astigmatism	HOA	coma	SA	Signed SA
SD	0.058	0.077	0.028	0.023	0.019	0.013	0.013
COR	0.116	0.153	0.055	0.045	0.039	0.025	0.027
ICC	0.999	0.999	0.995	0.862	0.757	0.925	0.983

SD, Standard deviation of the difference (D). COR, Coefficient of Repeatability (D). ICC, Intraclass Coefficient. TA, total aberrations. HOA, higher order aberrations. SA, spherical aberrations.

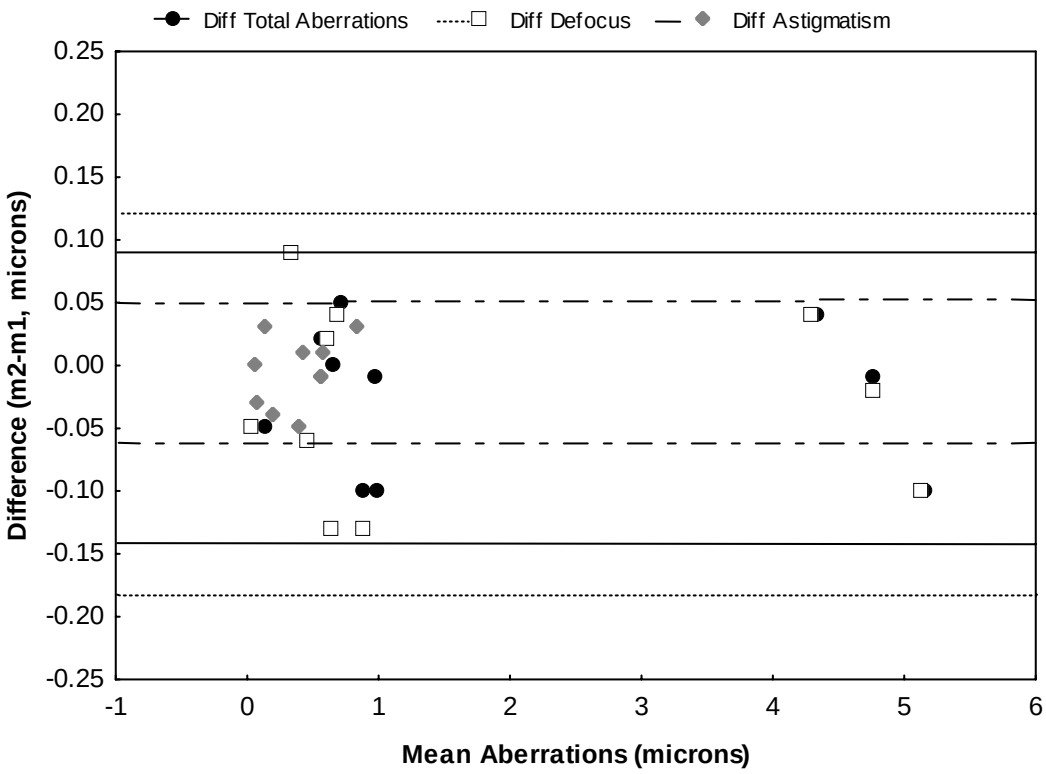

Figure 3-2. The limits of agreement of the total aberration, defocus and astigmatism.

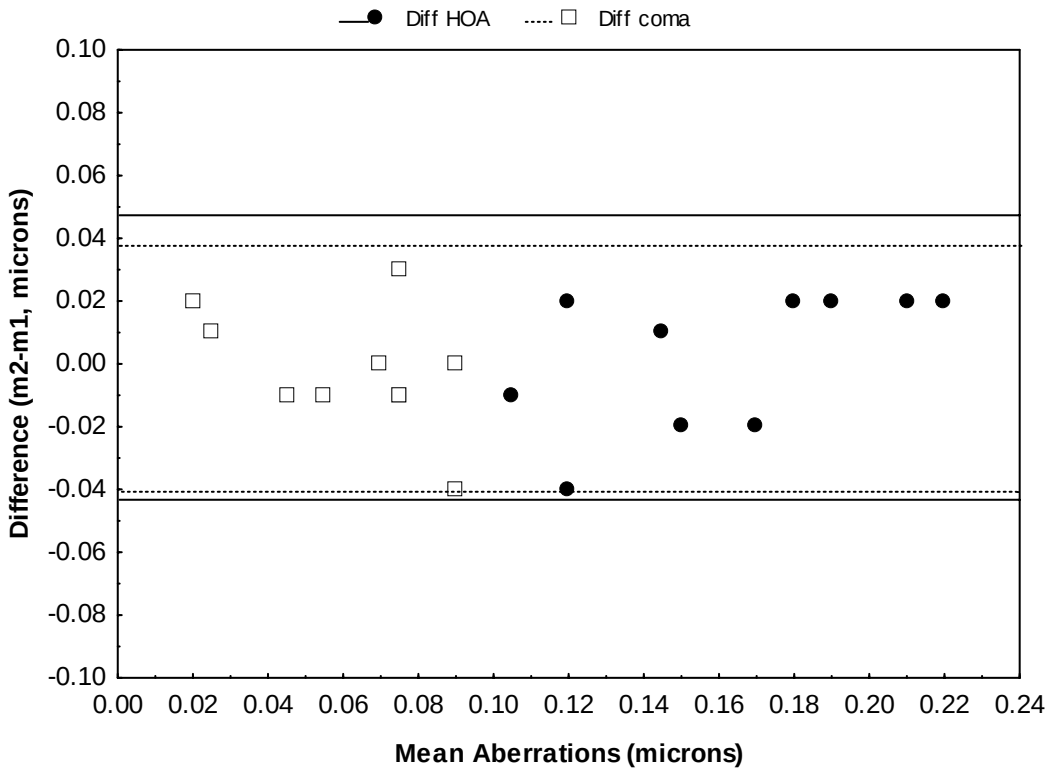

Figure 3-3. The limits of agreement of the HOAs and coma.

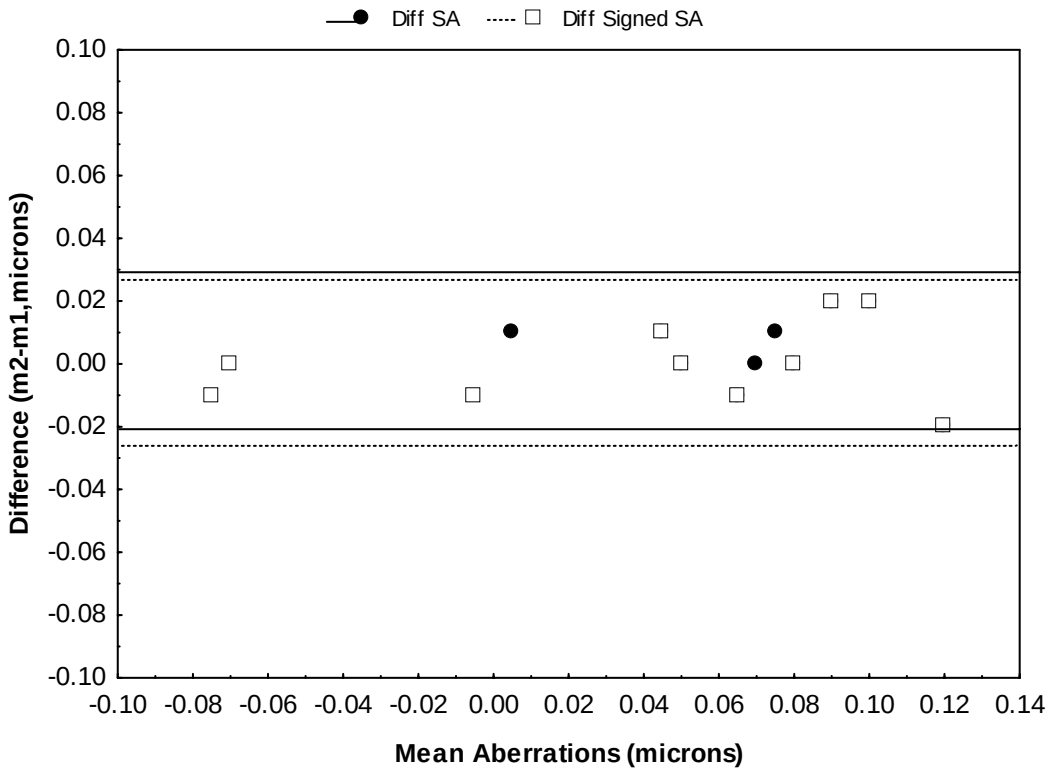

Figure 3-4. The limits of agreement of the SA and signed SA.

In general, the repeatability of the LadarWave™ aberration measurements, especially the total aberration, defocus and astigmatism, was very good in humans. The defocus term was comparable to a previous report (Porter et al., 2001). The repeatability of the HOA, coma and SA were slightly less than the lower order aberrations and total aberrations. But they are still reasonably repeatable. Although the repeatability of overall HOA and coma was relatively low, it is still better than that reported in previous studies (Mirshahi et al., 2003; Zadok et al., 2005).

3.1.3 Auto-refraction

Refractive error was measured using Nikon™ auto-refractor (NRK-8000; Nikon, Tokyo, Japan). Each autorefraction measurement was only used if the device's "confidence" metric was greater than 90%.

Three readings were taken and averaged for each measurement. For the repeatability of this device, 3 measures were taken and on the following day at the same time, 3 measures were again made in 20 subjects. There was no difference in sphere (or spherical equivalent) between the two days (both $p \geq 0.605$). The standard deviation of the mean difference of the measurement was 0.21D for the sphere and 0.37D for the spherical equivalent. The coefficient of repeatability was 0.42D and 0.74D for the sphere and spherical equivalent, respectively. The intraclass of coefficient (ICC) was 0.993 for the spherical refractive error and 0.990 for the spherical equivalent for three measurements. The 95% limits of agreement are illustrated in Figures 3-5 and 3-6.

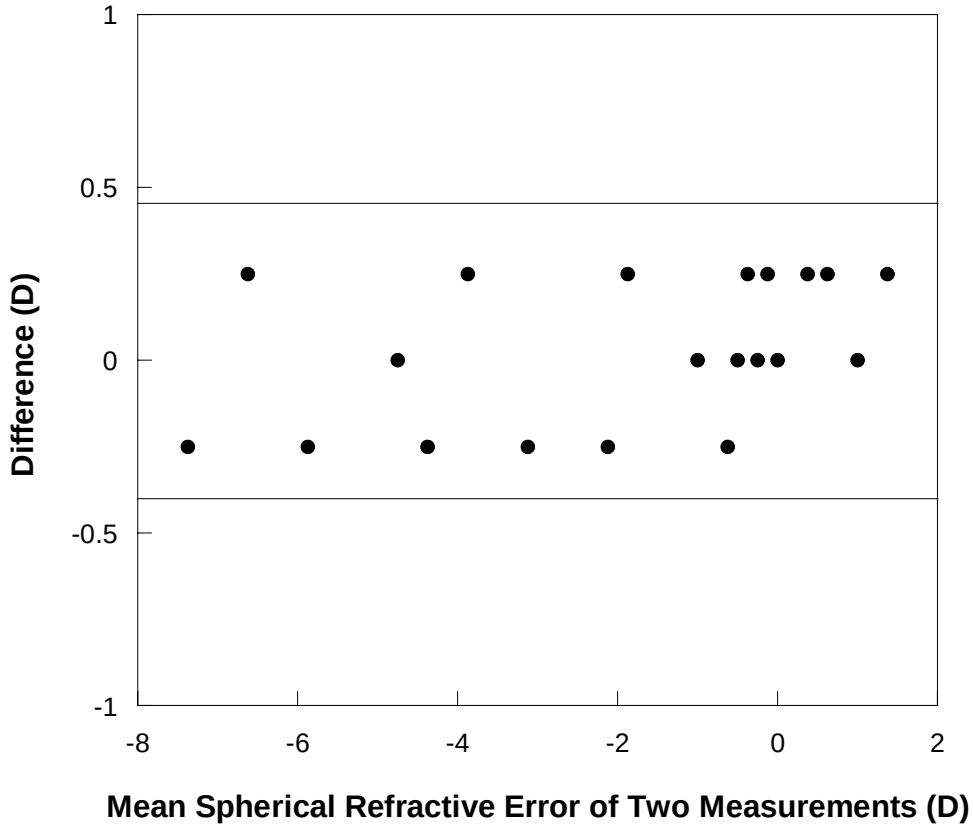

Figure 3-5. The limits of agreement of the spherical refractive error.

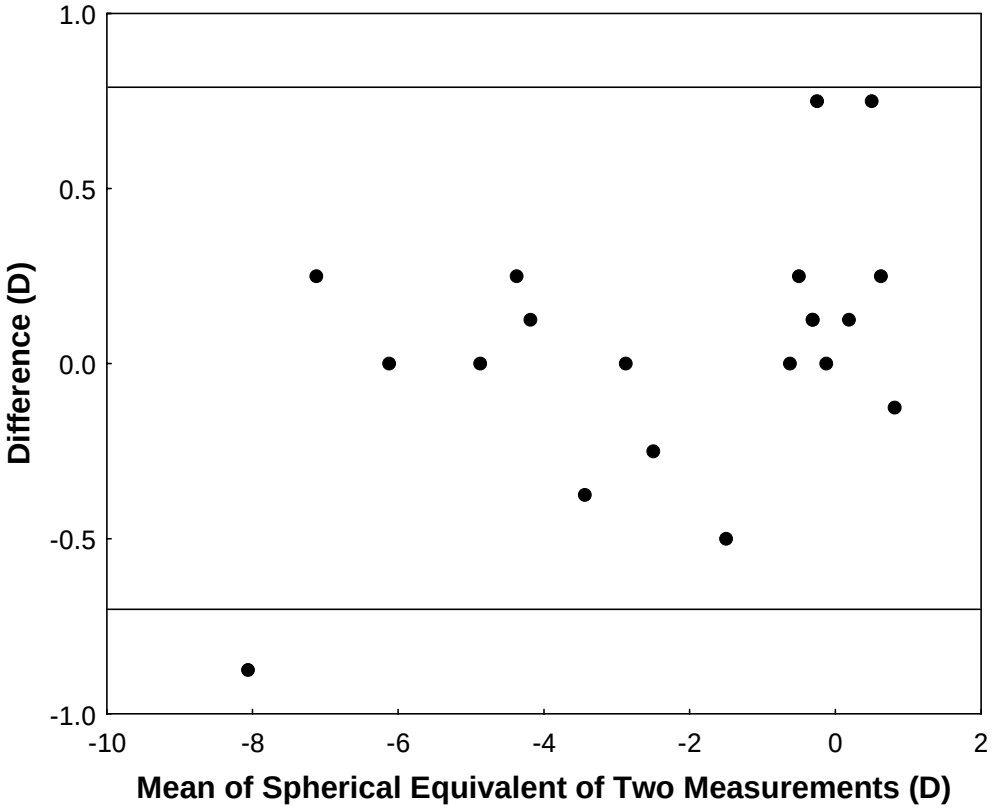

Figure 3-6. The limits of agreement of the spherical equivalent.

3.1.4 Orbscan II™ (Corneal Topography) System

Orbscan II™ was used to measure the radius of posterior best-fit sphere of the corneal posterior surface. Here, a best-fit sphere is the fit of the elevation data of the corneal surface using a sphere. The operation of the Orbscan II has been described previously (Liu et al., 1999; Iskander et al., 2001; Fakhry et al., 2002; Prisant et al., 2003).

Two consecutive measurements were taken with Orbscan II™ on one eye only (randomly selected) of twenty normal subjects. The radius of posterior best-fit sphere was measured. There was no difference in posterior best-fit sphere between two measurements (6.55±0.30mm vs. 6.55±0.28mm, mean±SD, t-test, p=0.766). The standard deviation of the mean difference of the measurement was 0.037mm. The coefficient of repeatability is 0.074mm. The intraclass of coefficient (ICC) was 0.992 for the posterior best-fit sphere radius of two measurements. The 95% limits of agreement (LoA) are illustrated in Figure 3-7.

In brief, the posterior best-fit sphere radius measurement was repeatable and was in agreement with a previous study (Moezzi, 2003).

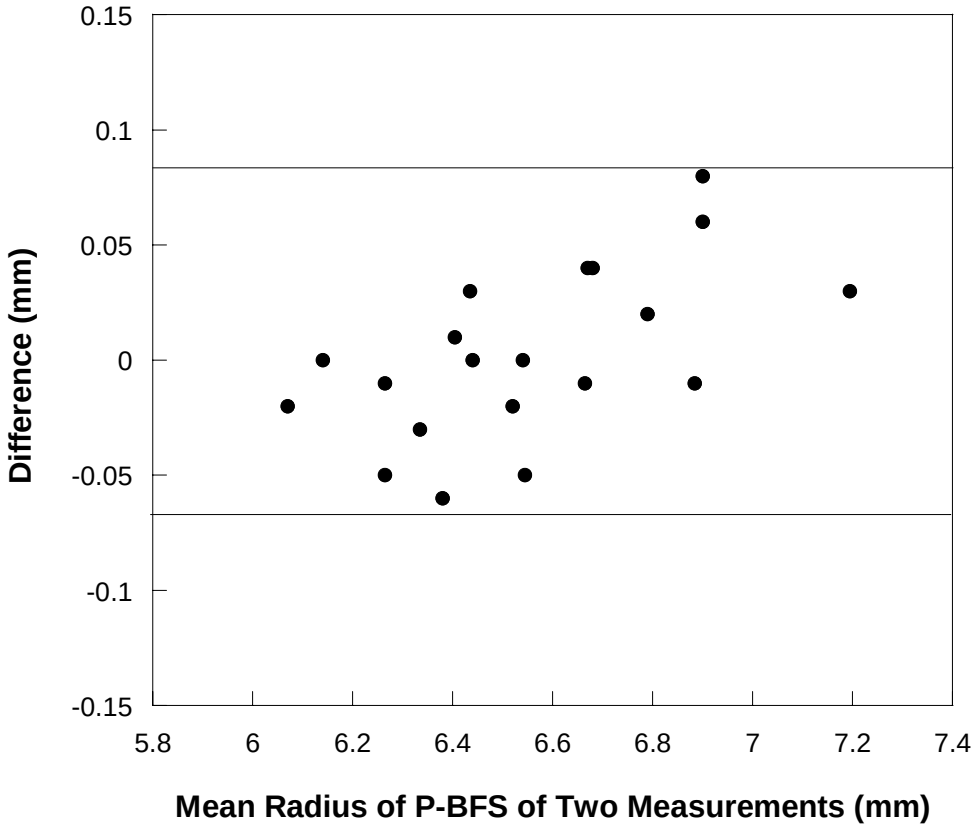

Figure 3-7. The limits of agreement of the radius of corneal posterior best-fit sphere.

3.1.5 Optical Coherence Tomography (OCT)

A Humphrey-Zeiss OCT (Humphrey system, CA, U.S.A) was used to obtain cross-sectional corneal images for one study only. OCT provides a reflectivity profile from which the corneal/epithelial thickness can be determined. The details of using OCT for corneal pachymetry have been described previously (Feng et al., 2001). A 1.13 mm scan length was used and the central 81 sagittal scans (of 100) were analyzed using custom software. A target with a series of fixation lights was used to control the eye position, so that meridional pachymetric data could be collected. Data along the meridian in the temporal cornea including the centre were collected over a 4.5-5.0 mm chord in approximately 1 mm steps. Only the central and mid-peripheral (2-3mm from the center) data were reported herein.

Since a recent experiment of repeatability of corneal and epithelial OCT thickness measures from our lab has recently been reported (Sin and Simpson, 2006), it was not redone in this dissertation.

3.2 Subjects

All subjects who were eligible to be involved in the study according to the inclusion and exclusion criteria were recruited for this study. Informed consent was obtained from all participants prior to enrolment in the study. This work received approval from Office of Research Ethics at the University of Waterloo (Waterloo, Ontario, Canada). All subjects were treated in accordance with the tenets of the Declaration of Helsinki (Ethical Principles for Medical Research Involving Human Subjects adopted by the 18th World Medical Association General Assembly Helsinki, Finland, June 1964; Forster et al., 2001). The details of each group of subjects for each study are listed in the relevant chapter

3.2.1 Inclusion Criteria

The participant was eligible for entry in the study if s/he:

1. Had undergone an oculo-visual examination in the last 2 years.
2. Was at least 18 years old and had full legal capacity to volunteer.
3. Had read and understood the Information Consent Letter.
4. Was willing and able to follow participant instructions.
5. Had sphere refractive error range of –2.00 to – 5.00D and corneal cyl < 1.50D (for CRT1, CRT2 and CRTHDK studies).
6. Was a non lens wearer or soft contact lens wearer.
7. Had not worn RGP's previously.
8. Was correctable through sphero/cylindrical refraction to 6/6 (20/20) or better in each eye.
9. Had corneal eccentricity between 0.4 and 0.8 measured by corneal topography
10. Had clear cornea.

3.2.2 Exclusion Criteria

The participant was ineligible for entry into the study if the s/he:

1. Had any systemic disease affecting ocular health.
2. Was using any systemic or topical medications that would affect ocular health.
3. Had an active ocular disease.
4. Had any clinically significant lid or conjunctival abnormalities, neovascularization, corneal scars or corneal opacities.
5. Had limbal or bulbar injection or corneal staining that, in the investigator's opinion, was clinically significant.
6. Had corneal distortion resulting from soft contact lens wear.
7. Was aphakic.
8. Had undergone surgery or an eye injury within eight weeks prior to enrolment for this study.
9. Was participating in any other type of research study.

3.3 Lenses

Following are the lens fitting philosophy for corneal refractive therapy for myopia and hyperopia (CRT® and CRT®H), respectively. The lens material, physical characteristics and parameters are reported in the relevant chapter. The lens was ordered for each eye, once an acceptable fit was obtained with the trial lens.

3.3.1 CRT® Lens Design and Fitting

"The CRT lens is designed to have congruent anterior and posterior surfaces (or harmonic surfaces) each consisting of three zones: the central spherical optic zone (OZ, 6mm

width), a mathematically designed sigmoid corneal proximity Return Zone (RZ, 1mm width, 400μm to 575 μm depth) and a non-curving Landing Zone (LZ, 1mm width, landing zone angle from 31^{o} to 36^{o}). The lens design also includes a convex elliptical edge terminus smoothly joining the anterior and posterior surfaces" (Figure 3-8) (CRT summary at http://www.fda.gov/cdrh/pdf/p870024s043.html.).

Each CRT® lens was fit using the Paragon slide rule. The flat K reading and refraction (or a fixed –3.50D for the STOK study only to match the 3.50D for CRTH lens in the STOK study) were used to calculate the base curve, return zone depth and landing zone angle for the initial lens. Lenses were adjusted to achieve centration, approximately 4mm of central touch, proper (1-1.5mm width) mid-peripheral clearance, proper (1-1.5mm width) peripheral alignment and edge clearance (Figure 3-9), according to the manufacturer's fitting guideline.

In the CRT1 study, a control lens was fit on flat K of the control eye.

3.3.2 CRTH® Lens Design and Fitting

The structure of the CRT®H lens is similar to the CRT® lens with following exception: The central spherical optic zone (OZ) is smaller with 5mm width and the return zone depth (RZD) is deeper, ranging between 575 and 750 μm.

CRT®H lens fit was based on that for myopia using the Paragon slide rule. The flat K reading and a refraction of –0.25D (the minimum value on the slide rule) were used to calculate the base curve, return zone depth and landing zone angle. The selected base curve was 0.7 mm (3.50D) steeper than the flat K, the depth of mid-peripheral return zone was 175 μm deeper than the calculated return zone depth (due to the small back optic zone diameter used for hyperopia, i.e. 5mm, rather than 6mm in the trial lens to counter the former looser

lens/corneal fitting relationship), and the landing zone angle was kept the same as the myopia fit. The lenses were adjusted to achieve centration, appropriate apical clearance (2-4 mm wide), para-central touch ("knee"), proper mid-peripheral pooling, peripheral alignment and edge clearance (Figure 3-10).

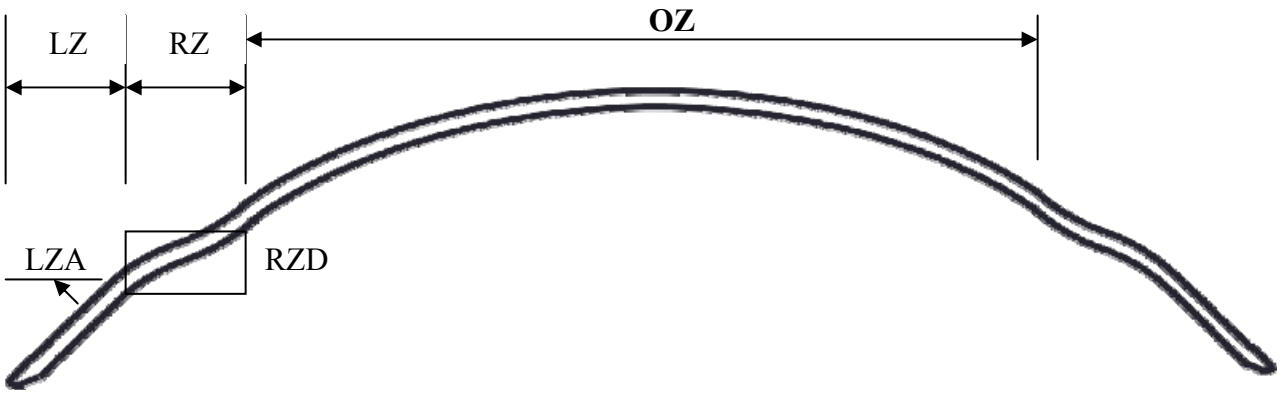

Figure 3-8. Schematic of CRT lens (Courtesy of Paragon Vision Sciences). OZ, Optic Zone; RZ, Return Zone; RZD, Return Zone Depth; LZ, Landing Zone; LZA, Landing Zone Angle.

Figure 3-9. Typical fluorescein pattern of CRT for myopia.

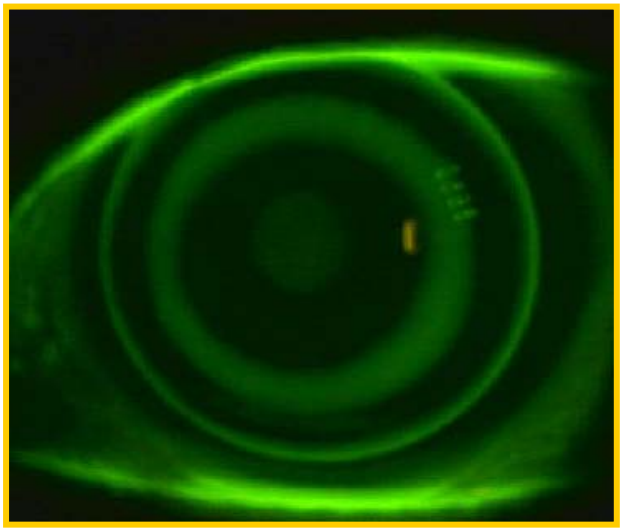

Figure 3-10. Typical fluorescein pattern of CRT for hyperopia

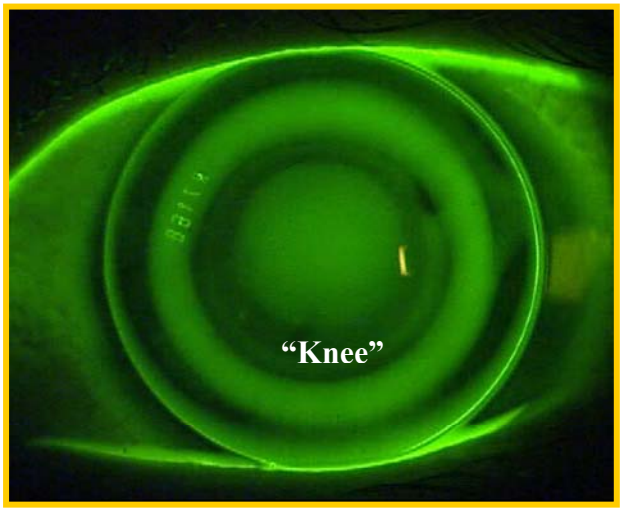

Chapter 4 (CRT1 study)

Corneal Shape after One Night of Corneal Refractive Therapy™ for Myopia

4.1 Abstract

Purpose: To determine the efficacy of Corneal Refractive Therapy for myopia (CRT®) by examining the myopia correction and corneal shape change after one night of CRT® lens wear.

Methods: Twenty participants wore CRT® HDS 100 contact lenses in one eye and control lenses in the contralateral eye (randomly selected) for one night while sleeping. Corneal topography and refractive error were measured using an Atlas™ corneal topographer and Nikon™ auto-refractor the night prior to lens insertion, immediately after lens removal on the following morning and at 20 and 60 minutes and 3, 6 and 12 hours later. Topographical changes were measured over an 8mm chord in 1mm steps.

Results: There were significant differences in corneal curvature between the two lenses ($p=0.001$) and at various corneal locations ($p<0.001$). The central cornea was flattened by 1.49±0.74D and steepened in the mid-periphery by 1.96±1.57D for the CRT lens-wearing eyes (all $p<0.001$) immediately after lens removal, whereas there was no location effect in the control eyes ($p=0.283$). The corneal shape regressed towards baseline ($p<0.001$ for the centre and $p=0.020$ for the mid-periphery), but did not return to baseline after 12 hours without lens wear ($p<0.001$). After one night of lens wear, myopia reduced from -3.34

±1.24D to -2.23±1.04D for the CRT lens wearing eyes (t-test, $p<0.001$) and no change in the control eyes (t-test, $p=0.196$).

Conclusions: After one night of lens wear, the CRT appears to be effective for myopic correction by flattening the central cornea and steepening the mid-periphery, whereas little change was found in the control eyes. The corneal shape change and refractive error did not return to baseline by 12 hours, indicating that the change in shape can be maintained.

4.2 Introduction

Orthokeratology has been used to correct the refractive error since 1960s (Jessen, 1962). Previous studies using traditional spherical lens design showed that the predictability and efficacy of the orthokeratology were poor and it was also time consuming (Kerns, 1978; Tredici, 1979; Binder et al., 1980; Polse et al., 1983b; Coon, 1984). Lens upward decentration and induced astigmatism frequently occurred (Kerns, 1976c; 1977a). With better understanding of the lens and cornea relationship, and the importance of lens centration to achieve success (Kerns, 1978), a reverse geometric curve (steeper secondary curve) was proposed by Stoyan and others (Phillips, 1995). This lens could reshape the cornea and change the refractive error more rapidly (Wlodyga, 1989).

Beside the introduction of the reverse geometry lens design, novel corneal topography measurement was another advance which assisted in selecting the appropriate candidates and monitoring the corneal shape change after the corneal reshaping, and also providing great details of the lens and cornea relationship. In addition, since overnight lens wear has numerous advantages in rigid gas permeable materials (Lui et al., 2000), high oxygen permeable (Dk) materials have been used to enable the overnight lens wear modality possible (Holden and Mertz, 1984).

Paragon Corneal Refractive Therapy (CRT®) lens for overnight corneal reshaping was approved by FDA (U.S.A) in June 2002. In this study, we examined the effects of CRT lens and conventional alignment rigid lens on the corneal shape change and myopic correction, so as to demonstrate the efficacy of CRT lens in non-surgical corneal reshaping.

4.3 Materials and Methods

4.3.1 Subjects

Twenty myopic subjects participated in this study. Their ages ranged from 21 to 31 years (mean± SD: 24.6±2.6) and they were mostly female (16F:4M). Spherical ametropia ranged from –1.00 to –5.75D, and corneal cylinder was less than 1.50D.

Refractive error and corneal curvature from keratometry of the 20 subjects are summarized in Table 4-1.

4.3.2 Lens Characteristics and Fitting

The RGP material used for both experimental and control lenses was Paragon HDS 100 (a 100 DK fluorosilicone acrylate material). Boston Simplicity™ (Simplicity; Bausch & Lomb, Rochester, NY) was used to condition the lenses prior to insertion. A summary of the experimental (CRT) and control lens parameters that were prescribed is found in Table 4-2.

CRT lens fitting can be found in Methods Chapter 3.

The number of the lens used in the CRT lens-wearing eyes was 2.65±1.50 (from 1 to 7 lenses) and 1.37±0.68 (from 1 to 3 lenses) for the control lens-wearing eyes on average.

4.3.3 Study Design

This was a double masked randomized controlled study. Paragon CRT lenses were fit on one eye of 20 myopes and the alignment lens in the contralateral eye (eye randomly selected). The examiner and subjects were masked to which eye wore which lens.

Table 4-1. Ocular Parameters (mean±SD)

	Experimental	Control	P values
Refractive Error			
Sphere	-3.11 ± 1.24	-3.09± 1.12	0.832
Cylinder	-0.46 ± 0.22	-0.49 ± 0.31	0.716
Auto-Keratometry			
Flat K	43.92 ± 1.74 (39.25 to 46.25)	43.82 ± 1.65 (39.62 to 46.25)	0.188
Cyl	-0.72 ± 0.43	-0.75 ± 0.48	0.776
Eccentricity Values	0.47 ± 0.08	0.46 ± 0.08	0.714

Table 4-2. Nominal Lens Parameters and Characteristics

	BOZR (mm)	RZD (μm)	LZA(degree)	TD (mm)	CT (mm)	Curves
Experimental	8.45 ± 0.50 (7.7 to 9.9)	540 ± 17 (525 to 575)	33.55º ± 0.83 (31 to 34)	10.50	0.15	tetracurve
Control	7.68 ± 0.83 (7.4 to 8.5)	n/a	n/a	10.00	0.15	tricurve

BOZR, Back Optic Zone Radius. RZD, Return Zone Diameter. LZA, Landing Zone Angle. TD, Total Diameter. CT, Center Thickness.

4.3.4 Procedures

Corneal topography and refractive error were measured at baseline on the night prior to the lens insertion. After the lenses had settled appropriately, participants retired in our laboratory at approximately 10 p.m. and were awakened at 7 a.m. the next morning. Measurements were repeated immediately after lens removal and 20 minutes and 1, 3, 6, 12 hours later on the following day.

4.3.5 Measurements

4.3.5.1 Corneal Topography

See Methods Chapter 3.

4.3.5.2 Auto-refraction

See Methods Chapter 3.

4.3.6 Statistical Analysis

Repeated measures analysis of variance (RM-ANOVA) was used to examine the main effects of the lens type, time and location in the corneal curvature and refractive error if applicable. Tukey Honestly Significantly Different (HSD) post hoc tests were used to determine whether there were differences in corneal curvature over time and at different locations. Planned paired t-tests were used to test the difference between two lens groups at baseline or the treatment effect after lens wear compared to the baseline. Differences were considered statistically significant when the likelihood of a type I error was ≤ 0.05. Data analysis was conducted using STATISTICA 6.0 (StatSoft Inc., Tulsa, Oklahoma, U.S.A.).

4.4 Results

A typical fluorescein pattern of CRT for myopia and a corneal topographic map after CRT lens wear is in Figure 4-1.

4.4.1 Corneal Topography

Figure 4-2 shows that averaged over location and time, there were statistical differences in horizontal corneal curvature between the two lenses wearing eyes (RM-ANOVA, $F_{(1, 19)}$=14.950, p=0.001) and at various corneal locations (RM-ANOVA, $F_{(8, 152)}$=16.122, p<0.001). The central cornea flattened from baseline by 1.49±0.74D immediately after the lens removal and 0.65±0.58D by 12 hours (t-tests, all p<0.001). The mid-periphery (3mm from centre) steepened from baseline by 1.96±1.57D immediately after the lens removal and 1.14±0.74D by 12 hours in the CRT lens-wearing eyes (t-tests, all p<0.001). There was no location effect in the control eyes (RM-ANOVA, $F_{(8, 152)}$=1.235, p=0.283). In the CRT lens-wearing eyes, the central corneal flattening and the mid-peripheral steepening regressed over time (RM-ANOVA, $F_{(5, 95)}$=36.759, p<0.001 for the centre and $F_{(5, 95)}$=2.830, p=0.020 for the mid-periphery) and did not recover to baseline by 12 hours (56.4% recovery centrally and 41.7% recovery mid-peripherally, all p<0.001).

4.4.2 Refractive Error (Spherical Equivalent)

Figure 4-3 shows that there was no difference in refractive error (spherical equivalent) between CRT and control lens-wearing eyes at baseline (t-test, p=0.914). After one night of lens wear, the myopia was reduced from -3.34±1.24D to -2.23±1.04D for the CRT lens-wearing eyes (t-test, p<0.001) and not in the control eyes (t-test, p=0.196). The refractive error regressed over time, but did not return to baseline by 12 hours in CRT lens-wearing eyes (post hoc tests, p<0.001). There was no significant difference in astigmatism between

CRT and control lens wearing eyes (RM-ANOVA, $F_{(1, 19)}$=0.053, p=0.821) over time (RM-ANOVA, $F_{(6, 114)}$=0.950, p=0.462).

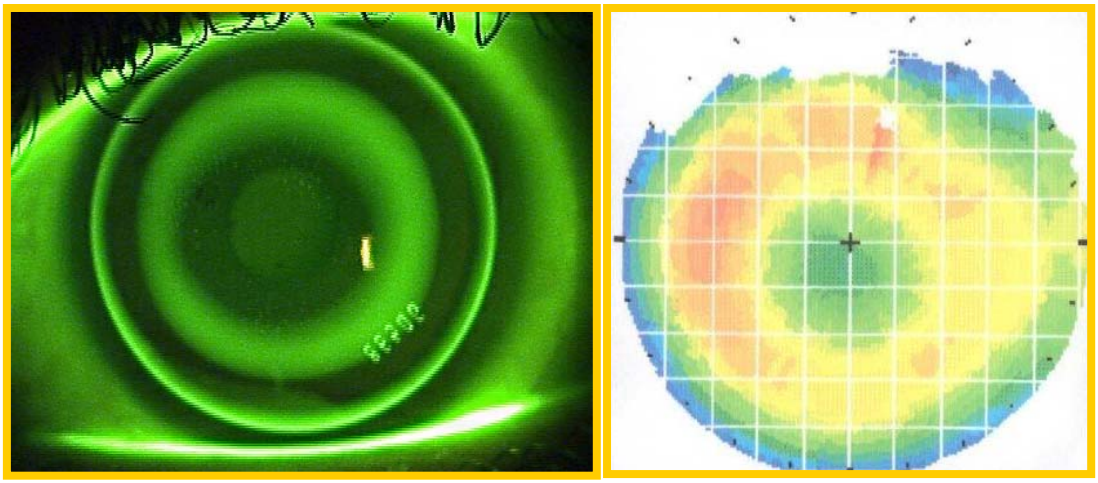

Figure 4-1. A typical fluorescein pattern of CRT for myopia (left panel) and a corneal topographic map after CRT lens wear (right panel). The central touch and the mid-peripheral pooling in the fluorescein pattern correspond to the central flattening (green) and mid-peripheral steepening (yellow and red) in the corneal topographic map.

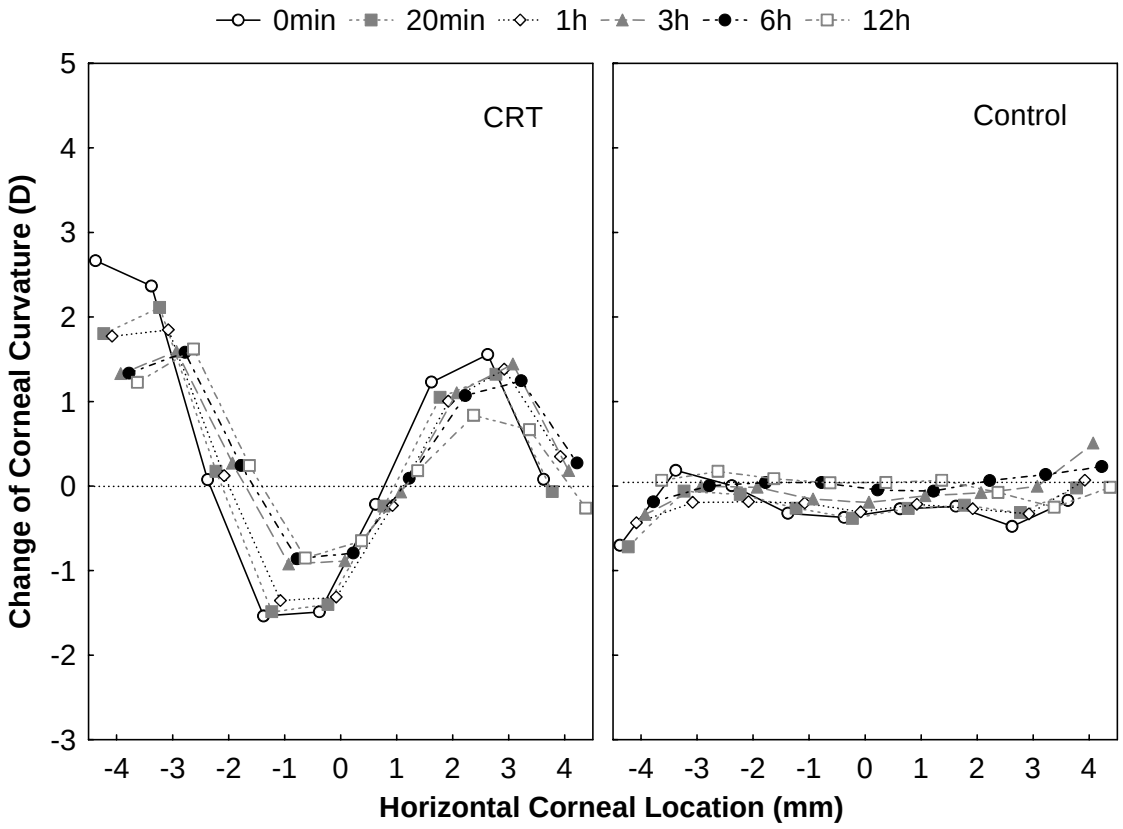

Figure 4-2. The change of horizontal corneal curvature (D) from baseline in the experimental and control eyes over time. Positive x-axis numbers refer to nasal corneal positions and negative to temporal corneal positions.

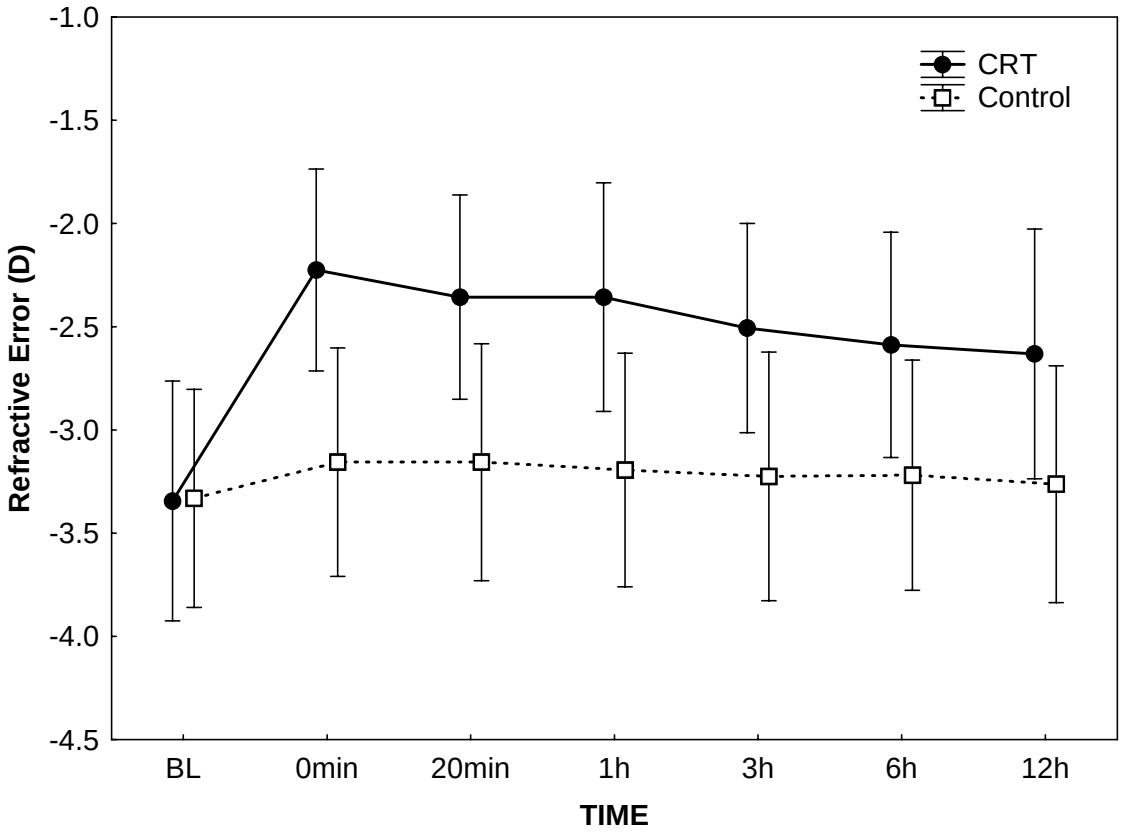

Figure 4-3. Refractive error in the experimental and control eyes over time. Error bars: 95% confidence intervals.

4.5 Discussion

To assess a new therapy, the efficacy and predictability are of concern for both the practitioners and the patients. After a single night of CRT lens wear, the central cornea flattened (1.49D) and mid-periphery steepened (1.96D) in the CRT lens-wearing eyes, but it did not change in the control eyes (Figure 4-2). Accordingly, myopia was corrected by 1.10D in CRT lens-wearing eyes, and it did not change in the control eyes (Figure 4-3). Our treatment effect was greater and quicker than a previous overnight study (Nichols et al., 2000). This difference may be due to different lenses used. Therefore, myopia correction using CRT lenses was quite predictable and rapid, in agreement with one night result of others (Alharbi and Swarbrick, 2003; Sridharan and Swarbrick, 2003). However, two other overnight studies were not comparable to ours due to different protocols used (for example, different times taken before data were collected, Mountford, 1997; Rah et al., 2002).

The significant differences between the experimental and control eyes in the corneal curvature and refractive changes might be due to the different lens designs. The control lens was fit on alignment to the corneal anterior surface. However, the CRT lens was fit flatter than the central corneal curvature and also steeper in the mid-periphery. Since the lens and corneal fitting relationship was different in two eyes, different corneal shape and refractive changes were found.

Since the topographical corneal curvature changes were similar to the topographical corneal/epithelial swelling after one night of CRT lens wear using OCT (Wang et al., 2003), it is reasonable to assume that the corneal/epithelial swelling might be involved in the corneal reshaping, resulting in myopic correction. After corneal reshaping, the corneal thickness changes have been reported (Swarbrick et al., 1998; Nichols et al., 2000; Wang et

al., 2003). In addition, investigators (Swarbrick et al., 1998; Wang et al., 2003) proposed that the epithelial redistribution might also play an important role in the corneal reshaping since the corneal epithelium is movable under the mechanical stress (Jones and Jones, 1995; Pritchard et al., 2000; Alharbi and Swarbrick, 2003).

As illustrated in Figures 4-2 and 4-3, the control corneal anterior surface and the refraction did not change. Similarly, there was no significant change in epithelial thickness in the control eyes. However, the central corneal swelling was greater than the CRT lens-wearing eyes and its horizontal corneal swelling profile differed from that of CRT lens wearing eyes (Wang et al., 2003). This parallel lack of change of corneal shape/refraction, and epithelium indirectly point to corneal epithelial thickness change taking part in the corneal reshaping. On the other hand, the role of corneal swelling in corneal reshaping needs further investigation, since the corneal swelling in CRT and control lens-wearing eyes recovered to baseline after 3 hours (Wang et al., 2003) and the corneal shape change and refractive error change did not returned to baseline after 12 hours.

In summary, after one night of lens wear, CRT appears to be effective for myopic correction by flattening the central cornea and steepening the mid-periphery, whereas little change was found in the control eyes. The corneal shape and refractive changes did not return to baseline by 12 hours, indicating that the change in shape can be maintained.

Chapter 5 (CRTH study)

Corneal Shape and Optical Performance after One Night of Corneal Refractive Therapy® for Hyperopia

This paper was accepted by Optometry and Vision Science (2006). The coauthors, Drs. Trefford Simpson, Luigina Sorbara and Desmond Fonn, permit the microfilming of this thesis.

5.1 Abstract

Purpose: To investigate corneal shape and optical performance after one night of Corneal Refractive Therapy for hyperopia (CRT®H).

Methods: Twenty subjects (spherical equivalent: -2.14 ±2.54 D) were fit with a Paragon CRT®H lens (Dk=100) on one eye (selected randomly). The other eye served as the control. Aberrations, refractive error and corneal topography at various locations along the horizontal meridian were measured at baseline prior to lens insertion, and immediately after lens removal and at 1, 3, 6, 12 and 28 hours later. Root mean square wavefront errors were measured using a 4.5mm pupil size.

Results: After one night of CRT®H lens wear, the central cornea steepened and para-central region flattened in the experimental eyes ($p<0.001$), whereas no significant location effect was found in the control eyes ($p=0.139$). Refractive error (mean ± SE) changed by 1.23 ± 0.21 D ($p<0.001$). The defocus increased by 0.58 ± 0.09 μm ($p<0.001$), respectively. Higher order aberrations, coma and spherical aberrations increased by factors of 2.69, 2.58 and 4.07, respectively (all $p<0.001$). Spherical aberrations shifted from positive to negative.

Astigmatism did not change over time ($p=0.771$). All parameters returned to baseline by 28 hours (all $p \geq 0.808$). Aberrations and refractive error did not change in the control eyes (all $p \geq 0.082$).

Conclusion: The CRT®H lens steepens the central cornea and flattens the para-central region which alters the ametropia by inducing a myopic shift. It appears to be effective for correcting hyperopia and also is reversible.

5.2 Introduction

Corneal Refractive Therapy (CRT®), also known as orthokeratology or non-surgical corneal reshaping, is used to correct refractive error by altering the corneal shape with rigid contact lenses. Recently, rapid improvement in technology and understanding of the modality has renewed clinical interests in Orthokeratology (Dave and Ruston, 1998; Swarbrick et al., 1998; Nichols et al., 2000; Sridharan and Swarbrick, 2003; Alharbi and Swarbrick, 2003; Tahhan et al., 2003; Wang et al., 2003; Sorbara et al., 2005). The advent of high Dk (oxygen permeability) materials, reverse geometry multicurve lens designs, and novel corneal topographers partially account for this renewed interest in orthokeratology (Lui et al., 2000). It has been demonstrated by a number of groups that corneal reshaping can correct myopia by flattening the central cornea and steepening the mid-periphery (Dave and Ruston, 1998; Swarbrick et al., 1998; Tahhan et al., 2003; Sridharan and Swarbrick, 2003; Alharbi and Swarbrick, 2003; Nichols et al., 2000; Lu et al., 2003; Sorbara et al., 2005). Corneal reshaping lenses may also correct hyperopia by steepening the central cornea and flattening the mid-periphery. In 1962, Jessen proposed that the techniques of "orthofocus" could reduce hyperopia by attempting to mold the cornea with a contact lens, which was fit steeper (Jessen, 1962). Other attempts (Sarver and Harris, 1967; Hill and Rengstorff, 1974) have been made to correct hyperopia without clear conclusions, but recently, Swarbrick et al. (2004) reported that steeply fitted rigid contact lenses could induce corneal steepening and myopic shifts in refraction over a 4-hour period.

Optical quality is perhaps most sensitively measured by wavefront sensors that quantify ocular aberrations. Although the optical performance after corneal refractive surgery (Oshika et al., 1999; Marcos et al., 2001; Marcos, 2001; Moreno-Barriuso et al., 2001;

Chalita and Krueger, 2004; Llorente et al., 2004b) and after myopic non-surgical corneal reshaping (Joslin et al., 2003; Hiraoka et al., 2005; Berntsen et al., 2005) has been monitored, the change in optical characteristics over time after overnight hyperopic corneal reshaping has not yet been determined. In this study, therefore, we investigated the dynamic variation of corneal shape and optical performance after one night of Corneal Refractive Therapy for hyperopia (CRT®H). The diurnal variation of the optical performance in the control eyes without lens wear was also determined.

5.3 Materials and Methods

5.3.1 Subjects

Twenty ametropes participated in this study after a screening appointment for eligibility (15 women and 5 men; mean age, 30.1±7.5 years; range, 22 – 48). Spherical ametropia ranged from + 1.25 to - 7.00D, and the cylinder was - 0.25 to - 1.50D. The respective number of hyperopic/emmetropic/ myopic participants was 4/2/14. The larger number of the myopes enrolled was due to the higher proportion of myopes in the recruitment pool.

5.3.2 Lens Characteristics and Fitting

The rigid gas permeable material used for CRT®H lens was Paragon HDS 100 (fluorosilicone acrylate). A summary of the lens characteristics and parameters is found in Table 5-1.

CRT®H lens fitting can be found in Methods Chapter 3.

The number of the lens used in the CRTH lens-wearing eyes was 2.45±1.70 (from 1 to 8 lenses) on average.

Table 5-1. Nominal Lens Characteristics and Parameters

Dk (cm^2/sec).(mlO_2/ ml.mmHg)	**CT** (mm)	**TD** (mm)	**BOZD** (mm)	**Power** (D)	**BOZR**(±SD) (mm)	**RZD** (±SD) (microns)	**LZA**(±SD) (degrees)
100×10^{-11}	0.15	10.5	5.0	-0.50	7.19±0.32 (6.7 to 7.7)	656±38 (600 to 725)	34±1 (31 to 36)

Dk, Oxygen permeability. CT, Centre Thickness. TD, Total Diameter. BOZD, Back Optic Zone Diameter. BOZR, Back Optic Zone Radius. RZD, Return Zone Depth. LZA, Landing Zone Angle.

5.3.3 Study Design

This was a single masked randomized controlled study. Paragon CRT®H lenses (Paragon Vision Sciences, Mesa, AZ) were fit on one eye of 20 ametropes (eyes randomly selected). The other eye served as the control. A designated investigator (LS) fit the lens, and the examiner (FL) was masked as to which was the experimental eye. During the study visit, a technician placed the lens on the eye and removed the lens in the morning in the lab.

5.3.4 Procedures

Corneal topography, root mean squared (RMS) wavefront errors and refractive error were measured at baseline, the night prior to lens insertion. After the lenses were correctly positioned on the eye, participants retired in the laboratory at approximately 10 p.m. and were awakened at 7 a.m. the next morning. The measurements were repeated immediately after lens removal, and 1, 3, 6, 12 and 28 hours later.

5.3.5 Measurements

5.3.5.1 Corneal Topography

See Methods Chapter 3.

5.3.5.2 Aberrations

See Methods Chapter 3.

5.3.5.3 Autorefraction

See Methods Chapter 3.

5.3.6 Statistical Analysis

Two- or three-way repeated measures analysis of variance (RM-ANOVA) was used for overall effects and Tukey Honestly Significantly Different post hoc tests were used to

determine the difference over time in aberrations, refractive error and corneal curvature. Planned paired t-tests were used to determine the difference in baseline aberrations and refractive error between experimental and control eyes and to determine the difference in aberrations, refractive error and corneal curvature after CRT®H lens wear relative to baseline. Polynomial regression was used to quantify the change of the horizontal corneal curvature from baseline immediately after the lens removal. Pearson correlation was used to determine the association between the changes of signed SA and refractive error. Significant difference was set at $p \leq 0.05$. Data analysis was conducted using STATISTICA 6.0 (StatSoft Inc., Tulsa, Oklahoma, U.S.A.) and bivariate regressions (York, 1966) were obtained using ProFit 5.01a (QuantumSoft, Zürich, Switzerland). The data are presented as mean±SE in the text.

5.4 Results

The refractive error and corneal curvature (auto-keratometry) baseline measurements are listed in Tables 2 and 3. There were no significant differences between the experimental and control eyes (t-test, all $p \geq 0.111$).

A typical fluorescein pattern of CRT for hyperopia and a corneal topographic map after CRTH lens wear is in Figure 5-1.

5.4.1 Corneal Topography

There was no difference in corneal curvature between experimental and control eyes at baseline (RM-ANOVA, $F_{(1,19)}=0.101$, $p=0.754$). After one night of CRT®H lens wear, the central cornea steepened by 0.85±0.15D (mean±SE) and the para-central region flattened by 1.34±0.19D from baseline (averaged temporal and nasal sides) in experimental eyes (RM-ANOVA, $F_{(8,152)}=6.823$, $p<0.001$, Figure 5-2). The central corneal steepening and para-

central corneal flattening regressed over time (RM-ANOVA, $F_{(5,95)}$=16.63 - 20.24, both p≤0.001) and recovered by 28 hours (post hoc test, both p≥0.830). No significant location effect was found in control eyes (RM-ANOVA, $F_{(8, 152)}$=1.568, p=0.139). However, the control cornea was flatter immediately after eye opening (0.18±0.05D vs. 0.38±0.10D for the centre and para-central region) and at 1 hour visit compared to baseline (t-test, all p≤0.031), but this flattening disappeared by 3 hours (t-test, all p≥0.130).

The profile of the change of horizontal corneal curvature in experimental and control eyes was different immediately after the lens removal (Figure 5-3). To characterise these differences, polynomial regression was used to quantify the change of corneal curvature from baseline versus corneal locations. Polynomial analysis showed that only a parabolic component in control eyes was different from zero (p<0.001). However, in experimental eyes, there were linear, quadratic, cubic, quartic and quintic components (all p≤0.005). The functions and correlation coefficients are:

$Y_{EXP}=0.651+(-0.885)*x+(-0.407)*x^2+(0.202)*x^3+(0.024)*x^4+(-0.009)*x^5$, R=0.99;

$Y_{CON}=(-0.136)+(-0.038)*x^2$, R =0.98.

5.4.2 Refractive Error (Spherical Equivalent)

There was no significant difference in refractive error between experimental and control eyes at baseline (t-test, p=0.224). After one night of CRT®H lens wear, refractive error (mean±SE) changed by 1.23±0.21 D (from -2.14±0.57 D to -3.38±0.60 D, t-test, p<0.001). It regressed over time (RM-ANOVA, $F_{(6,114)}$=26.893, p<0.001) and returned to baseline by 28 hours (post hoc test, p=0.458). However, it did not change in control eyes (from -2.28±0.60D to -2.26±0.60D, t-test, p=0.869) (Figure 5-4).

5.4.3 Aberrations

There were no significant differences between experimental and control eyes in defocus, astigmatism, HOAs, coma and SA at baseline (t-test, all $p \geq 0.323$). After one night of CRT®H lens wear, defocus (mean±SE) increased by 0.58±0.09 μm (from 1.76±0.37 μm to 2.34±0.37 μm, t-test, $p<0.001$, Figure 5-5). No difference was found in astigmatism between eyes (RM-ANOVA, $F_{(1,19)}<0.001$, $p=0.993$) and astigmatism did not change over time for either eye (RM-ANOVA, $F_{(6,114)}=0.547$, $p=0.771$). HOAs, coma and SA increased by factors of 2.69 (from 0.17±0.02 μm to 0.46±0.04 μm, Figure 5-6), 2.58 (from 0.10±0.02 μm to 0.27±0.03 μm, Figure 5-7) and 4.07 (from 0.05±0.01 μm to 0.20±0.03 μm), respectively (t-test, all $p<0.001$). Signed SA shifted from positive to negative (from 0.04±0.01 μm to - 0.11±0.05 μm, t-test, $p=0.011$, Figure 5-8). All parameters [except SA (post hoc test, $p=0.390$, Figure 5-8)] had not returned to baseline by 12 hours in experimental eyes (post hoc test, all $p \leq 0.009$) but did so by 28 hours (post hoc test, all $p \geq 0.808$, Figures 5-5 ~ 5-7). Aberrations did not change in control eyes (RM-ANOVA, $F_{(6,114)}= 0.370$ to 1.927, all $p \geq 0.082$, Figures 5-5 to 5-8).

5.4.4 Association of Changes of Signed Spherical Aberration and Refractive Error

There was a significant association between the changes in signed SA and refractive error from baseline immediately after the lens removal ($r = 0.603$, $p=0.005$, the bivariate regression is found in Figure 5-9). The larger the myopic shift (hyperopic correction), the greater the amount of negative SA induced by the CRT®H lenses. In addition, there were no differences between myopic eyes vs. hyperopic eyes in term of the change of refractive error (spherical equivalent) and the change of signed SA (both $p>0.05$).

Table 5-2: Refractive Error (D), (Mean±SD, N=20)

	Experimental Eyes	**Control Eyes**	**P-values**
Sphere	-1.86±2.64	-1.99±2.62	0.287
Cylinder	-0.56±0.42	-0.58±0.43	0.863
M (spherical equivalent)	-2.14±2.54	-2.28±2.67	0.224
J0	-0.04±0.32	0.01±0.31	0.327
J45	-0.01±0.16	0.03±0.18	0.559

J0 is the power of a Jackson crossed cylinder with axes at 90 degrees and 180 degrees. J45 is the power of a Jackson crossed cylinder with axes at 45 degrees and 135 degrees (Thibos and Horner, 2001).

Table 5-3: Auto-Keratometry (D, Mean±SD, N=20)

	Experimental Eyes	**Control Eyes**	**P-values**
Flat K	43.00±1.80 (40.12 to 46.00)	42.95±1.75 (40.12 to 45.75)	0.129
Cylinder	-0.71±0.42	-0.79±0.40	0.241
M (mean K)	43.36±1.75	43.35±1.73	0.828
J0	0.23±0.32	0.29±0.30	0.111
J45	0.01±0.14	0.06±0.15	0.453

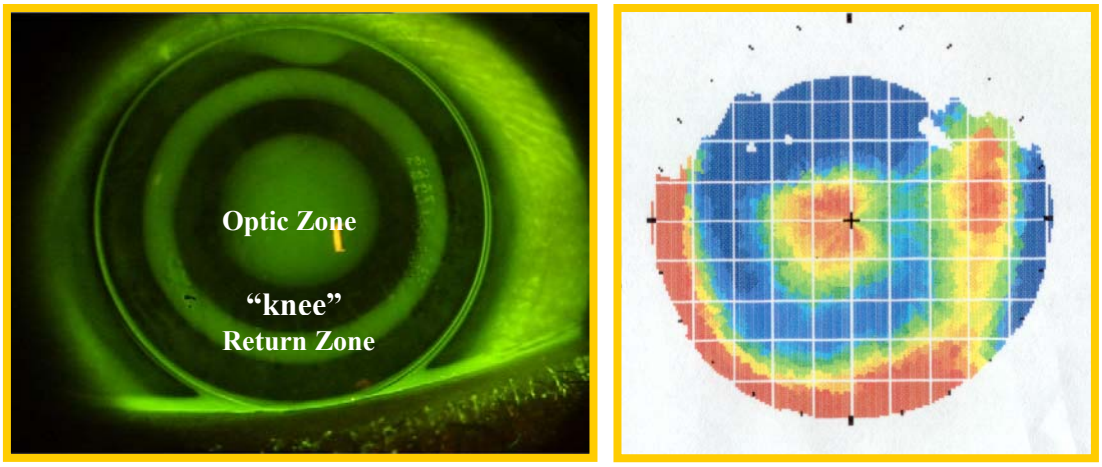

Figure 5-1. A typical fluorescein pattern of CRT for hyperopia (left panel) and a corneal topographic map after CRTH lens wear (right panel). The central pooling, para-central touch ("Knee") and the mid-peripheral pooling in the fluorescein pattern correspond to the central steepening (red), para-central flattening (blue) and mid-peripheral steepening (yellow and red) in the corneal topographic map.

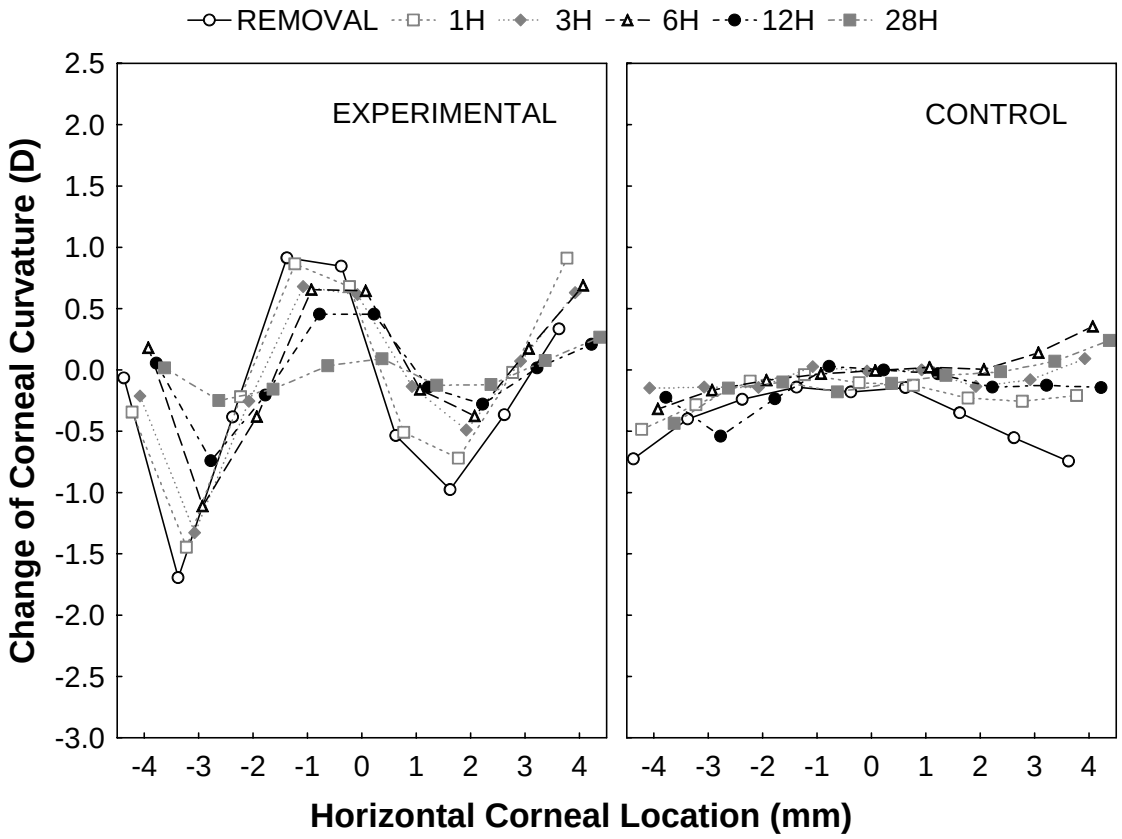

Figure 5-2. The change of horizontal corneal curvature (D) from baseline in the experimental and control eyes over time. Positive x-axis numbers refer to nasal corneal positions and negative to temporal corneal positions. REMOVAL, immediately after the lens removal following waking.

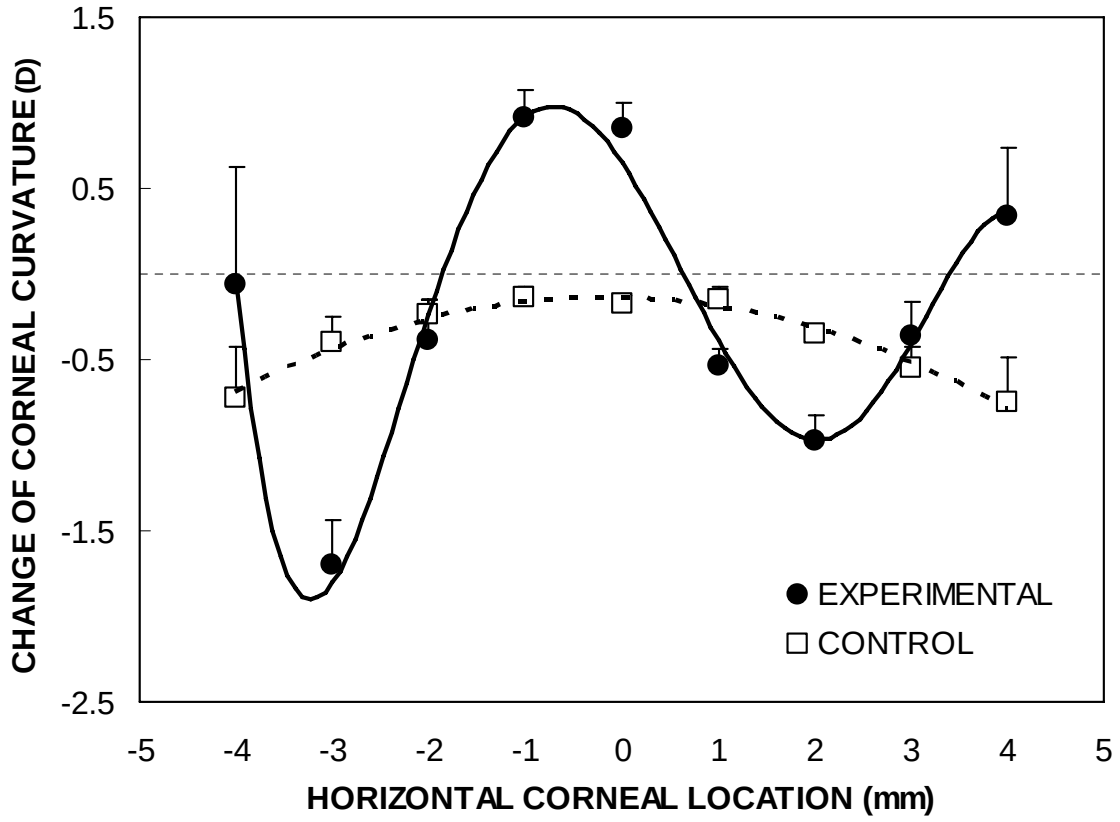

Figure 5-3. The change of horizontal corneal curvature (D) from baseline in experimental and control eyes immediately after the lens removal. Positive x-axis numbers refer to nasal corneal positions and negative to temporal corneal positions. Error bars: standard errors.

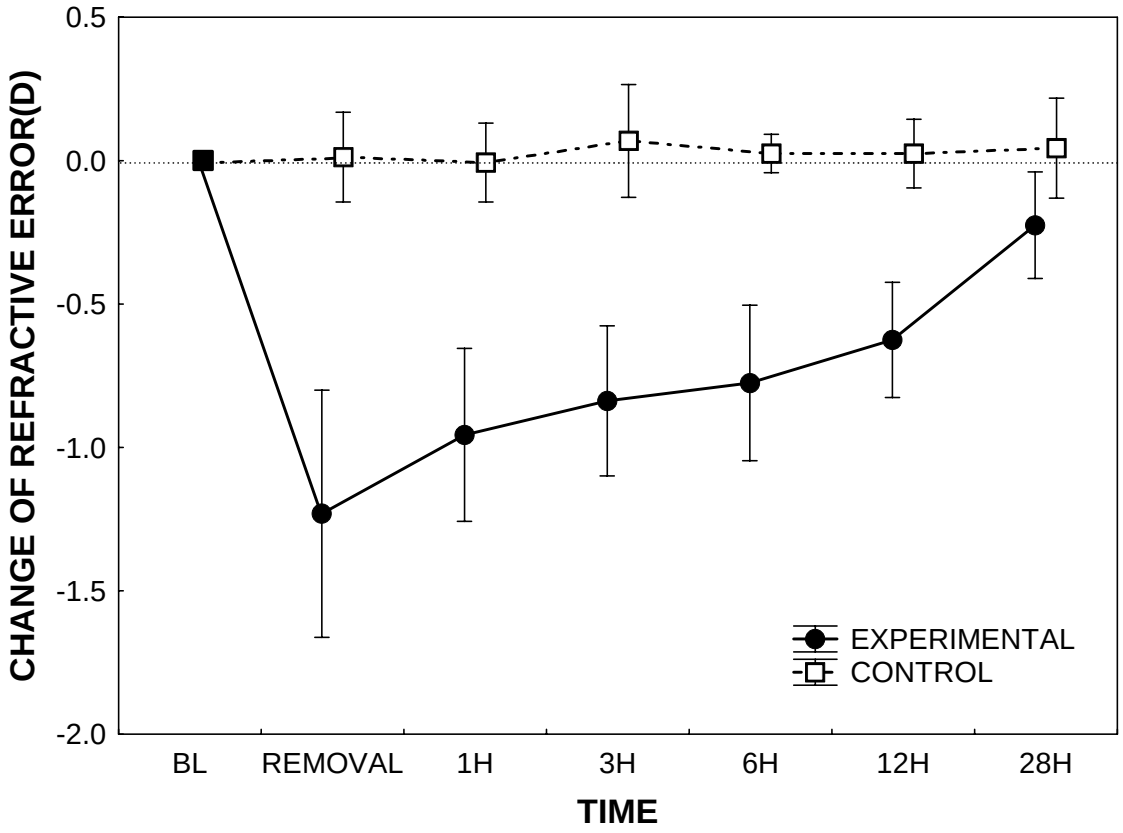

Figure 5-4. The change of refractive error from baseline in the experimental and control eyes over time. The solid square represents baseline for both experimental and control eyes. BL, baseline. REMOVAL, immediately after the lens removal following waking. Error bars: 95% confidence intervals.

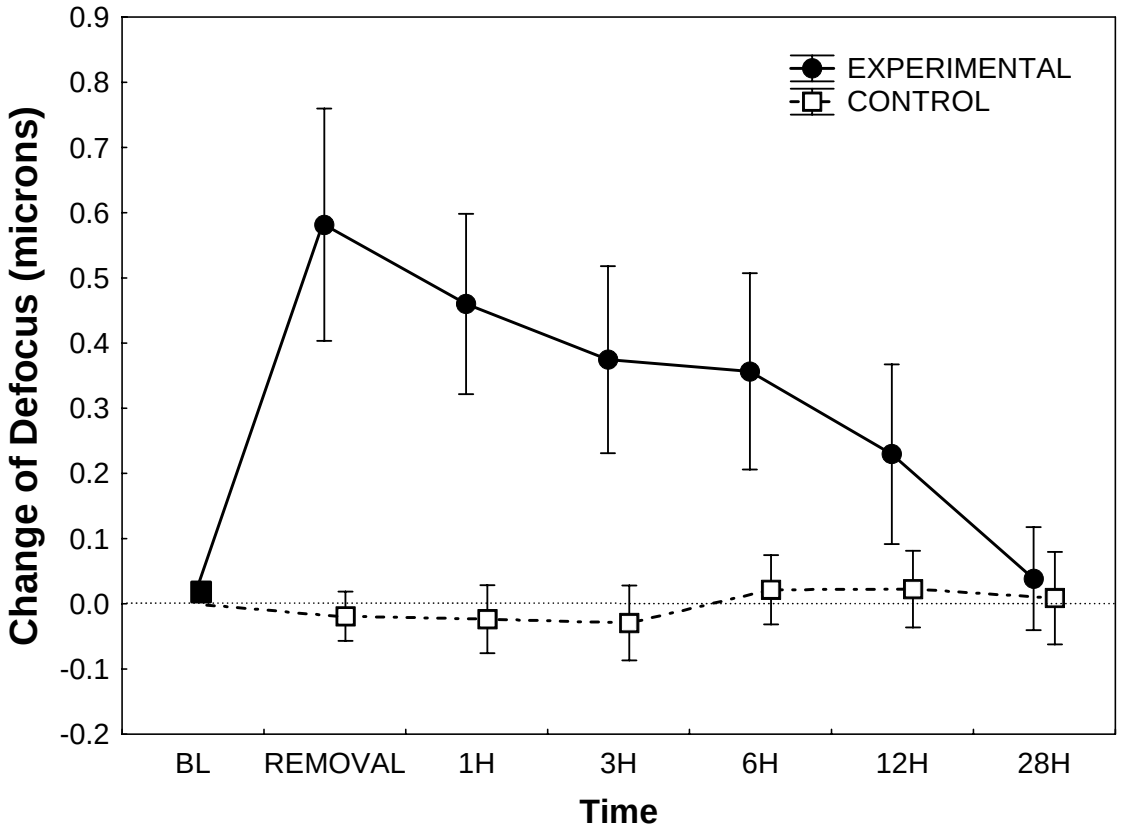

Figure 5-5. The change of defocus (Z_2^0) from baseline in the experimental and control eyes over time. The solid square represents baseline for both experimental and control eyes. BL, baseline. REMOVAL, immediately after the lens removal following waking. Error bars: 95% confidence intervals.

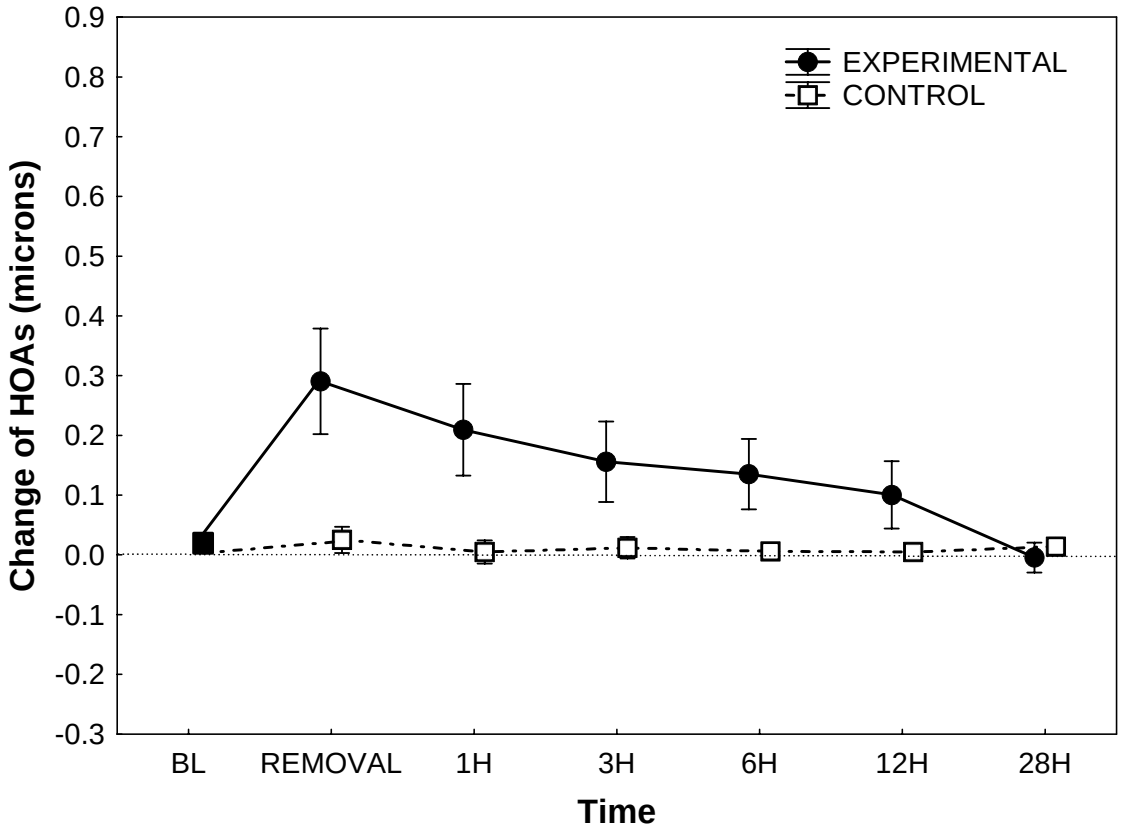

Figure 5-6. The change of higher order aberrations (HOAs) from baseline in the experimental and control eyes over time. The solid square represents baseline for both experimental and control eyes. BL, baseline. REMOVAL, immediately after the lens removal following waking. Error bars: 95% confidence intervals.

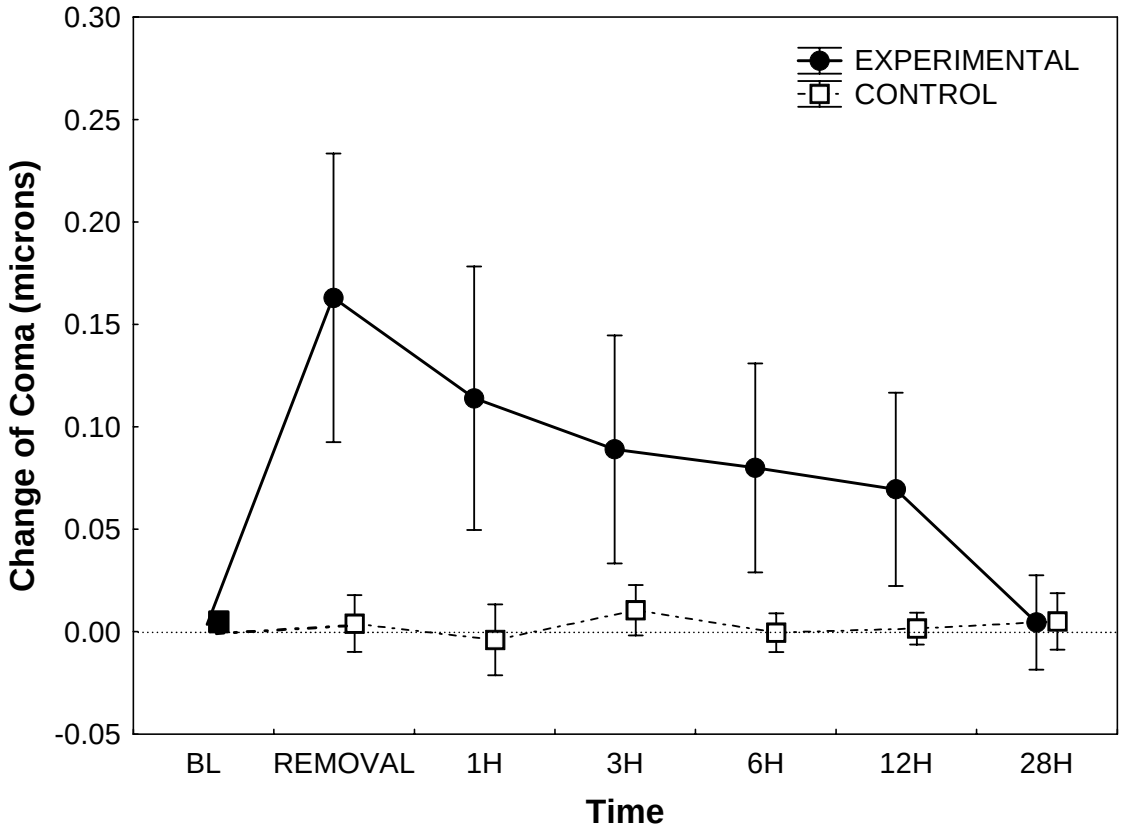

Figure 5-7. The change of coma ($Z_3^{\pm 1}$) from baseline in the experimental and control eyes over time. The solid square represents baseline for both experimental and control eyes. BL, baseline. REMOVAL, immediately after the lens removal following waking. Error bars: 95% confidence intervals.

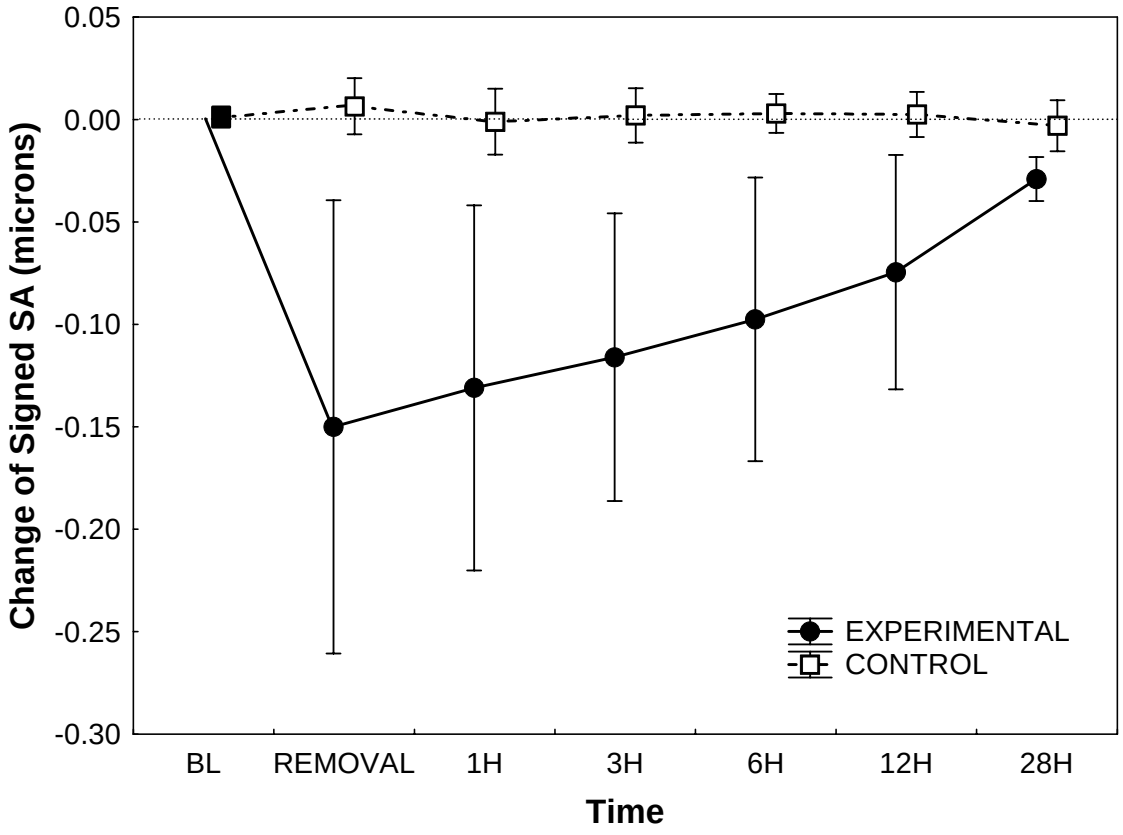

Figure 5-8. The change of signed spherical aberration (SA, Z_4^0) from baseline in the experimental and control eyes over time. The solid square represents baseline for both experimental and control eyes. BL, baseline. REMOVAL, immediately after the lens removal following waking. Error bars: 95% confidence intervals.

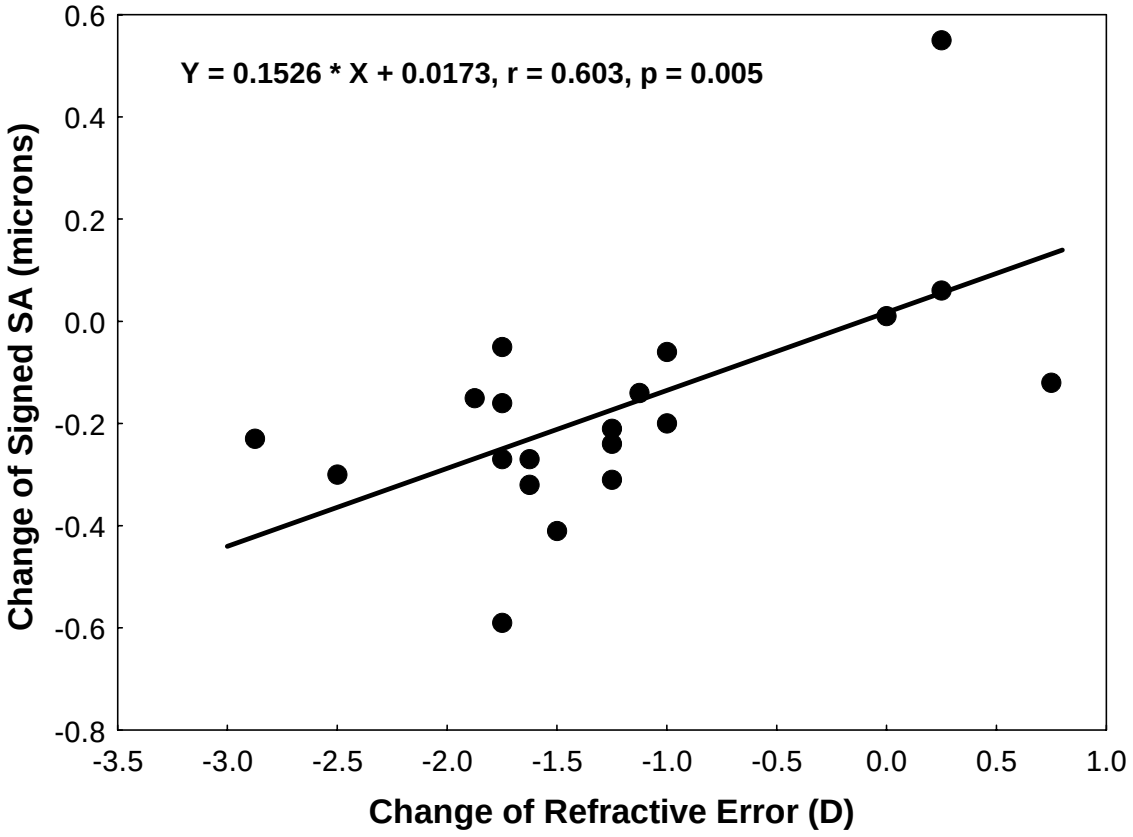

Figure 5-9. The relationship between the changes of refractive error and signed spherical aberration (SA) from baseline immediately after the lens removal.

5.5 Discussion

Rigid contact lenses can be used to correct hyperopia by steepening the central cornea (Jessen, 1962; Swarbrick et al., 2004). However, previous studies (Sarver and Harris, 1967; Hill and Rengstorff, 1974) have not been able to unequivocally show that steep lenses steepened the corneal curvature, perhaps due to lens fitting and/or lens design differences. In addition, because of changes in corneal curvature, an initially steep lens might not be steep after it is worn for some time. Recently, Swarbrick et al. (2004) reported that lenses with base curves approximately 0.3 mm steeper than the flattest K could successfully correct hyperopia or induce a myopic shift, approximately 0.4D, after 4 hours of PMMA lens wear, but not in the Boston XO lens. In the current study, the selected base curve was 0.7 mm steeper than the flat K, and the depth of the mid-peripheral return zone was 175 μm deeper than the calculated return zone depth, which determined the final sagittal depth of the initial lens (Sorbara et al., 2004). The lenses were worn for a single night for approximately 8 to 9 hours. As a result, the cornea steepened centrally and flattened para-centrally (Figures 5-2 and 3). There was a predictable increase in the defocus component, in the myopic direction (Figure 5-5), and refractive error became more myopic or less hyperopic (1.23D on average)(Figure 5-4), suggesting that CRT®H could be used to treat hyperopia. Furthermore, after one night of CRT®H lens wear, the optical effects did not return by 12 hours (except SA which lasted 6 hours), indicating that this overnight lens wear modality may be feasible for retaining reasonable daytime vision.

Change in corneal shape alters the ocular aberration structure. After one night of hyperopic corneal reshaping, the defocus component increased due to the mostly myopic

subjects enrolled (Figure 5-5). As might be expected, the HOAs, including coma and SA, increased (Figures. 5-6 to 5-8) but astigmatism did not change.

SA was the major component of HOAs induced by CRT®H, increasing by a factor of 4.07. Similar to hyperopic corneal refractive surgery (Llorente et al., 2004b; Yoon et al., 2005), signed SA shifted from positive to negative after one night of CRT®H lens wear. SA is relatively low in the population (Williams et al., 2000; He et al., 2003; Kelly et al., 2004) and this low SA is believed to be largely due to the balance of the corneal shape and the crystalline lens (Artal and Guirao, 1998; Artal et al., 2001). It has been hypothesized that the cornea reduces overall ocular SA by its aspheric prolate shape, which is steeper centrally and flatter in the periphery (Somani et al., 2004; Yebra-Pimentel et al., 2004), and perhaps by variation of the refractive index across the cornea (Vasudevan et al., 2004). CRT®H corrects hyperopia by steepening the central cornea and flattening the para-central region. This shape change alters the positive (Millodot and Sivak, 1979; He et al., 2003; Kelly et al., 2004) or negative (Artal and Guirao, 1998; Guirao et al., 2000) corneal SA to be less positive or more negative after hyperopic corneal reshaping. The balance of SA between the cornea and crystalline lens was disturbed, shifting ocular SA from positive to negative. Furthermore, uneven epithelial distribution (discussed later) may also alter the refractive index across the cornea, contributing to the imbalance of the SA.

The amount of the signed SA change was associated with the refractive error change. Similar to hyperopic corneal refractive surgery (Llorente et al., 2004b; Ma et al., 2004) and myopic non-surgical corneal reshaping (Hiraoka et al., 2005), the increment of SA was significantly related to the change of the refractive error immediately after the lens removal.

The greater the amount of the refractive error corrected, the more the negative SA induced (Figure 5-9).

Increased coma may have been due to slight lens decentration. Topography data in this study showed the centre of the treatment zone displaced 0.47±0.30 mm temporally and 0.09±0.27 mm inferiorly on average. This decentration outcome is comparable to myopic corneal reshaping (Yang et al., 2003). Lid-lens interaction has been hypothesized to affect the lens centration during blinking (Carney et al., 1997a), especially the forced and squeezed blinks from lens discomfort immediately after rigid lens insertion. Coma has been reported after myopic corneal reshaping due to lens decentration (Joslin et al., 2003; Yang et al., 2003; Hiraoka et al., 2005), and it also happened after hyperopic corneal reshaping in this study. Therefore, decentration-induced coma may be difficult to completely avoid in corneal reshaping.

After one night of CRT®H lens wear, the central cornea steepened and para-central cornea flattened (Figures 5-2 and 5-3). We hypothesize that the compression from the junction ("knee") between the return zone and the optic zone (Figure 5-1) presses the epithelium and forces it to migrate centrally (toward the optic zone) and also squeezes the epithelium to the mid-periphery (toward the return zone). Central and mid-peripheral negative forces (the space between the lens and cornea generating capillary suction) are also hypothesized to drive the tissue towards the centre and mid-periphery. The effect of lid tension through the contact lens may induce squeeze pressure (Lieberman and Grierson, 2000; Ehrmann et al., 2001) on para-central epithelial cells through the "knee" although the eyelid tension may be low during sleep. In addition, Allaire and Flack (1980) demonstrated that different thickness tear film profiles between a contact lens and the cornea induced

different hydraulic forces or pressures on the cornea. Similarly, Mountford (2004b) simulated a tear film profile to explain the hydraulic force underneath the myopic corneal reshaping lens. The different hydraulic forces resulting from the uneven tear film profile underneath the lens can also be assumed in hyperopic corneal reshaping. These hypotheses have been supported by a corneal morphological study (Haque et al., 2004a) suggesting that corneal reshaping was due to epithelium accumulation centrally, and by histological data in cats (Choo et al., 2004c; Hughes et al., 2004) that the epithelium was thicker centrally (Choo et al., 2004c; Hughes et al., 2004) and thinner para-centrally (Choo et al., 2004c).

Full recovery is a critical clinical issue in corneal reshaping. In this study, the corneal shape and all optical parameters had returned to baseline by 28 hours, indicating that CRT® for hyperopia was reversible. This temporary effect is a drawback in non-surgical corneal reshaping, but it may also be attractive for candidates who are concerned about the safety of corneal refractive surgery.

Diurnal variation of ocular aberrations and corneal shape might potentially have affected the outcome in this study. The contralateral eyes without lenses served as controls and no diurnal variation of aberrations was found in these eyes during this study, suggesting that the robust treatment effect was valid in experimental eyes. Although the control cornea was slightly flatter (0.18±0.05D) than baseline after one night of sleep [consistent with previous experiments (Kiely et al., 1982; Cronje and Harris, 1997)], this corneal flattening disappeared by 3 hours of eyes being open. In addition, the profile of the change of corneal curvature in experimental and control eyes was significantly different, i.e. the central corneal steepening and para-central flattening in experimental eyes, and no significant location effect

in control eyes (Figures 5-2 and 5-3), also indicating an effective corneal reshaping in experimental eyes.

Our result of no diurnal variation of HOAs in control eyes, especially coma and SA, is in accord with the report of Mierdel et al. (2004), who demonstrated no change of Zernike coefficients during the day in 22 eyes, except for the coefficient $Z_4^{\pm 2}$ (quantifying secondary astigmatism 90/180). This lack of diurnal variation in aberrations reflected relatively stable corneal shape at different corneal locations in the control eyes over time (Figure 5-2).

There are a number of issues that might warrant further investigation. An example of this is the large 95% confidence intervals in the experimental eyes (Figures 5-4 to 5-8) suggesting high treatment variability. The cause of this needs to be determined to make the clinical outcome more predictable. For instance, lens decentration might lead the "knee" to touch the central cornea, resulting in a myopic-like correction, an opposite effect. In addition, only one night of lens wear might be a source of transient variability. For example, as in myopic corneal reshaping (Mountford, 2004a), central topographic irregularities that appear as "central islands" and which occur in the earlier stage of treatment might resolve over time. A second issue is that the majority of subjects in this study were myopes, whose corneal shapes [corneal aberration structure (Llorente et al., 2004a)] perhaps are not exactly the same as those of hyperopes (Carney et al., 1997b; Llorente et al., 2004a), and who, theoretically, may have subtly different ocular structure. Therefore, further work is needed to clarify the treatment effect on hyperopes. A third issue relates to long term effects beyond a single night that need to be investigated. Finally, the safety of these lenses should be evaluated in a much lager clinical trial.

In summary, after one night of CRT®H lens wear, corneal refractive therapy steepens the central cornea and flattens the para-central region, altering the ametropia by inducing a myopic shift. It therefore appears to be effective for correcting hyperopia. HOAs increased in predictable ways and the optical effects did not return to baseline by 12 hours, but did so by 28 hours. No significant diurnal variation in optical performance was found in control eyes.

Chapter 6 (CRT2 study)

The Relationship between the Treatment Zone Diameter and Visual, Optical and Subjective Performance in Corneal Refractive Therapy® Lens Wearers

This paper was submitted to Ophthalmic and Physiologic Optics and is under revision. The coauthors, Drs. Trefford Simpson, Luigina Sorbara and Desmond Fonn, permit the microfilming of this thesis.

6.1 Abstract

Purpose: To investigate the stability of the Treatment Zone (TZ) size during Corneal Refractive Therapy (CRT®) over four weeks of lens wear, and to determine the relationship between TZ diameter and visual, optical and subjective performance.

Methods: Twenty-three myopic subjects wore CRT® lenses overnight and removed their lenses on awakening. Visual Acuity (VA), subjective vision, refractive error, aberrations, and corneal topography were measured at baseline, immediately after lens removal on the first day and 14 hours later, and these measurements were repeated on days 4, 10, and 28. The TZ including the Central Flattened Zone (CFZ) and the Annular Steepened Zone (ASZ) was demarcated by the change in corneal curvature from negative to positive and vice versa, using the tangential difference map from the Atlas corneal topographer. Repeated measures ANOVA examined time effects, Tukey HSD post hoc tests determined variable stabilization and planned paired t tests determined diurnal differences. Pearson correlation examined associations.

Results: After overnight CRT® lens wear, the central cornea flattened and the mid-periphery steepened (both $p<0.001$). After 4 weeks of lens wear, the CFZ (±SE) increased from 3.41±0.09 mm to 3.61±0.07 mm and the diameter of the ASZ increased from 8.17 ± 0.16 mm to 8.85 ± 0.14mm (both $p<0.001$). From day 10 onwards, the CFZ and ASZ diameter were stable in the morning ($p\geq0.404$). Throughout the day, the CFZ became smaller during the first 10 days (all $p\leq0.022$), whereas the ASZ diameter remained constant (all $p\geq0.079$). There were significant positive correlations between the CFZ or ASZ and refractive error, subjective vision, and spherical aberration. The CFZ was also correlated with astigmatism and higher order aberrations, and the ASZ was positively correlated with coma ($r=0.726$ to 0.961, all $p\leq0.042$). In addition, there were significant negative correlations between the CFZ or ASZ and total aberration and defocus and between the ASZ and VA ($r= - 0.707$ to $- 0.953$, all $p\leq0.050$).

Conclusion: The TZ changed during the first 10 days. Its size was associated with VA, refractive error, aberrations and subjective vision. The concept of a TZ is a useful metric of visual, optical and subjective performance in CRT® lens wearers.

6.2 Introduction:

Corneal Refractive Therapy (CRT®) has been demonstrated to be effective for myopic correction after a single night of CRT lens wear (Chapter 4). However, the relatively long term changes in corneal shape, visual, subjective and optical performance were unclear. A study of 4-weeks CRT® lens wear was conducted to characterize these estimates and to determine the stabilization of these outcome variables.

Corneal topography can be used to define and quantify the optical ablation (treatment zone, TZ) and transition zones after corneal refractive surgery (Endl et al., 2001; Partal and Manche, 2003; Kermani et al., 2003; Seo et al., 2004; Macsai et al., 2004). However, few studies have quantified the TZ in orthokeratology (Sridharan and Swarbrick, 2003; Tahhan et al., 2003; Owens et al., 2004). This concept is as important in orthokeratology (Alharbi and Swarbrick, 2003) as in corneal refractive surgery (Munnerlyn et al., 1988; Endl et al., 2001; Partal and Manche, 2003; Macsai et al., 2004) since the success of the treatment may be associated with the area of treatment.

Clinically, patients with good visual acuity and low or no residual refractive error may not be satisfied with a refractive procedure. Therefore, the assessment of a vision correction procedure should include both objective and subjective responses. As in corneal refractive surgery (Applegate et al., 2001), dissatisfaction with corneal reshaping may not be fully assessed by conventional measures such as visual acuity testing.

Ocular optical quality is perhaps most sensitively measured by wavefront sensors that quantify ocular aberrations. In addition to wavefront sensors, corneal topographers can detect subtle changes of the corneal shape, which also contribute to the vision quality, improving our understanding of the ocular response after corneal reshaping. To our knowledge, no

literature has linked corneal shape change in terms of the TZ with ocular aberrations in non-surgical corneal reshaping. In this study, we investigated the dynamic variation of the TZ during four weeks of CRT® lens wear, and determined the relationship between TZ diameter and visual, optical, and subjective performance in CRT® lens wearers.

6.3 Materials and Methods

6.3.1 Subjects

Thirty myopic subjects were enrolled and the data from the 23 who completed the study are reported here. The reasons for the seven subjects who discontinued from this study included uncomfortable lenses (2), poor vision (3), conjunctivitis (1) and corneal abrasion (1). The subjects' age ranged from 19 to 51 years (mean± SD: 26.1±7.6) with 4 subjects who were 30 or older than 30 years old (39.7±9.5). They were mostly female (16F:7M). Spherical ametropia ranged from –1.00 to – 5.00D, and corneal cylinder was less than 1.50D.

Refractive error and corneal curvature from keratometry of the 23 subjects are summarized in Table 6-1.

6.3.2 Lens Characteristics and Fitting

The rigid gas permeable (RGP) material used for CRT® lenses (Paragon Vision Sciences, Mesa, AZ) was Paragon HDS 100 (fluorosilicone acrylate). A summary of the lens characteristics and parameters that were prescribed is found in Table 6-2.

CRT® lens fitting can be found in Methods Chapter 3.

The number of the lens used for the right eyes was 2.48±1.47 (from 1 to 7 lenses) and 2.35±1.50 (from 1 to 7 lenses) for the left eyes on average.

Table 6-1. Ocular Parameters (D), (mean ± SD)

Refractive Error		**Auto-Keratometry**	
Sphere	**Cylinder**	**Flat K**	**Cylinder**
-2.72±1.06	-0.55±0.40	43.94±1.37 (41.37 to 46.38)	-0.64 ± 0.45

Table 6-2. Nominal Lens Characteristics and Parameters.

Dk (cm^2/sec).(mlO_2/ml.mmHg)	**CT** (mm)	**TD** (mm)	**BOZR**(±SD) (mm)	**RZD**(±SD) (micron)	**LZA** (±SD) (degree)
100×10^{-11}	0.15	10.5	8.39±0.37 (7.7 to 9.1)	530±50 (500 to 575)	33.17±0.97 (31 to 35)

Dk, Oxygen permeability. CT, Centre Thickness. TD, Total Diameter. BOZR, Back Optic Zone Radius. RZD, Return Zone Depth. LZA, Landing Zone Angle.

6.3.3 Study Design

This was a prospective cohort study.

6.3.4 Procedures

High/Low Contrast Visual Acuity (HCVA/LCVA), refractive error, Root-Mean-Squared (RMS) wavefront errors, and corneal topography were measured at baseline (day 0) on the night prior to lens insertion. After the lenses were applied, participants retired in our laboratory at approximately 10 p.m. and were awakened at 7 a.m. the next morning. Measurements were repeated immediately after lens removal on the first day and 14 hours later. Additional overnight visits took place on days 4, 10, and 28, when the same measurements were taken. After the first night of lens wear, the subjects were asked to continue to use their lenses every night before they went to sleep and to remove the lenses on waking.

Before the start of the study, a designated ophthalmic technician taught the subjects how to insert and remove the lens. Subjects were advised to wet the lenses with the provided re-wetting drops before going to sleep and upon awakening. The subjects were required to sleep with the lens in place for at least 8 hours each night.

6.3.5 Measurements

6.3.5.1 Visual Acuity

Uncorrected visual acuity was measured with computerized log MAR charts (logarithm of the minimum angle of recognition) at 90% and 10% contrast (HCVA and LCVA, respectively) with high illumination (approximately 500 lux) at 6 meters. The chart luminance was 98.2 cd m-2.

6.3.5.2 Subjective Visual Analogue Scale

The visual analogue scale used consisted of a 10 cm horizontal line divided into 10 sections with descriptors at each end. All subjects marked their daily logs to indicate the quality of their vision, with 1 representing poor and 100, excellent vision. Participants completed a daily log characterizing their subjective vision at the beginning (immediately after the lens removal) and the end (14 hours without lens wear) of each day.

6.3.5.3 Autorefraction

See Methods Chapter 3.

6.3.5.4 Aberrations

See Methods Chapter 3.

6.3.5.5 Corneal Topography

See Methods Chapter 3.

6.3.5.6 Definition of the TZ Diameter

The TZ comprising a Central Flattened Zone (CFZ) and a surrounding Annular Steepened Zone (ASZ) was induced by lens wear. The diameter of the ASZ is the sum of the diameter of CFZ and the width of each nasal and temporal components of the ASZ (ASZ = CFZ + ASZ_n + ASZ_t, ASZ_{n+t}=ASZ_n+ASZ_t), and these are illustrated in Figures 6-1 and 6-2. The TZ diameter was defined by the change in corneal curvature from negative to positive (ideally zero) along the horizontal meridian, and vice versa, using the tangential difference map from the corneal topographer. The TZ diameter was measured directly from the computer display.

6.3.6 Statistical Analysis

Repeated measures analyses of variance (RM-ANOVA) were used to examine the main effects of the day on the corneal curvature, TZ diameters, vision, refractive error and aberrations at the time of lens removal. Tukey Honestly Significantly Different (HSD) post hoc tests were used to determine when the dynamic outcome variables stabilized. Paired t tests (planned comparison) were used to determine the differences between morning and afternoon variables throughout the day. Polynomial non-linear regression was used to characterise corneal curvature at baseline and after 4 weeks of CRT® lens wear. Pearson correlation was used to determine associations among variables. Differences were considered statistically significant when the likelihood of a type I error was ≤ 0.05. Data analysis was conducted using STATISTICA 7.0 (StatSoft Inc., Tulsa, Oklahoma, U.S.A.) and bivariate regressions (York, 1966) were obtained using ProFit 5.01a (QuantumSoft, Zürich, Switzerland). One of two eyes randomly chosen was used for analysis. The data are presented as mean $\pm$ SE in the text.

6.4 Results

6.4.1 Corneal Topography

After CRT™ lens wear, the central cornea flattened and the mid-periphery steepened (Figures 6-1 and 6-2). The horizontal corneal curvature after corneal reshaping was different from baseline. Polynomial regression analysis showed that only a parabolic component of the corneal curvature was different from zero ($p<0.001$) at the baseline. However, there were quadratic, cubic and quartic components in the corneal curvature after 4 weeks of corneal reshaping (all $p \leq 0.027$). The functions and correlation coefficients (Figure 6-2) are:

$$Y_{Baseline} = 44.126 - 0.122*x - 0.205*x^2,\ R = 0.958;$$

Y_{D28T0}=41.737 + 0.505*x + 0.817*x^2 - 0.061*x^3 - 0.049*x^4, R =0.961.

The cornea flattened centrally from 44.61±0.31 D at baseline to 41.82±0.31 D on day 28 (RM-ANOVA, $F_{(8,176)}$=135.38, p<0.001) and steepened in the mid-periphery (3mm from the centre, average of temporal 3mm and nasal 3mm) from 41.89±0.33 D at baseline to 45.20±0.40 D on day 28 (RM-ANOVA, $F_{(8,176)}$=49.08, p<0.001). The central corneal curvature in the morning visit stabilized by day 10 (post hoc test, p=0.999) and the mid-periphery by day 4 (post hoc test, all p≥0.323). However, they regressed throughout the day (t-test, all p≤0.012). The central and mid-peripheral corneal curvatures at different times are illustrated in Figure 6-3.

6.4.2 The TZ Diameter

Figure 6-4 shows that after CRT® lens wear, the CFZ increased from 3.41±0.09 mm in day 1 morning to 3.61±0.07 mm on day 28 morning (RM-ANOVA, $F_{(3,66)}$ =5.843, p<0.001). There was no significant difference between the width of nasal and temporal ASZ (ASZ_n and ASZ_t) (RM-ANOVA, $F_{(1,22)}$=1.744, p=0.202). The sum of the nasal and temporal ASZ (ASZ_{n+t}) increased from 4.77±0.14 mm to 5.24±0.13 mm (RM-ANOVA, $F_{(3,66)}$=6.219, P<0.001) and the diameter of the ASZ increased from 8.17±0.16 mm to 8.85±0.14mm (RM-ANOVA, $F_{(3,66)}$ =10.631, p<0.001). From day 4, the ASZ_{n+t} was constant at the time of the lens removal (post hoc test: all p≥0.386), but the CFZ and the diameter of ASZ were stable from day 10 (post hoc test: both p≥0.404). From the beginning to the end of the day, the CFZ became smaller during the first 10 days (t-test, all p≤0.022), but on day 28, the difference between the early and later daily measurements was not significant (p=0.07). There was a trend for the ASZ_{n+t} to increase but not significantly (t-test, all p≥0.073, except on day 4,

p=0.016). The early and later daily measurements of the ASZ diameter were statistically the same on days 1, 4, 10 and 28 (t-test, all $p \geq 0.079$).

6.4.3 Visual Acuity

LogMAR uncorrected visual acuity improved significantly from 0.89±0.07 at baseline to -0.01±0.02 on day 28 morning for the HCVA and from 1.19±0.07 (baseline) to 0.31±0.02 (day 28) for the LCVA during the study period (RM-ANOVA, $F_{(8, 176)}=85.51$ to 97.05, both $p<0.001$). From day 4, the HCVA stabilized for the morning visit (post hoc test, p=0.230), and the LCVA stabilized by day 10 (post hoc test, p=0.999). However, the HCVA regressed throughout the day on days 1, 4 and 28 (t-test, all $p \leq 0.033$, except on day 10, p=0.144). The LCVA regressed throughout the day on days 1, 4, 10 and 28 (t-test, all $p \leq 0.005$)(Figure 6-5).

6.4.4 Refractive Error

After CRT® lens wear, myopia (spherical equivalent) reduced from -3.00±0.22 D at baseline to -0.40±0.16D on day 28 morning (RM-ANOVA, $F_{(8, 176)}=56.42$, $P<0.001$). From day 10, it was stable in the morning (post hoc test: p=0.963). Myopia regressed throughout the day on days 1, 4, 10 and 28 (t-test, all $p \leq 0.001$)(Figure 6-6). In addition, the spherical component decreased from -2.72±0.22D (baseline) to -0.17±0.09D (day 28)(RM-ANOVA, $F_{(8, 176)}=90.08$, $P<0.001$). Astigmatism did not change significantly during the study period from -0.55±0.08 D (baseline) to -0.46±0.07D (day 28)(RM-ANOVA, $F_{(8, 176)}=2.049$, P=0.051).

6.4.5 Ocular Aberrations

Total aberration and defocus decreased over the study period by factors of 2.65 (from 2.462 ±0.169μm at baseline to 0.928±0.101μm on day 28 morning) and 3.42 (from

2.427±0.170μm to 0.71±0.108μm), respectively (RM-ANOVA, $F_{(8,176)}$=62.64-76.23, both p<0.001). Astigmatism did not change (RM-ANOVA, $F_{(8, 176)}$=1.623, p=0.125). On the other hand, coma, SA and HOA increased by 2.27× (from 0.082±0.011μm to 0.186±0.025μm), 3.84× (from 0.045±0.006μm to 0.173 ±0.025μm) and 2.22× (from 0.139±0.016μm to 0.308±0.033μm), respectively (RM-ANOVA, $F_{(8,176)}$=3.86-11.49, all p<0.001). Total aberration and defocus were stable by day 10 (post hoc test: both p≥0.837), whereas HOA, coma and SA were stable by day 4 (post hoc test: all p≥0.631). Throughout the day, total aberration and defocus regressed (t-test, all p<0.001). HOA decreased throughout the day on days 1, 10 and 28 (t-test, all p≤0.025, except on day 4, p=0.276). SA decreased throughout the day on day 1 (t-test, p=0.003) and did not change from day 4 onwards (all p≥0.079). Coma was relatively stable throughout the day (t-test, all p≥0.105). The aberrations at different times are illustrated in Figures 6-7 and 6-8.

6.4.6 Subjective Vision

Subjective vision improved from 49.7±5.7 (immediately after lens removal on day 1) to 86.6±3.2 (on day 28) during the study period (RM-ANOVA, $F_{(3, 66)}$=40.32, p<0.001) and was stable by day 10 in the morning visit (post hoc test: p=0.545). Subjective vision deteriorated from the beginning to the end of the day (t-test, all p≤0.014) (Figure 6-9).

6.4.7 The Relationship between TZ and Visual, Optical, and Subjective Performance in CRT® Lens Wearers

The mean diameters of the CFZ and ASZ are significantly associated with the visual, optical, and subjective performance of CRT® lens wearers except for the CFZ vs. visual acuity and coma, and ASZ vs. astigmatism and HOA. In addition, the ASZ_{n+t} was not statistically associated with these parameters (all p>0.05).

Pearson correlation coefficients (r) and p values for the CFZ and ASZ, with HCVA/LCVA, ametropia (Rx, raw spherical equivalent), subjective vision (SV) and aberrations are shown in Table 6-3. Figure 6-10 shows the relationship between the ASZ and residual refractive error (spherical equivalent).

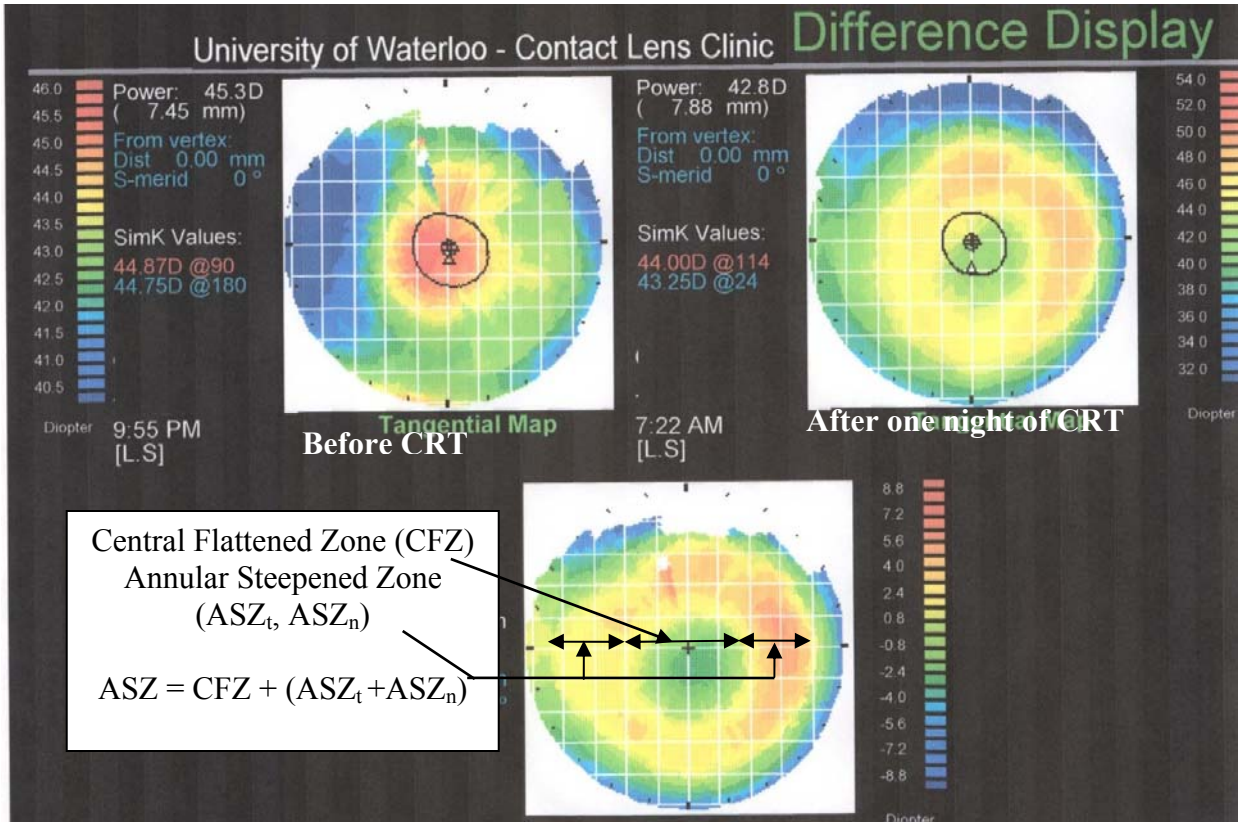

Figure 6-1. A normal corneal topography (pre-treatment) is shown with central steepening and flattening toward the periphery on the top left panel. After successful CRT®, corneal topography shows a "bull's eye" on the top right panel. In the tangential difference map in the bottom panel (subtraction of the pre- and post-treatment), the central area is the central flattened zone (CFZ), while a surrounding mid-peripheral circle is the annular steeped zone (ASZ). The diameter of the ASZ is the sum of the diameter of the CFZ, and the width of each nasal and temporal sides of the ASZ ($ASZ=CFZ+ASZ_n+ASZ_t$).

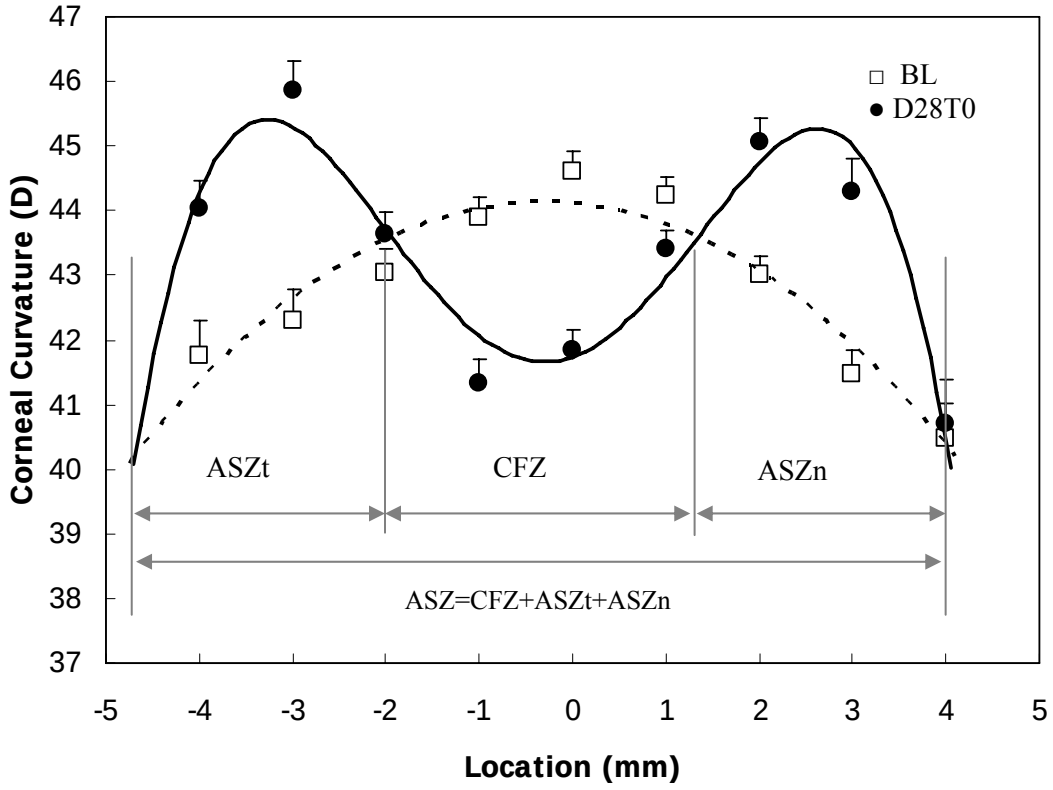

Figure 6-2. The horizontal corneal curvature (D) at baseline and after 4 weeks of CRT® lens wear illustrating the various treatment zones. CFZ is the central flattened zone. ASZ_t is the width of the temporal annular steepened zone. ASZ_n is the width of the nasal annular steepened zone. Positive x-axis numbers refer to nasal corneal positions and negative to temporal corneal positions. BL, baseline. D28T0, immediately after lens wear on day 28. Error bars: standard errors.

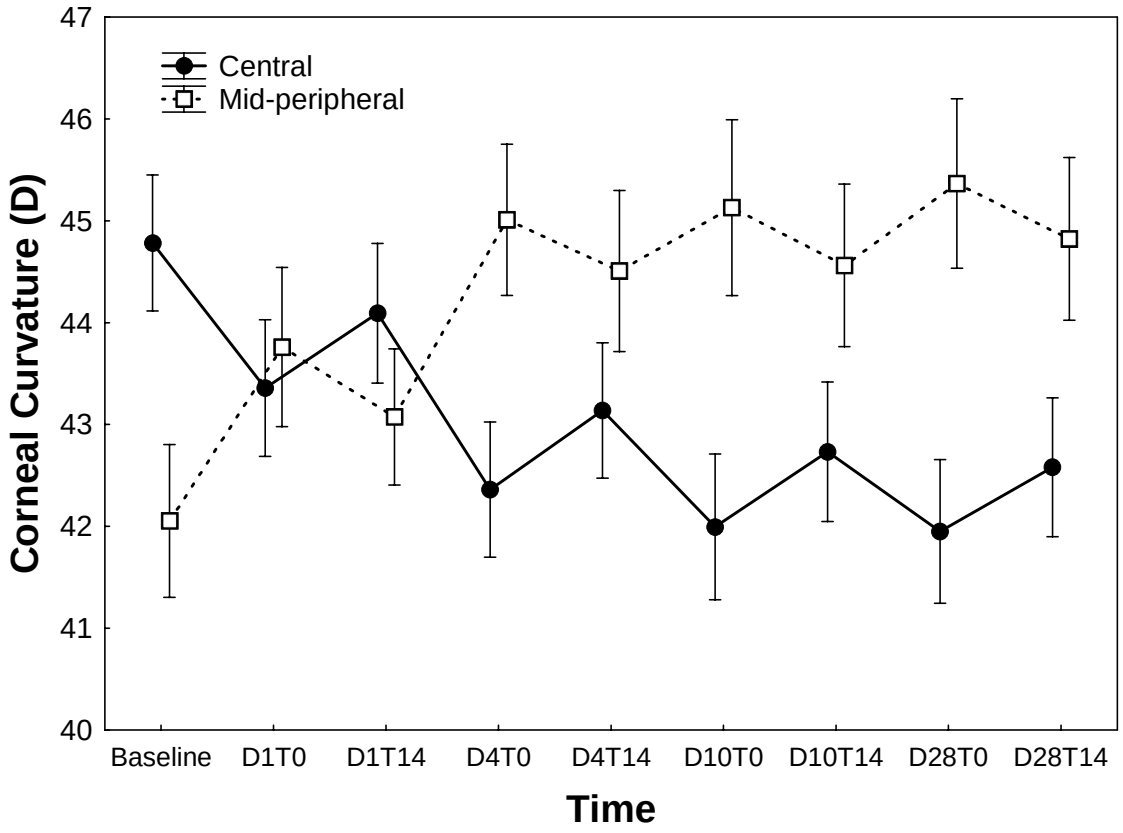

Figure 6-3. The central and mid-peripheral (3mm from the centre) corneal curvatures (D) at different times. D1T0, immediately after the lens removal on day 1. D1T14, 14 hours without lens wear on day 1, etc. Error bars: 95% confidence intervals.

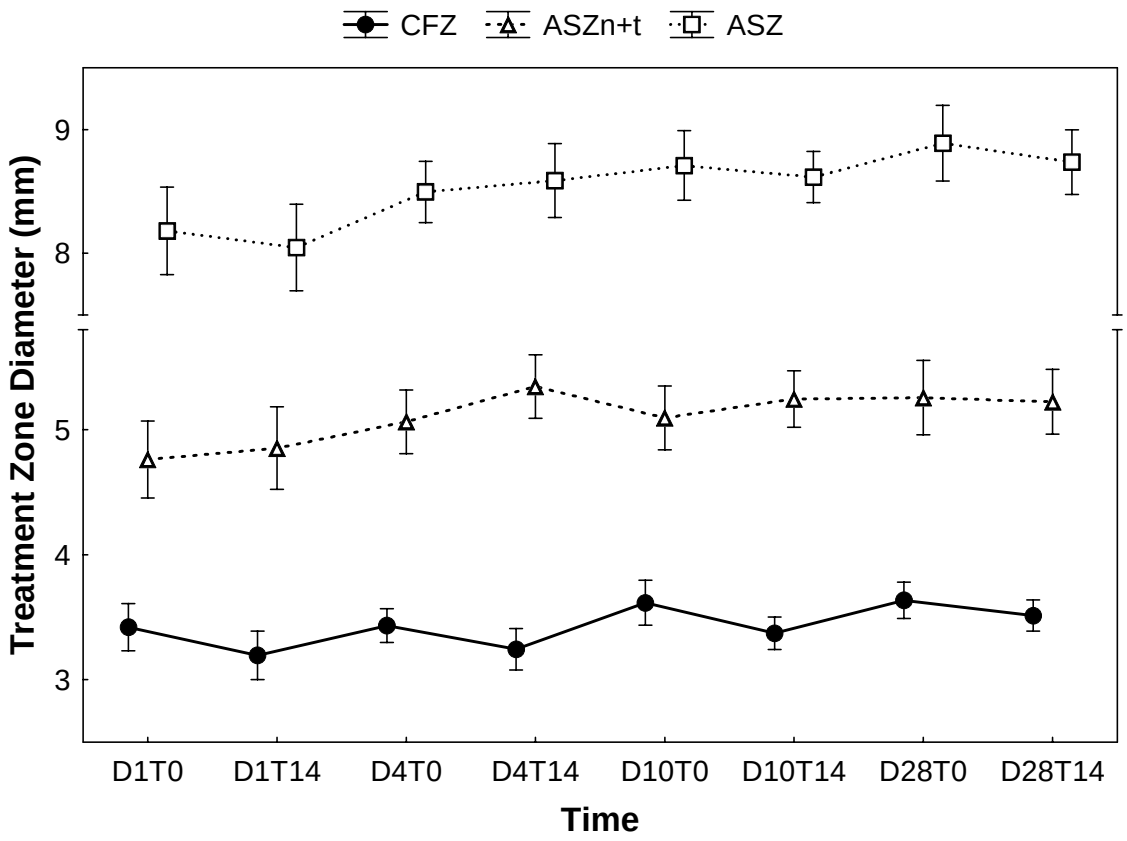

Figure 6-4. The CFZ, ASZ_{n+t} and ASZ at different times. CFZ is the central flattened zone, ASZ_{n+t} is the sum of the width of the nasal and temporal sides of annular steepened zone, ASZ is the diameter of annular steepened zone. D1T0, immediately after the lens removal on day 1. D1T14, 14 hours without lens wear on day 1, etc. Error bars: 95% confidence intervals.

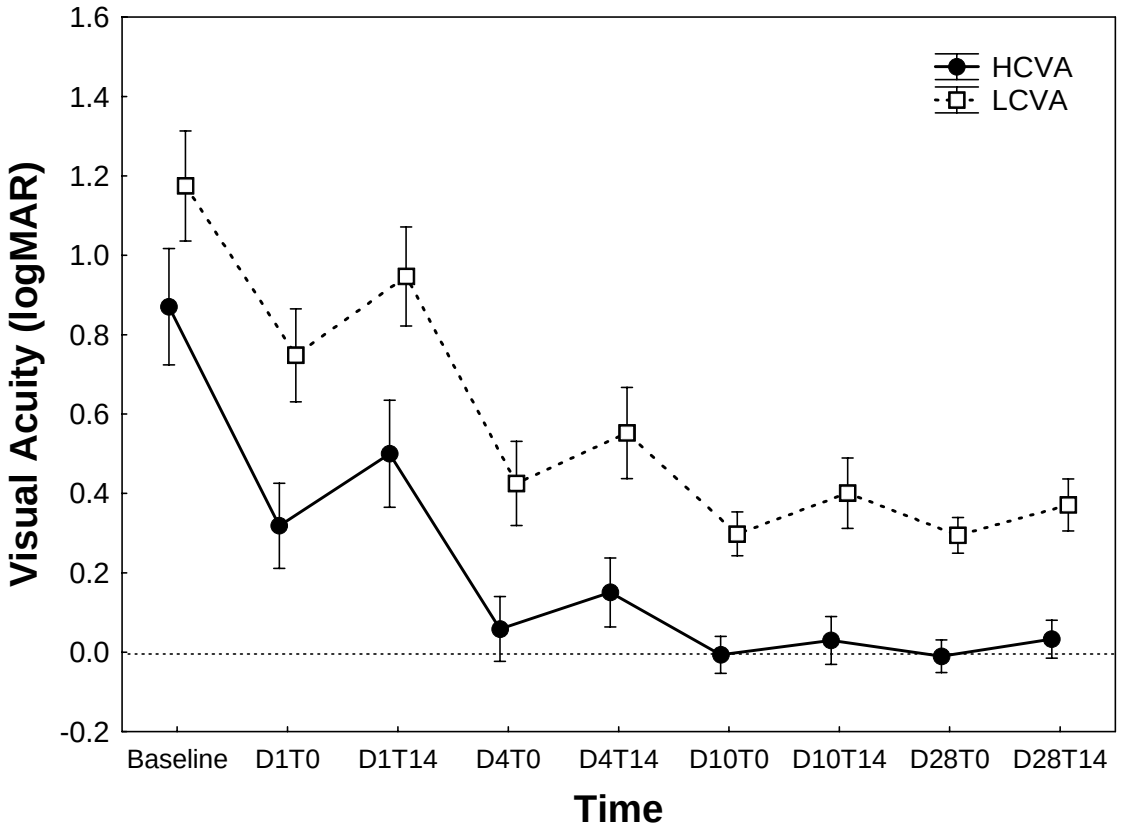

Figure 6-5. Visual acuity improved significantly during the study period. HCVA, high contrast visual acuity. LCVA, low contrast visual acuity. D1T0, immediately after the lens removal on day 1. D1T14, 14 hours without lens wear on day 1, etc. Error bars: 95% confidence intervals.

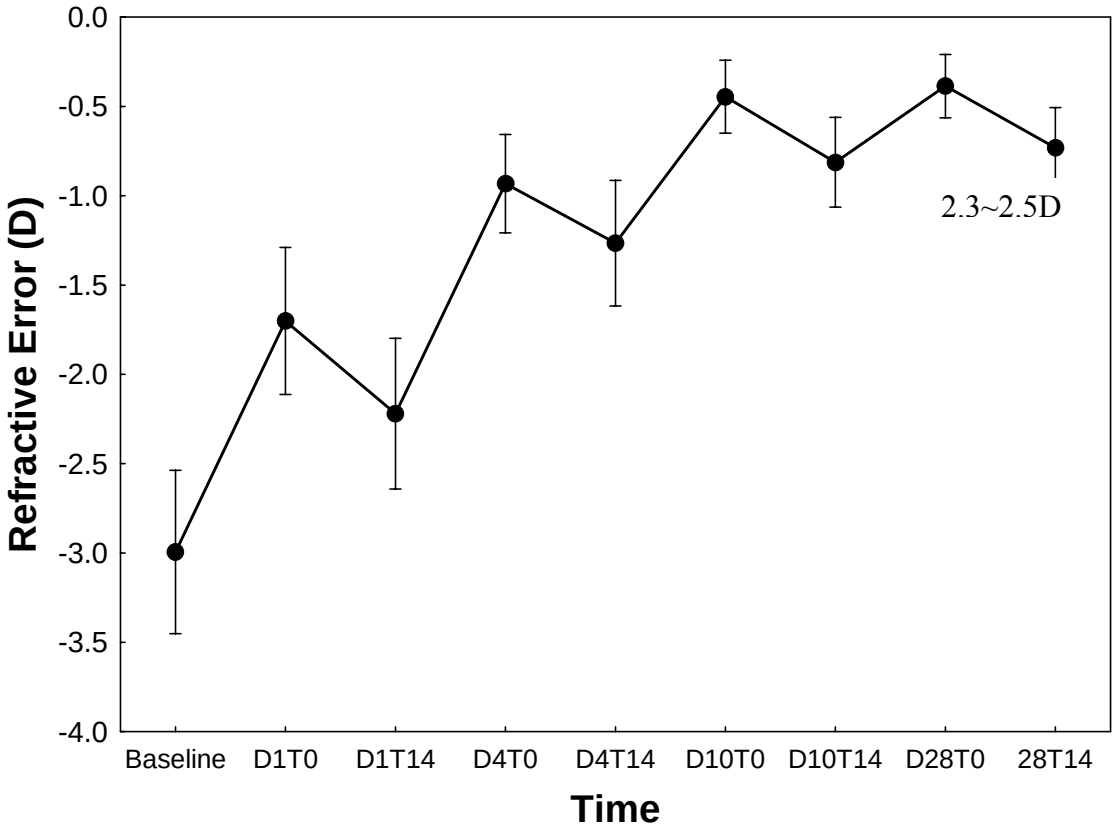

Figure 6-6. Refractive error (spherical equivalent) decreased significantly during the study period. D1T0, immediately after the lens removal on day 1. D1T14, 14 hours without lens wear on day 1, etc. Error bars: 95% confidence intervals.

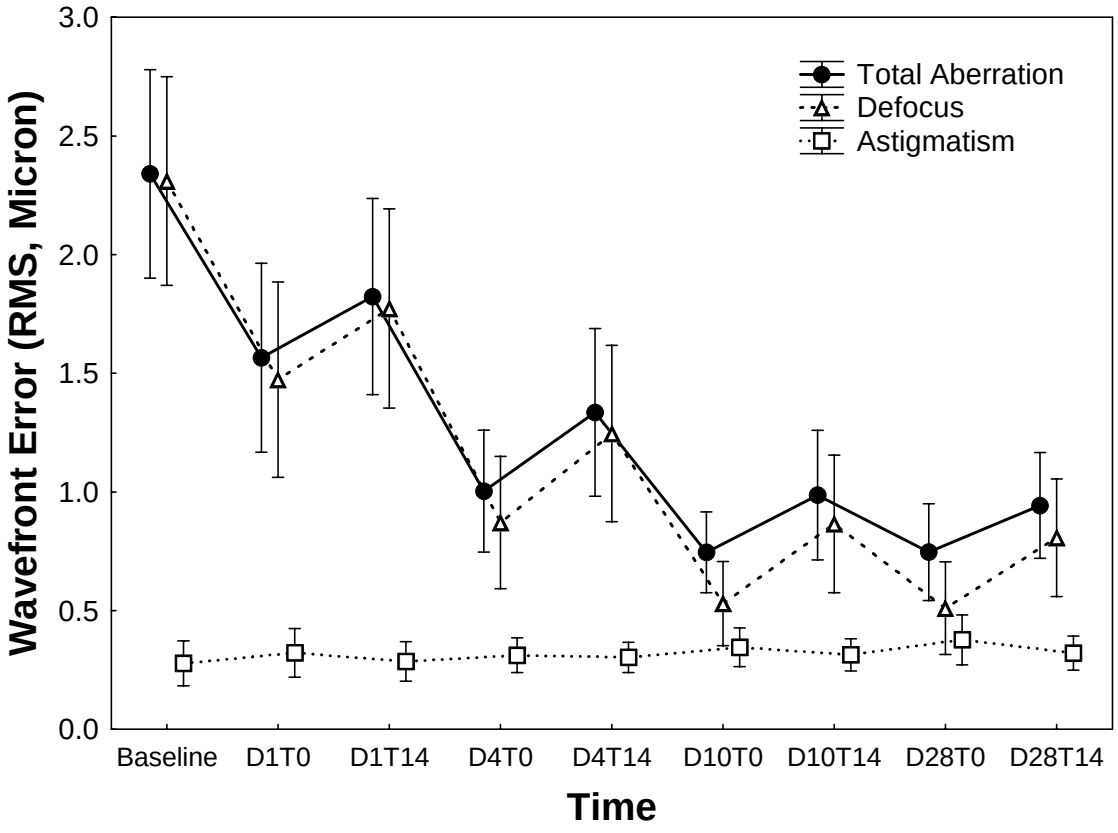

Figure 6-7. Total aberration and defocus significantly decreased, but astigmatism did not change over 4 weeks of CRT ™ lens wear. D1T0, immediately after the lens removal on day 1. D1T14, 14 hours without lens wear on day 1, etc. Error bars: 95% confidence intervals.

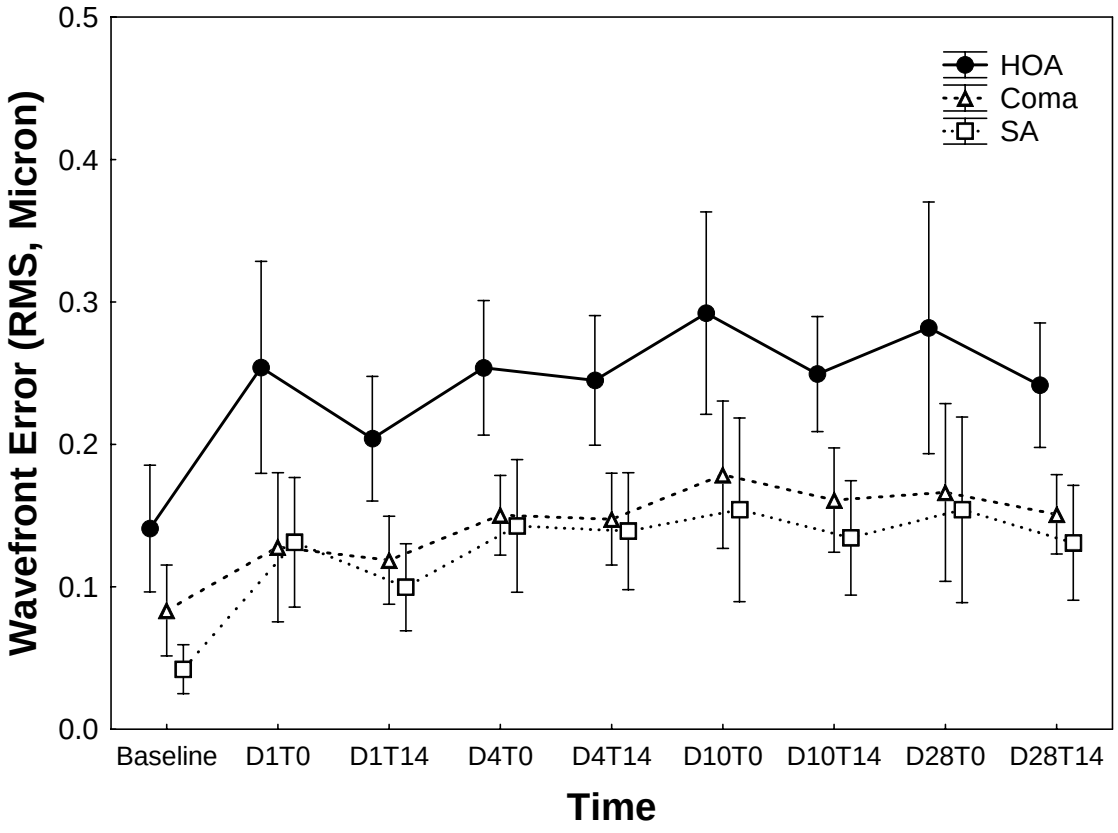

Figure 6-8. Higher order aberrations (HOA), coma and spherical aberration (SA) increased significantly during the study period. D1T0, immediately after the lens removal on day 1. D1T14, 14 hours without lens wear on day 1, etc. Error bars: 95% confidence intervals.

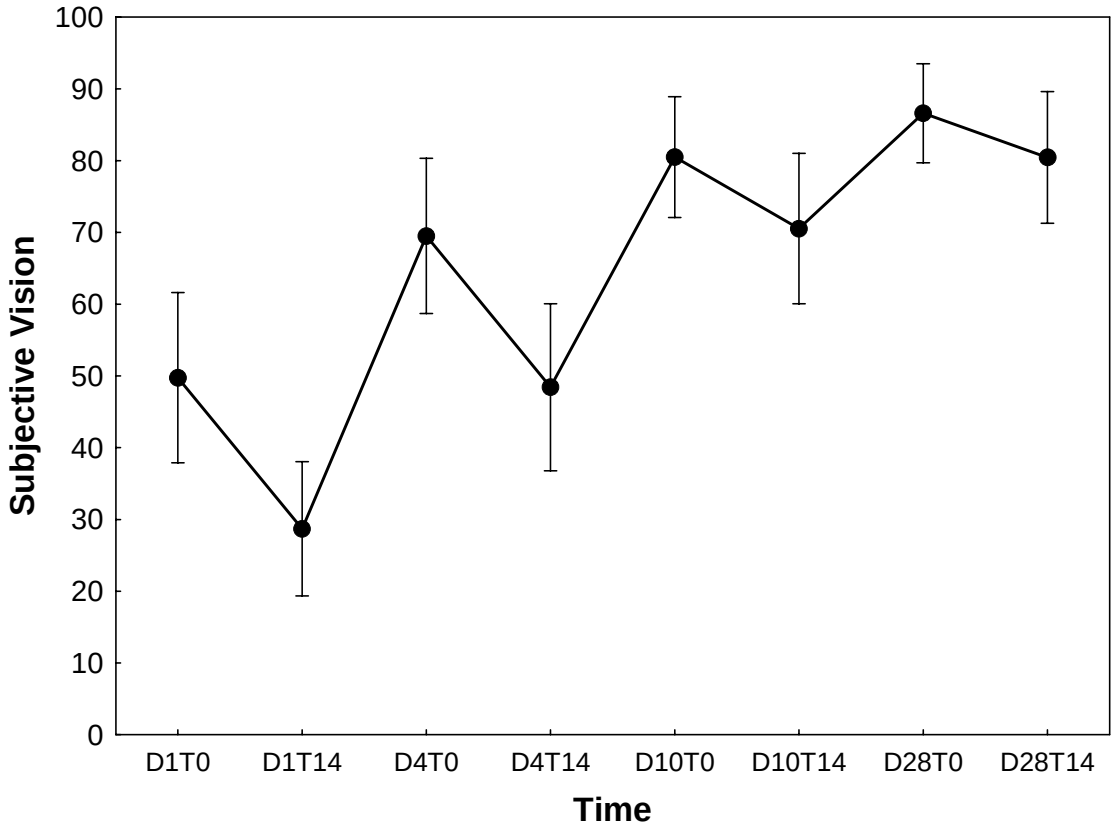

Figure 6-9. Subjective vision improved significantly during the study period. D1T0, immediately after the lens removal on day 1. D1T14, 14 hours without lens wear on day 1, etc. Error bars: 95% confidence intervals.

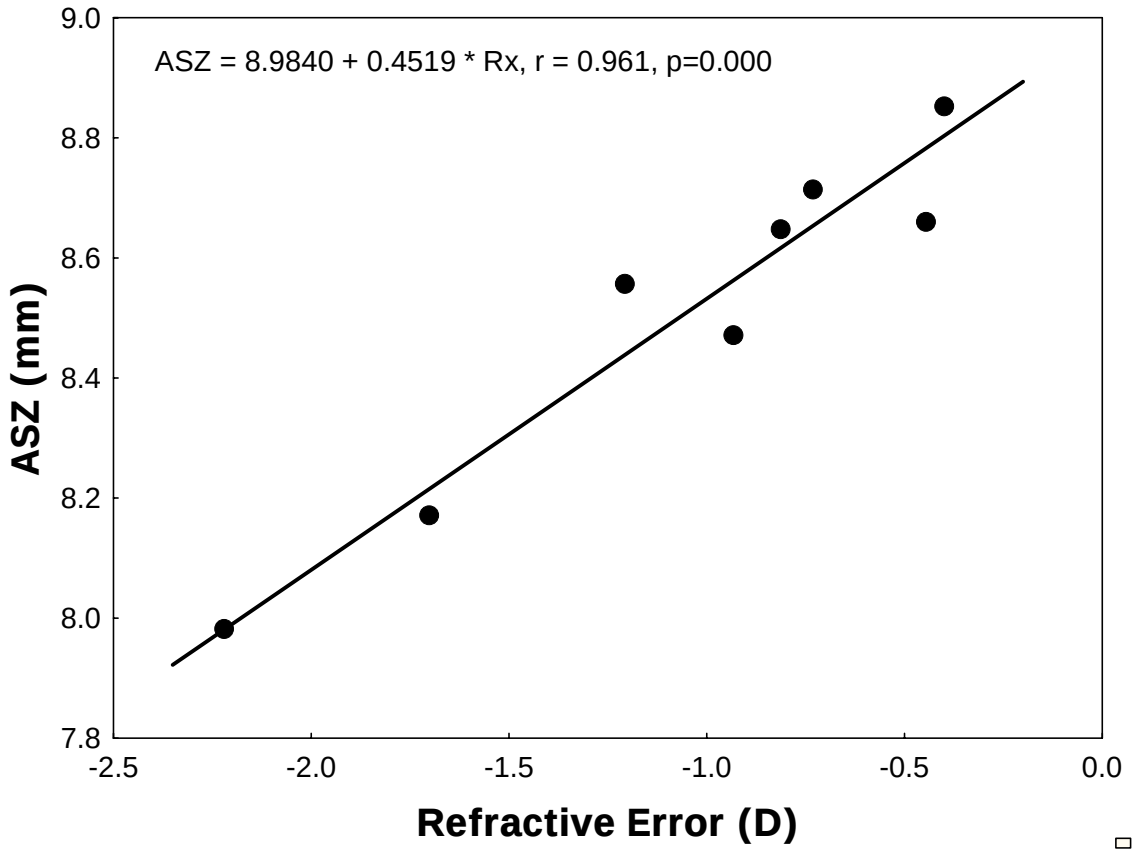

Figure 6-10. The relationship between the annular steepened zone (ASZ) and residual refractive error (spherical equivalent). Each datum is the average of the 23 subjects. The mean of the ASZ diameter and refractive error after eye opening (T0min) and after 14 hours (T14h) on 4 different days are graphed. The larger the ASZ, the lower the residual refractive error.

Table 6-3. The relationship between the TZ and visual, optical and subjective performance.

Performance		Visual		Subject-ive	Optical						
		HCVA	**LCVA**	**SV**	**Rx**	**TA**	**Defo**	**Asti**	**HOA**	**SA**	**COMA**
CFZ	r	-0.652	-0.701	0.862	0.726	-0.707	-0.735	0.926	0.787	0.735	0.687
	p	0.080	0.053	0.006*	0.042*	0.050*	0.038*	0.001*	0.020*	0.038*	0.060
ASZ	r	-0.953	-0.953	0.902	0.961	-0.952	-0.944	0.590	0.692	0.861	0.858
	p	<0.001*	<0.001*	0.002*	<0.001*	<0.001*	<0.001*	0.124	0.057	0.006*	0.006*

HCVA/LCVA, high/low contrast visual acuity. SV, subjective vision. Rx, refractive error. TA, total aberrations. Defo, defocus. Asti, astigmatism. HOA, higher order aberrations. SA, spherical aberration. CFZ, central flattened zone. ASZ, the diameter of annular steepened zone. r: Pearson correlation coefficient. p: p value. *: statistically significant.

Discussion

Generally, the cornea is steeper centrally and flattens towards the periphery (Dingeldein and Klyce, 1989; Bogan et al., 1990; Hayashi et al., 1995; Somani et al., 2004; Yebra-Pimentel et al., 2004). CRT®, a corneal reshaping method, reduces myopia by flattening the cornea centrally and steepening the mid-peripheral area (Figures 6-1 and 6-2) (Dave and Ruston, 1998; Swarbrick et al., 1998; Nichols et al., 2000; Sridharan and Swarbrick, 2003; Tahhan et al., 2003). Therefore, after successful CRT®, corneal topography images should have a new appearance, the pattern illustrated in the top right panel in Figure 6-1.

The dynamic characteristics of TZ diameter (both chronic – over weeks and acute – during each day) points to the balance of corneal shape alteration during lens wear and corneal shape regression after lens removal. When a corneal reshaping lens is worn, it affects central and non-central cornea differently (Alharbi and Swarbrick, 2003; Wang et al., 2003; Caroline and Choo, 2003). The tear film hydraulic force underneath the lens has been described by Mountford (Mountford, 2004b), and the effect of lid tension through the contact lens has been hypothesized to induce squeeze pressure (Lieberman and Grierson, 2000; Ehrmann et al., 2001; Mountford, 2004b) on central epithelial cells. The general effects of the these forces and pressures to induce structural changes have been supported by histological (Matsubara et al., 2004; Choo et al., 2004c) and morphological studies (Swarbrick et al., 1998; Alharbi and Swarbrick, 2003; Wang et al., 2003; Haque et al., 2004b; Wang et al., 2004; Ladage et al., 2004). Morphological studies (Swarbrick et al., 1998; Wang et al., 2003; Alharbi and Swarbrick, 2003) have also indicated stromal involvement in corneal reshaping. In addition, post corneal reshaping recovery studies

(Wang et al., 2003; Barr et al., 2004; Haque et al., 2004b; Soni et al., 2004; Sorbara et al., 2005) have demonstrated that recovery of corneal curvature, thickness, visual acuity, and refractive errors occurs gradually. Visual acuity returns to approximately 90% of baseline after two weeks without lens wear (Soni et al., 2004), suggesting stromal changes might be also involved in corneal reshaping. This inference rests on indirect evidence: After one week without lens wear (Matsubara et al., 2004), rabbits' epithelium returns to normal [but the rabbits' epithelium is slightly thinner than the humans' (Li et al., 1997; Reiser et al., 2005)]. Corneal epithelial turnover occurs in 5 to 7 days (Gipson, 1994) although not necessarily with contact lens wear (Lemp and Gold, 1986; Ladage et al., 2003). Therefore, if corneal reshaping only involved the epithelium, these parameters would be expected to return to baseline by one week without lens wear.

Corneal shape regression after lens removal involves a number of possible stromal and epithelial mechanisms. These include changes in redistribution and reduction of stromal water and the realignment of fibrils. In addition, corneal epithelial cells naturally migrate continuously, centripetally (Ren and Wilson, 1996; Davanger and Evensen, 1971; Estil et al., 2000), and vertically (Ren and Wilson, 1996; Estil et al., 2000; Ladage et al., 2003) and are shed (Lemp and Mathers, 1989; Ren and Wilson, 1997), so that the epithelium reverts to its original configuration. Regardless of how the recovery occurs (since it is likely that recovery involves a complex interaction among multiple mechanisms), the processes result in a tendency to return to the original corneal morphology once the lens is removed.

We showed that the change of corneal shape was accompanied by alteration in the ocular aberration. After CRT®, the total aberration decreased over the study period primarily because of a decrease of defocus, the major component of the ocular aberrations in this group

of myopes. The ratio of the defocus to the total aberration was 98.6% at baseline and 76.5% on day 28 (Figure 6-7). At the same time, the HOA, including coma and SA, increased (Figure 6-8). This increase in HOA is in accord with results of others (Joslin et al., 2003; Berntsen et al., 2005).

SA was the major component of HOA induced after CRT®, increasing by a factor of 3.84. SA is low in the population (Williams et al., 2000) and is believed to be largely due to the corneal and crystalline lens shape (Artal and Guirao, 1998; Artal et al., 2001) and refractive index (Vasudevan et al., 2004). It has been hypothesized that the cornea reduces the overall ocular SA by its aspheric shape (or a prolate ellipse), which is steeper centrally and flatter in the periphery (Somani et al., 2004; Yebra-Pimentel et al., 2004), and perhaps by a variation of the refractive index across the cornea (Vasudevan et al., 2004). CRT® corrects myopia by flattening the cornea centrally and steepening the mid-periphery, a reshaping of the cornea from a prolate ellipse to a sphere or an oblate ellipse. As a result, CRT® disturbs the balance between the cornea and crystalline lens's SA. Furthermore, epithelial and extracellular fluid redistribution may also alter the refractive index across the cornea, contributing to the imbalance of the SA.

Visual analogue scales are a simple, reproducible, and quick way to measure subjective vision (Papas and Schultz, 1997; Pointer, 2004) and have been used after other corneal reshaping technique including corneal refractive surgery (Rushhood et al., 1997; Cosar et al., 2004) and after corneal diseases (Weed and McGhee, 1998; Huang et al., 2004). In this study, patients' subjective vision measured by a subjective visual analogue scale was an important factor in determining the clinical impact of corneal reshaping. In general, factors that may influence patients' subjective vision during corneal reshaping include

uncorrected refractive error, the need to wear glasses later in the day and driving and vision problems in dim light. Among these factors, the need for correction later in the day results from residual refractive error. Night driving problems and symptoms in low luminance may be due to increased HOA when the pupil is dilated (Chalita and Krueger, 2004). From day 10 onwards, the conventional refractive error was corrected to within about half a diopter of emmetropia (Figure 6-6) and HCVA was approximately 6/6 (Figure 6-5). In addition, HOAs including coma and SA increased significantly (Figure 6-8) and subjective vision was good but not optimal and was rated as 80 - 85 out of 100 (Figure 6-9). This slightly less than perfect subjective vision might be due to not only the residual refractive error (Sorbara et al., 2005), but also the increased HOAs. This was confirmed by a significant negative correlation between the SA and subjective vision immediately after the lens removal on day 28 (Subjective vision = 96.6 - 57.8* SA, r = - 0.42, p=0.045). That is, the greater amount of the SA, the worse the subjective vision. Therefore, this suggests that, in this sample, HOAs after CRT® on average accounted for 15-20% of the rating of subjective vision at most.

Corneal reshaping reduces myopia by flattening the central cornea and steepening the mid-periphery, generating TZ's. In this study, the longer the lens was worn, the larger the TZ (Figure 6-4), the lower the residual refractive error, and the better were the visual acuity and subjective vision ratings (Table 6-3), as might be expected clinically. In addition, the longer the lens was worn, the larger the TZ generated, and the greater the HOA, coma and SA induced (Table 6-3). Owen et al. (2004) found a similarly increasing TZ during 4 weeks of BE™ lens wear. However, Tahhan et al. (2003) reported no relationship between the TZ size and subjective ratings or visual acuity measurements. Their results differed from ours perhaps because of differences in when measurements were made between these two studies.

In ours, data were collected immediately after lens removal and 14 hours after no lens wear. However, Tahhan et al. (2003) collected data either within 2 hours of the subjects waking after one night of lens wear, or 8 hours after lens removal at 1 week and 1 month of lens wear. Therefore, their TZ stability may have been due to its measurement after the most dynamic phase of corneal stabilization was completed. In addition, the use of different lenses, different corneal topographers, and different topographic maps (Klein and Mandell, 1995a; Klein and Mandell, 1995b) may also be a source of this discrepancy.

The surgically induced transition zone has not been entirely ignored in the literature but it has received less attention than the ablation zone (Endl et al., 2001; Partal and Manche, 2003; Kermani et al., 2003; Macsai et al., 2004; Seo et al., 2004). Few papers (Sridharan and Swarbrick, 2003; Tahhan et al., 2003; Owens et al., 2004) on corneal reshaping have reported the CFZ, but none have mentioned the ASZ. The diameters of the CFZ and ASZ are both related to the vision, residual refractive error, and to some of the aberrations (Table 6-3). We therefore suggest that both the CFZ and the ASZ data be included in future reports of the analysis of corneal reshaping experiments.

In summary, after CRT® the TZ changed during the first 10 days of lens use. Its size was associated with VA, refractive error, aberrations and subjective vision. The concept of a TZ appears to be a useful metric of visual, optical and subjective performance in CRT® lens wearers.

Chapter 7 (CRTHDK study)

The Effect of Oxygen Transmissibility on Corneal Shape and Optical Characteristics after One Night of Corneal Refractive Therapy® Lens Wear

This paper was submitted to Optometry and Vision Science and is under revision. The coauthors, Drs. Trefford Simpson, Luigina Sorbara and Desmond Fonn, permit the microfilming of this thesis.

7.1 Abstract

Purpose: To compare the effects of two different oxygen transmissible (Dk/t) lenses on corneal shape and optical performance after one night of Corneal Refractive Therapy (CRT®) for myopia.

Methods: Twenty myopic subjects were fit with Menicon Z [MZ] (Dk/t=90.6, Paragon CRT® lenses) on one eye and an Equalens II [EII] CRT® lens (Dk/t=47.2) on the contralateral eye (eye randomized). Corneal topography, refractive error and aberrations were measured before lens insertion (baseline), and the following day after overnight lens wear, on lens removal and 1, 3, 6, 12 hours later. Root mean squared wavefront errors were measured using 4.5 mm pupils.

Results: Averaged over position and time, the horizontal corneal curvature was statistically different between the MZ and EII lens-wearing eyes (p=0.011). The central cornea flattened similarly (p=0.886) and the mid-periphery steepened in both eyes (p=0.061) from baseline. The EII lens-wearing eyes were steeper in the mid-periphery than the MZ eyes immediately

after lens removal and at the 1-hour visit ($p \leq 0.032$). Central corneal flattening and mid-peripheral corneal steepening regressed over time (all $p<0.001$) but did not recover to baseline by 12 hours (all $p<0.004$). Myopia was reduced equally by 0.61±1.07D for the MZ-lens wearing eyes and 0.61±1.09D for the EII eyes ($p=0.969$). Coma increased by 1.85X (0.056±0.081 μm) for the MZ-lens wearing eyes and 1.72X (0.048±0.084 μm) for the EII eyes (both $p<0.001$). Spherical aberration increased by 4.55X (0.101±0.077 μm) for the MZ-lens wearing eyes and 4.31X (0.085±0.076 μm) for the EII eyes (both $p<0.001$), but there were no differences between the MZ and EII eyes (all $p \geq 0.308$). Coma and spherical aberration did not return to baseline by 12 hours (both $p \leq 0.007$).

Conclusion: After one night of CRT® lens wear, changes in corneal shape were slightly different, with more mid-peripheral steepening in the lower Dk (EII) lens-wearing eyes compared to the higher Dk (MZ) lens-wearing eyes. Change in central corneal curvature and optical performance were similar in both eyes.

7.2 Introduction

The availability of high oxygen permeability (Dk) material is one of the three important advancements (Lui et al., 2000), accounting for the renewed interest in Corneal Refractive Therapy (CRT)/ Orthokeratology or non-surgical corneal reshaping (Mountford, 1997; Dave and Ruston, 1998; Swarbrick et al., 1998; Nichols et al., 2000; Rah et al., 2002; Sridharan and Swarbrick, 2003; Alharbi and Swarbrick, 2003; Tahhan et al., 2003; Wang et al., 2003; Walline et al., 2004; Barr et al., 2004; Sorbara et al., 2005). New higher oxygen transmissible (Dk/t) materials (Benjamin, 1993) are desirable to produce the least corneal swelling beyond physiological edema (Mandell and Fatt, 1965; Holden and Mertz, 1984; Harvitt and Bonanno, 1999) when using these lenses at night. Overnight lens wear induces corneal swelling over and above eye closure. Therefore, using the highest Dk/t lens materials to minimize any swelling increment would be desirable.

In conventional gas permeable (GP) polymers, a silicone-containing methacrylate has been used to provide high oxygen permeability. The greater the proportion of silicone used in the material, the higher the Dk/t, but the less the hardness and mechanical strength of the material (Hom and Bruce, 2004). GP lenses for myopic corneal reshaping have been made from relatively high Dk/t materials (Benjamin, 1993) (Dk/t: approximately 35-70) (Mountford, 1997; Wang et al., 2003; Cho et al., 2003a; Sridharan and Swarbrick, 2003; Tahhan et al., 2003; Haque et al., 2004b; Sorbara et al., 2005). A higher Dk/t GP material, Menicon Z (Tisilfocon A, Dk/t: 90.6, MZ) (Menicon Co. Ltd. Nagoya, Japan), has been developed and was approved by the FDA (U.S.) for continuous wear up to 30 days (July 12, 2002). In addition, it is claimed that MZ is the first material to possess both high oxygen

permeability and high mechanical strength (www.menicon.com). Thus, it may be a promising material for corneal reshaping.

Corneal reshaping lenses primarily alter the corneal anterior surface to correct the refractive error. The effect of higher Dk/t on corneal reshaping after overnight lens wear is largely unknown, although the effect of lower Dk/t on corneal reshaping has been studied (Swarbrick et al., 2005; Swarbrick and Lum, 2006). In this study, two lenses with identical physical lens design (Paragon CRT®), but with different Dk/t [one the Equalens II (EII) with Dk/t 47.2 units ($\times 10^{-9}$ barrers/cm), the other with Dk/t 90.6 units, MZ] were worn for a single night to examine their effects on corneal shape and optical performance.

7.3 Materials and Methods

7.3.1 Subjects

Twenty healthy myopic subjects participated in this study. Their ages ranged from 19 to 35 years (mean± SD: 24.2±3.6) and they were mostly female (13F:7M). Spherical ametropia ranged from –0.25 to –5.25D, and corneal cylinder was less than 1.50D.

The refractive error and corneal curvatures are listed in Table 7-1. There were no significant differences between the MZ and EII lens-wearing eyes (all $p \geq 0.333$).

7.3.2 Lens Characteristics and Fitting

MZ and EII lenses were manufactured in the same Paragon CRT® design by the same laboratory. A summary of the MZ and EII lens characteristics and parameters that were used is found in Table 7-2. There were no significant differences in back optical zone radius, return zone depth and landing zone angle between the MZ and EII lenses (all $p \geq 0.163$).

CRT® lens fitting could be found in Methods Chapter 3.

The number of the lens used in MZ lens-wearing eyes was 1.65±0.75 (from 1 to 3 lenses) and 1.6±0.82 (from 1 to 4 lenses) for the EII lens wearing eyes on average.

Table 7-1: Ocular Parameters (Mean ±SD, Diopter, N=20)

	Menicon Z	Equalens II	P values
Refractive Error			
Sphere	-2.70±1.45	-2.65±1.43	0.745
Cylinder	-0.54±0.43	-0.46±0.33	0.333
Auto-Keratometry			
Flat K	43.30±1.24 (40.75 to 45.25)	43.38±1.37 (40.50 to 45.37)	0.403
Flat K (mm)	7.80±0.22 (7.46 to 8.28)	7.79±0.25 (7.44 to 8.33)	0.444
Cylinder	-0.62±0.44	-0.62±0.42	0.986

Table 7-2. Nominal Lens Characteristics and Parameters

Lens	**Material**	**Dk**	**Dk/t**	**BOZR** (±SD) (mm)	**RZD** (±SD) (microns)	**LZA** (±SD) (degrees)	**CT** (mm)	**TD** (mm)
Menicon Z	Fluoro-methacrylate and siloxanylstyrene (tisilfocon A)	163	90.6	8.48±0.47 (7.6 to 9.3)	525±19 (500 to 550)	33±1.08 (31 to 35)	0.18	10.5
Equalens II	Fluorosilicone acrylate (Boston XO)	85	47.2	8.48±0.46 (7.6 to 9.3)	525±18 (500 to 550)	33.1±1.12 (31 to 35)	0.18	10.5

Dk, oxygen permeability (10^{-11} cm^2/sec).(mlO_2/ ml.mmHg). Dk/t, oxygen transmissibility (10^{-9}cm/sec).(mlO_2/ ml.mmHg). BOZR, back optic zone radius. RZD, return zone depth. LZA, landing zone angle. CT, lens centre thickness. TD, lens total diameter.

7.3.3 Study Design

This was a double masked randomized study. Paragon CRT® lenses (MZ) were fit on one eye of 20 myopes with the same CRT® design EII lenses on the contralateral eye (eye randomized). The investigators and participants were masked about which eye (right vs. left) wore which lens (MZ vs. EII).

7.3.4 Procedures

Corneal topography, wavefront errors and refractive error were measured at baseline on the night prior to lens insertion. After the lenses had settled appropriately, participants retired in our laboratory at approximately 10 p.m. and were awakened at 7 a.m. the next morning. The measurements were repeated immediately after lens removal and 1, 3, 6, 12 hours later.

7.3.5 Measurements

7.3.5.1 Corneal Topography

See Methods Chapter 3.

7.3.5.2 Aberrations

See Methods Chapter 3.

7.3.5.3 Autorefraction

See Methods Chapter 3.

7.3.6 Statistical Analysis

Repeated measures analysis of variance (RM-ANOVA) was used to examine the main effects of the lens type, time and location of corneal curvature, the aberrations and refractive error if applicable. Tukey Honestly Significantly Different (HSD) post hoc tests

were used to determine whether there were differences in corneal curvature, aberrations and refractive error over time and at different locations. Planned paired t-tests were used to test the difference between the two lens wearing eyes at baseline and to determine the treatment effect after lens wear relative to the baseline. Polynomial non-linear regression analysis was used to characterise the change of horizontal corneal curvature at different corneal positions after one night of lens wear. Differences were considered statistically significant when the likelihood of a type I error was ≤ 0.05. Data analysis was conducted using STATISTICA 6.0 (StatSoft Inc., Tulsa, Oklahoma, U.S.A.).

7.4 Results

7.4.1 Corneal Topography

Averaged over location and time, MZ and EII lens-wearing eyes' horizontal corneal curvature changes were statistically different (RM-ANOVA, $F_{(1, 19)}=8.022$, $p=0.011$). The change of horizontal corneal curvature between the MZ and EII lens-wearing eyes is illustrated in Figure 7-1. The central cornea flattened similarly from baseline in both the MZ (1.22±0.65D) and EII (1.16±0.58D) lens-wearing eyes (RM-ANOVA, $F_{(1, 19)}=0.021$, $p=0.886$, Figures 7-1,7-2,7-4), and the mid-periphery (3mm from the centre) steepened in both the MZ (0.92±1.76D) and EII (1.35±1.52D) lens wearing eyes (RM-ANOVA, $F_{(1, 19)}=3.982$, $p=0.061$, Figures 7-1,7-3,7-4). In addition, EII lens-wearing eyes were steeper in the mid-periphery than the MZ eyes immediately after lens removal and at the 1-hour visit (t-test, both $p\leq0.032$, Figures 7-3 & 7-4). These differences resolved from 3 hours onwards (t-test, all $p\geq0.081$) (Figure 7-3). The central flattening and the mid-peripheral steepening regressed over time (RM-ANOVA, $F_{(4,76)}=7.705$-8.763, both $p<0.001$) and did not return to baseline after 12 hours without lens wear (40.3 vs. 40.7% recovery centrally and 53.8 vs.

54.4% recovery mid-peripherally for the MZ and EII lens wearing eyes, respectively) (post hoc tests, all $p<0.004$, Figures 7-2 and 7-3).

Polynomial regression analysis showed that linear, quadratic, cubic and quartic components were each significant in the fit of the profiles of horizontal corneal curvature change of both the MZ and EII lens-wearing eyes (all $p\leq0.040$). The details of the regression are shown in Figure 7-4.

7.4.2 Refractive Error (Spherical Equivalent)

There was no significant difference in refractive error between the MZ and EII lens-wearing eyes at baseline (t-test, $p=0.550$) and after one night of lens wear (RM-ANOVA, $F_{(1,19)}=0.378$, $p=0.546$). The refractive error was reduced equally by 0.61±1.07D and 0.61±1.09D for the MZ and EII lens-wearing eyes, respectively (t-test, $p=0.969$). The myopic correction regressed over time (RM-ANOVA, $F_{(5,95)}=5.598$, $p<0.001$). The refractive error did not return to baseline after 12 hours without lens wear (post hoc tests, all $p\leq0.006$, Figure 7-5).

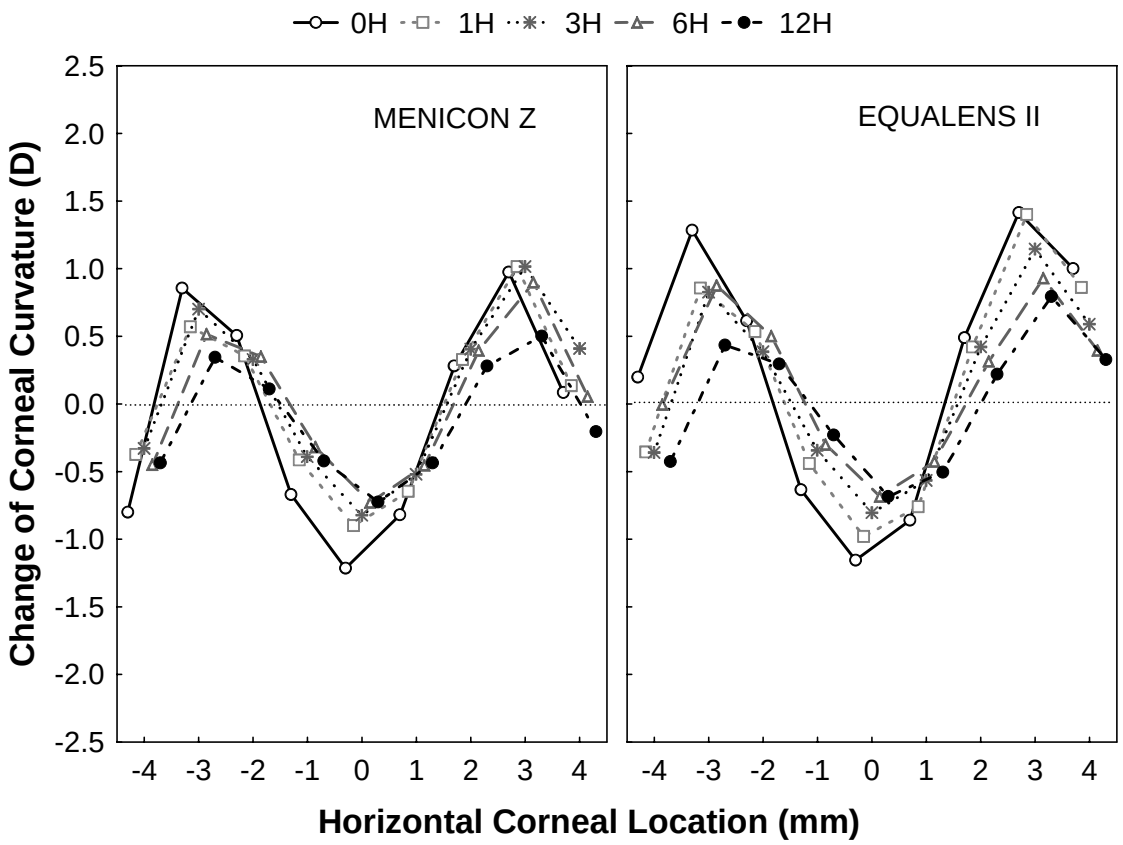

Figure 7-1. Change of the horizontal corneal curvature (D) from baseline in eyes wearing the MZ and EII lenses over time. Positive x-axis numbers refer to nasal corneal positions and negative to temporal corneal positions.

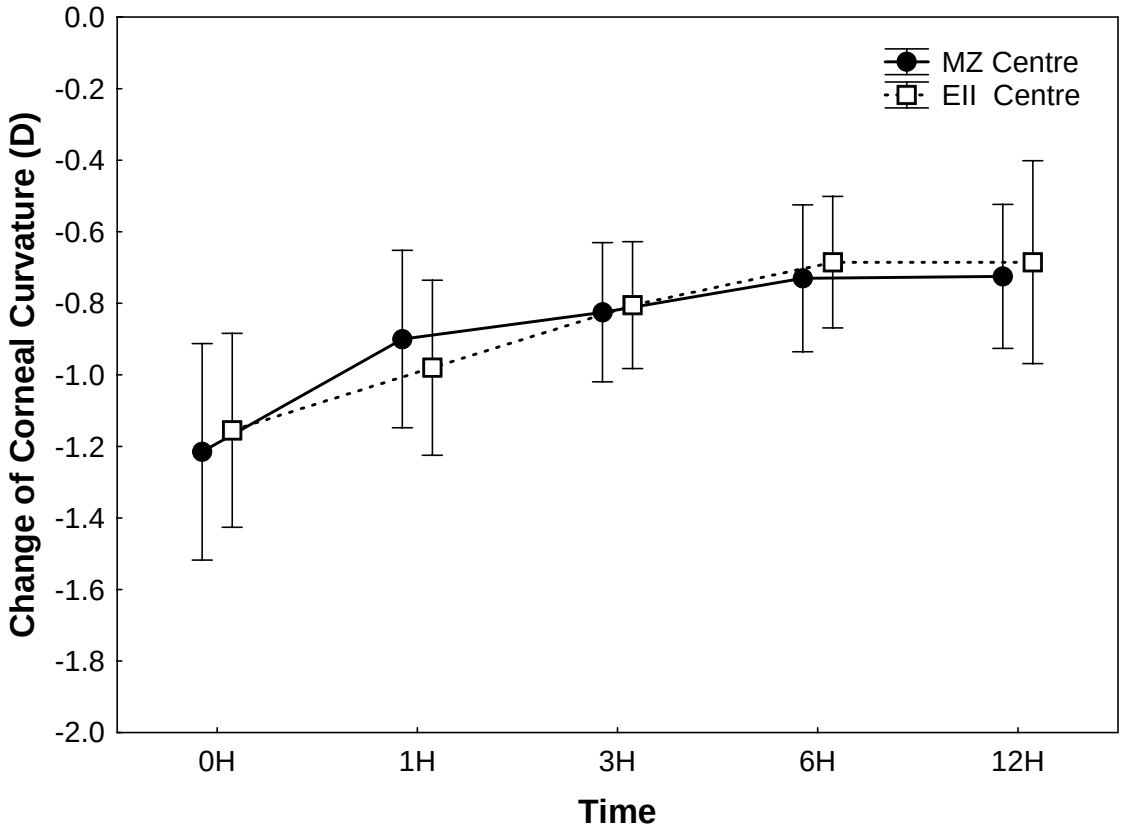

Figure 7-2. Change of central corneal curvature from baseline in the MZ and EII lens-wearing eyes over time. Error bars: 95% confidence intervals.

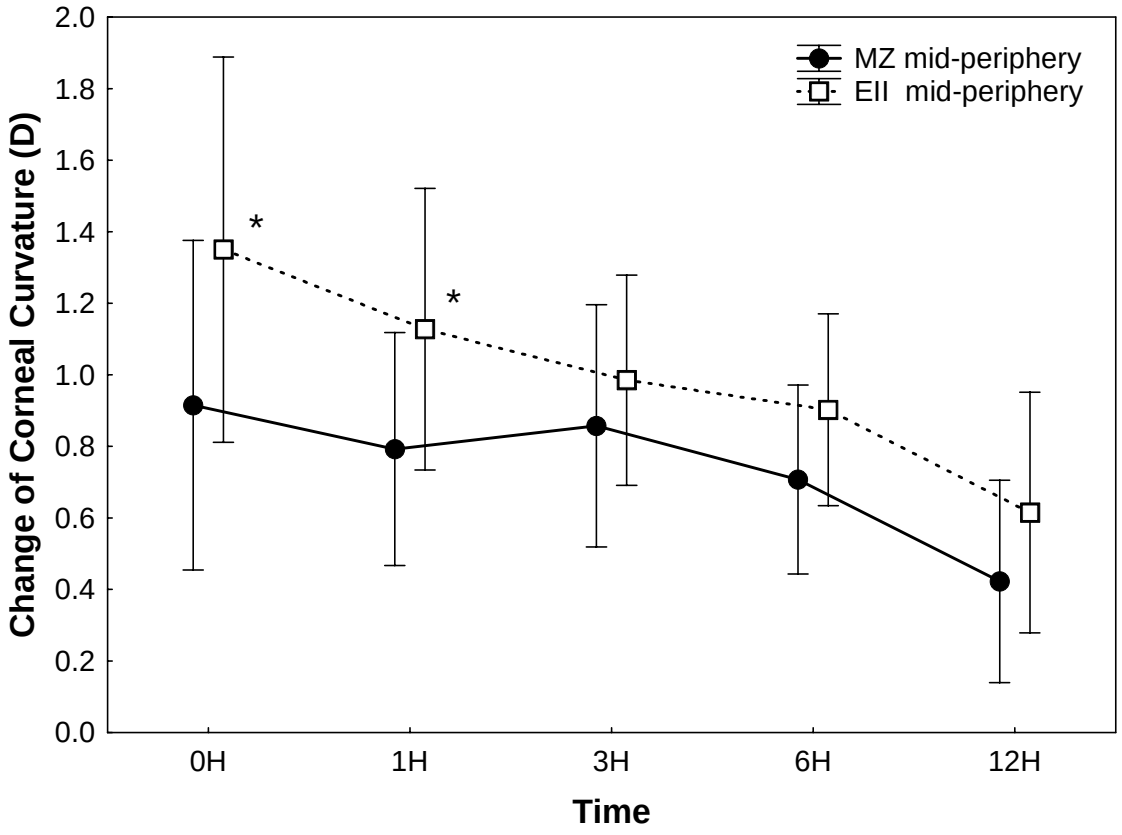

Figure 7-3. Change of mid-peripheral corneal curvature from baseline in the MZ and EII lens-wearing eyes over time. The asterisk denotes that there are significant differences in mid-peripheral corneal curvature between the MZ and EII lens wearing eyes. Error bars: 95% confidence intervals.

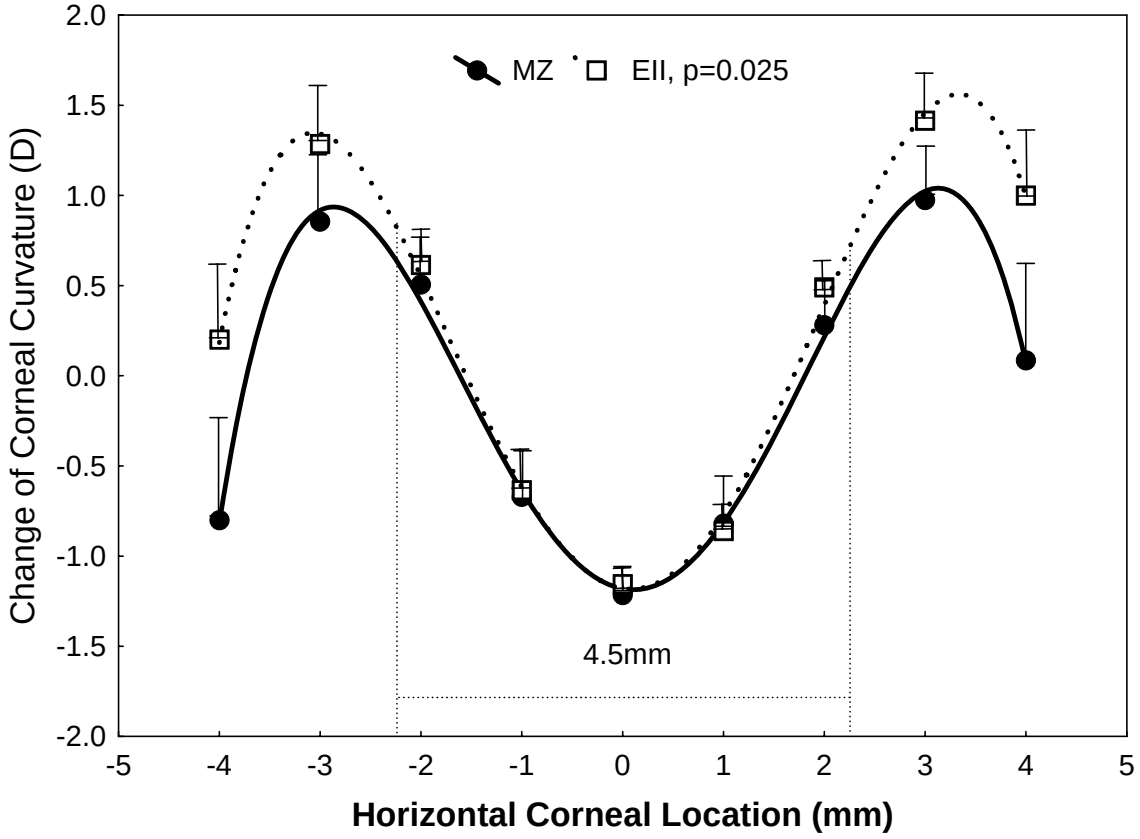

Figure 7-4. Comparison of the profile of the change of corneal curvature from baseline in the MZ and EII lens-wearing eyes immediately after lenses removal. The functions and correlation coefficients of the MZ and EII lens-wearing eyes are:

$Y_{MZ\ 0h} = -1.181-0.102*x+0.481*x^2+0.013*x^3-0.027*x^4$, R =0.998

$Y_{EII\ 0h} = -1.179-0.087*x+0.513*x^2+0.012*x^3-0.025*x^4$, R =0.998

MZ, Menicon Z. EII, Equalens II. Positive x-axis numbers refer to nasal corneal positions and negative to temporal corneal positions. Vertical dashed line denotes central 4.5 mm diameter. Error bars: standard errors.

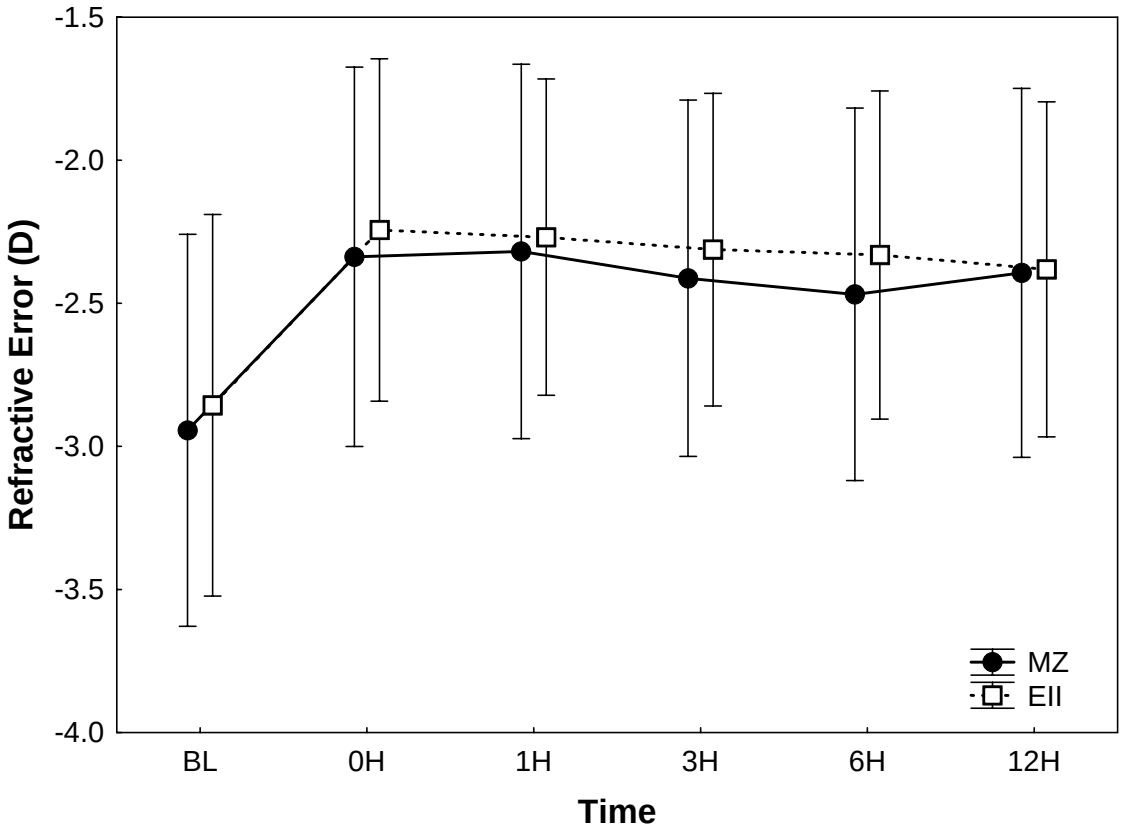

Figure 7-5. Refractive error (spherical equivalent) after one night of lens wear in MZ and EII lens-wearing eyes over time. Error bars: 95% confidence intervals.

7.4.3 Aberrations

There was no significant difference in total aberration, defocus, astigmatism, overall HOA, SA and coma between the MZ and EII lens-wearing eyes at baseline (t-tests, all $p \geq 0.338$) and after one night of lens wear (RM-ANOVA, $F_{(1,19)}=0.288$ to1.096, all $p \geq 0.308$). Total aberration decreased from 2.548±0.967 μm to 1.947±0.901 μm for the MZ lens-wearing eyes and 2.472±0.953 μm to 1.9±0.905 μm for the EII eyes (t-tests, both $p<0.001$, Figure 7-6). Defocus decreased from 2.522±0.974 μm to 1.896±0.908 μm for MZ lens-wearing eyes and from 2.442±0.967 μm to 1.844±0.911 μm for the EII eyes (t-tests, both $p<0.001$, Figure 7-7). Astigmatism did not change significantly in the MZ and EII lens-wearing eyes over time (RM-ANOVA, $F_{(5,95)}=0.614$ and 2.290, both $p \geq 0.052$, Figure 7-8). Overall HOA increased by 1.78× in the MZ lens-wearing eyes (from 0.139±0.044 μm to 0.248±0.094 μm) and 1.65× (from 0.138±0.049 μm to 0.228±0.105 μm) in the EII eyes (t-tests, both $p<0.001$, Figure 7-9). Coma increased by 1.85× in the MZ lens-wearing eyes (from 0.066±0.041 μm to 1.121±0.059 μm) and 1.72× (from 0.067±0.036 μm to 1.115±0.077 μm) in the EII eyes (t-tests, both $p<0.001$, Figure 7-10). SA increased by 4.55× in the MZ lens-wearing eyes (from 0.03±0.022 μm to 0.137±0.086μm) and 4.31× (from 0.026±0.025 μm to 0.11±0.074 μm) in the EII eyes from baseline (t-tests, both $p<0.001$, Figure 7-11). All aberrations, except for astigmatism, lasted at least 12 hours and did not return to baseline after 12 hours without lens wear (post hoc tests, all $p \leq 0.007$). The aberrations measured at different times are illustrated in Figures 7-6 to 7-11.

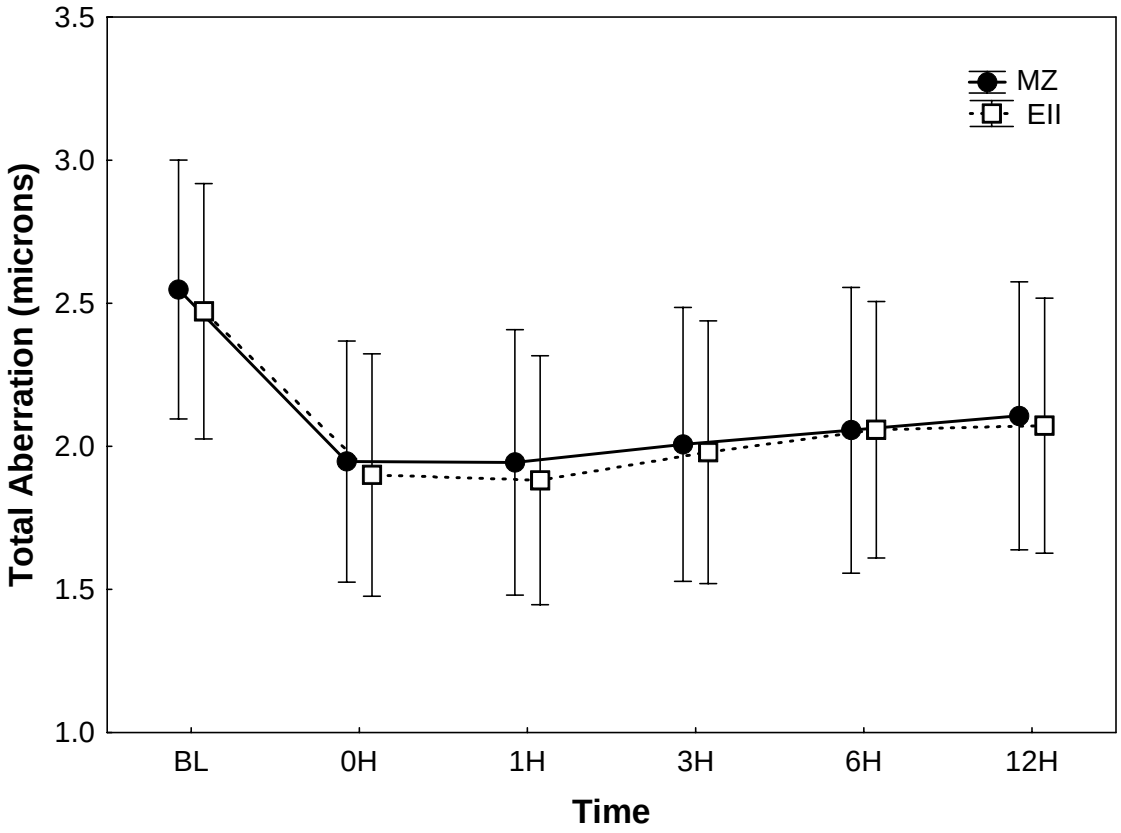

Figure 7-6. Total aberration after one night of lens wear in MZ and EII lens-wearing eyes over time. Error bars: 95% confidence intervals.

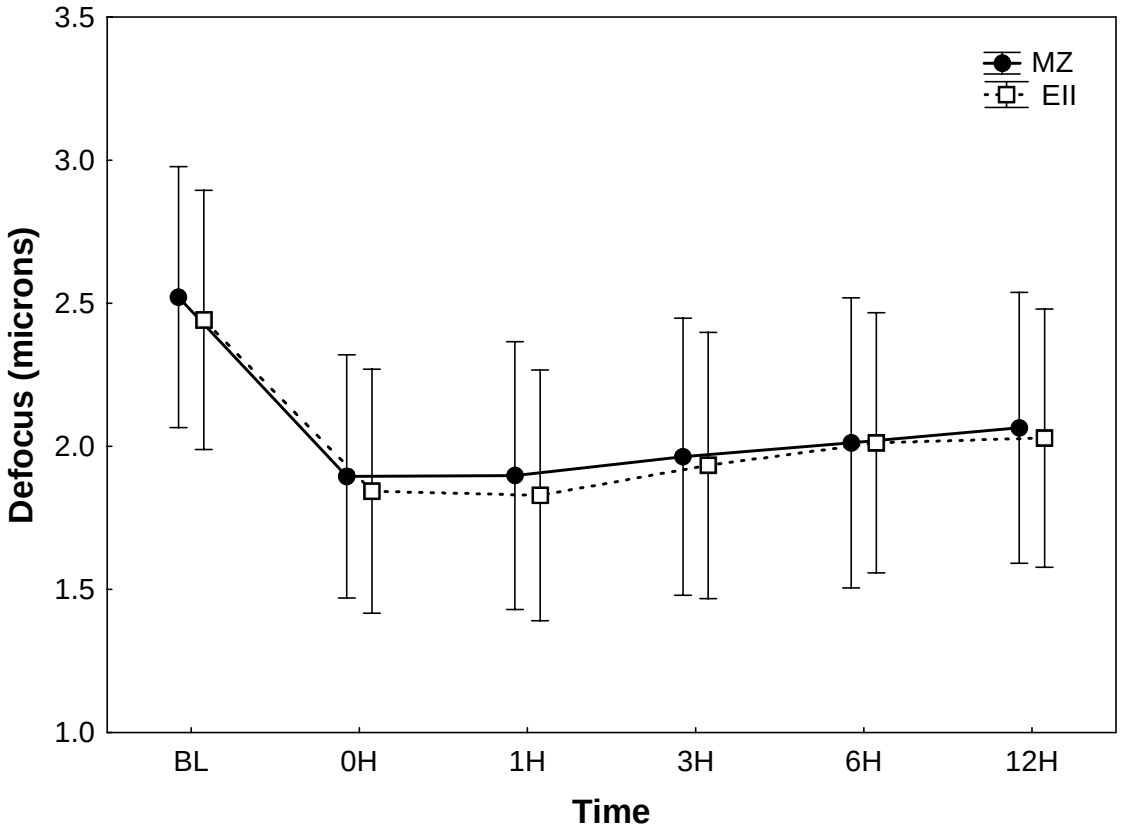

Figure 7-7. Defocus (Z_2^0) after one night of lens wear in MZ and EII lens-wearing eyes over time. Error bars: 95% confidence intervals.

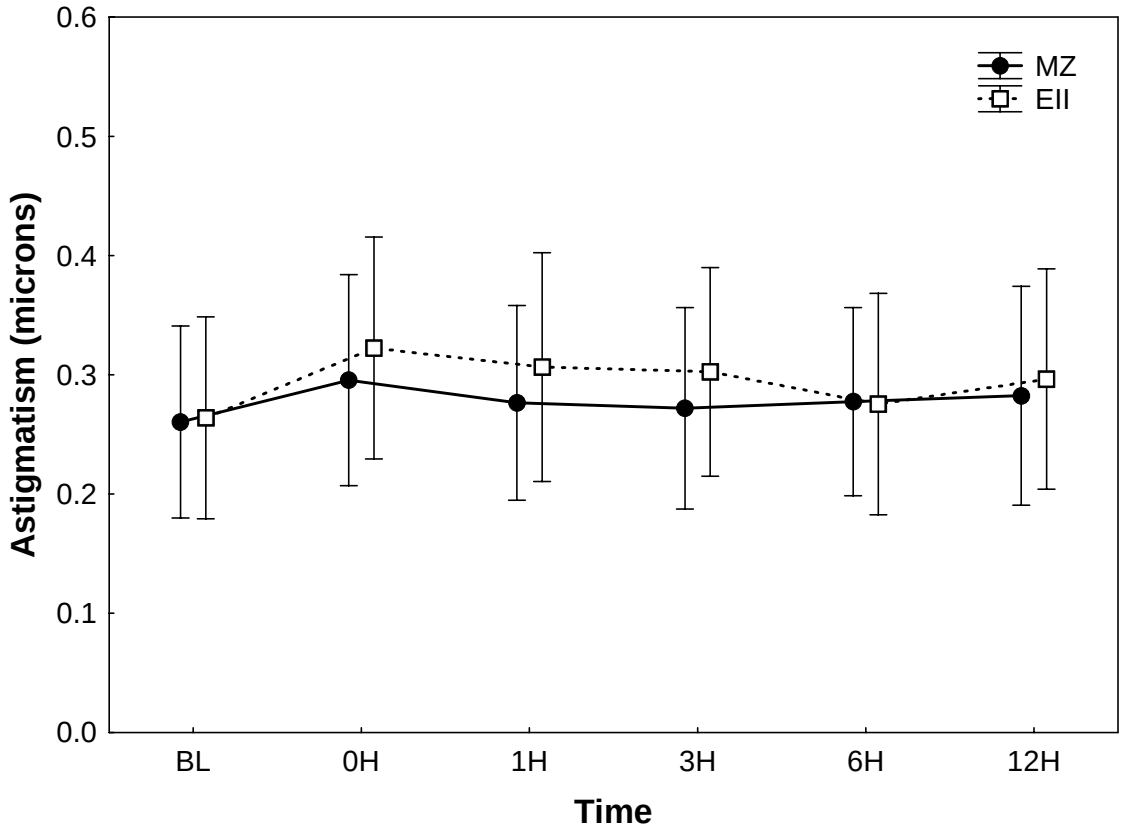

Figure 7-8. Astigmatism ($Z_2^{\pm 2}$) after one night of lens wear in MZ and EII lens-wearing eyes over time. Error bars: 95% confidence intervals.

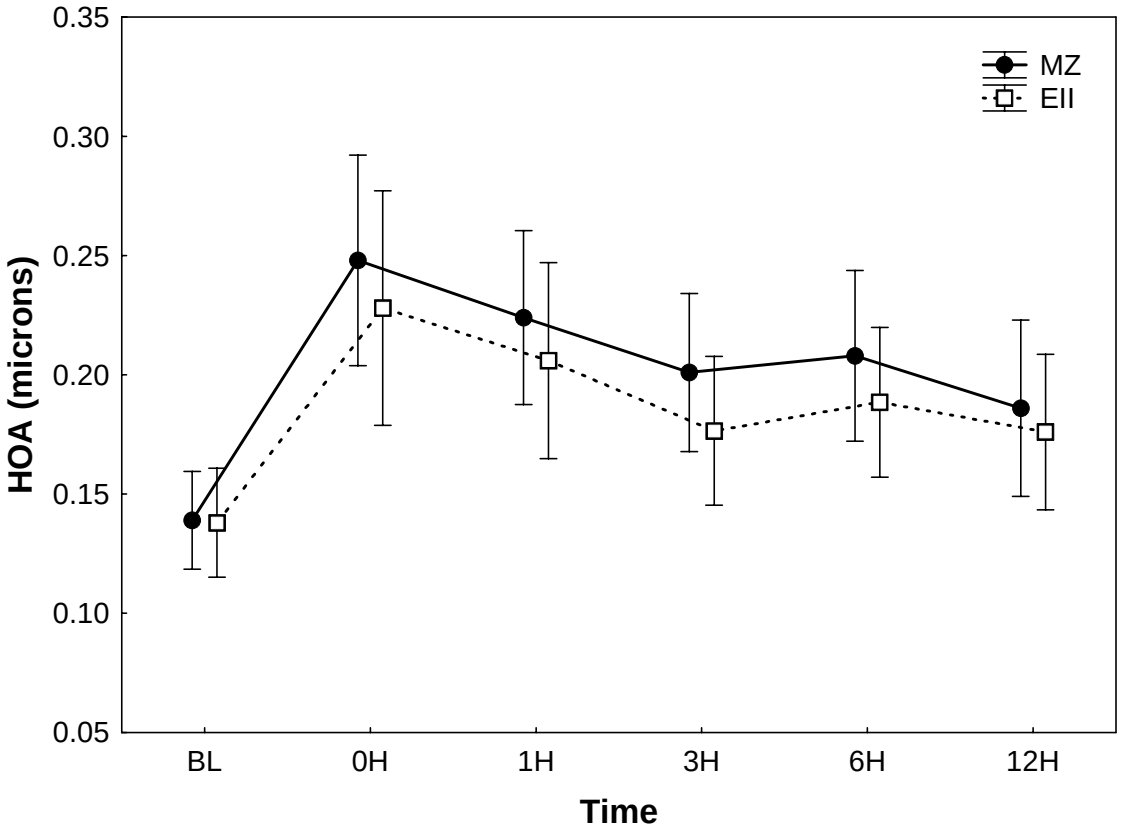

Figure 7-9. Higher order aberrations (HOA) after one night of lens wear in MZ and EII lens-wearing eyes over time. Error bars: 95% confidence intervals.

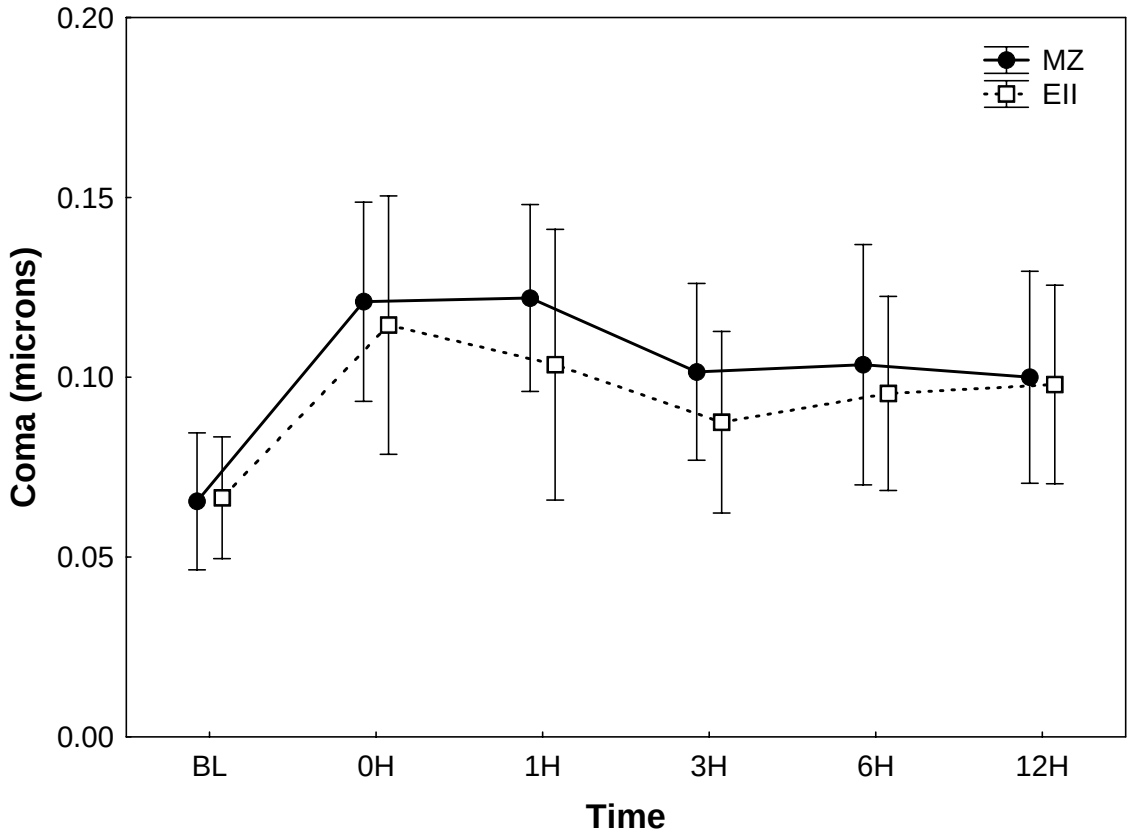

Figure 7-10. Coma ($Z_3^{\pm 1}$) after one night of lens wear in MZ and EII lens-wearing eyes over time. Error bars: 95% confidence intervals.

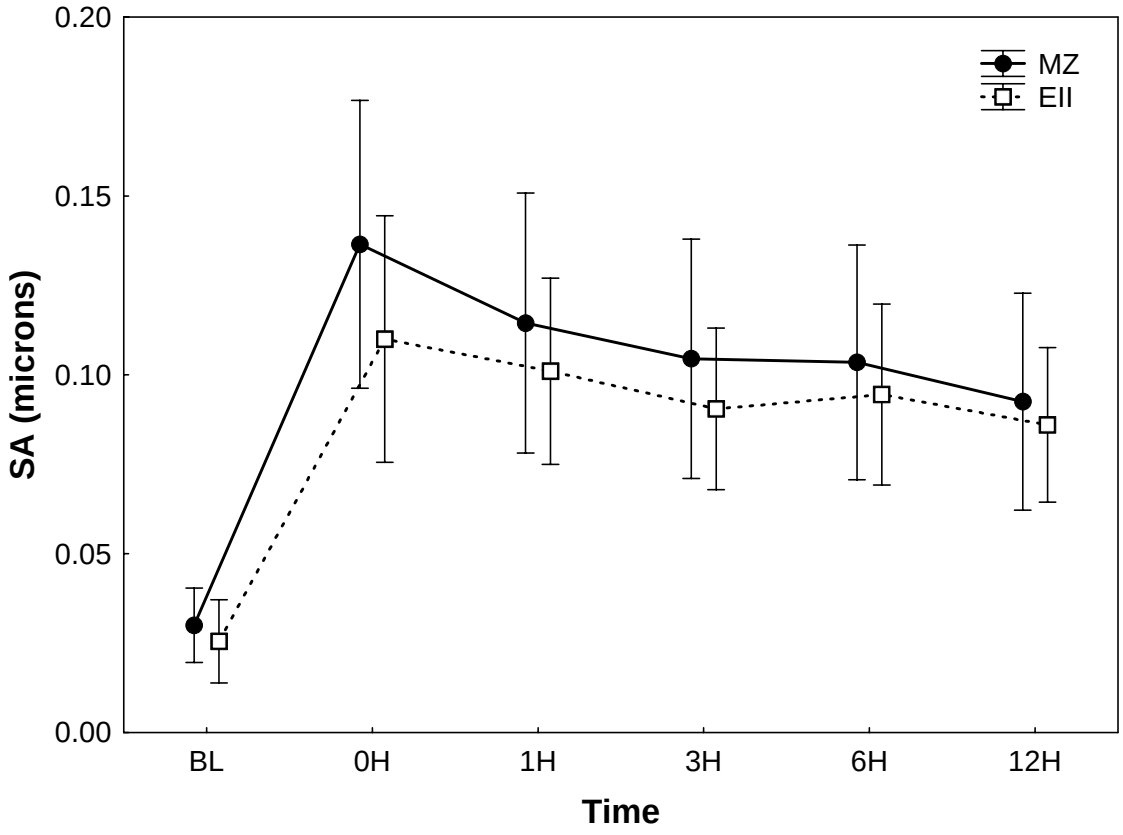

Figure 7-11. Spherical aberration (SA, Z_4^0) after one night of lens wear in MZ and EII lens-wearing eyes over time. Error bars: 95% confidence intervals.

7.5 Discussion

Corneal hypoxia and corneal health are of concern in overnight corneal reshaping. Higher Dk/t materials can provide more oxygen to the cornea and might minimize corneal swelling. However, from a clinical point of view, does a higher Dk/t lens material (MZ) have the same therapeutic effect as the lower Dk/t lens material (EII) on corneal reshaping for myopia in terms of corneal shape and optical performance?

In this study, myopia was reduced by flattening the central cornea and steepening the mid-periphery, which is similar to previous corneal reshaping studies (Swarbrick et al., 1998; Nichols et al., 2000; Sridharan and Swarbrick, 2003; Tahhan et al., 2003; Alharbi and Swarbrick, 2003). In addition, the flattening of the central cornea was similar after one night of MZ and EII lenses wear (Figures 7-1 and 7-2). This similarity of central corneal shape change may be due to the similar central compression induced underneath these two lenses, resulting in similar central epithelial thinning in the lens wearing eyes, as demonstrated using optical coherence tomography (OCT) (Haque et al., 2005). The similar central compression is presumably because of the identical physical characteristics of two lenses (Tab1e 7-2) and similar baseline corneal shape (central corneal curvature, Table 7-1) in the lens-wearing eyes.

MZ and EII lenses had different Dk/t (90.6 and 47.2 units) centrally, resulting in slightly but significantly different central corneal swelling (Haque et al., 2005), but the change of the central anterior corneal curvature was similar in the lens-wearing eyes. This similar anterior surface change may be due to corneal swelling occurring in the posterior direction (Kikkawa and Hirayama, 1970; Lee and Wilson, 1981; Moezzi et al., 2004).

Our findings differ from Swarbrick et al., who compared Boston ES (Dk/t = 8 units) to Boston XO (Dk/t = 45 units)(Swarbrick et al., 2005), and EO (Dk/t = 26 units) to Boston XO

(Swarbrick and Lum, 2006), and found apical corneal radius change differences after overnight lens wear. The difference may be due to more corneal edema induced in Boston ES and EO lens-wearing eyes compared to the Boston XO lens-wearing eyes.

When the cornea becomes edematous, the tissue fluid distribution depends on the characteristics of the stromal ground substance [e.g. hydrophilic keratan sulfate proteoglycan being located more posteriorly (Edelhauser et al., 1994)], and the balance of the external and internal pressure of the cornea. Since, in the corneal stroma, a great part of the fluid is free water, it can be moved by mechanical pressure (Maurice and Riley, 1970). The force underneath the CRT® lens will cause the fluid to flow to the site of least pressure, for instance, the post-lens space in the mid-periphery of a CRT® lens (Wang et al., 2003; Haque et al., 2004b; Haque et al., 2005; Alharbi et al., 2005; Sorbara et al., 2005). Therefore, this corneal reshaping lens induces greater edema in the mid-periphery compared to the centre, as demonstrated in previous studies (Wang et al., 2003; Haque et al., 2004b; Haque et al., 2005; Alharbi et al., 2005). The lower central and greater mid-peripheral corneal swelling is similar to that of the corneal curvature, the central corneal flattening and the mid-peripheral steepening after myopic corneal reshaping.

EII lens-wearing corneas were steeper in the mid-periphery than those wearing MZ lenses immediately after the lens removal and at 1-hour visit (Figures 7-3 and 7-4). This steepening difference in the mid-periphery may be due to the different amount of corneal swelling in the MZ and EII lens-wearing eyes, as demonstrated using the OCT (Haque et al., 2005). The steepening difference resolved after three hours without lens wear (Figure 7-3), which was consistent with the corneal deswelling time course (Feng et al., 2001; Wang et al., 2003; Haque et al., 2004b). In addition, the steepening difference also may be due to the

different amount of corneal epithelial swelling in the mid-periphery between MZ and EII lens-wearing eyes, as demonstrated using the OCT (Haque et al., 2005). Finally, it is also possible that on-eye lens flexure differences may occur in the mid-periphery due to the different materials used. The MZ lens with more silicone would be expected to have less mechanical strength (Hom and Bruce, 2004), perhaps resulting in narrower mid-peripheral post-lens space during eye closure, compared to the EII lens. We did not have the lens flexure data in the mid-periphery for these two lenses in this study.

After one night of corneal reshaping for myopia, the total aberration, defocus and refractive error decreased, and HOA (particularly SA) increased. This optical alteration was in agreement with previous reports (Joslin et al., 2003; Lu et al., 2004; Berntsen et al., 2005). In addition, the optical performance measured with 4.5mm pupils was similar after one night of MZ and EII lens wear (Figures 7-5 to 7-11). This similarity of the optical performance in the lens wearing eyes was primarily attributed to the similar anterior corneal shape change centrally (Figures 7-1, 7-2 and 7-4). The anterior corneal surface contributes greatly to the ocular aberrations, due to the greater refractive index difference between the tears and air relative to that in the posterior corneal surface and aqueous. In addition, the posterior corneal surface only contributes a small amount (2% at most) to ocular aberrations (Barbero et al., 2002).

After 12 hours without lens wear, by the time corneal edema would be expected to have resolved (Feng et al., 2001; Wang et al., 2003; Haque et al., 2004b; Haque et al., 2005), the corneal shape had not returned to baseline (Figures 7-1 to 7-3). This suggests that the corneal structural change was not solely because of the alteration in hydration. The central epithelial thinning (Alharbi and Swarbrick, 2003; Haque et al., 2004b; Haque et al., 2005)

and the mid-peripheral epithelial thickening (Haque et al., 2004b; Haque et al., 2005) did not completely return to baseline in the late afternoon, suggesting that the epithelial profile alteration is particularly important in corneal reshaping (Swarbrick et al., 1998; Alharbi and Swarbrick, 2003; Wang et al., 2003; Haque et al., 2004b; Haque et al., 2005). This corneal shape change resulting from epithelial change contributes to the maintenance of the myopic correction and optical performance in the late afternoon.

In summary, after one night of CRT® lens wear, the central cornea flattened and mid-periphery steepened. The total aberration, defocus and myopia decreased, whereas the overall HOA, coma and SA increased. In addition, optical performance and central corneal shape change was similar in the higher and lower Dk/t (MZ vs. EII) lens-wearing eyes. The mid-periphery of cornea in the lower Dk/t (EII) material lens-wearing eyes was steeper than the higher Dk/t (MZ) eyes, but these differences disappeared after three hours without lens wear.

Chapter 8 (STOK study)

Moldability of the Ocular Surface in Response to Local Mechanical Stress

8.1 Abstract

Purpose: To determine the moldability of the ocular surface by examining the acute effects of local mechanical stress on optical performance, corneal shape and corneal/epithelial thickness after corneal refractive therapy for myopia and hyperopia (CRT® and CRT®H).

Methods: 20 ametropes (spherical equivalent: - 2.08±2.31D) wore CRT® and CRT®H lenses in a random order on one eye (randomly selected). The lenses were worn for three separate time periods of 15, 30 and 60 minutes (randomly ordered, with each period taking place on a different day). Refractive error, aberrations, corneal topography, and corneal/epithelial thickness (using OCT) were measured before and after lens wear. The measurements were performed on the control eyes at 60 minutes only.

Results: With both CRT® and CRT®H lens wear, significant changes occurred in many parameters from the 15 minutes time point. The refractive error, total aberration and defocus decreased after CRT® lens wear (all $p<0.05$) and increased after CRT®H lens wear from baseline (all $p<0.05$). Astigmatism did not change (both $p>0.05$). Higher order aberrations (HOA), including coma and spherical aberration (SA), increased after CRT® and CRT®H lens wear (all $p<0.05$) from baseline, but the signed SA shifted from positive to negative after CRT®H lens wear ($p<0.05$). The central cornea flattened and the mid-periphery steepened after CRT® lens wear, whereas the central cornea steepened and mid-periphery flattened after CRT®H lens wear ($p<0.05$). The central cornea swelled less than the mid-

periphery after CRT® lens wear ($p<0.05$), whereas the central cornea swelled more than the para-central region after CRT®H lens wear ($p<0.05$). The central epithelium was thinner than the mid-periphery after CRT® lens wear ($p<0.05$) and thicker than the para-central region after CRT®H lens wear ($p<0.05$). Optical performance, corneal curvature and epithelial thickness did not change from baseline in the control eyes (all $p>0.05$).

Conclusions: CRT® lenses for myopia and hyperopia induce significant structural and optical changes in as little as 15 minutes. The cornea, particularly the epithelium, is remarkably moldable, with very rapid steepening and flattening possible in a small amount of time.

8.2 Introduction:

The characteristics of modern Orthokeratology (also known as corneal reshaping and corneal refractive therapy, CRT) of non-invasiveness, reversibility, predictability and enabling reasonable correction-free vision during waking hours has resulted in renewed interest in this modality in recent years (Mountford, 1997; Swarbrick et al., 1998; Fan et al., 1999; Nichols et al., 2000; Rah et al., 2002; Cho et al., 2003a; Alharbi and Swarbrick, 2003; Caroline and Choo, 2003; Soni et al., 2003; Tahhan et al., 2003; Wang et al., 2003; Barr et al., 2004; Cheung and Cho, 2004; Soni et al., 2004; Jayakumar and Swarbrick, 2005; Berntsen et al., 2005; Sorbara et al., 2005). Several groups have demonstrated the efficacy of myopic correction with corneal reshaping occurring after days, weeks and monthly use of the lenses (Mountford, 1997; Swarbrick et al., 1998; Nichols et al., 2000; Wang et al., 2003; Alharbi and Swarbrick, 2003; Tahhan et al., 2003; Soni et al., 2003; Sorbara et al., 2005). We and others have shown that epithelial profile alteration might play an important role in corneal reshaping for myopia (Swarbrick et al., 1998; Nichols et al., 2000; Wang et al., 2003; Alharbi and Swarbrick, 2003; Haque et al., 2004b; Jayakumar and Swarbrick, 2005) and hyperopia (Haque et al., 2004a) after overnight lens wear. A number of reports (Horner et al., 1992; Tahhan et al., 2001; Sridharan and Swarbrick, 2003; Jackson et al., 2004; Kamei et al., 2005; Jayakumar and Swarbrick, 2005) have shown how visual acuity, refraction and central corneal curvature can change after short amounts of myopic corneal reshaping lens wear. It is, however, unclear what corneal or superficial structural change (e.g. corneal/epithelial thickness) occurs on a short term basis (Jackson et al., 2004; Jayakumar and Swarbrick, 2005). Our group demonstrated that overnight corneal refractive therapy for hyperopia (CRT®H) steepened the central cornea and flattened the para-central region to correct

hyperopia or induce myopia (Haque et al., 2004a; Lu et al., 2006b; Sorbara et al., 2004). However, there have been no studies on the short-term effects of hyperopic corneal reshaping.

I therefore chose to examine the effects of brief use (15 to 60 minutes) of myopic and hyperopic corneal reshaping lenses on the same subjects with techniques allowing us to characterize the surface and structural change and optical alterations induced by the lenses.

8.3 Materials and Methods

8.3.1 Subjects

Twenty ametropes participated in this study after a screening appointment for eligibility. Their ages ranged from 20 to 39 years (mean± SD: 27.4±5.5) with 9 female and 11 male. Spherical ametropia ranged from + 1.25 to - 6.50D and the cylinder was from 0 to -2.00D. Spherical equivalent (mean±SD) of the baseline refractive error was: - 2.08 ± 2.31D.

8.3.2 Lens Characteristics and Fitting

The rigid gas permeable material used for both CRT® and CRT®H lenses (Paragon Vision Sciences, Mesa, AZ) was Paragon HDS 100 (fluorosilicone acrylate, oxygen permeability (Dk) =100 X 10^{-11} [cm^2.mlO_2]/ [s.ml.mmHg]). Both CRT® and CRT®H lenses had the same centre thickness (t) of 0.15 mm and had the same total diameter of 10.5mm. A summary of the lens characteristics and parameters that were used is found in Table 8-1.

CRT® and CRT®H lenses fitting could be found in Methods Chapter 3.

The number of the lens used in the CRT lens-wearing eyes was 1.95±0.83 (from 1 to 4 lenses) and 1.95±0.94 (from 1 to 4 lenses) for the CRTH lens-wearing eyes on average.

Table 8-1. Nominal Lenses Characteristics and Parameters

Lens	**BOZR** (±SD) (mm)	**BOZD** (mm)	**RZD** (±SD) (Microns)	**LZA** (±SD) (Degrees)	**Power** (Diopter)
CRT®	8.67±0.31 (8.0 to 9.2)	6.0	535±22 (500 to 575)	32.6±0.99 (31 to 34)	+0.50
CRT®H	7.16±0.29 (6.6 to 7.6)	5.0	685±29 (625 to 725)	33.3±0.97 (32 to 35)	-0.50

CRT, Corneal Refractive Therapy for myopia. CRTH, Corneal Refractive Therapy for Hyperopia.
BOZR, Back Optic Zone Radius. BOZD, Back Optic Zone Diameter. RZD, Return Zone Depth.
LZA, Landing Zone Angle.

8.3.3 Study Design

This was a randomized cross-over study. Twenty ametropes wore CRT® and CRT®H lenses in a random order on one eye only (eye randomly selected). The lenses were worn for three periods of 15, 30 and 60 minutes (randomly ordered) with each period occurring on a different day. The contralateral eye served as a control. Measurements were taken of the control eyes at the 60 minutes visit only.

8.3.4 Procedures

Corneal topography, root-mean-squared (RMS) wavefront errors, refractive error, and corneal/epithelial thickness were measured before lens insertion and immediately after lens removal. Lens fitting including centration, movement and fluorescein pattern was checked before participants closed their eyes and laid down on their back (with their faces up) in our laboratory.

Each study visit was scheduled after 10 a.m. to minimize the effects of diurnal variation (Cronje and Harris, 1997; Kiely et al., 1982; Feng et al., 2001). At least 24 hours (on average 72 hours) between each visit was designated to eliminate carryover effects from the previous visit. At least 48 hours (on average 72 hours) between CRT® and CRT®H lenses series was designated to eliminate carryover effects from the previous lens type. The wash out periods were based on previous short term and overnight corneal reshaping studies (Horner et al., 1992; Sorbara et al., 2004; Lu et al., 2006b; Haque et al., 2004a), which confirmed that after one day without lens wear, the induced changes would return to baseline.

After the initial study visit, i.e. from the second to the sixth visit, corneal topography was measured and the difference was determined using tangential difference maps to

determine any carry over from the previous treatment. If so, this visit was postponed until there were no differences from the previous measures of topography.

8.3.5 Measurements

8.3.5.1 Corneal Topography

See Methods Chapter 3.

8.3.5.2 Aberrations

See Methods Chapter 3.

8.3.5.3 Auto-refraction

See Methods Chapter 3.

8.3.5.4 Optical Coherence Tomography (OCT)

See Methods Chapter 3.

8.3.6 Statistical Analysis

Repeated measures analysis of variance (RM-ANOVA) were used to examine main effects of the lens type, lens wearing time, and corneal location on the wavefront errors, refractive error (spherical equivalent), and corneal curvature and corneal/epithelial thickness if applicable. Tukey Honestly Significantly Different (HSD) post hoc tests were used to determine whether there were differences among different lens wearing times and locations. Planned paired t-tests were used to determine the difference from baseline in these parameters after CRT® and CRT®H lens wear, and between the experimental and control eyes at the 60 minutes time point. A polynomial non-linear regression was used to examine the changes of the horizontal corneal curvature and corneal thickness at different corneal locations. Differences were considered statistically significant when the likelihood of a type I

error was ≤0.05. Data analysis was conducted using STATISTICA 6.0 (StatSoft Inc., Tulsa, Oklahoma, U.S.A.).

8.4 Results

The refractive error and corneal curvatures are listed in Table 8-2. There were no significant differences between the experimental and control eyes (all P≥0.143).

Table 8-2. Ocular Parameters (Mean ±SD, Diopter, N=20)

	Experimental eyes	Control eyes	P values
Refractive Error			
Sphere	- 1.85±2.31	-1.88±2.30	0.818
Cylinder	- 0.59±0.49	-0.61±0.44	0.694
Auto-keratometry			
Flat K	43.04±1.57 (40.25 to 46.37)	42.95±1.52 (40.25 to 46.12)	0.143
Cylinder	-0.66±0.47	-0.70±0.45	0.416

8.4.1 Corneal Topography

Figure 8-1 shows the corneal topographic maps before and after 30 minutes of CRT (top panel) and CRTH (bottom panel) lens wear in the same eye of a same subject (ID # 10), demonstrating that the corneal anterior surface is remarkably moldable.

8.4.1.1 Horizontal Corneal Curvature

Figure 8-2 shows that there were significant differences in the change of the horizontal corneal curvature after CRT® and CRT®H lens wear (RM-ANOVA, $F_{(1,19)}$=5.350, p=0.032). The central cornea flattened and mid-periphery (average of the temporal and nasal sides) steepened after 15, 30 and 60 minutes of CRT® lens wear, respectively (RM-ANOVA, $F_{(8,152)}$=19.481, p<0.001), whereas the central cornea steepened and para-central cornea flattened after CRT®H lens wearing (RM-ANOVA, $F_{(8,152)}$=6.570, p<0.001). The corneal curvature in the control eyes did not change from baseline (RM-ANOVA, $F_{(8,152)}$=1.633, p=0.120).

Polynomial regression analysis was used to quantify the change of horizontal corneal curvature at different corneal locations in the CRT® and CRT®H lens wearing eyes after 60 minutes. There were quadratic, cubic and quartic components in CRT® lens wearing eyes (all p≤0.022), but linear, quadratic, cubic, quartic and quintic components in the CRT®H lens wearing eyes (all p≤0.016). The functions and correlation coefficients were (Figure 8-3):

$Y_{CRT} = - 0.600 + 0.232*x + 0.291*x^2 - 0.031*x^3 - 0.016*x^4$, R=0.954;

$Y_{CRTH}= 0.106 - 0.400 *x - 0.091*x^2 + 0.118*x^3 + 0.005*x^4 - 0.006* x^5$, R=0.991.

8.4.1.2 Central Corneal Curvature

Figure 8-4 shows that there was a significant difference in the change of central corneal curvature (the average of the centre and temporal 1 mm due to slightly temporal lens

decentration) between the CRT® and CRT®H lens-wearing eyes (RM-ANOVA, $F_{(1,19)}$=159.52, p<0.001). There was no interaction between the lens type and time (RM-ANOVA, $F_{(2,38)}$=1.028, p=0.368). The central cornea flattened from baseline 0.69±0.26D, 0.71±0.47D, 0.73±0.39D after 15, 30 and 60 minutes of CRT® lens wear, respectively (t-test, all p<0.001), whereas the central cornea steepened from baseline 0.18±0.31D, 0.32±0.39D and 0.25±0.38D after CRT®H lens wear, respectively (t-test, all p≤0.019). There was no time effect after both CRT® and CRT®H lens wear (RM-ANOVA, $F_{(2,38)}$=0.107, p=0.898; $F_{(2,38)}$=1.492, p=0.238, respectively). Central corneal curvature in the control eyes did not change (t-test, both p≥0.115).

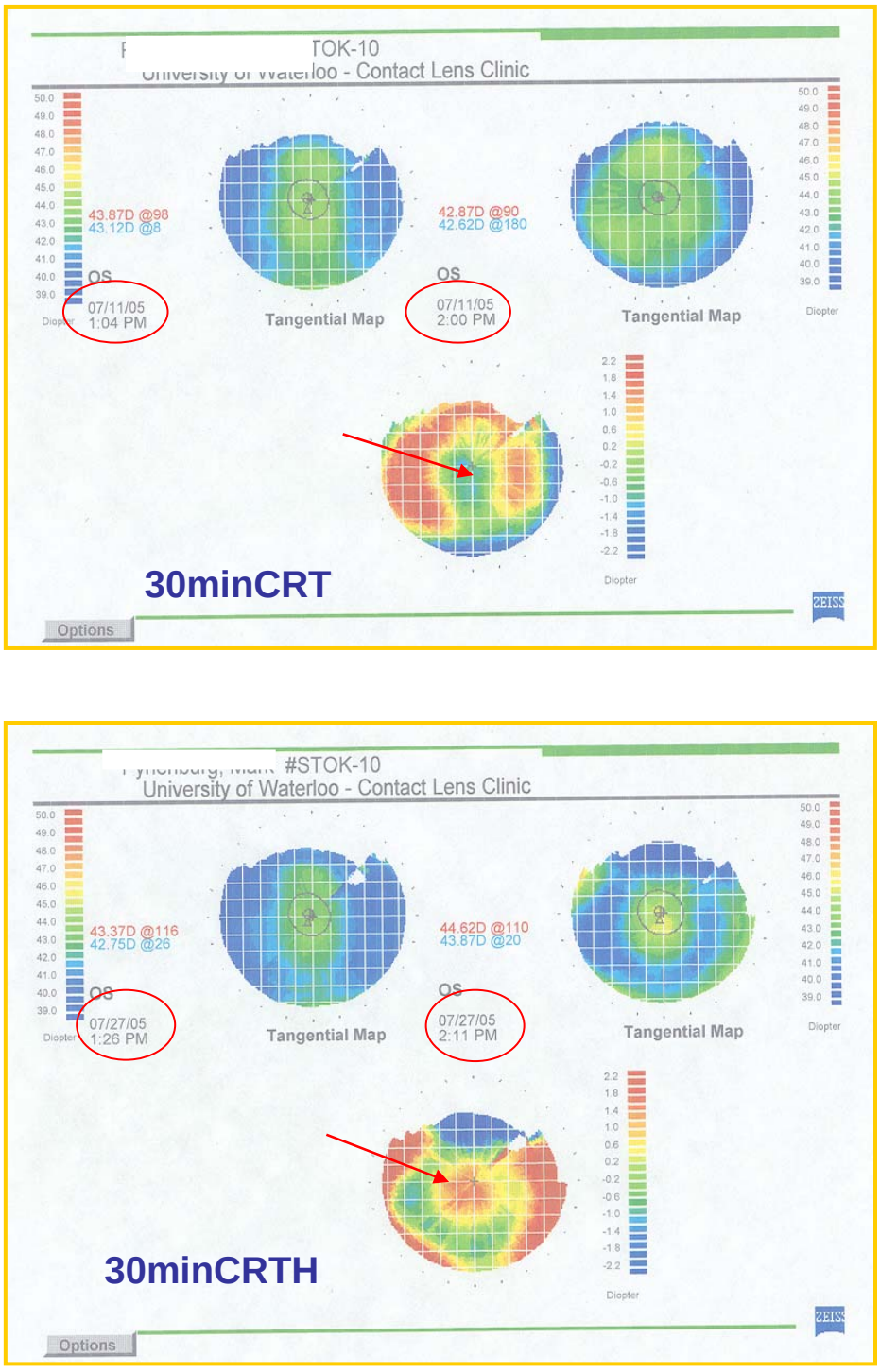

Figure 8-1. Corneal topographic maps before and after 30 minutes of CRT (top panel) and CRTH (bottom panel) lens wear in the same eye of a same subject (ID # 10). After 30 minutes of CRT lens wear, the central cornea flattened and mid-periphery steepened. However, after 30 minutes of CRTH lens wear, the central corneal steepened, the para-central region flattened and the mid-periphery steepened.

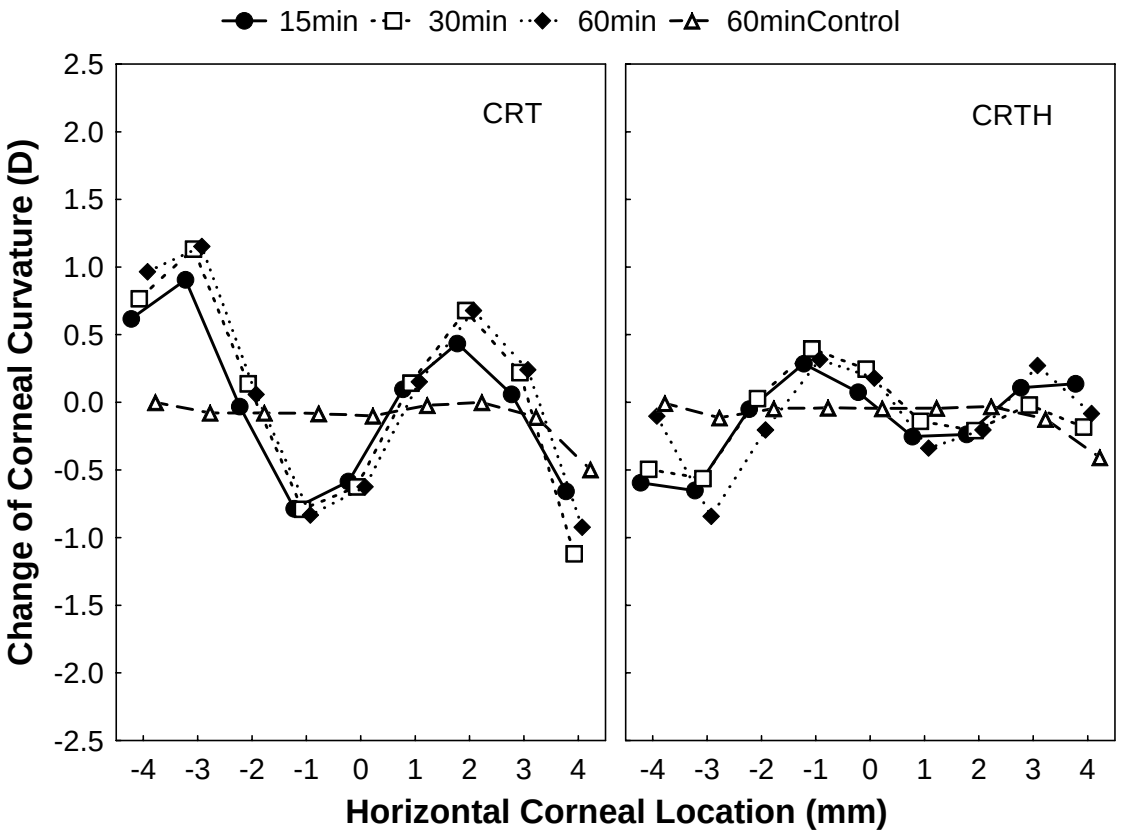

Figure 8-2. Changes of horizontal corneal curvature after 15, 30 and 60 minutes of CRT® and CRT®H lenses wear compared to controls. Positive x-axis numbers refer to nasal corneal positions and negative to temporal corneal positions.

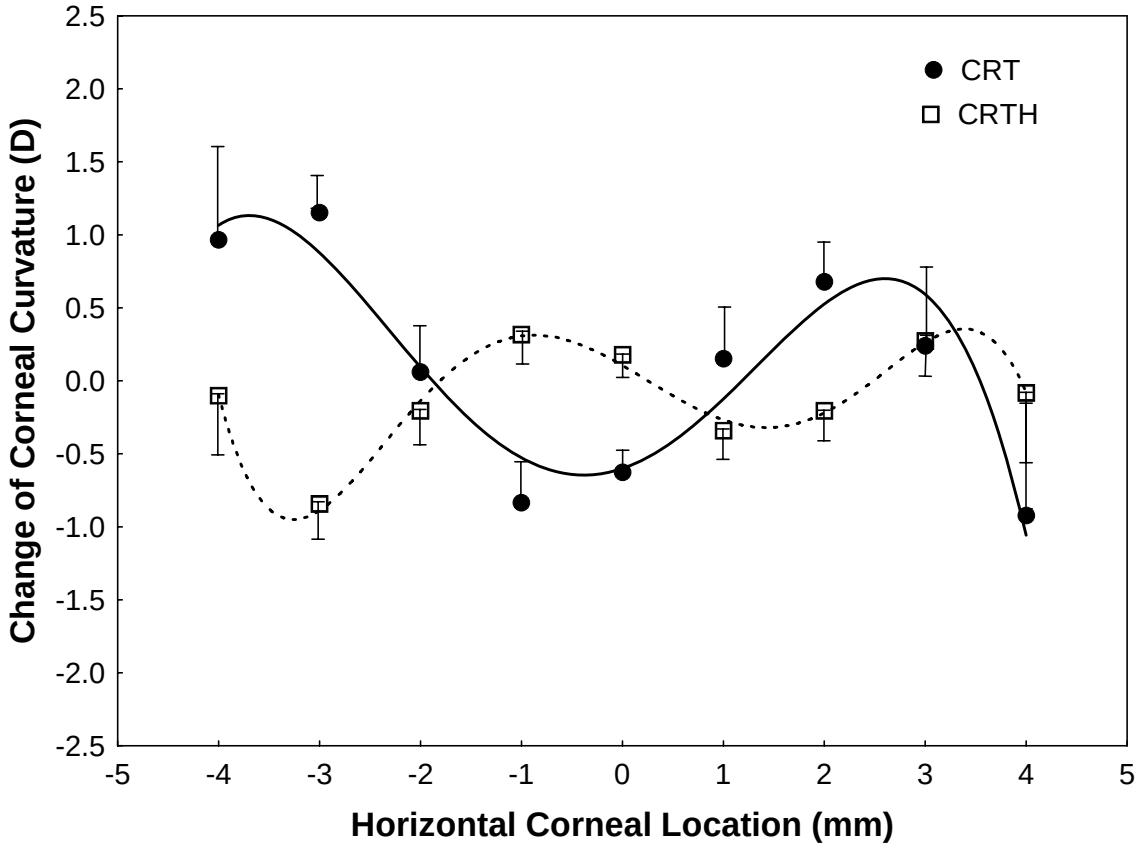

Figure 8-3. Changes of horizontal corneal curvature from baseline after 60 minutes of CRT® and CRT®H lens wear. Positive x-axis numbers refer to nasal corneal positions and negative to temporal corneal positions. Error bars: 95% confidence intervals

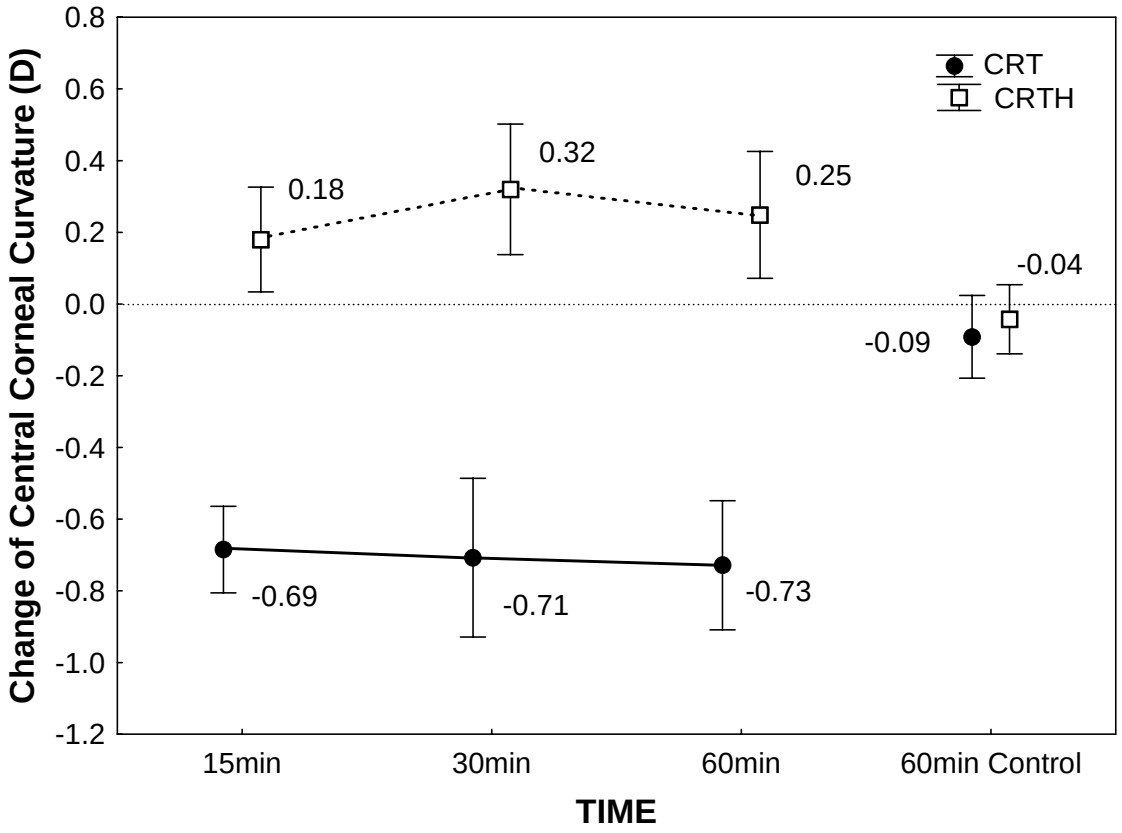

Figure 8-4. Changes of the central corneal curvature from baseline after 15, 30 and 60 minutes of CRT® and CRT®H lens wear compared to controls. Error bars: 95% confidence intervals.

8.4.2 Optical performance

8.4.2.1 Refractive Error (Spherical Equivalent)

Figure 8-5 shows that there was significant difference in the change of the refractive error after CRT® and CRT®H lens wear (RM-ANOVA, $F_{(1,19)}$=106.63, p<0.001). There was no interaction between the lens type and time (RM-ANOVA, $F_{(2,38)}$=2.785, p=0.074). Refractive error (mean±SD) decreased by 0.30±0.24D, 0.37±0.30D and 0.43±0.41D after 15, 30 and 60 minutes of CRT® lens wear, respectively (t-test, all p<0.001). Refractive error increased by 0.24±0.32D, 0.21±0.30D and 0.30±0.41D after 15, 30 and 60 minutes of CRT®H lens wear, respectively (t-test, all p≤0.005). The change of the refractive error was not significantly different at the three time points after CRT® and CRT®H lens wear, respectively (RM-ANOVA,$F_{(2,38)}$=1.778 p=0.183; $F_{(2,38)}$=0.537, p=0.589). Ametropia did not change in control eyes (t-test, both p≥0.399).

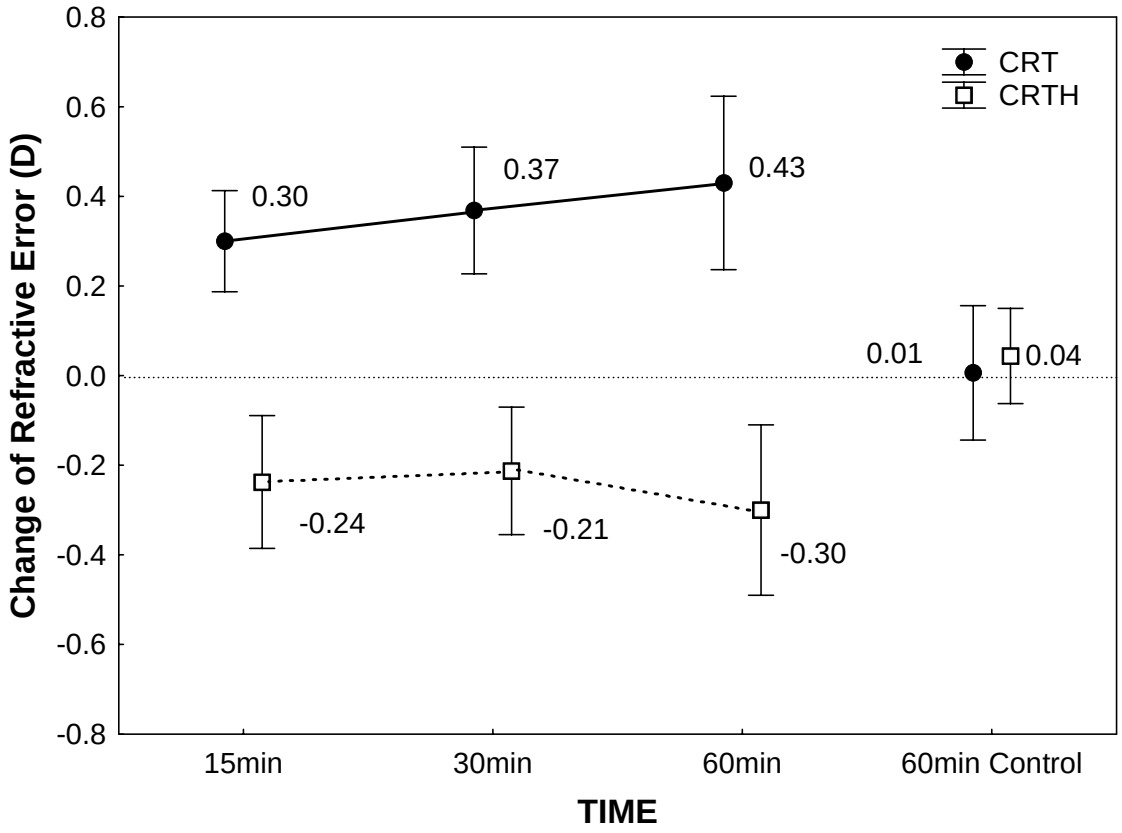

Figure 8-5. Changes of the refractive error after 15, 30 and 60 minutes of CRT® and CRT®H lens wear compared to controls. Error bars: 95% confidence intervals.

8.4.2.2 Aberrations

There were no significant differences in total aberration, defocus, astigmatism, HOAs, coma, and SA between the experimental and control eyes at baseline (t-test, all $p \geq 0.144$).

8.4.2.2.1 Total aberration

Figure 8-6 shows that there was a significant difference in the change of total aberration after CRT® and CRT®H lens wear (RM-ANOVA, $F_{(1,19)}=30.488$, $p<0.001$). Total aberration increased over time after CRT®H lens wear (RM-ANOVA, $F_{(2,38)}=7.988$, $p=0.001$), the change of the total aberration at 60 minutes being greater than at 15 and 30 minutes (post hoc test, both $p\leq0.017$). However, total aberration decreased similarly after CRT® lens wear (RM-ANOVA, $F_{(2,38)}=0.160$, both $p=0.852$). There was an interaction between the lens type and time (RM-ANOVA, $F_{(2,38)}=4.178$, $p=0.023$). A post hoc test yielded a statistically significant difference in the change of total aberration between two lenses at 15, 30 and 60 minutes (all $p\leq0.002$). Total aberration decreased by 0.131±0.295μm, 0.132±0.252μm and 0.153± 0.362μm after 15, 30 and 60 minutes of CRT® lens wear (t-test, $p=0.062$, 0.03, 0.074, respectively), and increased by 0.161±0.171μm, 0.146±0.183 and 0.312±0.152μm after CRT®H lens wear (t-test, all $p \leq0.002$). Total aberration did not change in the control eyes (t-test, $p\geq0.199$).

8.4.2.2.2 Defocus

Figure 8-7 shows that there was a significant difference in the change of defocus after CRT® and CRT®H lens wear (RM-ANOVA, $F_{(1,19)}=20.234$, $p<0.001$). Defocus increased over time (RM-ANOVA, $F_{(2,38)}=5.752$, $P=0.007$) after CRT®H lens wear. Increased defocus at 60 minutes was greater than at 15 and 30 minutes (post hoc test, both $p\leq0.028$). Defocus

decreased similarly after CRT® lens wear (RM-ANOVA, $F_{(2,38)}$=0.127, p=0.881). There was no interaction between the lens type and time (RM-ANOVA, $F_{(2,38)}$=2.828, p=0.072). Defocus decreased by 0.151±0.335μm, 0.17±0.251μm and 0.175± 0.369μm after 15, 30 and 60 minutes of CRT® lens wear, respectively (t-test, p=0.058, 0.007, 0.047, respectively), and increased by 0.144±0.204μm, 0.122±0.211 and 0.281±0.209μm after CRT®H lens wear (t-test, all p≤0.018). Defocus did not change in the control eyes (t-test, p≥0.311).

8.4.2.2.3 Astigmatism

Figure 8-8 shows that there was no difference in astigmatism after CRT® and CRT®H lens wear (RM-ANOVA, $F_{(1, 19)}$=0.367, p=0.552). Astigmatism did not change in the experimental eyes over time (RM-ANOVA, $F_{(2, 38)}$=2.119, p=0.134) and in the control eyes (t-test, all p≥0.313, except after 15 minutes of CRTH® lens wear, p=0.017).

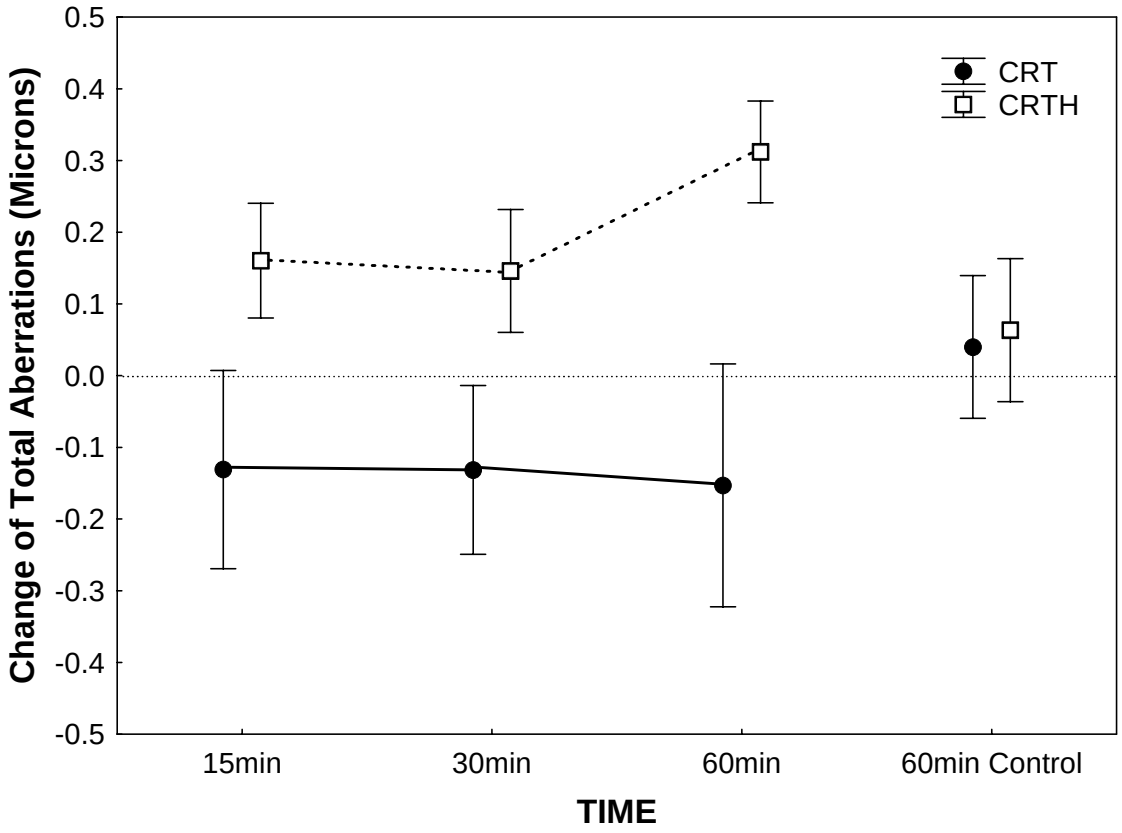

Figure 8-6. Changes of the total aberration after 15, 30 and 60 minutes of CRT® and CRT®H lens wear compared to controls. Error bars: 95% confidence intervals.

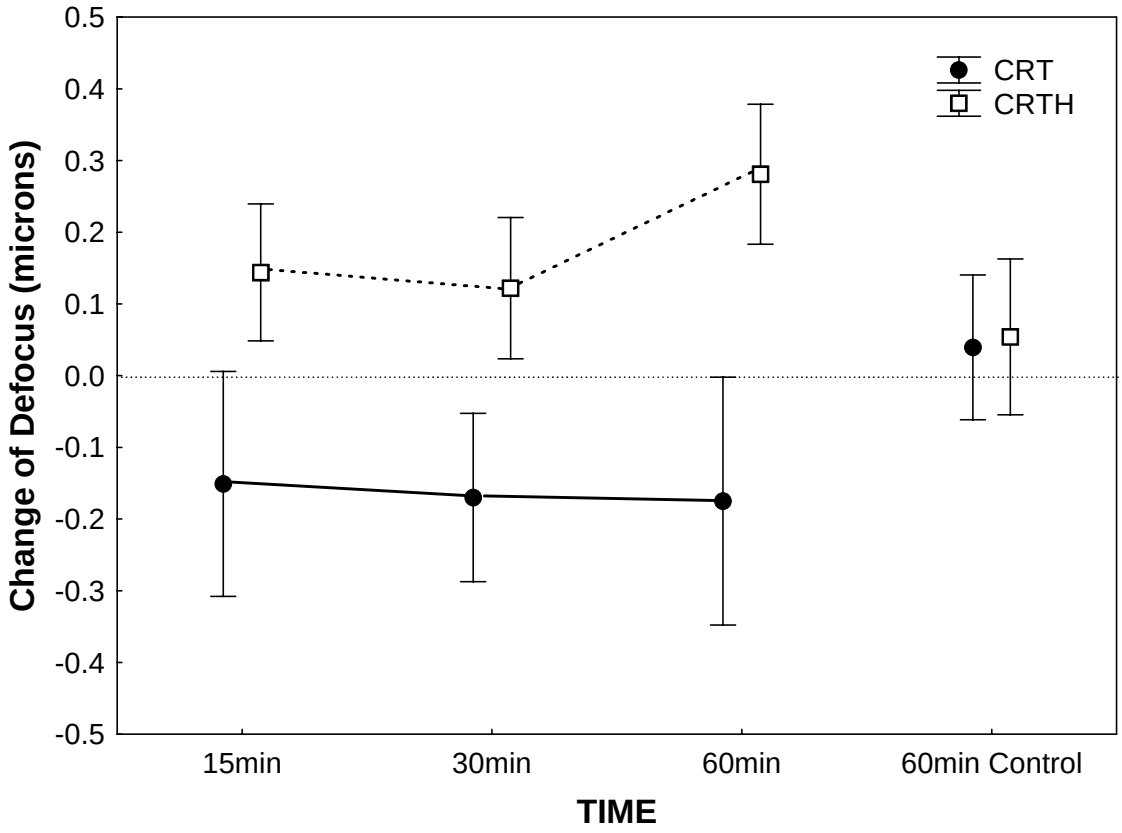

Figure 8-7. Changes of the defocus (Z_2^0) after 15, 30 and 60 minutes of CRT® and CRT®H lens wear compared to controls. Error bars: 95% confidence intervals.

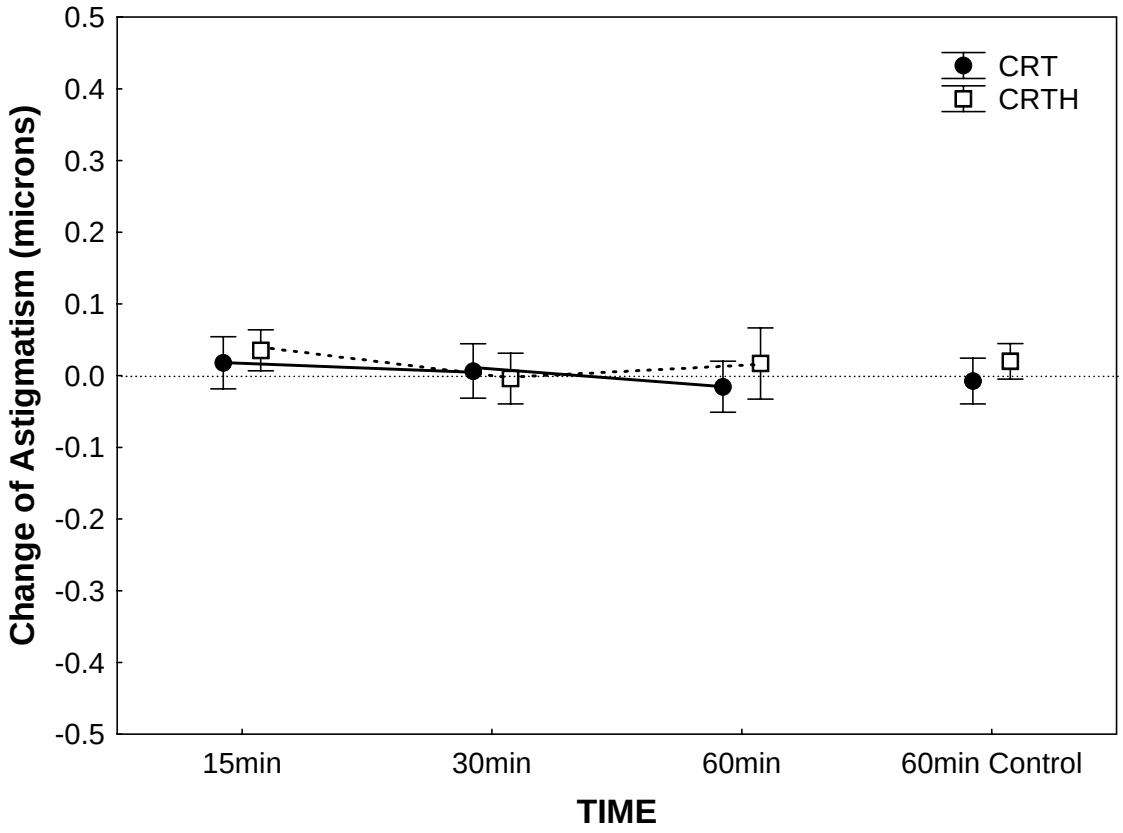

Figure 8-8. Changes of the astigmatism ($Z_2^{\pm 2}$) after 15, 30 and 60 minutes of CRT® and CRT®H lens wear compared to controls. Error bars: 95% confidence intervals.

8.4.2.2.4 Overall Higher Order Aberrations (HOAs)

There were no significant differences in overall HOAs, coma, and RMS SA between CRT® and CRT®H lens wear (RM-ANOVA, $F_{(1,19)}$=2.481 to 2.916, all p≥0.104).

HOAs increased over time (RM-ANOVA, $F_{(2,38)}$=4.290~5.959, both p≤0.021) after CRT® and CRT®H lenses wear. Post hoc tests showed that increased HOAs after CRT® lens wear at 60 minutes was greater than at 15 minutes (p=0.034). However, HOAs increased similarly after CRT®H lens wear (p≥0.187). There was no interaction among the lens type, wearing time and pre/post lens wear (RM-ANOVA, $F_{(2,38)}$=0.159, p=0.854). Figure 8-9 shows that overall HOAs increased by 0.061±0.067μm, 0.108±0.089μm and 0.125±0.082μm after 15, 30 and 60 minutes of CRT® lens wear and by 0.099±0.117μm, 0.143±0.110μm and 0.174±0.167μm after CRT®H lens wear, respectively (t-test, all p≤0.001). HOAs did not change in the control eyes (t-test, both p≥0.327).

8.4.2.2.5 Coma

Coma increased over time after CRT® lens wear (RM-ANOVA, $F_{(2,38)}$=4.085, p=0.025), and it increased similarly after CRT®H lens wear (RM-ANOVA, $F_{(2,38)}$=1.574, p=0.220). There was no interaction among the lens type, wearing time and pre/post lens wear (RM-ANOVA, $F_{(2,38)}$=0.287, p=0.752). Figure 8-10 shows that coma increased by 0.035±0.067μm, 0.068±0.094μm and 0.08±0.084μm after 15, 30 and 60 minutes of CRT® lens wear (t-test, all p≤0.031) and by 0.068±0.089μm, 0.107±0.087μm and 0.101±0.135μm after CRT®H lens wear, respectively (t-test, all p≤0.003). Coma did not change in the control eyes (t-test, both p≥0.382).

8.4.2.2.6 Spherical Aberration

Spherical Aberration (SA) increased over time after CRT®H lens wear (RM-ANOVA, $F_{(2,38)}$=8.599, p<0.001), and it increased similarly after CRT® lens wear (RM-ANOVA, $F_{(2,38)}$=1.130, p=0.333). There was no interaction among the lens type, wearing time and pre/post lens wear (RM-ANOVA, $F_{(2,38)}$=1.98, p=0.152). Figure 8-11 shows that SA increased by 0.027±0.05μm, 0.028±0.047μm and 0.044±0.054μm after 15, 30 and 60 minutes of CRT® lens wear (t-test, all p≤0.028) and by 0.037±0.061μm, 0.04±0.063μm and 0.085±0.064μm after CRT®H lens wear, respectively (t-test, all p≤0.016). SA did not change in the control eyes (t-test, both p≥ 0.290).

Figure 8-12 shows that there was no interaction between the lens wearing time and pre/post CRT®H lens wear (RM-ANOVA, $F_{(2,38)}$=1.188, p=0.316). Signed SA shifted from positive to negative by 0.055±0.089μm, 0.053±0.088μm and 0.076±0.128μm after 15, 30 and 60 minutes of CRT®H lens wear, respectively (t-test, all p≤0.016), whereas signed SA did not change in the control eyes (t-test, p=0.214).

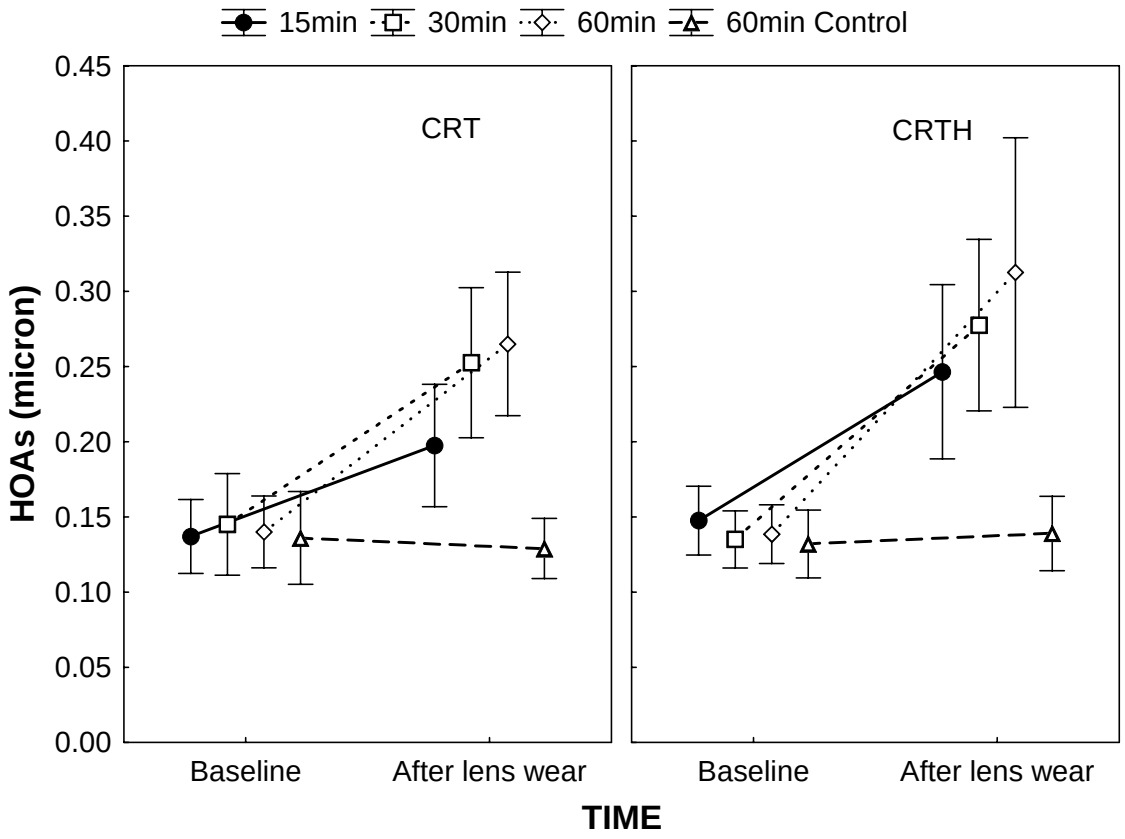

Figure 8-9. HOAs after 15, 30 and 60 minutes of CRT® and CRT®H lens wear compared to controls. Error bars: 95% confidence intervals.

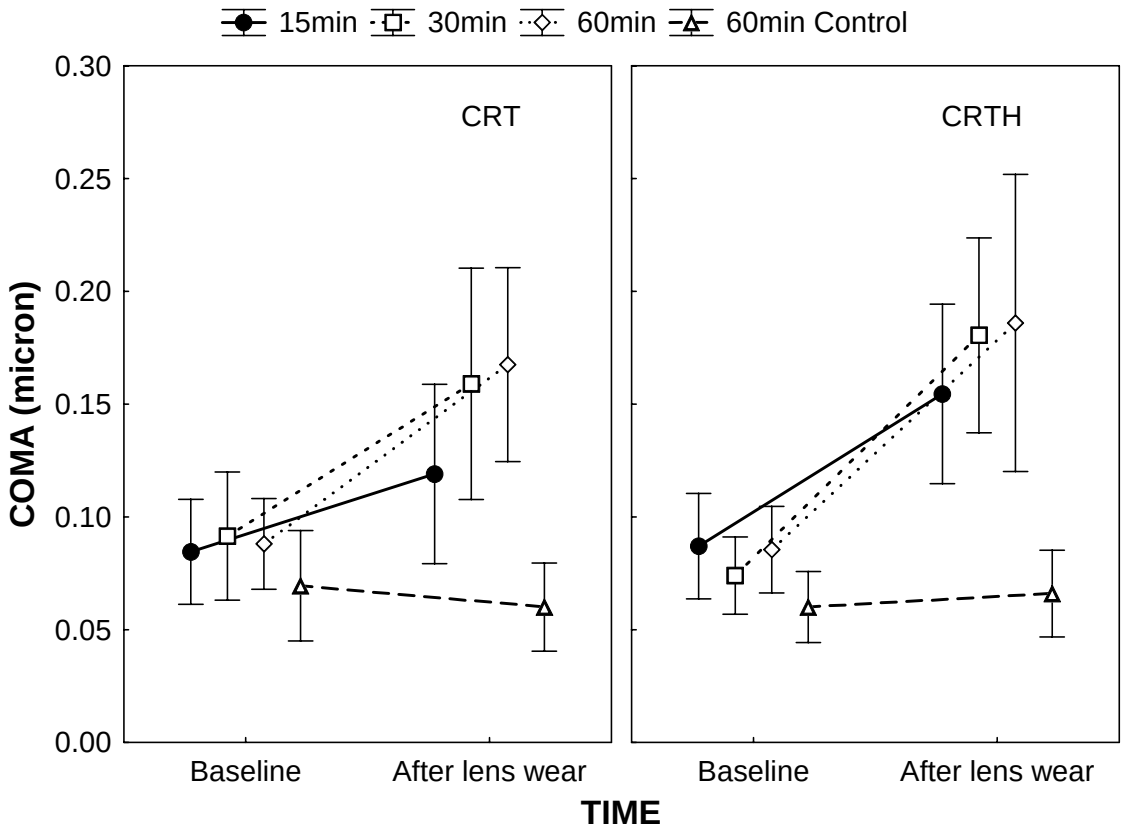

Figure 8-10. Coma ($Z_3^{\pm 1}$) after 15, 30 and 60 minutes of CRT® and CRT®H lens wear compared to controls. Error bars: 95% confidence intervals.

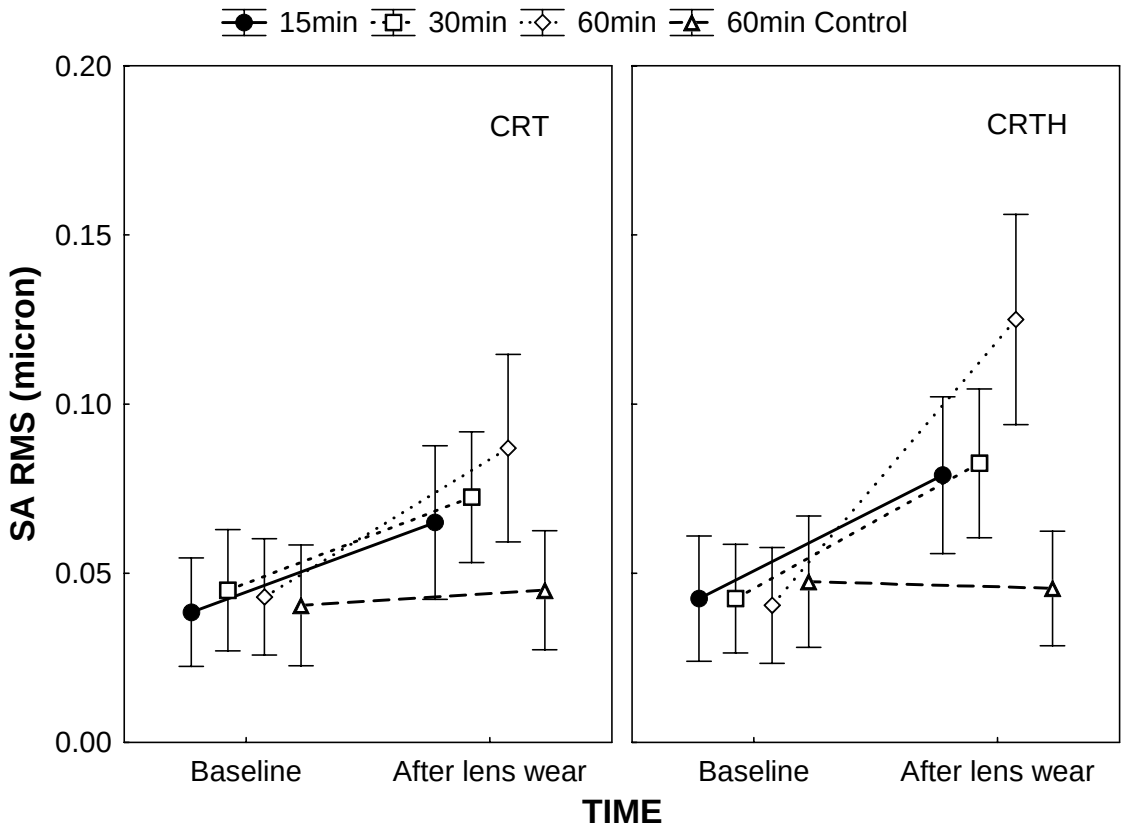

Figure 8-11. SA (RMS, Z_4^0) after 15, 30 and 60 minutes of CRT® and CRT®H lens wear compared to controls. Error bars: 95% confidence intervals.

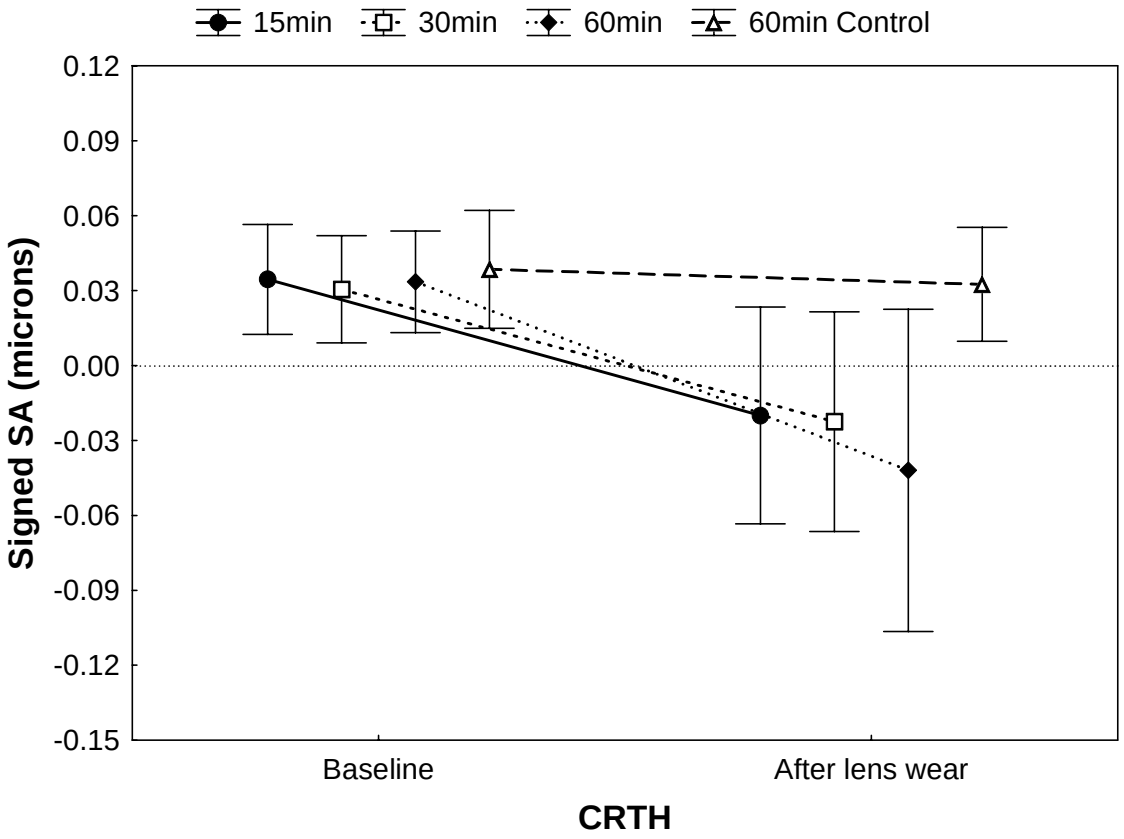

Figure 8-12. Signed SA before and after 15, 30 and 60 minutes of CRT®H lens wear compared to controls. Error bars: 95% confidence intervals.

8.4.3 Corneal and Epithelial Thickness

8.4.3.1 Corneal Swelling (Percentage Change of Corneal Thickness)

Figure 8-13 shows that after CRT® lens wear, the central corneal swelling was less than the mid-peripheral (RM-ANOVA, $F_{(1,19)}$=7.944, p=0.011). There was no significant location effect in the control eyes (RM-ANOVA, $F_{(1,19)}$=1.475, p=0.239). The central and mid-peripheral corneal swelling increased over time (RM-ANOVA, $F_{(2,38)}$= 8.839-10.828, both p<0.001). The central and mid-peripheral corneal swelling at 30 and 60 minutes was significantly greater than at 15 minutes (post hoc test, all p≤0.041). There was no interaction between the location and lens wearing time on corneal swelling after CRT lens wear (RM-ANOVA, $F_{(2,38)}$=0.034, p=0.966). The central cornea swelled by 0.40±0.25%, 1.36±0.28% and 2.00±0.28% after 15, 30 and 60 minutes of CRT® lens wear, respectively (t-test, both p<0.001, except at 15 minutes, p=0.130). After the same amount of lens wear, the mid-peripheral cornea swelled by 1.10±0.27%, 2.21±0.28% and 2.82±0.38%, respectively (t-test, all p<0.001). The control cornea swelled by 1.62±0.20% centrally and 1.22±0.23% mid-peripherally (t-test, both p<0.001). There was no significant difference in central corneal swelling between the CRT® lens-wearing eyes and control eyes after 60 minutes (t-test, p=0.246), whereas the mid-peripheral corneal swelling was greater in the CRT® lens wearing eyes than the control eyes (t-test, p=0.002), as illustrated in Figure 8-13.

After CRT®H lens wear, the central corneal swelling was greater than the mid-peripheral (RM-ANOVA, $F_{(1,19)}$=47.391, p<0.001), as illustrated in Figure 8-14. However, there was no significant location effect on the control eyes (RM-ANOVA, $F_{(1,19)}$=1.536, p=0.230). The central corneal swelling increased over time (RM-ANOVA, $F_{(2,38)}$=10.200, P<0.001). The central corneal swelling at 30 and 60 minutes was significantly greater than

that at 15 minutes, respectively (post hoc test, $p \leq 0.036$). There was no significant time effect on the mid-peripheral corneal swelling (RM-ANOVA, $F_{(2,38)}=2.567$, $P=0.090$). There was no interaction between the location and lens wearing time on corneal swelling after CRT®H lens wear (RM-ANOVA, $F_{(2,38)}=2.046$, $p=0.143$). The central cornea swelled by 1.36±0.20%, 2.34±0.14% and 3.06±0.41% after 15, 30 and 60 minutes of CRT®H lens wear, respectively (t-test, all $p<0.001$) and the mid-peripheral cornea swelled by 0.74±0.30%, 0.67±0.35% and 1.74±0.40% after 15, 30 and 60 minutes, respectively (t-test, all $p \leq 0.024$). However, the control cornea swelled by 1.28±0.30% centrally and 0.82±0.33% in the mid-periphery (t-test, both $p \leq 0.021$). The central corneal swelling was greater in the CRT®H lens wearing eyes relative to the control eyes after 60 minutes (t-test, $p=0.002$). There was no statistically significant difference in the para-central corneal swelling between the CRT®H eyes and control eyes (t-test, $p=0.064$), as illustrated in Figure 8-14.

To illustrate (in Figure 8-15) the different distributions of the corneal thickness percentage changes after CRT® and CRT®H lenses wear cross the cornea, we assumed the corneal swelling from the nasal cornea was symmetrical. Polynomial analysis was used to quantify the corneal swelling at different corneal locations after 60 minutes of CRT® and CRT®H lenses wear. There were statistically significant quadratic, quartic and sixth order components in CRT® lens wearing eyes (all $p \leq 0.001$), and quadratic and quartic components in the CRT®H lens wearing eyes (both $p \leq 0.006$). The functions and correlation coefficients were:

$$Y_{CRT}=2.003+(-0.14e\text{-}5)*x+0.514*x^2+(0.58e\text{-}6)*x^3-0.096*x^4+(-0.42e\text{-}7)*x^5+0.004*x^6,\ R=0.996;$$

$$Y_{CRTH}=3.02+(0.111e\text{-}7)*x-0.342*x^2+(-0.48e\text{-}8)*x^3+0.016*x^4+(0.245e\text{-}$$

9)*x^5,R=0.989.

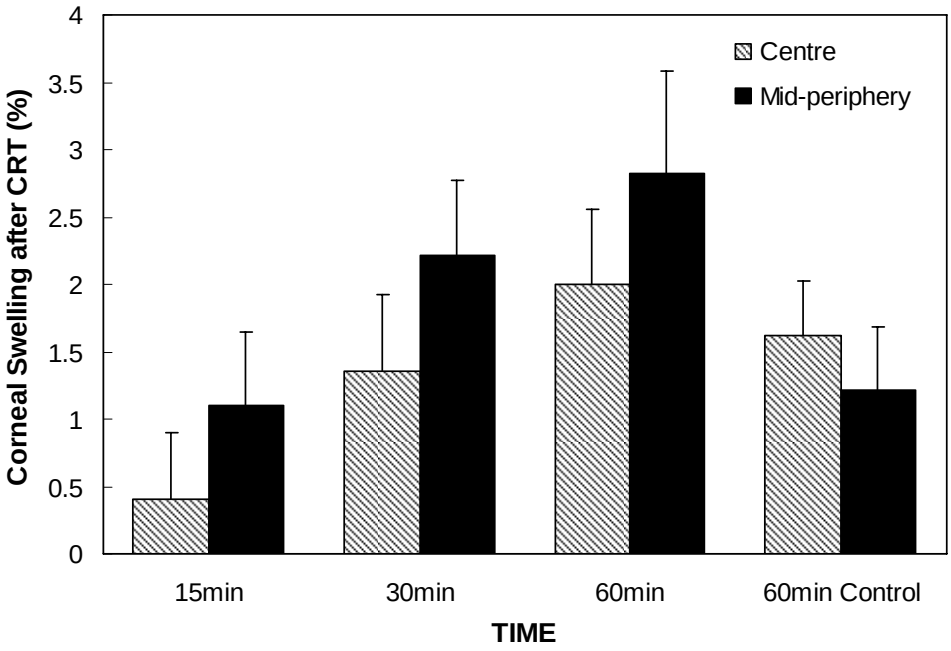

Figure 8-13. Percentage change of corneal thickness (corneal swelling) centrally and mid-peripherally (T2) after CRT® lens wear over time compared to controls. Error bars: 95% confidence intervals.

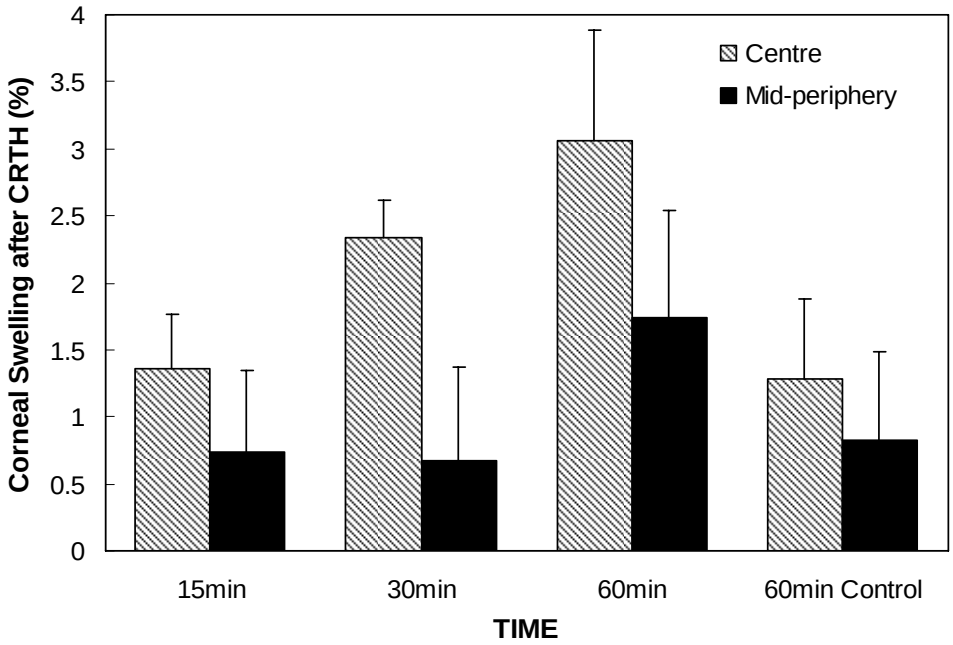

Figure 8-14. Percentage change of corneal thickness (corneal swelling) centrally and mid-peripherally (T2) after CRT®H lens wear over time compared to controls. Error bars: 95% confidence intervals.

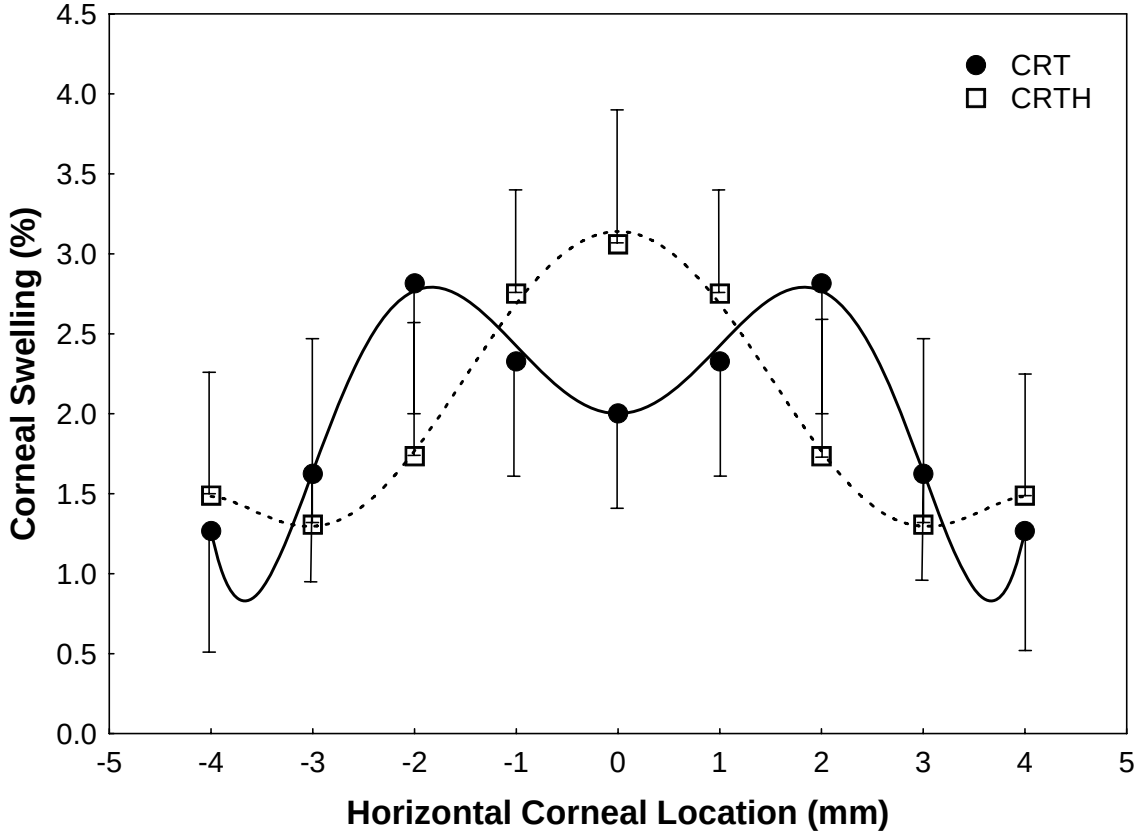

Figure 8-15. Profiles of the corneal swelling after 60 minutes of CRT® and CRT®H lens wear. Positive x-axis numbers refer to nasal corneal positions and negative to temporal corneal positions. Error bars: 95% confidence intervals.

8.4.3.2 Percentage Change in Epithelial Thickness

The percentage change in central epithelial thickness after CRT® and CRT®H lens wear depended on the location (RM-ANOVA, $F_{(1,19)}$=67.986, p<0.001). As is apparent in Figure 8-16, the epithelium in the centre was thinner after CRT® lens wear (t-test, all p≤0.047) and the epithelium in the mid-periphery was generally thicker (t-test, both p≤0.014, except p=0.166 for 15minutes). There was no significant time effect on the central and mid-peripheral epithelial swelling (RM-ANOVA, $F_{(2,38)}$=0.378, p=0.687; $F_{(2,38)}$=0.726, p=0.491). The central corneal epithelium thinned by 2.64±1.25%, 2.44±0.94% and 3.73±1.08% after 15, 30 and 60 minutes of CRT® lens wear, respectively, whereas the mid-peripheral epithelium thickened by 1.89±1.31%, 3.07±0.83% and 4.03±1.49%, respectively. The central and mid-peripheral epithelial thickness did not change in the control eyes (t-test, all p≥0.718).

As is apparent in Figure 8-17, the epithelium in the centre was not thicker (t-test, all p≥0.109) but the mid-periphery was thinner (t-test, both p≤0.048, except p=0.140 for 15 minutes) after CRT®H lens wear. There was no significant time effect on the central and mid-peripheral epithelial thickness changes (RM-ANOVA, $F_{(2,38)}$=0.208, p=0.813; $F_{(2,38)}$=0.329, p=0.722). The central corneal epithelium thickened by 1.19±1.08%, 1.83±1.14% and 2.20±1.31% at 15, 30 and 60 minutes, respectively, and the mid-peripheral epithelium thinned by 1.48±0.96%, 2.13±0.85% and 2.51±1.19%, respectively. The central and mid-peripheral epithelium did not change in the control eyes (t-test, all p≥0.852).

To illustrate (in Figure 8-18) the different distributions of the corneal epithelial thickness changes after CRT® and CRT®H lenses wear cross the cornea, we assumed the change of corneal epithelium from the nasal cornea was symmetrical. Polynomial regression

analysis showed that there were quadratic, and quartic components in CRT® lens wearing eyes (both $p \leq 0.001$), and quadratic, quartic and six order components in the CRT®H lens wearing eyes (all $p \leq 0.029$). The functions and correlation coefficients were:

$Y_{CRT} = - 2.944 + (0.198e\text{-}7)*x + 1.557*x^2 + (-0.26e\text{-}8)*x^3 - 0.087*x^4$, $R = 0.985$;

$Y_{CRTH} = 2.955 + (-0.23e\text{-}5)*x - 2.685*x^2 + (0.852e\text{-}6)*x^3 + 0.355*x^4 + (-0.39e\text{-}7)*x^5 - 0.012*x^6$, $R = 0.991$.

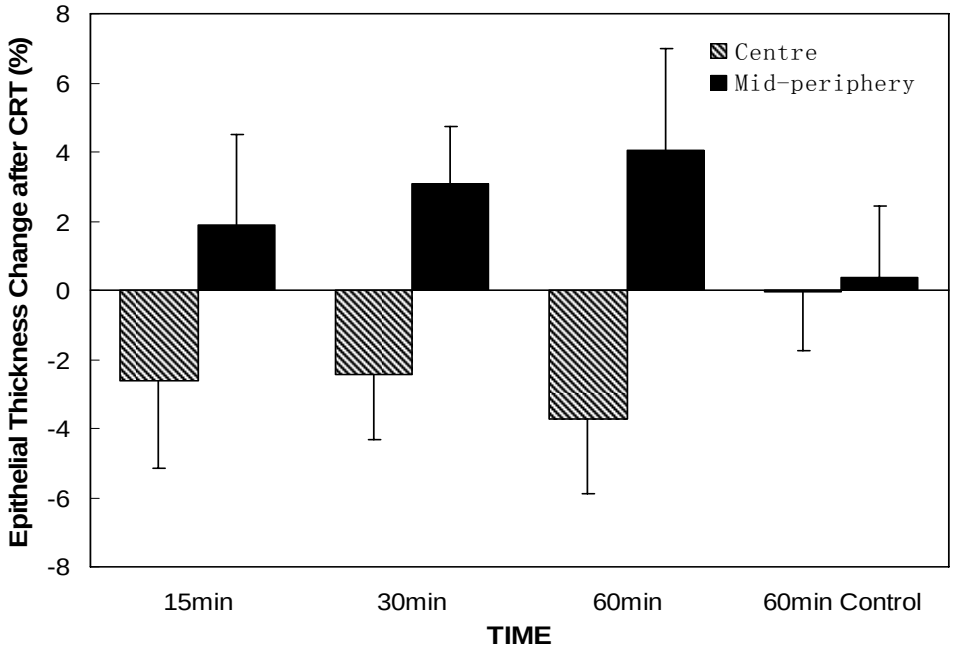

Figure 8-16. Percentage changes in epithelial thickness centrally (average of centre and T1) and mid-peripherally (average of T2 and T3) after CRT® lens wear over time compared to controls. Error bars: 95% confidence intervals.

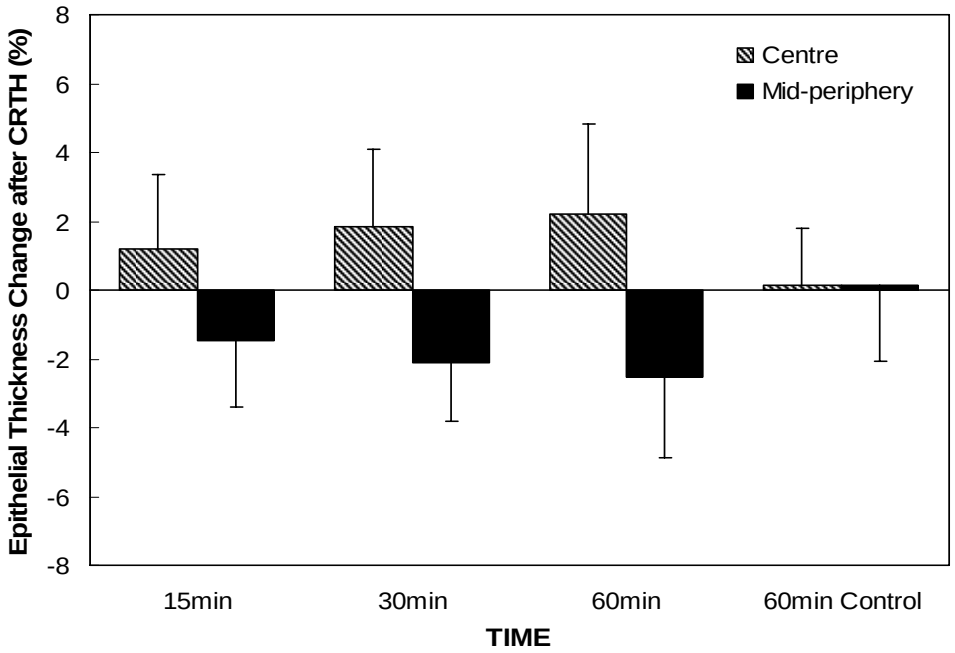

Figure 8-17. Percentage changes in epithelial thickness centrally (average of centre and T1) and mid-peripherally (average of T2 and T3) after CRT®H lens wear over time compared to controls. Error bars: 95% confidence intervals.

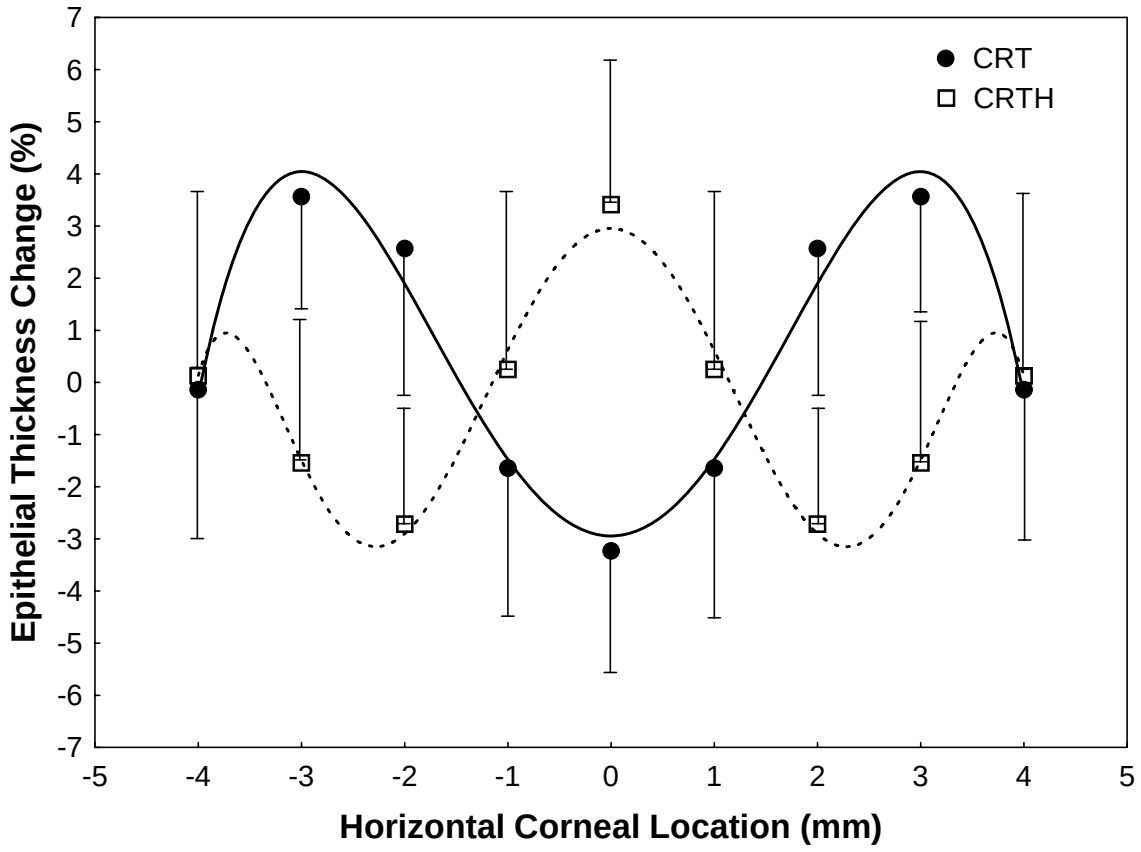

Figure 8-18. Profiles of the percentage change in corneal epithelial thickness after CRT® and CRT®H lens wear. Positive x-axis numbers refer to nasal corneal positions and negative to temporal corneal positions. Error bars: 95% confidence intervals.

8.5 Discussion

Clinically, the efficacy of corneal reshaping partially depends on how moldable the cornea is (Tredici, 1979). After minutes of CRT® for myopia, refractive error and corneal curvature changed significantly, similar to the previously reported short term myopic corneal reshaping studies (Horner et al., 1992; Tahhan et al., 2001; Sridharan and Swarbrick, 2003; Jackson et al., 2004; Kamei et al., 2005; Jayakumar and Swarbrick, 2005). However, it is unclear how the corneal structure, particularly the epithelium, changed (Jackson et al., 2004; Jayakumar and Swarbrick, 2005). In this short term study, after CRT® lens wear, the epithelium became thinner centrally and thicker mid-peripherally (Figure 8-16). Jayakumar and Swarbrick (2005) reported that after 1 hour of orthokeratology (BE) lens wear, the central epithelium became thinner (using optical pachymeter in 20 young adults). However, Jackson et al. (2004) reported that after 1 hour of CRT® lens wear, epithelial thickness did not change in 10 subjects. The negative findings from the latter study may be due to their smaller sample size and different pachymetric techniques used.

This study demonstrated for the first time that CRT®H lens could steepen the central cornea and flatten the para-central region (Figures 8-2 and 8-3) after short amounts of lens wear, altering the ametropia by inducing myopia (Figures 8-5 and 8-7). In addition, as is illustrated in Figure 8-17, the direction of the epithelial thickness change was opposite between the centre and para-central region after even the shortest amount of lens wear.

Corneal swelling and epithelial thickness percentage change patterns were different after CRT® and CRT®H lens wear, in spite of using the same Dk/t material and with the same duration of treatment. The swelling and percentage change patterns were consistent with the lens design, particularly the geometry of the lens back surfaces. The central cornea

swelled less than the mid-periphery after CRT® lens wear, whereas the central cornea swelled more than the para-central region after CRT®H lens wear (Figures 8-13 to 8-15). The central epithelium was thinner than the mid-periphery after CRT® lens wear and thicker than the para-central region after CRT®H lens wear (Figures 8-16 and 8-17). These findings are in agreement with McMonnies' hypothesis, who discussed corneal molding matching the lens shape (McMonnies, 2005).

The epithelial change was evident and different after CRT® and CRT®H lens wear (Figures 8-16 and 8-17). This difference may be due to different hydraulic force profiles underneath the two lenses and various eyelid tensions induced across the ocular surface as discussed in Chapters 5 and 6. In addition, the intraocular pressure, which is in an opposite direction to the eyelid tension, might also be involved in the formation of the different epithelial profiles after corneal reshaping (McMonnies, 2005). Beside the mechanical pressures, the characteristic of the epithelium is also a critical factor in this epithelial change. When a rigid corneal reshaping lens (CRT® or CRT®H) is placed on the eye, a sandwich-like system, rigid lens/epithelium/Bowman's layer, is formed. Compared to the rigid lens and Bowman's layer (Hoeltzel et al., 1992), the epithelium is the most moldable structure with lower elastic modulus, and, therefore, the epithelium is relatively easier to deform. The alteration of the epithelium profile depends on lens shapes; we found differences between the CRT® and CRT®H lens-wearing eyes.

In this current study, the same participant and the same eye wore both the myopic and hyperopic corneal reshaping lenses in a random order but opposite changes of corneal and epithelial thickness occurred after as little as 15 minutes (Figures 8-13, 8-14, 8-16 and 8-17), indicating that the cornea was highly moldable. This relatively rapid response of the ocular

surface under local mechanical pressure has also been observed in clinical practice, for instance, dimple veiling (Zadnik, 1988; Jones and Jones, 1995) when air bubbles become trapped between the contact lens and the ocular surface, and epithelial changes in the cornea secondary to mucin balls (Pritchard et al., 2000; Ladage et al., 2002) occurring with silicone hydrogel lens wear. Recently, it has also been shown that silicone hydrogel or conventional soft contact lenses can reshape the cornea unintentionally (Mountford, 2003) and intentionally (Choo et al., 2005; Evans et al., 2005).

The absence of difference in the central corneal swelling between the CRT® lens-wearing eyes and the control eyes after 60 minutes (Figure 8-13) provided support for the hypothesis that myopic corneal reshaping lenses could block the central stromal edema response (Alharbi et al., 2005). Theoretically, the para-central touch in the CRT®H lens wearing eye might block the para-central corneal swelling, and this was confirmed by the lack of a difference in para-central corneal swelling between the CRT®H lens-wearing eyes and control eyes after 60 minutes (Figure 8-14).

The corneal shape and optical performance changed in complementary ways, in accord with earlier overnight studies (Joslin et al., 2003; Lu et al., 2004; Lu et al., 2006b; Berntsen et al., 2005; Lu et al., 2005), but these changes occurred in as little as 15 minutes. After CRT® lens wear, the central cornea flattened and the mid-periphery steepened, whereas the central cornea steepened and the para-central region flattened after CRT®H lens wear (Figures 8-2 and 8-3). Consequently, ocular refractive power, total aberration and defocus decreased after CRT® lens wear. As anticipated, they increased after CRT®H lens wear (Figures 8-5 to 8-7). In addition, overall HOAs, coma and SA increased after both CRT® and

CRT®H lenses wear (Figures 8-9 to 8-11). Signed SA shifted from positive to negative after CRT®H lens wear (Figure 8-12).

Coma increased after short term of CRT® and CRT®H lens wear, in amounts comparable to previous overnight studies (Joslin et al., 2003; Lu et al., 2004; Lu et al., 2005; Berntsen et al., 2005; Lu et al., 2006b). Increased coma might be due to slight lens decentration, and topography data in this study showed that the centre of the central treatment zone was displaced (mean distance ± SD) by 0.64±0.44mm after 60 minutes of CRT® lens wear, and 0.59±0.35mm after 60 minutes of CRT®H lens wear. These decentration outcomes were also comparable to previous reports (Yang et al., 2003; Lu et al., 2006b).

The efficacy of the corneal reshaping is not the major outcome in this short-term study, but clinically, myopia was corrected after CRT® lens wear and was induced after CRT®H lens wear. In addition, despite attempting the same amount of "correcting" power, ±3.50D, the hyperopic refractive error change was approximately 2/3 that of the myopic change (Figure 8-5). The greater refractive error change after myopic corneal reshaping lens wear than after hyperopic was in agreement with the corneal curvature change (Figures 8-2 to 8-4). Similarly, the epithelial change after hyperopic corneal reshaping also suggests that this lens design for myopia appears more effective (Figures 8-16 and 8-17).

The variation of the epithelial change was evident after corneal reshaping lens wear, suggesting that the moldability of all corneas in this study were not the same and each individual was different. Correspondingly, the success of the each individual varied. Exploring the factors that may affect or predict the success will be beneficial in corneal reshaping.

In summary, significant changes in corneal structure and shape, and optical performance occurred in as little as 15 minutes after CRT® for myopia and hyperopia. The cornea, particularly the epithelium, is remarkable moldable, with very rapid steepening and flattening possible in a small amount of time.

Chapter 9

Corneal Posterior Surface Change after Corneal Reshaping

9.1 Introduction

The Orbscan II is the only commercial corneal topographer that is reported to provide the quantitative information of corneal posterior surface. Since the mechanisms of the corneal reshaping are not yet fully elucidated, some theories, such as, corneal bending, are yet to be explored. The change of the corneal posterior surface provides insight into a specific hypothetical mechanism of corneal reshaping and therefore the topic of the following experiment.

9.2 Methods

The radius of posterior best-fit spheres from Orbscan II from previously reported studies in this thesis, specifically the CRT1, CRT2, CRTHDK and CRTH studies was determined. The best-fit sphere is referred to the fit of the elevation data of the corneal surface using a sphere. An Orbscan II was used for the measurements, the operation of which has been described previously (Liu et al., 1999; Iskander et al., 2001; Fakhry et al., 2002; Prisant et al., 2003; Lu et al., 2006a).

9.3 Results

9.3.1 The radius of posterior best-fit sphere at different times in the CRT1 study.

Figure 9-1 shows that there is no difference in the radius of posterior best fit sphere (mean±95% confidence interval) between CRT® lens wearing eyes and control lens-wearing eyes (RM-ANOVA, $F_{(1,19)}$=0.734, p=0.402) except that the posterior surface was steeper at

the single time point immediately after CRT® lens removal (post hoc test, p=0.025). It did not change in the control eyes (RM-ANOVA, $F_{(6,114)}$=3.003, p=0.099).

9.3.2 The radius of posterior best-fit sphere at different time in the CRT2 study.

Figure 9-2 shows that there is no difference in the radius of posterior best fit sphere (mean±95% confidence interval) in two eyes (RM-ANOVA, $F_{(1,15)}$=0.019, p=0.892). The posterior surface did not change during 4 weeks of CRT® lens wear (RM-ANOVA, $F_{(8,120)}$=0.599 – 0.969, both p≥0.465).

9.3.3 The radius of posterior best-fit sphere at different time in the CRTHDK study

Figure 9-3 shows that there is no difference in the radius of posterior best fit sphere (mean±95% confidence interval) between the MZ and EII lens wearing eyes (RM-ANOVA, $F_{(1,19)}$=0.027, p=0.870). The posterior surface did not change significantly after one night of the MZ and EII lens wear (RM-ANOVA, $F_{(5, 95)}$=2.036 – 4.521, p>0.05).

9.3.4 The radius of posterior best-fit sphere at different time in the CRTH study

Figure 9-4 shows that there is no difference in the radius of posterior best fit sphere (mean±95% confidence interval) between CRT®H lens wearing eyes and control eyes (no lenses) (RM-ANOVA, F(1,19)=1.126, p=0.302). The posterior surface did not change after one night of CRT®H lens wear (RM-ANOVA, $F_{(6, 114)}$=2.338, p=0.143). However, it was steeper immediately after one night of sleep in the control eyes (post hoc test, p=0.037) and returned toward baseline after 1 hour without lens wear (post hoc test, all p≥0.062).

In brief, after overnight of CRT® lens wear, the radius of posterior best-fit sphere did not change in the CRT2, CRTHDK studies, whereas it became transiently steeper in the CRT1 study.

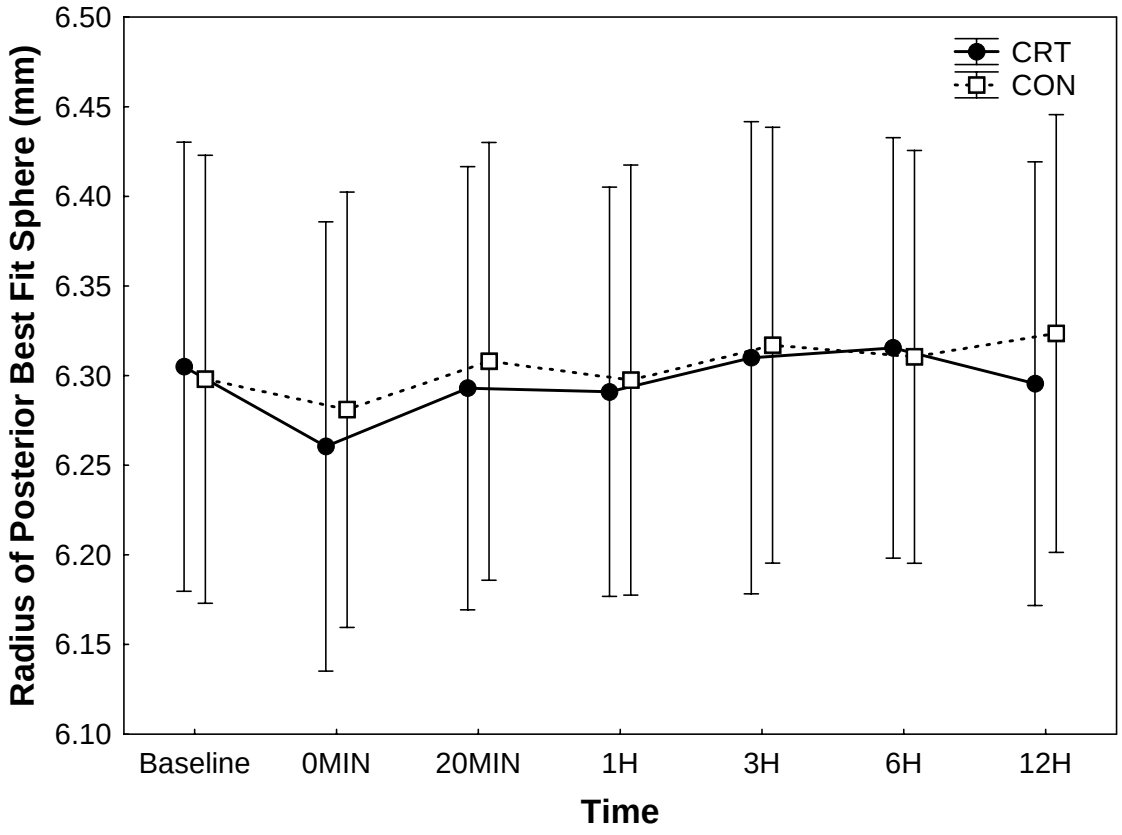

Figure 9-1. The radius of posterior best-fit sphere in the CRT® and control lens-wearing eyes over time. Error bars: 95% confidence intervals.

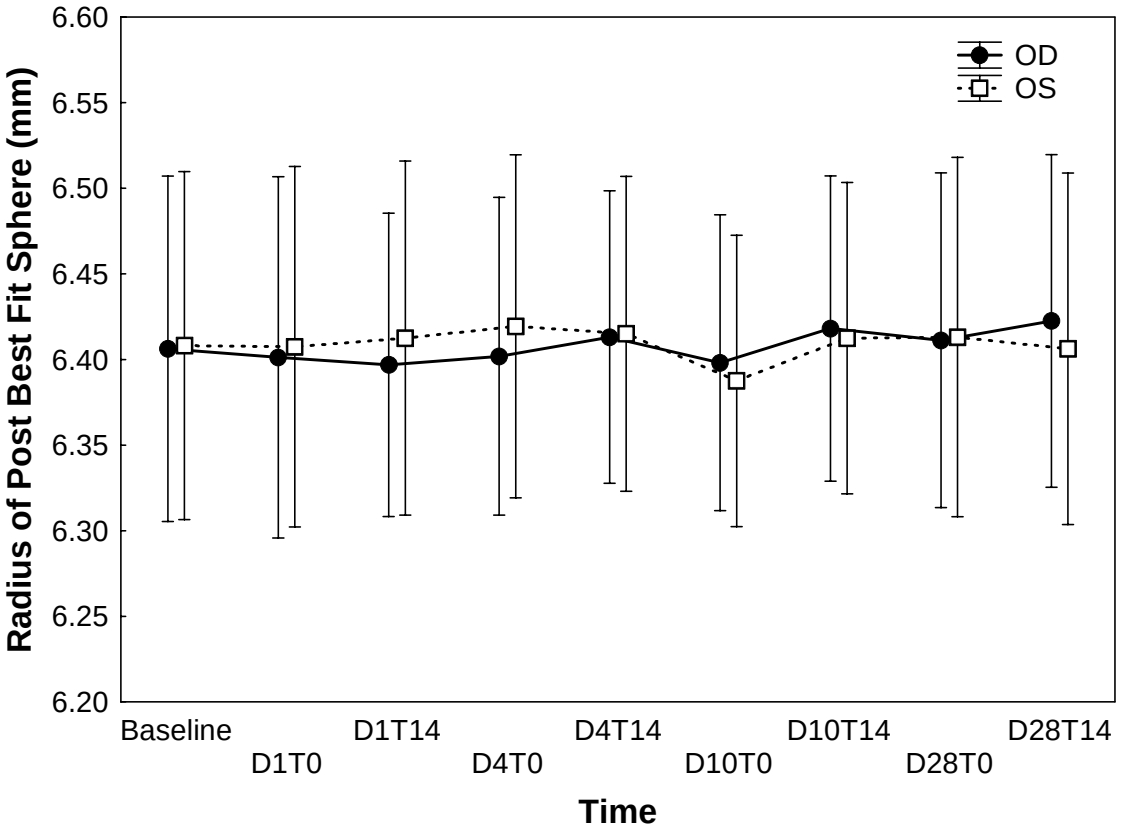

Figure 9-2. The radius of posterior best-fit sphere in the CRT® lens-wearing eyes over time for the CRT2 study. Error bars: 95% confidence intervals.

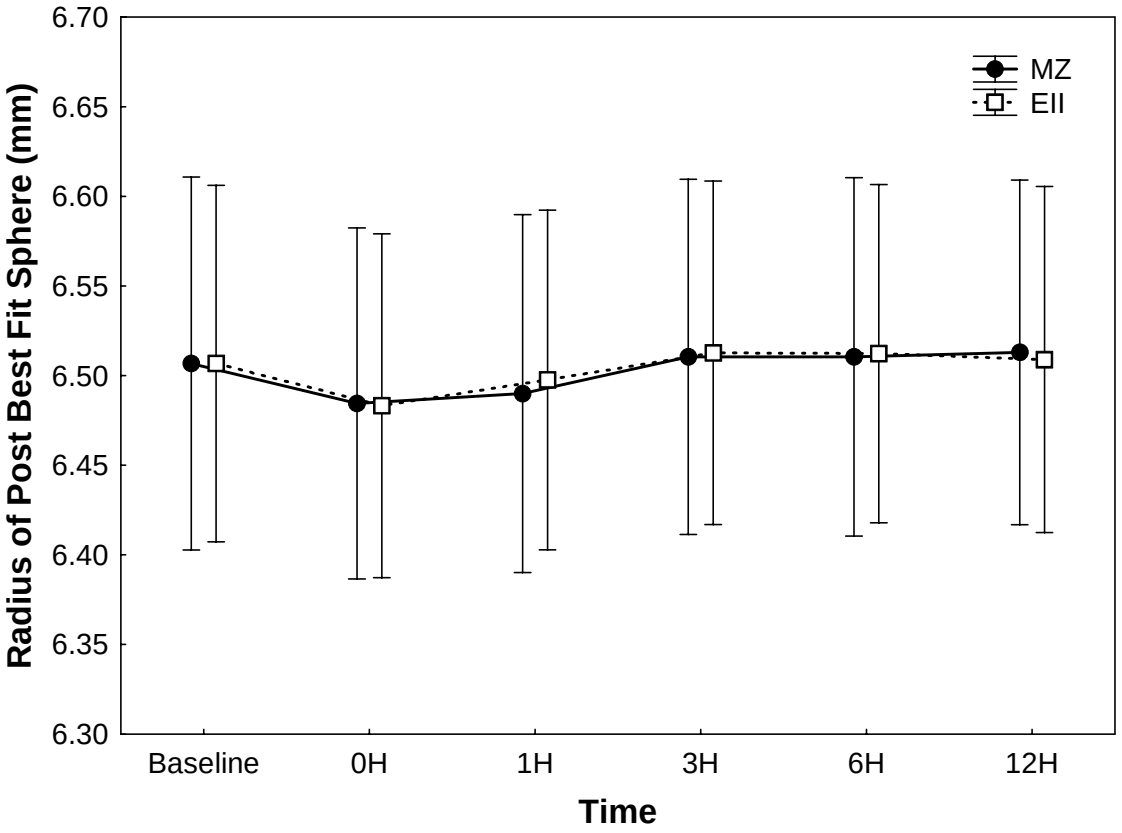

Figure 9-3. The radius of posterior best-fit sphere in the MZ and EII lens-wearing eyes over time for the CRTHDK study. Error bars: 95% confidence intervals.

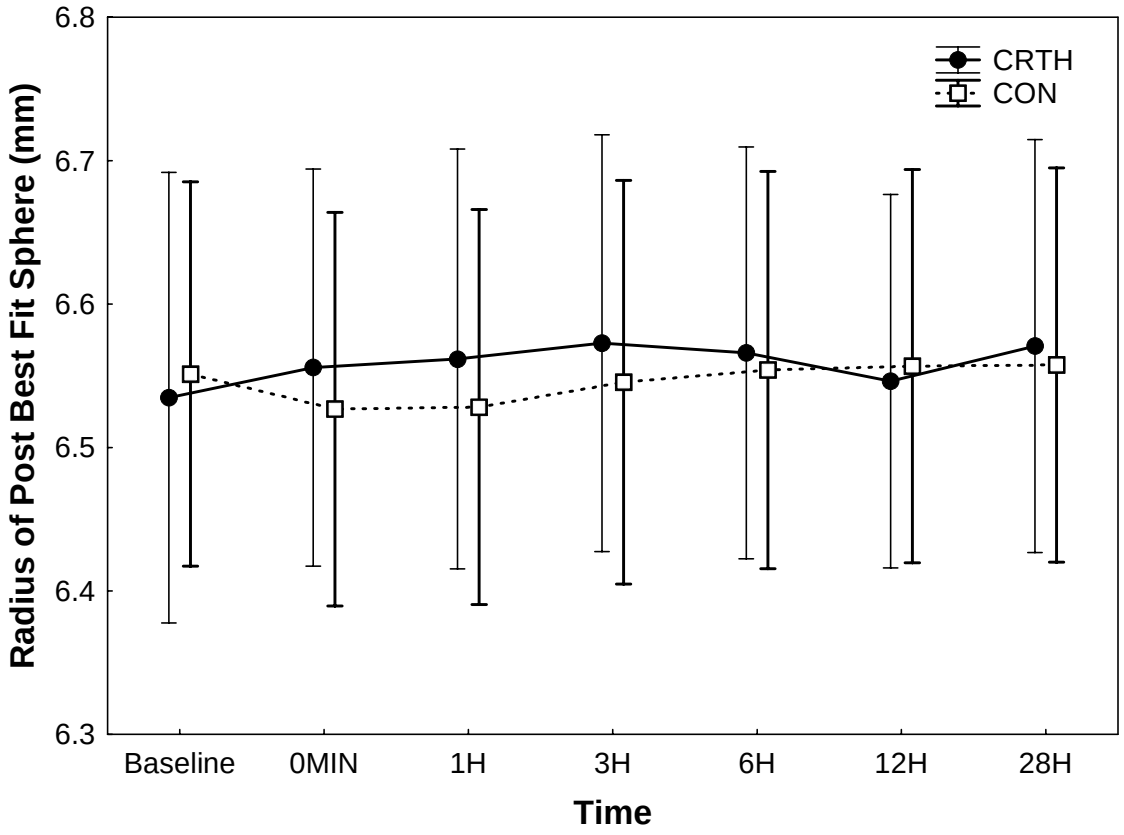

Figure 9-4. The radius of posterior best-fit sphere in the CRT®H and control eyes over time for the CRTH study. Error bars: 95% confidence intervals.

9.4 Discussion

Experimental results of corneal posterior shape change through corneal reshaping methods allow us to examine one specific hypothesis proposed for CRT effects. If the cornea were a plastic, the mechanical stress induced by the CRT® lens and eyelid may force the cornea to bend centrally. This corneal bending theory proposes that the corneal posterior surface after corneal reshaping is flattened for myopia, and steepened for the hyperopic therapy. However, this hypothesis was not supported by the data from the experiments. The corneal posterior surface did not change in two studies (CRT2 and CRTHDK) and even became steeper in one (CRT1). Moreover, the corneal posterior surface did not change after hyperopic therapy either. These results indicate that the corneal bending theory does not account for the result in these studies.

Owens et al. (2004) reported that a flattening of the posterior surface occurred during the early adaptive stages (one week) of OK lens wear. The difference between my results and theirs may be ascribed to technical differences and perhaps the relative small sample sizes in the experiments I analysed. This potential low power is a side effect of the analysis not being a primary outcome in the experiments I conducted.

The cornea is not a piece of plastic (Roberts, 2000). The results of this and the previous experiments (Swarbrick et al., 1998; Matsubara, 2002; Alharbi and Swarbrick, 2003; Wang et al., 2003; Wang et al., 2004; Ladage et al., 2004; Matsubara et al., 2004; Choo et al., 2004c; Haque et al., 2004b) point to surface alteration due to changes particularly in the epithelium, and not because the cornea simply bends.

Chapter 10 Summary and General Discussion

10.1 Summary and Significance

The Efficacy of the CRT® for Myopia and Hyperopia

Perhaps of most concern in corneal reshaping is its efficacy. The lack of controlled, masked and randomized experiments might result in biased and unscientific conclusions in clinical trials. In the one night corneal reshaping for myopia and hyperopia studies (CRT1 and CRTH), masked randomized and controlled procedures were used to examine treatment effectiveness. The CRT® lens flattened the central cornea and steepened the mid-periphery to correct myopia. The CRT®H lens steepened the central cornea and flattened the para-central region to induce myopia or to correct hyperopia. No significant meridional changes were found in the control eyes. Therefore, CRT® and CRT®H were demonstrated to be effective to correct myopia and hyperopia, respectively.

Corneal shape change alters the ocular aberration structure. After one night of CRT®H lens wear, defocus increased since the majority of the subjects were myopes. The HOAs, including coma and SA, increased and signed SA shifted from positive to negative. However, the astigmatism did not change. The aberration data, particularly the HOAs, provide insight in the optical quality after corneal reshaping and show that the reduction in ametropia is accompanied by potentially detrimental HOAs.

Relatively Long-Term (four weeks) Effects of Corneal Reshaping

A study of 4-weeks CRT® lens wear was conducted to quantify the relatively long term changes in corneal shape, visual, subjective and optical performance and to determine

the stabilization of these outcome variables. The second goal of this study was to link the corneal shape change in terms of the treatment zone diameter with other outcome variables.

After 4 weeks of CRT® lens wear, the central cornea flattened and mid-periphery steepened. The treatment zone diameter including the central flattened zone and annular steepened zone increased over time and was stable from day 10 onwards. Myopia reduced by 2.30 to 2.50D, and visual acuity and subjective vision improved significantly. Total aberration and defocus decreased significantly, but astigmatism did not change. HOAs including coma and SA increased. In general, all parameters except astigmatism were stable by day 10. Interestingly, the treatment zone size was associated with many parameters, suggesting that the concept of the treatment zone size is a useful metric for visual, optical and subjective performance in the CRT® lens wearers. These relationships were illustrated in Figure 10-1.

The Effects of lens Dk/t on the Corneal Shape and Optical Performance

The higher Dk/t lens material provides more oxygen to the cornea and potentially has less of a negative impact on its health. However, since the increased Dk/t material might have less mechanical strength compared to the lower Dk/t material, the question arose whether the higher Dk/t material would compromise its clinical effect. This study demonstrated that the central corneal shape and optical performance was similar in the higher Dk (MZ) and lower Dk (EII) lens-wearing eyes, the exception being the mid-peripheral corneal shape. The mid-peripheral cornea was steeper in the lower Dk lens-wearing eyes relative to the higher Dk lens-wearing eyes. This experimental result would suggest that practitioners choose higher Dk/t rigid lens material for all their CRT patients.

Moldability of the Ocular Surface in Response to Acute Local Mechanical Forces

Clinically, the efficacy of corneal reshaping partially depends on how moldable the cornea is. The STOK (short term) study was designed to examine how quickly and by how much the corneal surface changed. This study demonstrated that significant changes in many estimates of corneal structure and shape, reflected in some optical characteristics, occurred in as little as 15 minutes of CRT® lens wear for myopia and hyperopia. The patterns of the corneal and epithelial thickness change were different after short amounts of CRT® and CRT®H lens wear, and were consistent with lens designs, particularly the back geometry of the lens. The rapid change of the ocular surface under mechanical pressure in CRT® for myopia and hyperopia indicated that the cornea could be manipulated in a planned manner with the rigid contact lens. The cornea, particularly the epithelium, is remarkably moldable, with rapid steepening and flattening possible in a small amount of time.

This study demonstrated for the first time that CRT®H lens steepens the central cornea and flattens the mid-periphery after short amounts of lens wear with eye closure, altering the ametropia by inducing myopia.

10.2 General Discussion

Corneal Biomechanical Behavior in Non-Surgical Corneal Reshaping

After myopic corneal reshaping, the central corneal flattened and the mid-periphery steepened: A central flattened zone and a mid-peripheral annular steepened zone was generated. Previous morphological studies have suggested that the epithelium profile alteration was responsible for this corneal shape change from the centre to the mid-periphery (Swarbrick et al., 1998; Alharbi and Swarbrick, 2003; Wang et al., 2003; Haque et al., 2004b). Histological data in rabbits and cats (Matsubara, 2002; Choo et al., 2004c; Matsubara et al., 2004) have also supported this contention; the central epithelium appeared thinner (Matsubara et al., 2004; Choo et al., 2004a; Matsubara, 2002; Choo et al., 2004c) and the basal epithelium was vertically elongated with more layers of wing-like cells in the mid-periphery (Matsubara et al., 2004; Choo et al., 2004c). At the cellular level, the suppression of the turnover of epithelial cells after RGP lens wear (Ladage et al., 2001; Ladage et al., 2003; Ren et al., 1999), decreasing cell desquamation after RGP and orthokeratology lens wear in humans (Ren et al., 2002; Guo et al., 2004), enlargement of epithelial cell surface area after orthokeratology lens wear (Ladage et al., 2004), and decreased corneal epithelial cell density (Wang et al., 2004) may also account for these morphological changes. Basal cell mitosis may also contribute to epithelial remolding by increasing cell numbers in the mid-periphery (Matsubara et al., 2004).

The steepening in the mid-periphery corresponds to histologically larger and/or thicker basal cells (Choo et al., 2004c; Matsubara et al., 2004) and/or a greater numbers of cell layers (Choo et al., 2004c; Matsubara et al., 2004). These local morphological changes may be due to mechanical forces that could transfer the intracellular fluid and inorganic ions

to the adjacent cells (from centre to periphery) through the gap junctions (Alberts et al., 1994). The negative force underneath the lens in the mid-periphery may also contribute to this local morphological change. In addition, the greater number of cell layers (Matsubara et al., 2004; Choo et al., 2004c) in the mid-periphery may be due to less cell shedding (Guo et al., 2004), cell mitosis from basal epithelial cells (Matsubara et al., 2004), cell proliferation from limbal stem cells (Lavker et al., 2004) and restriction of the epithelial centrifugal movement by the alignment zone in the mid-periphery.

Besides the hypotheses regarding the epithelium, the stroma has been speculated to be involved in corneal reshaping. First, redistribution of stromal extracellular fluid has been proposed (Swarbrick et al., 1998; Wang et al., 2003; Alharbi and Swarbrick, 2003). Under normal physiological conditions, the cornea contains 78% water, which is incompressible (Maurice and Riley, 1970). In addition, only a small fraction of the water in the corneal stroma can be bound or structurally organized by intermolecular forces. The greater part of the tissue fluid may move around by mechanical pressure (Maurice and Riley, 1970). A second hypothesis involving the stroma proposes stromal remodeling to be involved in corneal reshaping. Mechanical compressive forces and intraocular pressure during CRT® lens wear are applied to the central stroma. Although the collagen fibrils' tensile strength and resilience can oppose the external force (Friend and Hassell, 1994) and the glycosaminoglycans (GAGs) are thought to play a role in resisting compressive forces in tissue (Alberts et al., 1994), if the applied force is greater than the opposing force, the ground substance may be redistributed and the collagen fibrils may be deformed. Hyaluronan, a GAG, may be degraded by the enzyme hyaluronidase to regulate the space within the tissue (Alberts et al., 1994). In addition, Petroll et al. (2004) demonstrated that corneal fibroblasts

responded rapidly to changes in local mechanical stress in vitro. A third line of evidence suggesting stromal involvement is based on the post corneal reshaping recovery studies (Wang et al., 2003; Barr et al., 2004; Haque et al., 2004b; Soni et al., 2004; Sorbara et al., 2005). These indicate a stromal role in addition to the epithelium (see detailed Discussion in the CRT2 study in Chapter 6).

After CRT® lens removal, the corneal shape regresses for a number of possible reasons. The return to normality may be the result of epithelial movement and the shear force of the upper eyelid. Corneal epithelial cells naturally migrate continuously, centripetally (Davanger and Evensen, 1971; Ren and Wilson, 1996; Estil et al., 2000), and vertically (Ren and Wilson, 1996; Estil et al., 2000; Ladage et al., 2003), so that the altered epithelial profile may revert to its original configuration. In addition, the shear force of the eyelid may contribute to the recovery of the normal anterior surface by increasing epithelial shedding (Lemp and Mathers, 1989; Ren and Wilson, 1997) or by releasing an autocrine/paracrine signal, such as ATP, to modulate paracellular activities (Srinivas et al., 2002). A second reason may be that since lenses are not worn, increased oxygen availability may affect epithelial metabolism and the basal epithelial mitosis may recover (Shin et al., 2005). Also, because of the absence of central compression and mid-peripheral tension, the free fluid (water) in the stroma may return to its original distribution, the collagen fibrils may revert to their initial position and the stromal ground substance may revert to its original structure.

The functions of the shear force of the eyelid have been discussed in Chapter 1. Briefly, the shear force of the eyelid is tangential to the corneal surface. It assists the epithelial desquamation (Ren and Wilson, 1997) and spreads tears uniformly to maintain the

tear film as an optically smooth refractive layer (Trinkaus-Randall et al., 1998). The shear force acts as a smoother.

Beside the eyelid involvement in the smoothing function, the corneal epithelium also adjusts its thickness to preserve a smooth corneal surface in order to maintain optimal optical function. The corneal epithelium thins over elevations, e.g., over Salzmann's nodules (Freddo and Warning III, 1998) or over the cone in the advanced keratoconus (Dillon et al., 1992), or on the elevated area of the intrastromal ring (Dawson et al., 2005), and the corneal epithelium thickens over focal defect after the LASIK or PRK (Spadea et al., 2000; Dawson et al., 2005; Kramer et al., 2005). However, the mechanism through which this adjustment is accomplished is unknown. The pressure exerted by the eyelid orthogonal to the ocular surface may provide a mechanical signal that provides feedback to regulate epithelial growth controlling normal epithelial structures preventing cellular proliferation and excessive layers.

The post-lens space in the mid-periphery (steeper return zone) in the CRT® lens, and in the center (steeper central optic zone) in the CRT®H lens would be a place where the eyelid could not reach. The epithelium fills this gap up to the posterior surface of the lens since the epithelium migrates vertically (Ren and Wilson, 1996; Estil et al., 2000; Ladage et al., 2003). Overnight CRT works partly because the relatively uniform mechanical signals from the lid are replaced by those from the posterior surface of the lens. Where the lens is steep, proliferation towards the surface continues. Where there is touch, this proliferation is inhibited. The surface of the epithelium eventually resembles the back surface of the lens, the surrogate of the inner eyelid during sleep.

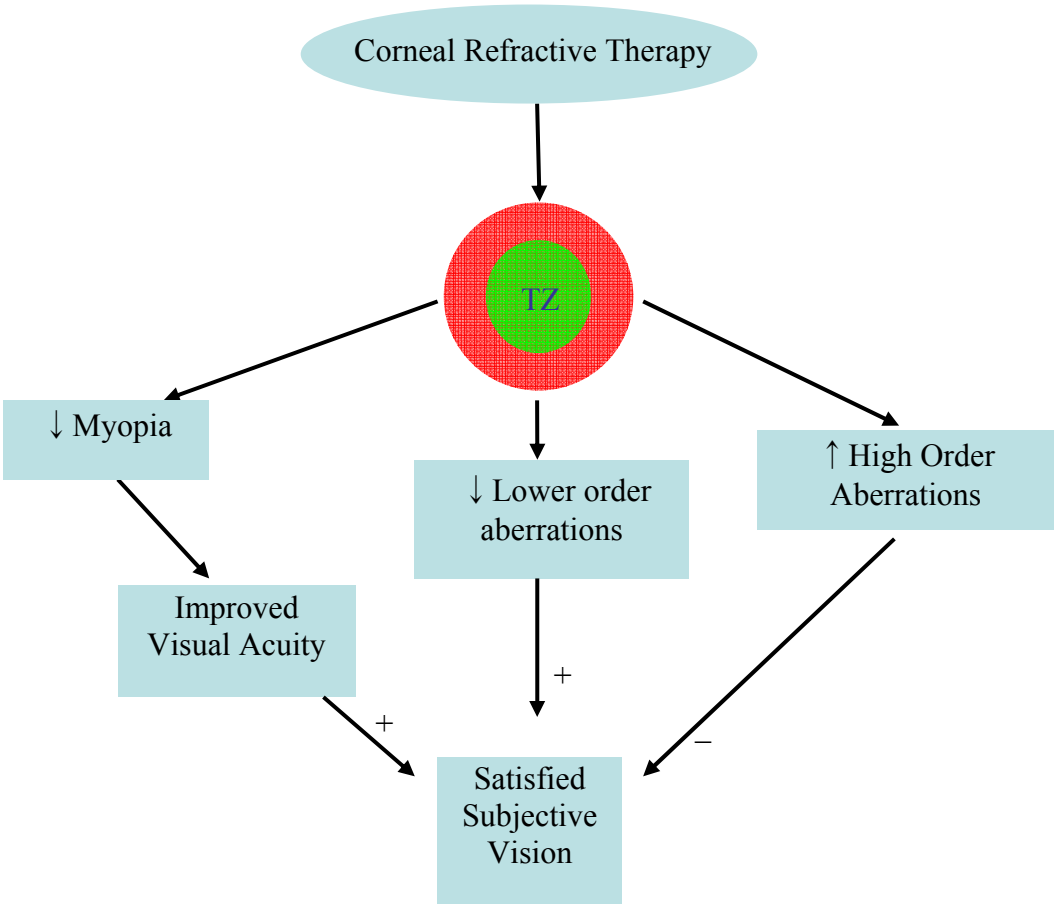

Figure 10-1. The flow chart of the relationships between the treatment zone diameter and visual, optical and subjective performance after corneal refractive therapy.

Chapter 11 Future Work

Modeling the corneal structural (corneal/epithelial thickness) change and corneal shape change to predict the refraction change: Understanding the biomechanics of cornea will help to understand the clinical response to CRT® lenses.

The effect of the corneal edema on the corneal reshaping: Further research is required to cover a broad range of the Dk/t of the lens materials to examine the effects of different Dk/ts on the corneal reshaping (Lu et al., 2005; Haque et al., 2005; Swarbrick et al., 2005; Swarbrick and Lum, 2006). The relationship between corneal edema and the clinical response to CRT can be examined. The cutoff of the Dk/t of the lens material may need to be modified to optimize the clinical response and corneal health.

Multi-layered corneal epithelial response under mechanical stress: Robertson et al. (2005) successfully developed a telomerase-immortalized human corneal epithelial cell line. A well-stratified epithelium (five to seven cell layers) was produced. This cultivated multi-layered corneal epithelium could be used to study the epithelial response *in vitro* under mechanical stress, which will assist to elucidate the biomechanical influences on the corneal epithelium. It also could be used to characterise the receptors or channels signaling the mechanical force influencing the cells during blinking, eye closure and CRT® lens wear.

The safety of non-surgical corneal reshaping: As microbial keratitis incidence increases, the safety of the corneal reshaping should be examined in a large scale and long-term clinical trial, so that its incidence can be exactly determined. In addition, due to more microbial keratitis cases occurring in Asians, it would be important to investigate the corneal epithelial response (i.e. pachymetric change, bacterial bindings to the epithelial, e.g.

Pseudomonas Aeruginosa, oxygen consumption) before and after corneal reshaping in different ethnic groups, particularly in young children.

Success of Orthokeratology: A large-scale clinical trial attempting to determine which clinical and lab outcome variables are useful as clinical success predictors for corneal reshaping is vital in order to make the technique clinically viable, provided it is safe.

Maintenance of the corneal reshaping effect: One of the drawbacks of corneal reshaping is its transience. Understanding if it can be made permanent appears to be an important piece of research.

Corneal reshaping for other refractive errors: Although hyperopic corneal reshaping was addressed in one of my studies, its utility is still unclear. Customizing the hyperopic corneal reshaping lens for each prescription and understanding in more detail how the hyperopic lens works requires examination. Corneal reshaping for astigmatism appears to be a worthwhile experimental pursuit.

In brief, although there are still many unanswered questions, directed research will not only elucidate mechanisms of corneal reshaping, but provide important insight into corneal biomechanical characteristics and physiological mechanisms.

Appendices

Appendix A CRT 1 Study - Refractive Error (D)

Time	BL	0min	20min	1h	3h	6h	12h
Experimental							
Sphere (mean)	-3.11	-1.94	-2.08	-2.06	-2.28	-2.35	-2.41
Sphere (SD)	1.24	0.93	0.96	1.10	1.04	1.11	1.20
Cylinder (mean)	-0.46	-0.58	-0.56	-0.59	-0.46	-0.47	-0.44
Cylinder (SD)	0.22	0.58	0.49	0.46	0.32	0.32	0.39
Control							
Sphere (mean)	-3.09	-2.91	-2.90	-2.95	-2.96	-2.98	-3.04
Sphere (SD)	1.21	1.12	1.19	1.16	1.28	1.19	1.18
Cylinder (mean)	-0.49	-0.49	-0.51	-0.49	-0.53	-0.49	-0.45
Cylinder (SD)	0.31	0.42	0.36	0.40	0.30	0.31	0.42

BL, baseline. 0min, immediately after lens removal. 1h, 1h without lens wear, etc.

Appendix B CRT1 Study - Horizontal Corneal Curvature (D)

Experimental Eyes

Time	Location	T4	T3	T2	T1	C	N1	N2	N3	N4
BL	mean	42.17	42.62	43.18	43.92	44.63	44.01	42.87	41.33	40.03
	SD	1.67	1.46	1.50	1.60	1.85	1.82	1.71	1.89	2.16
0min	mean	44.84	44.98	43.26	42.39	43.14	43.80	44.10	42.89	40.11
	SD	2.77	1.93	1.52	1.84	1.88	1.95	1.69	2.85	4.17
20min	mean	43.97	44.73	43.36	42.43	43.23	43.78	43.92	42.65	39.96
	SD	2.40	1.79	1.46	1.88	2.09	2.03	1.59	2.40	4.15
1h	mean	43.94	44.47	43.31	42.57	43.31	43.78	43.88	42.71	40.38
	SD	1.76	1.82	1.52	1.75	2.08	2.15	1.70	2.57	3.77
3h	mean	43.50	44.21	43.45	43.00	43.74	43.94	43.97	42.78	40.21
	SD	2.20	1.69	1.55	1.78	1.99	2.02	1.72	2.37	3.45
6h	mean	43.51	44.20	43.43	43.06	43.84	44.11	43.94	42.58	40.30
	SD	1.59	1.59	1.52	1.92	2.03	1.87	1.69	2.36	3.31
12h	mean	43.40	44.24	43.43	43.07	43.98	44.20	43.71	42.00	39.77
	SD	1.62	1.27	1.37	1.90	2.05	1.81	1.55	2.19	3.10

T4, temporal 4mm from centre. C, centre. N4, nasal 4mm from centre.

BL, baseline. 0min, immediately after lens removal. 1h, 1h without lens wear, etc.

Appendix C CRT1 Study - Horizontal Corneal Curvature (D)

Control Eyes

Time	Location	T4	T3	T2	T1	C	N1	N2	N3	N4
BL	mean	42.24	42.57	43.09	43.91	44.65	44.04	42.83	41.46	40.33
	SD	1.73	1.57	1.45	1.53	1.69	1.71	1.69	2.00	2.40
0min	mean	41.54	42.76	43.10	43.59	44.28	43.77	42.59	40.98	40.16
	SD	2.45	1.84	1.53	1.43	1.66	1.75	1.66	1.75	2.03
20min	mean	41.52	42.51	42.99	43.65	44.27	43.78	42.60	41.15	40.30
	SD	1.98	2.00	1.46	1.35	1.55	1.72	1.69	1.88	2.15
1h	mean	41.81	42.38	42.91	43.71	44.35	43.83	42.56	41.13	40.40
	SD	1.87	1.88	1.51	1.45	1.58	1.71	1.61	1.87	2.23
3h	mean	41.91	42.57	43.08	43.76	44.46	43.93	42.75	41.45	40.84
	SD	1.62	1.71	1.54	1.51	1.64	1.65	1.66	1.88	2.18
6h	mean	42.05	42.58	43.13	43.95	44.61	43.99	42.89	41.60	40.56
	SD	2.03	1.92	1.60	1.50	1.61	1.69	1.77	2.15	2.46
12h	mean	42.31	42.75	43.18	43.95	44.69	44.11	42.75	41.21	40.31
	SD	1.71	1.80	1.49	1.46	1.75	1.81	1.62	1.81	2.38

T4, temporal 4mm from centre. C, centre. N4, nasal 4mm from centre.

BL, baseline. 0min, immediately after lens removal. 1h, 1h without lens wear, etc.

Appendix D CRTH Study – Refractive Error (D)

Time	BL	0min	1h	3h	6h	12h	28h
Experimental							
Sphere (mean)	-1.86	-2.89	-2.66	-2.63	-2.50	-2.40	-2.05
Sphere (SD)	2.47	2.60	2.43	2.62	2.56	2.54	2.63
Cylinder (mean)	-0.56	-0.98	-0.88	-0.71	-0.84	-0.74	-0.64
Cylinder (SD)	0.420	0.71	0.63	0.59	0.58	0.46	0.44
Control							
Sphere (mean)	-1.99	-1.95	-2.04	-1.96	-1.95	-1.98	-1.91
Sphere (SD)	2.62	2.64	2.62	2.71	2.67	2.70	2.82
Cylinder (mean)	-0.58	-0.63	-0.49	-0.49	-0.60	-0.55	-0.64
Cylinder (SD)	0.43	0.46	0.41	0.57	0.44	0.43	0.45

BL, baseline. 0min, immediately after lens removal. 1h, 1h without lens wear, etc.

Appendix E CRTH Study – Aberrations (μm)

Experimental Eyes

Aberrations	Time	BL	0min	1h	3h	6h	12h	28h
Total aberration	Mean	1.85	2.47	2.33	2.24	2.22	2.11	1.91
	SD	1.59	1.57	1.63	1.65	1.67	1.66	1.63
Defocus	Mean	1.76	2.34	2.22	2.14	2.12	1.99	1.80
	SD	1.63	1.65	1.69	1.70	1.73	1.74	1.71
Astigmatism	Mean	0.29	0.33	0.33	0.31	0.31	0.32	0.31
	SD	0.21	0.19	0.21	0.20	0.22	0.22	0.21
HOA	Mean	0.17	0.46	0.38	0.33	0.31	0.27	0.17
	SD	0.10	0.17	0.16	0.14	0.13	0.13	0.09
Coma	Mean	0.10	0.27	0.22	0.19	0.18	0.17	0.11
	SD	0.08	0.14	0.14	0.12	0.11	0.11	0.08
SA (RMS)	Mean	0.05	0.20	0.16	0.13	0.12	0.09	0.04
	SD	0.04	0.15	0.12	0.10	0.10	0.09	0.02
Signed SA	Mean	0.04	-0.11	-0.09	-0.07	-0.05	-0.03	0.02
	SD	0.04	0.23	0.19	0.15	0.15	0.12	0.04

BL, baseline. 0min, immediately after lens removal. 1h, 1h without lens wear, etc.

HOA, higher order aberrations. SA (RMS), spherical aberration (Root-Mean-Squared).

Appendix F CRTH Study – Aberrations (μm)

Control Eyes

Aberrations	Time	BL	0min	1h	3h	6h	12h	28h
Total aberration	Mean	1.92	1.90	1.90	1.89	1.94	1.93	1.93
	SD	1.60	1.60	1.63	1.63	1.66	1.62	1.62
Defocus	Mean	1.81	1.79	1.79	1.78	1.83	1.83	1.82
	SD	1.67	1.66	1.69	1.70	1.72	1.68	1.69
Astigmatism	Mean	0.31	0.30	0.31	0.31	0.32	0.31	0.32
	SD	0.23	0.28	0.25	0.24	0.25	0.23	0.25
HOA	Mean	0.16	0.19	0.17	0.18	0.17	0.17	0.18
	SD	0.10	0.08	0.07	0.07	0.09	0.09	0.11
Coma	Mean	0.09	0.10	0.09	0.10	0.09	0.09	0.10
	SD	0.07	0.06	0.05	0.06	0.07	0.07	0.08
SA (RMS)	Mean	0.05	0.05	0.05	0.05	0.05	0.05	0.05
	SD	0.05	0.04	0.05	0.05	0.05	0.05	0.05
Signed SA	Mean	0.04	0.05	0.04	0.05	0.05	0.05	0.04
	SD	0.05	0.04	0.05	0.05	0.05	0.05	0.05

BL, baseline. 0min, immediately after lens removal. 1h, 1h without lens wear, etc.

HOA, higher order aberrations. SA (RMS), spherical aberration (Root-Mean-Squared).

Appendix G CRTH Study – Horizontal Corneal Curvature (D)

Experimental Eyes

Time	Location	T4	T3	T2	T1	C	N1	N2	N3	N4
BL	mean	41.45	42.10	42.56	43.19	43.82	43.39	41.95	40.23	39.22
	SD	1.77	1.51	1.62	1.65	1.69	1.71	1.713	2.02	2.47
0min	mean	41.39	40.4	42.17	44.11	44.66	42.86	40.97	39.87	39.56
	SD	2.94	1.24	1.37	1.98	2.12	1.56	1.36	1.95	3.09
1h	mean	41.11	40.65	42.34	44.06	44.50	42.88	41.23	40.21	40.13
	SD	3.36	1.80	1.53	2.04	2.05	1.53	1.25	1.77	2.63
3h	mean	41.24	40.77	42.30	43.87	44.43	43.26	41.46	40.30	39.85
	SD	2.70	1.57	1.53	1.89	2.05	2.19	1.45	1.85	3.00
6h	mean	41.63	40.99	42.18	43.85	44.46	43.23	41.57	40.41	39.91
	SD	2.48	1.50	1.28	1.86	1.94	1.67	1.46	1.89	2.70
12h	mean	41.63	40.99	42.18	43.85	44.46	43.23	41.57	40.41	39.91
	SD	2.48	1.50	1.28	1.86	1.94	1.67	1.46	1.89	2.70
28h	mean	41.47	41.85	42.40	43.23	43.91	43.27	41.83	40.31	39.49
	SD	1.87	1.52	1.53	1.80	1.89	1.75	1.67	2.02	2.60

T4, temporal 4mm from centre. C, centre. N4, nasal 4mm from centre.

BL, baseline. 0min, immediately after lens removal. 1h, 1h without lens wear, etc.

Appendix H CRTH Study – Horizontal Corneal Curvature (D)

Control Eyes

Time	Location	T4	T3	T2	T1	C	N1	N2	N3	N4
BL	mean	41.68	42.14	42.50	43.08	43.75	43.31	42.02	40.32	39.29
	SD	1.56	1.45	1.52	1.61	1.70	1.59	1.65	1.90	2.34
0min	mean	40.96	41.74	42.26	42.94	43.57	43.16	41.67	39.76	38.55
	SD	1.93	1.58	1.54	1.56	1.73	1.56	1.64	1.97	2.48
1h	mean	41.20	41.86	42.41	43.04	43.65	43.18	41.79	40.06	39.08
	SD	1.51	1.51	1.65	1.54	1.62	1.51	1.66	1.92	2.20
3h	mean	41.53	42.00	42.36	43.11	43.74	43.31	41.88	40.24	39.38
	SD	1.71	1.56	1.47	1.53	1.70	1.58	1.70	2.15	2.55
6h	mean	41.36	41.98	42.42	43.05	43.75	43.33	42.02	40.46	39.65
	SD	1.69	1.77	1.59	1.60	1.77	1.73	1.67	1.89	2.23
12h	mean	41.46	41.60	42.27	43.11	43.75	43.28	41.88	40.19	39.15
	SD	1.52	1.93	1.57	1.58	1.70	1.63	1.71	2.06	2.46
28h	mean	41.25	41.99	42.40	42.90	43.64	43.26	42.00	40.39	39.53
	SD	1.52	1.60	1.54	1.47	1.65	1.61	1.80	2.12	2.55

T4, temporal 4mm from centre. C, centre. N4, nasal 4mm from centre.

BL, baseline. 0min, immediately after lens removal. 1h, 1h without lens wear, etc.

Appendix I CRT2 Study -Treatment Zone (mm)

	Time	D1T0	D1T14	D4T0	D4T14	D10T0	D10T14	D28T0	D28T14
CFZ	Mean	3.41	3.14	3.40	3.22	3.59	3.41	3.61	3.51
	SD	0.41	0.49	0.32	0.38	0.40	0.32	0.33	0.31
ASZn+t	Mean	4.77	4.84	5.07	5.34	5.07	5.24	5.24	5.20
	SD	0.66	0.71	0.55	0.54	0.54	0.48	0.62	0.55
ASZ	Mean	8.17	7.98	8.47	8.56	8.66	8.65	8.85	8.71
	SD	0.76	0.81	0.54	0.66	0.63	0.47	0.66	0.58

D1T0, immediately after lens removal on day 1, etc. CFZ, central flattened zone. ASZn+t, the sum of the width of the nasal and temporal sides of annular steepened zone. ASZ, annular steepened zone.

Appendix J CRT2 Study -Corneal Curvature (D)

	Time	BL	D1T0	D1T14	D4T0	D4T14	D10T0	D10T14	D28T0	D28T14
Central	Mean	44.61	43.18	43.94	42.19	42.98	41.83	42.56	41.82	42.45
	SD	1.46	1.45	1.47	1.42	1.42	1.52	1.47	1.46	1.42
Mid-peripheral	Mean	41.89	43.54	42.87	44.85	44.34	44.91	44.47	45.21	44.53
	SD	1.56	1.69	1.46	1.56	1.69	1.88	1.67	1.86	1.82

BL, baseline. D1T0, immediately after lens removal on day 1, etc.

Appendix K CRT2 Study -Visual Acuity (logMAR)

	Time	BL	D1T0	D1T14	D4T0	D4T14	D10T0	D10T14	D28T0	D28T14
HCVA	Mean	0.89	0.36	0.54	0.07	0.17	0.00	0.03	-0.01	0.05
	SD	0.32	0.27	0.31	0.18	0.21	0.10	0.13	0.09	0.13
LCVA	Mean	1.19	0.78	0.98	0.44	0.58	0.31	0.40	0.31	0.40
	SD	0.33	0.28	0.29	0.24	0.29	0.13	0.19	0.12	0.20

BL, baseline. D1T0, immediately after lens removal on day 1, etc. HCVA, high contrast visual acuity. LCVA, low contrast visual acuity.

Appendix L CRT2 Study -Refractive Error (D)

	Time	BL	D1T0	D1T14	D4T0	D4T14	D10T0	D10T14	D28T0	D28T14
Sphere	Mean	-2.72	-1.38	-1.95	-0.67	-1.01	-0.16	-0.59	-0.17	-0.47
	SD	1.06	0.95	0.99	0.63	0.84	0.48	0.60	0.42	0.50
Cylinder	Mean	-0.55	-0.65	-0.54	-0.53	-0.50	-0.57	-0.45	-0.46	-0.52
	SD	0.40	0.38	0.39	0.35	0.35	0.36	0.35	0.33	0.34

BL, baseline. D1T0, immediately after lens removal on day 1, etc.

Appendix M CRT2 Study –Aberrations (μm)

	Time	BL	D1T0	D1T14	D4T0	D4T14	D10T0	D10T14	D28T0	D28T14
Total aberration	Mean	2.46	1.82	2.04	1.22	1.45	0.93	1.16	0.93	1.13
	SD	0.81	0.81	0.79	0.61	0.72	0.46	0.60	0.48	0.52
Defocus	Mean	2.43	1.72	1.99	1.08	1.36	0.72	1.04	0.71	1.00
	SD	0.81	0.84	0.81	0.64	0.76	0.51	0.63	0.52	0.57
Astigmatism	Mean	0.29	0.35	0.31	0.35	0.30	0.35	0.35	0.39	0.34
	SD	0.23	0.23	0.19	0.19	0.12	0.19	0.18	0.19	0.16
HOA	Mean	0.15	0.28	0.21	0.28	0.26	0.31	0.27	0.31	0.26
	SD	0.07	0.17	0.08	0.14	0.09	0.14	0.11	0.16	0.09
Coma	Mean	0.08	0.15	0.12	0.17	0.16	0.19	0.18	0.19	0.16
	SD	0.05	0.13	0.06	0.09	0.07	0.10	0.11	0.12	0.07
SA (RMS)	Mean	0.05	0.14	0.10	0.16	0.15	0.17	0.15	0.17	0.15
	SD	0.03	0.09	0.05	0.10	0.08	0.11	0.08	0.12	0.08

BL, baseline. D1T0, immediately after lens removal on day 1, etc. HOA, higher order aberrations. SA (RMS), spherical aberration (Root-Mean-Squared).

Appendix N CRT2 Study -Subjective Vision

	Time	D1T0	D1T14	D4T0	D4T14	D10T0	D10T14	D28T0	D28T14
Subjective Vision	Mean	49.76	28.70	69.50	48.43	80.50	70.54	86.61	80.46
	SD	27.44	21.62	25.00	26.91	19.45	24.25	15.94	21.22

D1T0, immediately after lens removal on day 1, etc.

Appendix O CRTHDK Study – Refractive Error (D)

Group	Time	BL	0min	1h	3h	6h	12h
Menicon Z	Sphere (mean)	-2.70	-2.01	-2.04	-2.14	-2.25	-2.15
	Sphere (SD)	1.45	1.37	1.37	1.37	1.41	1.38
	Cylinder (mean)	-0.54	-0.65	-0.59	-0.55	-0.55	-0.54
	Cylinder (SD)	0.43	0.38	0.35	0.41	0.36	0.39
Equalens II	Sphere (mean)	-2.65	-1.96	-2.01	-2.09	-2.10	-2.16
	Sphere (SD)	1.43	1.29	1.18	1.18	1.26	1.25
	Cylinder (mean)	-0.46	-0.63	-0.54	-0.56	-0.51	-0.49
	Cylinder (SD)	0.33	0.40	0.38	0.35	0.35	0.26

BL, baseline. 0min, immediately after lens removal. 1h, 1h without lens wear, etc.

Appendix P CRTHDK Study – Aberrations (μm)

Menicon Z Lens Wearing Eyes

Aberrations	Time	BL	0min	1h	3h	6h	12h
Total aberration	Mean	2.55	1.95	1.94	2.01	2.06	2.11
	SD	0.97	0.90	0.99	1.02	1.07	1.00
Defocus	Mean	2.52	1.90	1.90	1.96	2.01	2.07
	SD	0.97	0.91	1.00	1.03	1.08	1.01
Astigmatism	Mean	0.26	0.30	0.28	0.27	0.28	0.28
	SD	0.17	0.19	0.17	0.18	0.17	0.20
HOA	Mean	0.14	0.25	0.22	0.20	0.21	0.19
	SD	0.04	0.09	0.08	0.07	0.08	0.08
Coma	Mean	0.07	0.12	0.12	0.10	0.10	0.10
	SD	0.04	0.06	0.06	0.05	0.07	0.06
SA (RMS)	Mean	0.03	0.14	0.11	0.10	0.10	0.09
	SD	0.02	0.09	0.08	0.07	0.07	0.06

BL, baseline. 0min, immediately after lens removal. 1h, 1h without lens wear, etc.

HOA, higher order aberrations. SA (RMS), spherical aberration (Root-Mean-Squared).

Appendix Q CRTHDK Study – Aberrations (μm)

Equalens II Lens Wearing Eyes

Aberrations	Time	BL	0min	1h	3h	6h	12h
Total aberration	Mean	2.47	1.90	1.88	1.98	2.06	2.07
	SD	0.95	0.91	0.93	0.98	0.96	0.95
Defocus	Mean	2.44	1.84	1.83	1.93	2.01	2.03
	SD	0.97	0.91	0.94	0.99	0.97	0.96
Astigmatism	Mean	0.26	0.32	0.31	0.30	0.28	0.30
	SD	0.18	0.20	0.21	0.19	0.20	0.20
HOA	Mean	0.14	0.23	0.21	0.18	0.19	0.18
	SD	0.05	0.11	0.09	0.07	0.07	0.07
Coma	Mean	0.07	0.11	0.10	0.09	0.10	0.10
	SD	0.04	0.08	0.08	0.05	0.06	0.06
SA (RMS)	Mean	0.03	0.11	0.10	0.09	0.09	0.09
	SD	0.02	0.07	0.06	0.05	0.05	0.05

BL, baseline. 0min, immediately after lens removal. 1h, 1h without lens wear, etc.

HOA, higher order aberrations. SA (RMS), spherical aberration (Root-Mean-Squared).

Appendix R CRTHDK Study – Horizontal Corneal Curvature (D)

Menicon Z Lens Wearing Eyes

Time	Location	T4	T3	T2	T1	C	N1	N2	N3	N4
BL	mean	41.33	41.77	42.72	43.66	44.14	43.58	42.62	41.78	41.06
	SD	1.43	1.23	1.12	1.27	1.41	1.34	1.36	1.70	1.99
0min	mean	40.53	42.63	43.23	42.99	42.92	42.76	42.90	42.75	41.15
	SD	3.55	2.80	1.42	1.51	1.40	1.85	1.47	2.58	3.75
1h	mean	40.95	42.34	43.08	43.25	43.24	42.93	42.95	42.79	41.20
	SD	3.13	2.22	1.23	1.48	1.44	1.58	1.41	2.29	3.21
3h	mean	41.00	42.47	43.05	43.27	43.31	43.06	43.03	42.79	41.47
	SD	2.52	1.97	1.24	1.41	1.42	1.41	1.42	2.16	2.77
6h	mean	40.88	42.29	43.07	43.34	43.41	43.12	43.02	42.68	41.12
	SD	2.38	1.98	1.27	1.43	1.44	1.45	1.34	2.05	2.62
12h	mean	40.89	42.12	42.83	43.24	43.41	43.14	42.90	42.28	40.86
	SD	2.20	1.74	1.06	1.23	1.31	1.38	1.20	1.92	2.45

T4, temporal 4mm from centre. C, centre. N4, nasal 4mm from centre.

BL, baseline. 0min, immediately after lens removal. 1h, 1h without lens wear, etc.

Appendix S CRTHDK Study – Horizontal Corneal Curvature (D)

Equalens II Lens Wearing Eyes

Time	Location	T4	T3	T2	T1	C	N1	N2	N3	N4
BL	mean	40.91	41.67	42.65	43.56	44.15	43.68	42.67	41.64	41.06
	SD	1.16	1.13	1.20	1.33	1.40	1.46	1.28	1.49	1.81
0min	mean	41.11	42.96	43.26	42.93	43.00	42.82	43.16	43.05	42.06
	SD	2.89	2.28	1.43	1.77	1.40	1.29	1.22	1.94	2.75
1h	mean	40.55	42.53	43.18	43.12	43.17	42.92	43.09	43.04	41.92
	SD	2.48	1.94	1.43	1.68	1.48	1.42	1.23	1.76	2.52
3h	mean	40.55	42.50	43.03	43.22	43.35	43.12	43.09	42.78	41.65
	SD	1.92	1.57	1.41	1.75	1.47	1.34	1.27	1.75	2.33
6h	mean	40.90	42.55	43.15	43.26	43.47	43.26	42.98	42.57	41.45
	SD	1.90	1.81	1.40	1.52	1.45	1.40	1.13	1.64	2.48
12h	mean	40.48	42.11	42.94	43.33	43.47	43.18	42.89	42.43	41.39
	SD	1.98	1.70	1.19	1.53	1.29	1.26	1.11	1.75	2.21

T4, temporal 4mm from centre. C, centre. N4, nasal 4mm from centre.

BL, baseline. 0min, immediately after lens removal. 1h, 1h without lens wear, etc.

Appendix T STOK Study – Refractive Error (D)

			Experimental						Control	
			15min BL	15min	30min BL	30min	60min BL	60min	60min BL	60min
CRT	Sph	Mean	-1.85	-1.54	-1.75	-1.38	-1.76	-1.35	-1.88	-1.85
		SD	2.31	2.26	2.35	2.30	2.24	2.27	2.29	2.33
	Cyl	Mean	-0.59	-0.61	-0.56	-0.58	-0.56	-0.53	-0.61	-0.65
		SD	0.49	0.47	0.44	0.42	0.42	0.40	0.44	0.47
CRTH	Sph	Mean	-1.80	-1.98	-1.81	-1.94	-1.83	-2.06	-2.01	-1.99
		SD	2.32	2.45	2.36	2.41	2.31	2.37	2.37	2.38
	Cyl	Mean	-0.54	-0.66	-0.55	-0.73	-0.56	-0.69	-0.64	-0.60
		SD	0.46	0.53	0.45	0.53	0.44	0.51	0.48	0.48

Sph, Sphere. Cyl, Cylinder. 15min BL, baseline for the 15 minutes visit. 15min, after 15min lens wear, etc.

Appendix U STOK Study – Aberrations (μm)

CRT

		Experimental						Control	
		15min BL	15min	30min BL	30min	60min BL	60min	60min BL	60min
Total Aberration	Mean	1.79	1.66	1.84	1.71	1.82	1.67	1.90	1.94
	SD	1.48	1.40	1.45	1.35	1.45	1.31	1.42	1.47
Defocus	Mean	1.71	1.56	1.77	1.60	1.75	1.58	1.83	1.87
	SD	1.53	1.46	1.49	1.42	1.50	1.36	1.47	1.51
Astigmatism	Mean	0.26	0.27	0.27	0.27	0.27	0.25	0.29	0.28
	SD	0.19	0.19	0.20	0.18	0.19	0.16	0.22	0.24
HOA	Mean	0.14	0.20	0.15	0.25	0.14	0.27	0.14	0.13
	SD	0.05	0.09	0.07	0.11	0.05	0.10	0.07	0.04
Coma	Mean	0.08	0.12	0.09	0.16	0.09	0.17	0.07	0.06
	SD	0.05	0.08	0.06	0.11	0.04	0.09	0.05	0.04
SA (RMS)	Mean	0.04	0.07	0.05	0.07	0.04	0.09	0.04	0.05
	SD	0.03	0.05	0.04	0.04	0.04	0.06	0.04	0.04

15min BL, baseline for the 15 minutes visit. 15min, after 15min lens wear, etc.

HOA, higher order aberrations. SA (RMS), spherical aberration (Root-Mean-Squared).

Appendix V STOK Study – Aberrations (μm)

CRTH

		Experimental						Control	
		15min BL	15min	30min BL	30min	60min BL	60min	60min BL	60min
Total Aberration	Mean	1.90	2.06	1.89	2.04	1.84	2.15	1.93	1.99
	SD	1.50	1.54	1.51	1.55	1.46	1.46	1.45	1.50
Defocus	Mean	1.83	1.97	1.82	1.95	1.76	2.04	1.85	1.91
	SD	1.54	1.58	1.55	1.60	1.51	1.53	1.50	1.55
Astigmatism	Mean	0.26	0.30	0.27	0.27	0.27	0.29	0.27	0.29
	SD	0.20	0.20	0.19	0.20	0.19	0.18	0.21	0.22
HOA	Mean	0.15	0.25	0.14	0.28	0.14	0.31	0.13	0.14
	SD	0.05	0.12	0.04	0.12	0.04	0.19	0.05	0.05
Coma	Mean	0.09	0.15	0.07	0.18	0.09	0.19	0.06	0.07
	SD	0.05	0.09	0.04	0.09	0.04	0.14	0.03	0.04
SA (RMS)	Mean	0.04	0.08	0.04	0.08	0.04	0.13	0.05	0.05
	SD	0.04	0.05	0.03	0.05	0.04	0.07	0.04	0.04
Signed SA	Mean	0.03	-0.02	0.03	-0.02	0.03	-0.04	0.04	0.03
	SD	0.05	0.09	0.05	0.09	0.04	0.14	0.05	0.05

15min BL, baseline for the 15 minutes visit. 15min, after 15min lens wear, etc.

HOA, higher order aberrations. SA (RMS), spherical aberration (Root-Mean-Squared).

Appendix W STOK Study – Horizontal Corneal Curvature (D)

CRT

Time	Location	T4	T3	T2	T1	C	N1	N2	N3	N4
Experimental										
15min BL	Mean	41.68	42.04	42.51	43.32	43.91	43.34	42.02	40.56	39.55
	SD	1.55	1.45	1.40	1.51	1.58	1.55	1.74	2.18	2.44
15min	Mean	42.30	42.95	42.47	42.53	43.32	43.44	42.45	40.62	38.89
	SD	1.73	1.63	1.47	1.50	1.58	1.65	1.76	2.28	2.75
30min BL	Mean	41.66	42.00	42.49	43.35	43.90	43.36	41.99	40.55	39.67
	SD	1.56	1.41	1.42	1.55	1.58	1.58	1.74	2.26	2.52
30min	Mean	42.43	43.14	42.63	42.56	43.28	43.50	42.67	40.77	38.55
	SD	2.03	1.60	1.53	1.63	1.65	1.67	1.88	2.51	3.46
60min BL	Mean	41.55	42.02	42.52	43.29	43.84	43.32	42.02	40.62	39.76
	SD	1.53	1.40	1.40	1.50	1.56	1.63	1.70	2.16	2.50
60min	Mean	42.52	43.17	42.58	42.46	43.21	43.47	42.70	40.86	38.83
	SD	2.50	1.72	1.66	1.76	1.69	1.58	1.85	2.65	3.18
Control										
60min BL	Mean	41.53	42.07	42.52	43.25	43.84	43.25	41.82	40.29	39.56
	SD	1.23	1.48	1.44	1.38	1.47	1.58	1.74	2.17	2.67
60min	Mean	41.53	41.99	42.44	43.17	43.74	43.23	41.82	40.18	39.06
	SD	1.05	1.30	1.38	1.42	1.52	1.51	1.71	2.27	2.88

T4, temporal 4mm from centre. C, centre. N4, nasal 4mm from centre.

15min BL, baseline for the 15 minutes visit. 15min, after 15min lens wear, etc.

Appendix X STOK Study – Horizontal Corneal Curvature (D)

CRTH

Time	Location	T4	T3	T2	T1	C	N1	N2	N3	N4
Experimental										
15min BL	Mean	41.75	42.14	42.58	43.33	43.95	43.34	42.04	40.59	39.64
	SD	1.49	1.41	1.45	1.55	1.58	1.61	1.78	2.16	2.36
15min	Mean	41.42	41.61	42.52	43.57	44.02	43.14	41.81	40.58	39.51
	SD	1.19	1.29	1.35	1.47	1.53	1.57	1.69	2.30	3.04
30min BL	Mean	41.72	41.99	42.44	43.26	43.83	43.30	41.96	40.55	39.68
	SD	1.49	1.47	1.43	1.49	1.49	1.58	1.76	2.20	2.35
30min	Mean	41.35	41.61	42.45	43.55	44.07	43.26	41.77	40.35	39.36
	SD	1.17	1.16	1.31	1.57	1.63	1.64	1.65	2.12	2.88
60min BL	Mean	41.65	42.02	42.51	43.34	43.89	43.37	41.96	40.54	39.67
	SD	1.46	1.40	1.43	1.55	1.58	1.59	1.77	2.18	2.33
60min	Mean	41.68	41.56	42.32	43.47	44.07	43.21	41.75	40.43	39.45
	SD	1.22	1.21	1.33	1.62	1.68	1.64	1.71	2.25	2.76
Control										
60min BL	Mean	41.51	42.16	42.51	43.19	43.80	43.30	41.87	40.31	39.60
	SD	1.18	1.34	1.42	1.50	1.51	1.55	1.72	2.16	2.43
60min	Mean	41.50	42.05	42.46	43.15	43.76	43.26	41.84	40.18	39.19
	SD	1.26	1.38	1.35	1.38	1.47	1.55	1.72	2.21	2.72

T4, temporal 4mm from centre. C, centre. N4, nasal 4mm from centre.

15min BL, baseline for the 15 minutes visit. 15min, after 15min lens wear, etc.

Appendix Y STOK Study – Corneal Thickness (μm)

CRT

Time	Location	C	T1	T2	T3	T4	T5
Experimental							
15min BL	Mean	511.01	518.20	540.00	581.50	638.00	713.00
	SD	26.61	25.97	28.08	29.43	32.39	35.96
15min	Mean	513.03	521.60	545.80	585.50	644.80	720.20
	SD	26.63	25.71	25.80	29.66	37.78	38.07
30min BL	Mean	509.38	518.40	540.40	584.50	642.50	714.20
	SD	28.48	28.72	27.87	27.65	32.06	36.00
30min	Mean	516.20	523.20	552.25	591.80	647.70	723.10
	SD	27.31	27.64	26.91	29.66	32.00	37.79
60min BL	Mean	511.40	519.10	543.07	582.97	642.74	716.80
	SD	26.57	26.57	27.61	27.89	29.74	31.49
60min	Mean	521.65	531.20	558.20	592.40	650.90	728.90
	SD	28.07	28.60	26.61	28.64	32.26	36.05
Control							
60min BL	Mean	510.78	520.47	546.45	588.40	651.70	723.80
	SD	27.35	26.58	28.19	24.52	27.39	43.13
60min	Mean	519.00	528.80	553.10	595.70	659.90	733.70
	SD	26.63	25.22	28.64	27.71	31.47	47.10

T4, temporal 4mm from centre. C, centre. 15min BL, baseline for the 15 minutes visit. 15min, after 15min lens wear, etc.

Appendix Z STOK Study – Corneal Thickness (μm)

CRTH

Time	Location	C	T1	T2	T3	T4	T5
Experimental							
15min BL	Mean	511.50	518.60	543.50	585.10	639.63	719.30
	SD	25.11	25.13	25.51	23.73	27.65	31.89
15min	Mean	518.40	526.40	547.50	588.00	645.50	721.00
	SD	25.08	25.31	26.80	26.56	28.60	33.86
30min BL	Mean	511.37	520.80	544.25	585.10	637.00	712.00
	SD	25.57	26.55	25.50	22.15	21.04	30.33
30min	Mean	523.30	529.70	547.80	588.60	644.50	719.60
	SD	25.84	25.51	24.40	23.83	30.11	34.01
60min BL	Mean	511.89	520.40	546.00	585.40	638.60	714.60
	SD	26.68	26.85	27.02	29.03	29.11	28.79
60min	Mean	527.50	534.70	555.40	592.80	648.00	723.00
	SD	28.06	28.18	27.75	27.85	29.25	33.39
Control							
60min BL	Mean	513.30	522.70	545.50	586.10	651.10	728.20
	SD	27.81	28.85	27.69	28.15	33.34	36.79
60min	Mean	519.85	526.90	549.80	593.20	654.00	735.80
	SD	28.30	26.06	25.08	27.99	27.77	39.90

T4, temporal 4mm from centre. C, centre. 15min BL, baseline for the 15 minutes visit. 15min, after 15min lens wear, etc.

Appendix AA STOK Study – Epithelial Thickness (μm)

CRT

Time	Location	C	T1	T2	T3	T4	T5
Experimental							
15min BL	Mean	48.99	48.40	47.80	49.00	50.30	53.10
	SD	3.97	4.48	3.30	4.42	4.82	4.08
15min	Mean	47.45	46.90	48.80	49.50	50.70	53.30
	SD	3.63	2.86	3.27	4.20	5.12	4.87
30min BL	Mean	49.84	49.50	49.40	49.40	51.30	54.90
	SD	3.74	4.25	4.31	3.68	5.24	3.86
30min	Mean	48.20	48.60	50.70	51.20	51.30	54.30
	SD	4.35	4.16	5.67	4.96	6.66	3.96
60min BL	Mean	49.30	49.60	49.75	50.35	50.35	54.60
	SD	3.51	3.82	4.66	4.12	3.91	4.11
60min	Mean	47.90	47.10	51.60	52.25	50.80	53.70
	SD	2.20	4.61	4.08	5.77	4.18	4.65
Control							
60min BL	Mean	48.90	48.85	49.70	49.60	50.90	54.90
	SD	3.40	3.86	4.37	3.98	3.46	3.64
60min	Mean	48.50	49.10	49.30	50.10	51.30	55.90
	SD	3.78	3.28	3.80	3.64	4.46	4.23

T4, temporal 4mm from centre. C, centre. 15min BL, baseline for the 15 minutes visit. 15min, after 15min lens wear, etc.

Appendix BB STOK Study – Epithelial Thickness (μm)

CRTH

Time	Location	C	T1	T2	T3	T4	T5
Experimental							
15min BL	Mean	48.30	48.10	48.30	48.30	49.14	54.50
	SD	2.77	1.65	3.51	2.54	3.49	5.98
15min	Mean	49.40	48.15	47.20	47.80	50.00	55.30
	SD	3.56	3.79	3.07	3.30	3.49	5.08
30min BL	Mean	47.67	48.50	48.60	49.30	51.00	54.30
	SD	3.45	3.17	3.19	3.63	3.87	4.17
30min	Mean	49.24	48.50	47.30	48.45	51.00	54.95
	SD	3.99	3.17	4.12	3.50	4.96	4.54
60min BL	Mean	48.38	48.30	48.80	50.20	50.70	56.80
	SD	3.27	2.62	3.33	4.58	3.57	4.02
60min	Mean	49.40	49.30	48.30	48.00	49.40	56.00
	SD	3.73	4.12	5.36	4.15	4.55	5.51
Control							
60min BL	Mean	47.80	48.60	49.20	50.30	50.60	56.50
	SD	3.55	3.44	3.69	3.39	3.32	4.58
60min	Mean	48.00	48.50	49.30	50.20	50.10	57.00
	SD	3.89	3.99	4.12	3.55	4.96	5.93

T4, temporal 4mm from centre. C, centre. 15min BL, baseline for the 15 minutes visit. 15min, after 15min lens wear, etc.

Bibliography

(July 12, 2002), Vol. 2006 U.S. Food and Drug Administration Website.

Alberts, B., Bray, D., Lewis, J., Raff, M., Robert, K. and Watson, J. (1994) *Molecular biology of the cell,* Garland publishing, Inc., New York.

Alharbi, A., La Hood, D. and Swarbrick, H. A. (2005) Overnight orthokeratology lens wear can inhibit the central stromal edema response *Invest Ophthalmol Vis Sci,* **46,** 2334-40.

Alharbi, A. and Swarbrick, H. A. (2003) The effects of overnight orthokeratology lens wear on corneal thickness *Invest Ophthalmol Vis Sci,* **44,** 2518-23.

Allaire, P. E. and Flack, R. D. (1980) Squeeze forces in contact lenses with a steep base curve radius *Am J Optom Physiol Opt,* **57,** 219-227.

Applegate, R. A., Hilmantel, G. and Thibos, L. N. (2001) Visual performance assessment In *Customized corneal ablation: the quest for supervision*(Eds, MacRae, S., Krueger, R. R. and Applegate, R. A.) SLACK Incorporated, Thorofare, pp. 81-92.

Applegate, R. A., Thibos, L. N., Bradley, A., Marcos, S., Roorda, A., Salmon, T. O. and Atchison, D. A. (2000) Reference axis selection: subcommittee report of the OSA Working Group to establish standards for measurement and reporting of optical aberrations of the eye *J Refract Surg,* **16,** S656-8.

Araki-Sasaki, K., Nishi, I., Yonemura, N., Takatsuka, H., Mutoh, K., Matsumoto, K., Asari, S. and Tanihara, H. (2005) Characteristics of Pseudomonas corneal infection related to orthokeratology *Cornea,* **24,** 861-3.

Artal, P. and Guirao, A. (1998) Contributions of the cornea and lens to the aberrations of the human eye *Optics Letters,* **23,** 1713-1715.

Artal, P., Guirao, A., Berrio, E. and Williams, D. R. (2001) Compensation of corneal aberrations by the internal optics in the human eye *J Vis,* **1,** 1-8.

Barbero, S., Marcos, S. and Merayo-Lloves, J. (2002) Corneal and total optical aberrations in a unilateral aphakic patient *J Cataract Refract Surg,* **28,** 1594-600.

Barr, J. T., Rah, M. J., Jackson, J. M. and Jones, L. A. (2003) Orthokeratology and corneal refractive therapy: a review and recent findings *Eye Contact Lens,* **29,** S49-53; discussion S57-9, S192-4.

Barr, J. T., Rah, M. J., Meyers, W. and Legerton, J. (2004) Recovery of refractive error after corneal refractive therapy *Eye Contact Lens,* **30,** 247-51; discussion 263-4.

Battaglioli, J. L. and Kamm, R. D. (1984) Measurements of the compressive properties of scleral tissue *Invest Ophthalmol Vis Sci,* **25,** 59-65.

Benjamin, W. J. (1993) EOP and Dk/L: the quest for hyper transmissibility *J Am Optom Assoc,* **64,** 196-200.

Berkley, D. (1971) Influence of IOP on corneal fluid pressure, tissue stress and thickness. *Exp Eye Res,* **11,** 132-139.

Berntsen, D. A., Barr, J. T. and Mitchell, G. L. (2005) The effect of overnight contact lens corneal reshaping on higher-order aberrations and best-corrected visual acuity *Optom Vis Sci,* **82,** 490-7.

Binder, P. S., May, C. H. and Grant, S. C. (1980) An evaluation of orthokeratology *Ophthalmology,* **87,** 729-44.

Bland, J. and Altman, D. (1986) Statistical methods for assessing agreement between two methods of clinical measurement. *Lancet***,** 307-310.

Bogan, S. J., Waring, G. O., 3rd, Ibrahim, O., Drews, C. and Curtis, L. (1990) Classification of normal corneal topography based on computer-assisted videokeratography *Arch Ophthalmol,* **108,** 945-9.

Brand, R. J., Polse, K. A. and Schwalbe, J. S. (1983) The Berkeley Orthokeratology Study, Part I: General conduct of the study *Am J Optom Physiol Opt,* **60,** 175-86.

Bruce, A. S. and Brennan, N. A. (1990) Corneal pathophysiology with contact lens wear *Surv Ophthalmol,* **35,** 25-58.

Burton, E. (1942) Progressive Myopia: a possible etiologic factor. *Trans Amer Ophthal Soc***,** 340.

Carkeet, N. L., Mountford, J. A. and Carney, L. G. (1995) Predicting success with orthokeratology lens wear: a retrospective analysis of ocular characteristics *Optom Vis Sci,* **72,** 892-8.

Carney, L. G. (1975) Hydrophilic lens effects on central and peripheral corneal thickness and corneal topography *Am J Optom Physiol Opt,* **52,** 521-3.

Carney, L. G., Mainstone, J. C., Carkeet, A., Quinn, T. G. and Hill, R. M. (1997a) Rigid lens dynamics: lid effects *Clao J,* **23,** 69-77.

Carney, L. G., Mainstone, J. C. and Henderson, B. A. (1997b) Corneal topography and myopia. A cross-sectional study *Invest Ophthalmol Vis Sci,* **38,** 311-20.

Caroline, P. J. (2001) Contemporary orthokeratology *Cont Lens Anterior Eye,* **24,** 41-6.

Caroline, P. J. and Choo, J. D. (2003) Modern corneal reshaping with contact lenses *Ophthalmol Clin North Am,* **16,** 405-13.

Chalita, M. R. and Krueger, R. R. (2004) Correlation of aberrations with visual acuity and symptoms *Ophthalmol Clin North Am,* **17,** 135-42, v-vi.

Cheung, S. W. and Cho, P. (2004) Subjective and objective assessments of the effect of orthokeratology--a cross-sectional study *Curr Eye Res,* **28,** 121-7.

Cho, P., Cheung, S. W. and Edwards, M. H. (2003a) Practice of orthokeratology by a group of contact lens practitioners in Hong Kong. Part 2: orthokeratology lenses *Clin Exp Optom,* **86,** 42-6.

Cho, P., Chui, W. S. and Cheung, S. W. (2003b) Reversibility of corneal pigmented arc associated with orthokeratology *Optom Vis Sci,* **80,** 791-5.

Cho, P., Lam, A. K., Mountford, J. and Ng, L. (2002) The performance of four different corneal topographers on normal human corneas and its impact on orthokeratology lens fitting *Optom Vis Sci,* **79,** 175-83.

Choo, J., Caroline, P. and Harlin, D. (2004a) How Does the Cornea Change Under Corneal Reshaping Contact Lenses? *Eye & Contact Lens,* **33,** 211-13.

Choo, J., Caroline, P., Harlin, D. and Meyers, W. (2004b) Morphologic changes in cat stroma following 14 continuous wear of Paragon CRT lenses *Optom Vis Sci,* **81,** 28.

Choo, J. D., Caroline, P., Harlin, D. D. and Meyers, W. (2004c) Morphologic changes in cat epithelium following overnight lens wear with Paragon CRT lens for corneal reshaping *IOVS.,* **45,** E-abstract 1552.

Choo, J. D., Caroline, P. J., Holden, B. A., Evans, S. R., Ho, A. and Bergenske, P. D. (2005) Soft Contact Lenses Can Induce Orthokeratology like Topographical Changes *Invest. Ophthalmol. Vis. Sci.,* **46,** E-Abstract 2062.

Conway, H. D. (1982) The motion of a contact lens over the eye during blinking *Am J Optom Physiol Opt,* **59,** 770-3.

Coon, L. J. (1982) Orthokeratology: part I historical perspective *J Am Optom Assoc,* **53,** 187-95.

Coon, L. J. (1984) Orthokeratology. Part II: Evaluating the Tabb method *J Am Optom Assoc,* **55,** 409-18.

Cosar, C. B., Saltuk, G. and Sener, A. B. (2004) Wavefront-guided laser in situ keratomileusis with the Bausch & Lomb Zyoptix system *J Refract Surg,* **20,** 35-9.

Cristol, S. M., Edelhauser, H. F. and Lynn, M. J. (1992) A comparison of corneal stromal edema induced from the anterior or the posterior surface *Refract Corneal Surg,* **8,** 224-9.

Cronje, S. and Harris, W. F. (1997) Short-term keratometric variation in the human eye *Optom Vis Sci,* **74,** 420-4.

Dart, J. K., Stapleton, F. and Minassian, D. (1991) Contact lenses and other risk factors in microbial keratitis *Lancet,* **338,** 650-3.

Davanger, M. and Evensen, A. (1971) Role of the pericorneal papillary structure in renewal of cornel epithelium *Nature,* **229,** 560-561.

Dave, T. and Ruston, D. (1998) Current trends in modern orthokeratology *Ophthalmic Physiol Opt,* **18,** 224-33.

Dawson, D. G., Edelhauser, H. F. and Grossniklaus, H. E. (2005) Long-term histopathologic findings in human corneal wounds after refractive surgical procedures *Am J Ophthalmol,* **139,** 168-78.

Dickinson, F. (1971) The relationship of the eyelids to contact lens performance *Br J Physiol Opt,* **26,** 22-8.

Dierick, H. G. and Missotten, L. (1992) Is the corneal contour influenced by a tension in the superficial epithelial cells? A new hypothesis *Refract Corneal Surg,* **8,** 54-9; discussion 60.

Dillon, E. C., Eagle, R. C., Jr. and Laibson, P. R. (1992) Compensatory epithelial hyperplasia in human corneal disease *Ophthalmic Surg,* **23,** 729-32.

Dingeldein, S. A. and Klyce, S. D. (1989) The topography of normal corneas *Arch Ophthalmol,* **107,** 512-8.

Dixon, J. M. (1964) Ocular Changes Due to Contact Lenses *Am J Ophthalmol,* **58,** 424-43.

Edelhauser, H. F., Geroski, D. H. and Ubels, J. (1994) Physiology In *The Cornea*(Eds, Smolin, G. and Thoft, R.) Little Brown, Toronto, pp. 25-47.

Efron, N. and Ang, J. H. (1990) Corneal hypoxia and hypercapnia during contact lens wear *Optom Vis Sci,* **67,** 512--521.

Ehrmann, K., Francis, I. and Stapleton, F. (2001) A novel instrument to quantity the tension of upper and lower eyelids *Cont Lens Anterior Eye,* **24,** 65-72.

Endl, M. J., Martinez, C. E., Klyce, S. D., McDonald, M. B., Coorpender, S. J., Applegate, R. A. and Howland, H. C. (2001) Effect of larger ablation zone and transition zone on corneal optical aberrations after photorefractive keratectomy *Arch Ophthalmol,* **119,** 1159-64.

Erickson, P., Comstock, T. L., Doughty, M. J. and Cullen, A. P. (1999) The cornea swells in the posterior direction under hydrogel contact lenses *Ophthalmic Physiol Opt,* **19,** 475-80.

Estil, S., Primo, E. J. and Wilson, G. (2000) Apoptosis in shed human corneal cells *Invest Ophthalmol Vis Sci,* **41,** 3360-4.

Evans, S. R., Ho, A. and Choo, J. D. (2005) Orthokeratologylike Effects of Everted Soft Contact Lenses: A Mechanical Model *Invest Ophthalmol vis Sci,* **46,** E-Abstract 2059.

Fakhry, M. A., Artola, A., Belda, J. I., Ayala, M. J. and Alio, J. L. (2002) Comparison of corneal pachymetry using ultrasound and Orbscan II *J Cataract Refract Surg,* **28,** 248-52.

Fan, L., Jun, J., Jia, Q., Wangqing, J., Xinjie, M. and Yi, S. (1999) Clinical study of orthokeratology in young myopic adolescents *Int. Contact Lens Clin,* **26,** 113-116.

Feng, Y., Varikooty, J. and Simpson, T. L. (2001) Diurnal variation of corneal and corneal epithelial thickness measured using optical coherence tomography *Cornea,* **20,** 480-3.

Forster, H. P., Emanuel, E. and Grady, C. (2001) The 2000 revision of the Declaration of Helsinki: a step forward or more confusion? *Lancet,* **358,** 1449-53.

Freddo, T. and Warning III, G. (1998) Chapter 6. Pathologic response in the cornea In *Corneal disorders: clinilcal diagnosis and management*(Eds, Leibowitz, H. and Warning III, G.) W.B. Saunders company, Toronto, pp. 154-200.

Friend, J. and Hassell, J. (1994) Biochemistry of the cornea In *The cornea: Scientific foundations and clinical practice*(Eds, Smolin, G. and Thoft, R.) Little Brown, Toronto, pp. 47-67.

Fung, Y. (1995) Stress, strain, growth, and remodeling of living organisms. In *Theoretical, Experimental, and Numerical Contributions to the Mechanics of Fluids and Solids.*(Ed, Casey, J., Crochet, MJ.) Birkhauser Verlag, Basel, pp. 78.

Gipson, I. (1994) Anatomy of the conjunctiva, cornea, and limbus In *The Cornea: Scientific foundations and clinical practice*(Eds, Smolin, G. and Thoft, R.) Little brown, Toronto, pp. 3-24.

Grant, S. C. (1980) Orthokeratology. I. A safe and effective treatment for a disabling problem. *Survey Of Ophthalmology,* **24,** 291-297.

Greenberg, M. H. and Hill, R. M. (1973) The physiology of contact lens imprints *Am J Optom Arch Am Acad Optom,* **50,** 699-702.

Guirao, A., Redondo, M. and Artal, P. (2000) Optical aberrations of the human cornea as a function of age *J Opt Soc Am A Opt Image Sci Vis,* **17,** 1697-702.

Guo, Y., Nguyen, M., Soni, S. and Wison, G. (2004) Cell Shedding in Overnight Orthokeratology *Invest. Ophthalmol. Vis. Sci.,* **45,** E-abstract 1581.

Haque, S., Fonn, D., Sorbara, L. and Simpson, T. (2004a) Corneal and epithelial thickness changes following one night of CRT gas permeable lens wear for hyperopia, measured with optical coherence tomography *Optom Vis Sci,* **81,** 27.

Haque, S., Fonn, D., Simpson, T. and Jones, L. (2004b) Corneal and epithelial thickness changes after 4 weeks of overnight corneal refractive therapy lens wear, measured with optical coherence tomography *Eye Contact Lens,* **30,** 189-93.

Haque, S., Fonn, D., Simpson, T. and Jones, L. (2005) Corneal, Stromal and epithelial thickness changes following overnight CRT, comparing two high DK lens materials *Optom Vis Sci,* **82,** E - abstract 050041.

Harris, M. G. and Appelquist, T. D. (1974) The effect of contact lens diameter and power on flexure and residual astigmatism *Am J Optom Physiol Opt,* **51,** 266-70.

Harvitt, D. M. and Bonanno, J. A. (1999) Re-evaluation of the oxygen diffusion model for predicting minimum contact lens Dk/t values needed to avoid corneal anoxia *Optom Vis Sci,* **76,** 712-9.

Hayashi, K., Hayashi, H. and Hayashi, F. (1995) Topographic analysis of the changes in corneal shape due to aging *Cornea,* **14,** 527-32.

He, J. C., Gwiazda, J., Thorn, F. and Held, R. (2003) Wave-front aberrations in the anterior corneal surface and the whole eye *J Opt Soc Am A Opt Image Sci Vis,* **20,** 1155-63.

Hennighausen, H., Feldman, S. T., Bille, J. F. and McCulloch, A. D. (1998) Anterior-posterior strain variation in normally hydrated and swollen rabbit cornea *Invest Ophthalmol Vis Sci,* **39,** 253-62.

Herman, J. P. (1983) Flexure of rigid contact lenses on toric corneas as a function of base curve fitting relationship *J Am Optom Assoc,* **54,** 209-13.

Hill, J. F. and Rengstorff, R. H. (1974) Relationship between steeply fitted contact lens base curve and corneal curvature changes *Am J Optom Physiol Opt,* **51,** 340-2.

Hiraoka, T., Matsumoto, Y., Okamoto, F., Yamaguchi, T., Hirohara, Y., Mihashi, T. and Oshika, T. (2005) Corneal higher-order aberrations induced by overnight orthokeratology *Am J Ophthalmol,* **139,** 429-36.

Hjortdal, J. O. (1995) Extensibility of the normo-hydrated human cornea *Acta Ophthalmol Scand,* **73,** 12-7.

Hjortdal, J. O. (1996) Regional elastic performance of the human cornea *J Biomech,* **29,** 931-42.

Hjortdal, J. O. (1998) On the biomechanical properties of the cornea with particular reference to refractive surgery *Acta Ophthalmol Scand Suppl***,** 1-23.

Hjortdal, J. O. and Jensen, P. K. (1995) In vitro measurement of corneal strain, thickness, and curvature using digital image processing *Acta Ophthalmol Scand,* **73,** 5-11.

Hoeltzel, D. A., Altman, P., Buzard, K. and Choe, K. (1992) Strip extensiometry for comparison of the mechanical response of bovine, rabbit, and human corneas *J Biomech Eng,* **114,** 202-15.

Holden, A., Sweeney, D. and Collin, H. (1989) The effects of RGP and silicone elastomer lens binding on corneal structure *Invest Ophthalmol Vis Sci***,** 481.

Holden, B. A. (1988) The Glenn A. Fry award lecture 1988: the ocular response to contact lens wear *Optom Vis Sci,* **66,** 717--733.

Holden, B. A. and Mertz, G. W. (1984) Critical oxygen levels to avoid corneal edema for daily and extended wear contact lenses *Invest Ophthalmol Vis Sci,* **25,** 1161-7.

Holden, B. A., Stephenson, A., Stretton, S., Sankaridurg, P. R., O'Hare, N., Jalbert, I. and Sweeney, D. F. (2001) Superior epithelial arcuate lesions with soft contact lens wear *Optom Vis Sci,* **78,** 9-12.

Holden, B. A., Sweeney, D. F., Sankaridurg, P. R., Carnt, N., Edwards, K., Stretton, S. and Stapleton, F. (2003) Microbial keratitis and vision loss with contact lenses *Eye Contact Lens,* **29,** S131-4; discussion S143-4, S192-4.

Hom, M. M. and Bruce, A. S. (2004) Oxygen and the Cornea: Material Properties In *Manual of Gas Permeable Contact Lenses*(Eds, Bennett, E. S. and Hom, M. M.) Butterworth-Heinemann, pp. 30-47.

Horner, D., Armitage, K., Wormsley, K., Mandell, R. and Soni, P. (1992) Corneal molding recovery after contact lens wear *Optom Vis Sci,* **12 (suppl)**.

Hsiao, C. H., Lin, H. C., Chen, Y. F., Ma, D. H., Yeh, L. K., Tan, H. Y., Huang, S. C. and Lin, K. K. (2005) Infectious keratitis related to overnight orthokeratology *Cornea,* **24,** 783-8.

Huang, B., Mirza, M. A., Qazi, M. A. and Pepose, J. S. (2004) The effect of punctal occlusion on wavefront aberrations in dry eye patients after laser in situ keratomileusis *Am J Ophthalmol,* **137,** 52-61.

Hughes, B., Caroline, P., Choo, J., Gondo, M. and Bergmanson, J. P. G. (2004) 24 hour orthok-induced epithelial alternations in cats. *Optom Vis Sci,* **81,** 73.

Hung, G., Hsu, F. and Stark, L. (1977) Dynamics of the human eyeblink *Am J Optom Physiol Opt,* **54,** 678-90.

Iskander, N. G., Anderson Penno, E., Peters, N. T., Gimbel, H. V. and Ferensowicz, M. (2001) Accuracy of Orbscan pachymetry measurements and DHG ultrasound pachymetry in primary laser in situ keratomileusis and LASIK enhancement procedures *J Cataract Refract Surg,* **27,** 681-5.

Jackson, J. M., Bildstein, T., Anderson, J., Leak, B. and Buresh, K. (2004) Short-Term Corneal Changes with Corneal Regractive Refractive Therapy (CRT) *Invest Ophthalmol Vis Sci,* **E-abstract,** 64.

Jalbert, I. and Stapleton, F. (2005) The corneal stroma during contact lens wear *Cont Lens Anterior Eye,* **28,** 3-12.

Jayakumar, J. and Swarbrick, H. A. (2005) The effect of age on short-term orthokeratology *Optom Vis Sci,* **82,** 505-11.

Jeandervin, M. and Barr, J. (1998) Comparison of repeat videokeratography: repeatability and accuracy *Optom Vis Sci,* **75,** 663-9.

Jessen, G. (1962) Orthofocus techniques *Contacto,* **6,** 200-204.

Joe, J. J., Marsden, H. J. and Edrington, T. B. (1996) The relationship between corneal eccentricity and improvement in visual acuity with orthokeratology *J Am Optom Assoc,* **67,** 87-97.

Jones, L. and Jones, D. (1995) Dimple-veil staining *Optician,* **210,** 32.

Joslin, C., Wu, S., Mcmahon, T. and Shahidi, M. (2003) Higher-order wavefront aberrations in corneal refractive therapy *Optom Vis Sci,* **80,** 805-811.

Jue, B. and Maurice, D. M. (1986) The mechanical properties of the rabbit and human cornea *J Biomech,* **19,** 847-53.

Kamei, Y., Cassar, K., Shen, J. and Soni, P. S. (2005) Short-term corneal changes in closed eye condition with orthokeratology lenses. *Invest Ophthalmol Vis Sci,* **46,** E-abstract: 2060.

Kelly, J. E., Mihashi, T. and Howland, H. C. (2004) Compensation of corneal horizontal/vertical astigmatism, lateral coma, and spherical aberration by internal optics of the eye *J Vis,* **4,** 262-71.

Kermani, O., Schmiedt, K., Oberheide, U. and Gerten, G. (2003) Early results of nidek customized aspheric transition zones (CATz) in laser in situ keratomileusis *J Refract Surg,* **19,** S190-4.

Kerns, R. L. (1976a) Research in orthokeratology. Part I: Introduction and background *J Am Optom Assoc,* **47,** 1047-51.

Kerns, R. L. (1976b) Research in orthokeratology. Part II: Experimental design, protocol and method *J Am Optom Assoc,* **47,** 1275-85.

Kerns, R. L. (1976c) Research in orthokeratology. Part III: results and observations *J Am Optom Assoc,* **47,** 1505-15.

Kerns, R. L. (1977a) Research in orthokeratology. Part IV: Results and observations *J Am Optom Assoc,* **48,** 227-38.

Kerns, R. L. (1977b) Research in orthokeratology. Part V: Results and observations--recovery aspects *J Am Optom Assoc,* **48,** 345-59.

Kerns, R. L. (1977c) Research in orthokeratology. Part VI: statistical and clinical analyses *J Am Optom Assoc,* **48,** 1134-47.

Kerns, R. L. (1977d) Research in orthokeratology. Part VII: examination of techniques, procedures and control *J Am Optom Assoc,* **48,** 1541-53.

Kerns, R. L. (1978) Research in orthokeratology. Part VIII: results, conclusions and discussion of techniques *J Am Optom Assoc,* **49,** 308-14.

Kiely, P. M. and Carney, L. G. (1978) Influence of lid pressure and corneal topography *Aust J Optom,* **61,** 390-392.

Kiely, P. M., Carney, L. G. and Smith, G. (1982) Diurnal variations of corneal topography and thickness *Am J Optom Physiol Opt,* **59,** 976-82.

Kikkawa, Y. and Hirayama, K. (1970) Uneven swelling of the corneal stroma *Invest Ophthalmol,* **9,** 735-41.

Klein, S. A. and Mandell, R. B. (1995a) Axial and instantaneous power conversion in corneal topography *Invest Ophthalmol Vis Sci,* **36,** 2155-9.

Klein, S. A. and Mandell, R. B. (1995b) Shape and refractive powers in corneal topography *Invest Ophthalmol Vis Sci,* **36,** 2096-109.

Klyce, S. D. and Beuerman, R. (1997) Structure and Function of the Cornea In *The Cornea*(Eds, Kaufman, H., Barron, B. and McDonald, M. B.) Butterworth-Heinemann, Boston, pp. 3-50.

Komai, Y. and Ushiki, T. (1991) The three-dimensional organization of collagen fibrils in the human cornea and sclera *Invest Ophthalmol Vis Sci,* **32,** 2244-58.

Kramer, T. R., Chuckpaiwong, V., Dawson, D. G., L'Hernault, N., Grossniklaus, H. E. and Edelhauser, H. F. (2005) Pathologic findings in postmortem corneas after successful laser in situ keratomileusis *Cornea,* **24,** 92-102.

Ladage, P., Yamamoto, N., Robertson, D., Jester, J., Petroll, W. and Cavanagh, H. (2004) Pseudomonas aeruginosa corneal binding after 24-hour orthokeratology lens wear. *Eye & Contact Lens,* **30,** 173-178.

Ladage, P. M., Jester, J. V., Petroll, W. M., Bergmanson, J. P. and Cavanagh, H. D. (2003) Vertical movement of epithelial basal cells toward the corneal surface during use of extended-wear contact lenses *Invest Ophthalmol Vis Sci,* **44,** 1056-63.

Ladage, P. M., Petroll, W. M., Jester, J. V., Fisher, S., Bergmanson, J. P. and Cavanagh, H. D. (2002) Spherical indentations of human and rabbit corneal epithelium following extended contact lens wear *Clao J,* **28,** 177-80.

Ladage, P. M., Yamamoto, K., Ren, D. H., Li, L., Jester, J. V., Petroll, W. M., Bergmanson, J. P. and Cavanagh, H. D. (2001) Proliferation rate of rabbit corneal epithelium during overnight rigid contact lens wear *Invest Ophthalmol Vis Sci,* **42,** 2804-12.

Lavker, R. M., Tseng, S. C. and Sun, T. T. (2004) Corneal epithelial stem cells at the limbus: looking at some old problems from a new angle *Exp Eye Res,* **78,** 433-46.

Lebow, K. (1991) Orthokeratology In *Clinical contact lens practice*(Eds, Bennett, E. and Weisman, B.) Philadelphia : Lippincott-Raven, pp. Chap 49:1-5.

Lee, D. and Wilson, G. (1981) Non-uniform swelling properties of the corneal stroma *Curr Eye Res,* **1,** 457-61.

Lemp, M. A. and Gold, J. B. (1986) The effects of extended-wear hydrophilic contact lenses on the human corneal epithelium *Am J Ophthalmol,* **101,** 274-7.

Lemp, M. A. and Mathers, W. D. (1989) Corneal epithelial cell movement in humans *Eye,* **3 (Pt 4),** 438-45.

Levy, B. (1982) Permanent corneal damage in a patient undergoing orthokeratology. *American Journal Of Optometry And Physiological Optics,* **59,** 697-699.

Li, H. F., Petroll, W. M., Moller-Pedersen, T., Maurer, J. K., Cavanagh, H. D. and Jester, J. V. (1997) Epithelial and corneal thickness measurements by in vivo confocal microscopy through focusing (CMTF) *Curr Eye Res,* **16,** 214-21.

Lieberman, D. and Grierson, J. (2000) The lid influence on corneal shape *Cornea,* **19,** 336-342.

Liesegang, T. J. (2002) Physiologic changes of the cornea with contact lens wear *Clao J,* **28,** 12-27.

Liu, Z., Huang, A. J. and Pflugfelder, S. C. (1999) Evaluation of corneal thickness and topography in normal eyes using the Orbscan corneal topography system *Br J Ophthalmol,* **83,** 774-8.

Llorente, L., Barbero, S., Cano, D., Dorronsoro, C. and Marcos, S. (2004a) Myopic versus hyperopic eyes: axial length, corneal shape and optical aberrations *J Vis,* **4,** 288-98.

Llorente, L., Barbero, S., Merayo, J. and Marcos, S. (2004b) Total and corneal optical aberrations induced by laser in situ keratomileusis for hyperopia *J Refract Surg,* **20,** 203-16.

Lu, F., Sorbara, L., Kort, R., Fonn, D., Simpson, T. and Jones, L. (2003) Topographic Keratometric Effects of Corneal Refractive Therapy After One Night of Lens Wear. *IOVS.,* **44,** E-abstract 3699.

Lu, F., Simpson, T., Sorbara, L. and Fonn, D. (2004) The Relationship between the Treatment Zone Diameter and Visual, Optical and Subjective Performance in Corneal Refractive Therapy Lens Wearers *IOVS.,* **45,** E-abstract: 1576.

Lu, F., Simpson, T., Sorbara, L. and Fonn, D. (2005) Corneal shape and optical performance after one night of two different oxygen transmissibility corneal refractive therapy lens wear. *Optom Vis Sci,* **82,** E-abstract 050042.

Lu, F., Simpson, T., Fonn, D., Sorbara, L. and Jones, L. (2006a) Validity of pachymetric measurements by manipulating the acoustic factor of Orbscan II *Eye Contact Lens,* **32,** 78-83.

Lu, F., Simpson, T., Sorbara, L. and Fonn, D. (2006b) Corneal Shape and Optical Performance after One Night of Hyperopic Corneal Refractive Therapy Lens Wear *Optom Vis Sci,* **Accepted**.

Lui, W. O. and Edwards, M. H. (2000) Orthokeratology in low myopia. Part 1: efficacy and predictability *Cont Lens Anterior Eye,* **23,** 77-89.

Lui, W. O., Edwards, M. H. and Cho, P. (2000) Contact lenses in myopia reduction - from orthofocus to accelerated orthokeratology *Cont Lens Anterior Eye,* **23,** 68-76.

Lydon, D. and Tait, A. (1988) Lid-Pressure: Its measurement and probable effects on the shape and form of the cornea-rigid contact lens system *Journal of the B.C.L.A.,* **11,** 11-22.

Ma, L., Atchison, D. A., Albietz, J. M., Lenton, L. M. and McLennan, S. G. (2004) Wavefront aberrations following laser in situ keratomileusis and refractive lens exchange for hypermetropia *J Refract Surg,* **20,** 307-16.

Macsai, M. S., Stubbe, K., Beck, A. P. and Ravage, Z. B. (2004) Effect of expanding the treatment zone of the Nidek EC-5000 laser on laser in situ keratomileusis outcomes *J Cataract Refract Surg,* **30,** 2336-43.

Mandell, R. B. (1996) A guide to videokeratography *ICLC,* **23,** 205-228.

Mandell, R. B. and Fatt, I. (1965) Thinning of the human cornea on awakening *Nature,* **208,** 292-3.

Marcos, S. (2001) Aberrations and visual performance following standard laser vision correction *J Refract Surg,* **17,** S596-601.

Marcos, S., Barbero, S., Llorente, L. and Merayo-Lloves, J. (2001) Optical response to LASIK surgery for myopia from total and corneal aberration measurements *Invest Ophthalmol Vis Sci,* **42,** 3349-56.

Martin, D. K. and Holden, B. A. (1986) Forces developed beneath hydrogel contact lenses due to squeeze pressure *Phys Med Biol,* **31,** 635-49.

Matsubara, M. (2002) Histological change of cornea by orthokeratology lens *1st Global orthokeraology symposium, Toronto, Canada,* **1,** Course # 7F.

Matsubara, M., Kamei, Y., Takeda, S., Mukai, K., Ishii, Y. and Ito, S. (2004) Histologic and Histochemical Changes in Rabbit Cornea Produced by an Orthokeratology Lens *Eye & Contact Lens,* **30,** 198?04.

Maurice, D. (1988) Mechanics of the cornea. In *The cornea: transactions of the world congress on the cornea III.* (Ed, Cavanagh, H.) Raven Press Ltd., New York, pp. 187-93.

Maurice, D. and Riley, M. (1970) The cornea In *Biochemistry of the eye*(Ed, CN., G.) Academic Press Inc, New York, pp. 1-14.

Maurice, D. M. (1999) Some puzzles in the microscopic structure of the stroma *J Refract Surg,* **15,** 692-4.

McMonnies, C. W. (2005) The biomechanics of keratoconus and rigid contact lenses *Eye Contact Lens,* **31,** 80-92.

McTigue, J. W. (1967) The human cornea: a light and electron microscopic study of the normal cornea and its alterations in various dystrophies *Trans Am Ophthalmol Soc,* **65,** 591-660.

Mierdel, P., Krinke, H. E., Pollack, K. and Spoerl, E. (2004) Diurnal fluctuation of higher order ocular aberrations: correlation with intraocular pressure and corneal thickness *J Refract Surg,* **20,** 236-42.

Miller, D. (1967) Pressure of the lid on the eye *Arch Ophthalmol,* **78,** 328-30.

Millodot, M. and Sivak, J. (1979) Contribution of the cornea and lens to the spherical aberration of the eye *Vision Res,* **19,** 685-7.

Mirshahi, A., Buhren, J., Gerhardt, D. and Kohnen, T. (2003) In vivo and in vitro repeatability of Hartmann-Shack aberrometry *J Cataract Refract Surg,* **29,** 2295-301.

Moezzi, A. M. (2002) Contact lens-induced corneal swelling measured with the Orbscan II corneal topographer. *School of Optometry*, University of Waterloo. Waterloo. Master Thesis. 44-47.

Moezzi, A. M., Fonn, D., Simpson, T. L. and Sorbara, L. (2004) Contact lens-induced corneal swelling and surface changes measured with the Orbscan II corneal topographer *Optom Vis Sci,* **81,** 189-93.

Moller, P. M. (1954) Tissue pressure in the orbit *Acta Ophthalmol (Copenh),* **32,** 597-604.

Moller, P. M. (1955) The pressure in the orbit *Acta Ophthalmol (Copenh)***,** 1-100.

Moreno-Barriuso, E., Lloves, J. M., Marcos, S., Navarro, R., Llorente, L. and Barbero, S. (2001) Ocular aberrations before and after myopic corneal refractive surgery: LASIK-induced changes measured with laser ray tracing *Invest Ophthalmol Vis Sci,* **42,** 1396-403.

Mountford, J. (1997) An analysis of the changes in corneal shape and refractive error induced by accelerated orthokeratology *International Contact Lens Clinic,* **24,** 128-144.

Mountford, J. (1998) A mathematical model for corneal shape changes associated with ortho-K *Contact Lens Spectrum,* **June,** 39-45.

Mountford, J. (2003) Siliconehydrogel.org.

Mountford, J. (2004a) History and general principles In *Orthokeratolgoy: Principles and Practice*(Eds, Mountford, J., Ruston, D. and Dave, T.) Butterworth-Heinemann, Toronto, pp. 1-17.

Mountford, J. (2004b) A model of forces acting in orthokeratology In *Orthokeratology: Principle and practice*(Eds, Mountford, J., Ruston, D. and Dave, T.) Butterworth-Heinemann, Toronto, pp. 269-302.

Muller, L. J., Pels, E. and Vrensen, G. F. (2001) The specific architecture of the anterior stroma accounts for maintenance of corneal curvature *Br J Ophthalmol,* **85,** 437-43.

Munnerlyn, C. R., Koons, S. J. and Marshall, J. (1988) Photorefractive keratectomy: a technique for laser refractive surgery *J Cataract Refract Surg,* **14,** 46-52.

Nichols, J. J., Marsich, M. M., Nguyen, M., Barr, J. T. and Bullimore, M. A. (2000) Overnight orthokeratology *Optom Vis Sci,* **77,** 252-9.

Oshika, T., Klyce, S. D., Applegate, R. A., Howland, H. C. and El Danasoury, M. A. (1999) Comparison of corneal wavefront aberrations after photorefractive keratectomy and laser in situ keratomileusis *Am J Ophthalmol,* **127,** 1-7.

Owens, H., Garner, L. F., Craig, J. P. and Gamble, G. (2004) Posterior corneal changes with orthokeratology *Optom Vis Sci,* **81,** 421-6.

Papas, E. B. and Schultz, B. L. (1997) Repeatability and comparison of visual analogue and numerical rating scales in the assessment of visual quality *Ophthalmic Physiol Opt,* **17,** 492-8.

Partal, A. E. and Manche, E. E. (2003) Diameters of topographic optical zone and programmed ablation zone for laser in situ keratomileusis for myopia *J Refract Surg,* **19,** 528-33.

Petroll, W. M., Vishwanath, M. and Ma, L. (2004) Corneal fibroblasts respond rapidly to changes in local mechanical stress *Invest Ophthalmol Vis Sci,* **45,** 3466-74.

Phillips, A. J. (1995) Orthokeratology - an alternative to excimer laser? *J Brit Contact Lens Assoc,* **18,** 65-71.

Pointer, J. S. (2004) A novel visual analogue scale (VAS) device: an instrument based on the VAS designed to quantify the subjective visual experience *Ophthalmic Physiol Opt,* **24,** 181-5.

Polse, K. A., Brand, R. J., Keener, R. J., Schwalbe, J. S. and Vastine, D. W. (1983a) The Berkeley Orthokeratology Study, part III: safety *Am J Optom Physiol Opt,* **60,** 321-8.

Polse, K. A., Brand, R. J., Schwalbe, J. S., Vastine, D. W. and Keener, R. J. (1983b) The Berkeley Orthokeratology Study, Part II: Efficacy and duration *Am J Optom Physiol Opt,* **60,** 187-98.

Polse, K. A., Brand, R. J., Vastine, D. W. and Schwalbe, J. S. (1983c) Corneal change accompanying orthokeratology. Plastic or elastic? Results of a randomized controlled clinical trial *Arch Ophthalmol,* **101,** 1873-8.

Porter, J., Guirao, A., Cox, I. G. and Williams, D. R. (2001) Monochromatic aberrations of the human eye in a large population *J Opt Soc Am A Opt Image Sci Vis,* **18,** 1793-803.

Portney, L. and Watkins, M. (2000) *Foundations of clinical research: applications to practice.,* Prentice Hall Health, New Jersey.

Pouliquen, Y. J. (1984) 1984 Castroviejo lecture. Fine structure of the corneal stroma *Cornea,* **3,** 168-77.

Prisant, O., Calderon, N., Chastang, P., Gatinel, D. and Hoang-Xuan, T. (2003) Reliability of pachymetric measurements using orbscan after excimer refractive surgery *Ophthalmology,* **110,** 511-5.

Pritchard, N., Jones, L., Dumbleton, K. and Fonn, D. (2000) Epithelial inclusions in association with mucin ball development in high-oxygen permeability hydrogel lenses *Optom Vis Sci,* **77,** 68-72.

Rah, M. J., Jackson, J. M., Jones, L. A., Marsden, H. J., Bailey, M. D. and Barr, J. T. (2002) Overnight orthokeratology: preliminary results of the Lenses and Overnight Orthokeratology (LOOK) study *Optom Vis Sci,* **79,** 598-605.

Randleman, J., Russell, B. and Ward, M. (2003) Risk factors and prognosis for corneal ectasia after LASIK *Ophthalmology* **110,** 267-275.

Reiser, B. J., Ignacio, T. S., Wang, Y., Taban, M., Graff, J. M., Sweet, P., Chen, Z. and Chuck, R. S. (2005) In vitro measurement of rabbit corneal epithelial thickness using ultrahigh resolution optical coherence tomography *Vet Ophthalmol,* **8,** 85-8.

Ren, D. H., Petroll, W. M., Jester, J. V. and Cavanagh, H. D. (1999) The effect of rigid gas permeable contact lens wear on proliferation of rabbit corneal and conjunctival epithelial cells *Clao J,* **25,** 136-41.

Ren, D. H., Yamamoto, K., Ladage, P. M., Molai, M., Li, L., Petroll, W. M., Jester, J. V. and Cavanagh, H. D. (2002) Adaptive effects of 30-night wear of hyper-O(2) transmissible contact lenses on bacterial binding and corneal epithelium: a 1-year clinical trial *Ophthalmology,* **109,** 27-39; discussion 39-40.

Ren, H. and Wilson, G. (1996) Apoptosis in the corneal epithelium *Invest Ophthalmol Vis Sci,* **37,** 1017-25.

Ren, H. and Wilson, G. (1997) The effect of a shear force on the cell shedding rate of the corneal epithelium *Acta Ophthalmol Scand,* **75,** 383-7.

Riley, C., Horner, D. and Soni, P. (1992) Polycon II vs. OK-3 lenses in the acute reduction of myopia. *Optom Vis Sci,* **69 suppl,** 156.

Roberts, C. (2000) The cornea is not a piece of plastic *J Refract Surg,* **16,** 407-413.

Robertson, D. M., Li, L., Fisher, S., Pearce, V. P., Shay, J. W., Wright, W. E., Cavanagh, H. D. and Jester, J. V. (2005) Characterization of growth and differentiation in a telomerase-immortalized human corneal epithelial cell line *Invest Ophthalmol Vis Sci,* **46,** 470-8.

Rom, M. E., Keller, W. B., Meyer, C. J., Meisler, D. M., Chern, K. C., Lowder, C. Y. and Secic, M. (1995) Relationship between corneal edema and topography *Clao J,* **21,** 191-4.

Rushhood, A., Nassim, H. and Azeemuddin, T. (1997) Patient satisfaction after photorefractive keratectomy for low myopia using the visual analogue scale *J Refract Surg,* **13,** S438-440.

Sarver, M. D. and Harris, M. G. (1967) Corneal lenses and "spectacle blur" *Am J Optom Arch Am Acad Optom,* **44,** 502-4.

Schein, O. D., Glynn, R. J., Poggio, E. C., Seddon, J. M. and Kenyon, K. R. (1989) The relative risk of ulcerative keratitis among users of daily-wear and extended-wear soft contact lenses. A case-control study. Microbial Keratitis Study Group *N Engl J Med,* **321,** 773-8.

Seo, K. Y., Lee, J. B., Kang, J. J., Lee, E. S. and Kim, E. K. (2004) Comparison of higher-order aberrations after LASEK with a 6.0 mm ablation zone and a 6.5 mm ablation zone with blend zone *J Cataract Refract Surg,* **30,** 653-7.

Shin, Y. J., Kim, M. K., Wee, W. R., Lee, J. H., Shin, D. B., Lee, J. L., Xu, Y. G. and Choi, S. W. (2005) Change of proliferation rate of corneal epithelium in the rabbit with orthokeratology lens *Ophthalmic Res,* **37,** 94-103.

Sin, S. and Simpson, T. (2006) The repeatability of corneal and corneal epithelial thickness measurements using optical coherence tomography *Optom Vis Sci,* **83** (6), 360-5.

Smolek, M. K. (1993) Interlamellar cohesive strength in the vertical meridian of human eye bank corneas *Invest Ophthalmol Vis Sci,* **34,** 2962-9.

Smolek, M. K. and McCarey, B. E. (1990) Interlamellar adhesive strength in human eyebank corneas *Invest Ophthalmol Vis Sci,* **31,** 1087-95.

Somani, S., Tuan, K. A. and Chernyak, D. (2004) Corneal asphericity and retinal image quality: a case study and simulations *J Refract Surg,* **20,** S581-5.

Soni, P. S., Nguyen, T. T. and Bonanno, J. A. (2003) Overnight orthokeratology: visual and corneal changes *Eye Contact Lens,* **29,** 137-45.

Soni, P. S., Nguyen, T. T. and Bonanno, J. A. (2004) Overnight orthokeratology: refractive and corneal recovery after discontinuation of reverse-geometry lenses *Eye Contact Lens,* **30,** 254-62.

Sorbara, L., Fonn, D., Simpson, T., Lu, F. and Kort, R. (2005) Reduction of myopia from corneal refractive therapy *Optom Vis Sci,* **82,** 512-8.

Sorbara, L., Lu, F., Fonn, D. and Simpson, T. (2004) Refractive and keratometric effects of corneal refractive therapy for hyperopia after one night of lens wear. *Optom Vis Sci,* **81,** 72.

Spadea, L., Fasciani, R., Necozione, S. and Balestrazzi, E. (2000) Role of the corneal epithelium in refractive changes following laser in situ keratomileusis for high myopia *J Refract Surg,* **16,** 133-9.

Sridharan, R. and Swarbrick, H. (2003) Corneal response to short-term orthokeratology lens wear *Optom Vis Sci,* **80,** 200-6.

Srinivas, S. P., Mutharasan, R. and Fleiszig, S. (2002) Shear-induced ATP release by cultured rabbit corneal epithelial cells *Adv Exp Med Biol,* **506,** 677-85.

Stapleton, F. (2003) Contact lens-related microbial keratitis: what can epidemiologic studies tell us? *Eye Contact Lens,* **29,** S85-9; discussion S115-8, S192-4.

Sun, X., Zhao, H., Deng, S., Zhang, Y., Wang, Z., Li, R., Luo, S. and Jin, X. (2006) Infectious keratitis related to orthokeratology *Ophthalmic Physiol Opt,* **26,** 133-6.

Swarbrick, H., Jayakumar, J., Co, W., He, D., Siu, C. and Yau, B. (2005) Overnight Corneal Edema Can Modulate the Short term Clinical Response to Orthokeratology Lens Wear *Invest Ophthalmol Vis Sci 2005;46: E-Abstract 2056.*

Swarbrick, H. A., Hiew, R., Kee, A. V., Peterson, S. and Tahhan, N. (2004) Apical clearance rigid contact lenses induce corneal steepening *Optom Vis Sci,* **81,** 427-35.

Swarbrick, H. A. and Holden, B. A. (1996) Effects of lens parameter variation on rigid gas-permeable lens adherence *Optom Vis Sci,* **73,** 144-55.

Swarbrick, H. A. and Lum, E. (2006) Lens Dk/t Influences the Clinical Response in Overnight Orthokeratology *Invest. Ophthalmol. Vis. Sci.,* **47,** E-abstract 110.

Swarbrick, H. A., Wong, G. and O'Leary, D. J. (1998) Corneal response to orthokeratology *Optom Vis Sci,* **75,** 791-9.

Tahhan, N., Du Toit, R., Papas, E., Chung, H., La Hood, D. and Holden, A. B. (2003) Comparison of reverse-geometry lens designs for overnight orthokeratology *Optom Vis Sci,* **80,** 796-804.

Tahhan, N., Sridharan, R., Du Toit, R. and Papas, E. (2001) Corneal topographical changes after fifteen minutes of reverse geometry lens wear. *Optom Vis Sci***, 78s**, 61.

Thibos, L. N. and Horner, D. (2001) Power vector analysis of the optical outcome of refractive surgery *J Cataract Refract Surg*, **27**, 81-85.

Thibos, L. N., Applegate, R. A., Schwiegerling, J. T. and Webb, R. (2002) Standards for reporting the optical aberrations of eyes *J Refract Surg,* **18,** S652-60.

Tredici, T. J. (1979) Symposium: Clinical management of physiologic myopia. Role of orthokeratology: a perspective *Ophthalmology,* **86,** 698-705.

Trinkaus-Randall, V., Edelhauser, H. F., Leibowitz, H. and Freddo, T. (1998) Corneal structure and function In *Corneal disorders: clinical diagnosis and management*(Eds, Leibowitz, H. and Warning III, G.) W.B. Saunders company, Toronto, pp. 2-32.

Tseng, C. H., Fong, C. F., Chen, W. L., Hou, Y. C., Wang, I. J. and Hu, F. R. (2005) Overnight orthokeratology-associated microbial keratitis *Cornea,* **24,** 778-82.

Van Horn, D. L., Doughman, D. J., Harris, J. E., Miller, G. E., Lindstrom, R. and Good, R. A. (1975) Ultrastructure of human organ-cultured cornea. II. Stroma and epithelium *Arch Ophthalmol,* **93,** 275-7.

Vasudevan, B., Sivak, J. and Simpson, T. (2004) Refractive index of the human corneal epithelium *invest Ophthalmol Vis Sci,* **45,** E-Abstract 2882.

Vihlen, F. and Wilson, G. (1983) The relation between eyelid tension, corneal toricity, and age. *Invest Ophthalmol Vis Sci,* **24,** 1367-1373.

Walline, J. J., Holden, B. A., Bullimore, M. A., Rah, M. J., Asbell, P. A., Barr, J. T., Caroline, P. J., Cavanagh, H. D., Despotidis, N., Desmond, F., Koffler, B. H., Reeder, K., Swarbrick, H. A. and Wohl, L. G. (2005) The current state of corneal reshaping *Eye Contact Lens,* **31,** 209-14.

Walline, J. J., Rah, M. J. and Jones, L. A. (2004) The Children's Overnight Orthokeratology Investigation (COOKI) pilot study *Optom Vis Sci,* **81,** 407-13.

Walton, D. (1983) Glaucoma, infants and children In *Pediatric Ophthalmology*(Ed, Harley, R.) WB Saunders, Philadelphia, pp. 587.

Wang, J., Fonn, D., Simpson, T. L., Sorbara, L., Kort, R. and Jones, L. (2003) Topographical thickness of the epithelium and total cornea after overnight wear of reverse-geometry rigid contact lenses for myopia reduction *Invest Ophthalmol Vis Sci,* **44,** 4742-6.

Wang, Q., Leach, N., Giannoni, A. G., Parker, K. and Miller, W. (2004) The effect of orthokeratology on corneal cell densities *Optom Vis Sci,* **81,** 28.

Wang, Z., Chen, J. and Yang, B. (1999) Posterior corneal surface topographic changes after laser in situ keratomileusis are related to residual corneal bed thickness *Ophthalmology,* **106,** 406-9; discussion 409-10.

Watt, K. and Swarbrick, H. A. (2005) Microbial keratitis in overnight orthokeratology: review of the first 50 cases *Eye Contact Lens,* **31,** 201-8.

Weed, K. H. and McGhee, C. N. (1998) Referral patterns, treatment management and visual outcome in keratoconus *Eye,* **12 (Pt 4),** 663-8.

Wilhelmus, K. R. (2005) Acanthamoeba keratitis during orthokeratology *Cornea,* **24,** 864-6.

Williams, D., Yoon, G. Y., Porter, J., Guirao, A., Hofer, H. and Cox, I. (2000) Visual benefit of correcting higher order aberrations of the eye *J Refract Surg,* **16,** S554-9.

Wlodyga, R. B., C. (1989) Corneal mouldings: the easy way *Contact Lens Spectrum,* **4,** 58-65.

Yang, X., Gong, X. M., Dai, Z. Y., Wei, L. and Li, S. X. (2003) Topographical evaluation on decentration of orthokeratology lenses *Zhonghua Yan Ke Za Zhi,* **39,** 335-8.

Yebra-Pimentel, E., Gonzalez-Jeijome, J. M., Cervino, A., Giraldez, M. J., Gonzalez-Perez, J. and Parafita, M. A. (2004) [Corneal asphericity in a young adult population. Clinical implications] *Arch Soc Esp Oftalmol,* **79,** 385-92.

Yepes, N., Lee, S. B., Hill, V., Ashenhurst, M., Saunders, P. P. and Slomovic, A. R. (2005) Infectious keratitis after overnight orthokeratology in Canada *Cornea,* **24,** 857-60.

Ying-Cheng, L., Chao-Kung, L., Ko-Hua, C. and Wen-Ming, H. (2006) Daytime Orthokeratology Associated With Infectious Keratitis by Multiple Gram-Negative Bacilli: Burkholderia cepacia, Pseudomonas putida, and Pseudomonas aeruginosa *Eye Contact Lens,* **32,** 19-20.

Yoon, G., Macrae, S., Williams, D. R. and Cox, I. G. (2005) Causes of spherical aberration induced by laser refractive surgery *J Cataract Refract Surg,* **31,** 127-35.

York, D. (1966) Least-squares fitting of a straight line *Can J Phys,* **44,** 1079-1086.

Zadnik, K. (1988) A case of dimple veiling/staining. *Contact Lens Forum,* **13,** 69.

Zadnik, K., Friedman, N. E. and Mutti, D. O. (1995) Repeatability of corneal topography: the "corneal field" *J Refract Surg,* **11,** 119-25.

Zadok, D., Levy, Y., Segal, O., Barkana, Y., Morad, Y. and Avni, I. (2005) Ocular higher-order aberrations in myopia and skiascopic wavefront repeatability *J Cataract Refract Surg,* **31,** 1128-32.